N° :______

Thèse de doctorat

Présentée et soutenue publiquement à
Université Lille I Sciences et Technologies

pour obtenir le grade de
Docteur
Spécialité : Molécules et matières condensées

par
Jeremy CIRET

Investigation of Intumescent Coatings for Fire Protection - Application to Jet-Fire

Thèse dirigée par
Prof. Serge BOURBIGOT et Prof. Sophie DUQUESNE

Soutenue le 16 février 2010 devant la Commission d'Examen composée de :
Prof. Jean-Bernard Vogt, Président du jury
Dr. Jannick Duchet-Rumeau, Rapporteur
Prof. Laurent Autrique, Rapporteur
Dr. Rachel Butler, Examinateur
Prof. Serge Bourbigot, Directeur de thèse
Prof. Sophie Duquesne, Co-directeur de thèse

N° :______

Thèse de doctorat

Présentée et soutenue publiquement à
Université Lille I Sciences et Technologies

pour obtenir le grade de
Docteur
Spécialité : Molécules et matières condensées

par
Jeremy CIRET

Investigation of Intumescent Coatings for Fire Protection - Application to Jet-Fire

Thèse dirigée par
Prof. Serge BOURBIGOT et Prof. Sophie DUQUESNE

Soutenue le 16 février 2010 devant la Commission d'Examen composée de :
Prof. Jean-Bernard Vogt, Président du jury
Dr. Jannick Duchet-Rumeau, Rapporteur
Prof. Laurent Autrique, Rapporteur
Dr. Rachel Butler, Examinateur
Prof. Serge Bourbigot, Directeur de thèse
Prof. Sophie Duquesne, Co-directeur de thèse

Acknowledgements

My first thank goes to Dr. J.M. Lefebvre and to Prof. R. Delobel for having welcomed me in the LSPES Laboratory (UMR CNRS 8008) and in the PERF group, giving me the opportunity to work on this interesting project and to benefit of all the knowledge and skills provided either by the laboratory and CREPIM.

My sincere thanks go to my supervisors in the PERF group, Prof. Serge Bourbigot and Prof. Sophie Duquesne, who provided me with the best scientific and moral support I could ever have desired. I am especially grateful to them for their trust and guidance experienced for the whole period of the PhD, which, combined with their continuous and stimulating participation, kept me highly motivated and enthusiastic.

During the entire PhD, I was able to take advantage of a strong partnership with my industrial sponsor. I particularly would like to acknowledge Dr. Paul Jackson for his generous scientific and technical contribution and his strong impulse in the project. I also would like to thank Dr Rachel Butler with whom I created a very enjoyable and efficient collaboration. I finally thank the many other people of the company with whom I collaborate to bring this project to a successful conclusion.

I also sincerely thank all of the current and former members of the PERF Laboratory for their help and friendship over the last three years: Gaëlle, Michou, Brigitte, Nadine. To my labmates Maude, Fabienne, Aurore, Virginie, Mathilde (x2), Oriane, Séverine, Caroline, Fatima, Yohann, Thomas, Loulou, Damien, Nicolas, Antoine, Jeremie,... thanks for the fun and support for these three years! I also would like to acknowledge the technicians Pierre, and Mickaël for their help.

Particular thanks are addressed to Bertrand Revel for his expertise in NMR, to Christophe Penvern and Maxence Vandewalle for the numerous XRD analyses.

Finally, I would like to thank my parents, my sisters and of course, my girlfriend Dr. Christelle Réti (met thanks to this thesis) for their never-ending support, patience and affection.

Content

List of figures

Table captions

Résumé français

Cette thèse s'intéresse aux comportements de quatre peintures intumescentes (appelées dans la suite du mémoire IF-1, IF-2, IF-3 et IF-4) élaborées à base d'une résine époxyde et destinées à protéger contre le feu les structures métalliques de plateformes offshores (Tableau 1). L'utilisation de telles peintures protectrices dans un environnement si hostile que les plateformes pétrolières ou les sites pétrochimiques requiert évidemment des performances supérieures aux protections thermiques classiques. Nous décrivons dans le premier chapitre les principaux risques d'incendie possibles sur un site d'hydrocarbures. Nous avons détaillé les particularités du « jet-fire », l'un des feux les plus puissants et les plus dangereux pour les hommes et la structure métallique de la plateforme, alimenté par une fuite continue et directionnelle d'hydrocarbures. Nous nous sommes intéressés également aux moyens mis en œuvre pour le combattre, non pas en l'évitant (un feu est toujours lié à un accident et donc évitable mais imprévisible) mais en comprenant son action et en limitant son effet sur la structure. Pour cela l'utilisation de revêtements protecteurs, en particulier les peintures intumescentes à base de résine époxyde (intumescence signifie la formation d'un bouclier protecteur carboné expansé faisant office de barrière thermique et limitant les transferts de gaz de dégradation combustibles pouvant alimenter la flamme), et les tests développés pour évaluer leur performance ont été détaillés. Dans le second chapitre, nous avons étudié le comportement des formulations intumescentes lors d'un test de résistance au jet-fire. Puis nous avons tenté dans les troisième et quatrième chapitres de comprendre et d'expliquer ces comportements grâce à des outils expérimentaux permettant d'étudier les propriétés physiques de nos revêtements intumescents et l'évolution chimique de ses formulations. Enfin, le dernier chapitre de ce manuscrit s'est attaché au développement d'un test à l'échelle laboratoire permettant de reproduire les phénomènes caractéristiques du jet-fire. Cet outil expérimental permet de mimer les comportements des formulations intumescentes à petite échelle de manière rapide et fiable.

D'un point de vue de la gestion des risques, les plateformes pétrolières sont connues pour leur haut degré de risque à cause de leur situation insulaire, de leur aménagement congestionné et bien sur à cause de l'inflammabilité des produits extraits, les hydrocarbures. Malheureusement il a fallu attendre des drames pour prendre en compte ces circonstances et l'accident de Piper Alpha en 1988 a permis l'élaboration de plusieurs rapports étudiant les feux spécifiques aux plateformes offshores. Ces rapports ont permis de mettre en évidence la particulière dangerosité du « jet-fire ». Le jet-fire est une flamme turbulente résultant de la combustion d'hydrocarbures libérés en continu dans une direction particulière avec une importante quantité de mouvement. Ainsi les deux paramètres importants d'un tel phénomène sont clairement exprimés dans sa définition : une direction et une vitesse significative dangereuses pour les hommes et les structures qui pourraient être « frappées » par la flamme. Pour limiter les dommages structurels et les températures élevées, l'utilisation de matériaux isolants est donc étudiée. Cependant la force de la flamme et l'environnement agressif (corrosion, climat) imposent l'utilisation de résines intumescentes à base époxydes (les résines à base époxy sont les plus résistantes aux conditions agressives).

Une peinture intumescente utilisée pour la protection des structures métalliques est généralement constituée de trois composants principaux (Tableau 1):

- La source acide susceptible de libérer un acide inorganique (par exemple l'acide phosphorique) lorsqu'il est soumis à une élévation de température. Le polyphosphate d'ammonium (APP) ou des phosphates de mélamine sont généralement utilisés; dans notre cas les quatre formulations comportent de l'APP. Dans IF-1, de l'acide borique est également ajouté comme source acide additionnelle.
- La source de carbone contenant des groupes hydroxyle (-OH) susceptibles de réagir avec la source acide. Dans le cas des résines époxyde, la source carbonée peut être constituée par le polymère lui-même, c'est le cas pour IF-2, ou bien un composé spécifique est ajouté, souvent des polyols, du pentaérythritol (PER) pour IF-3 ou bien du dipentaérythritol (dPER) pour IF-4 ; l'enrobant de l'APP utilisé dans IF-1.
- L'agent d'expansion libérant sous l'action de la chaleur une quantité importante de gaz ininflammables provoquant l'expansion de la structure phospho-carbonée, comme par exemple la mélamine, ou dans notre cas le polyphosphate d'ammonium (APP) qui joue un double rôle (dégagement d'ammoniac).

En plus de ses composés actifs dans le processus de l'intumescence, les formulations sont complexes et contiennent des additifs et des charges couramment utilisé dans les peintures. La formulation exacte n'est pas connu néanmoins la présence de TiO_2 est avérée.

Tableau 1 : Tableau récapitulatif de la composition des formulations intumescentes

Peintures intumescentes	Matrice polymère	Source acide	Source de carbone	Agent gonflant
IF-1	Prépolymère de type DGEBA + polyaminoamide	APP enrobé + Acide borique	Résine époxy + THEIC (enrobant l'APP)	APP
IF-2	Prépolymère de type DGEBA + polyaminoamide	APP	Résine époxy	APP
IF-3	Prépolymère de type DGEBA + polyaminoamide	APP	Résine époxy + PER	APP
IF-4	Prépolymère de type DGEBA + polyaminoamide	APP	Résine époxy + dPER	APP

Le processus de développement de l'intumescence est généralement décrit de la manière suivante. L'acide libéré lors de la dégradation de la source acide réagit avec l'agent source de carbone pour produire une structure phospho-carbonée. L'agent gonflant se décompose ensuite et entraîne un dégagement important de produits gazeux, ce qui provoque le gonflement du bouclier et la création de la structure intumescente, une couche protectrice isolante (Figure 1).

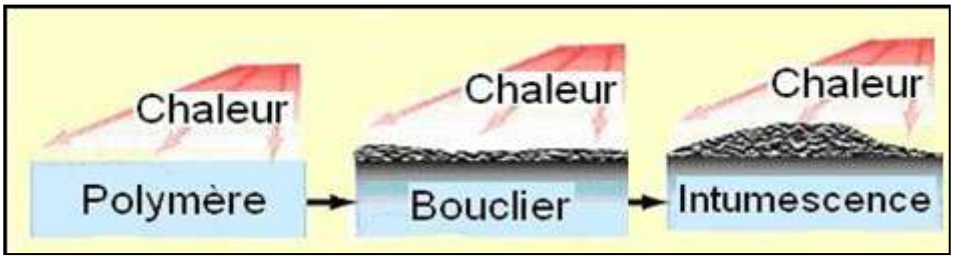

Figure 1 : Développement de la couche protectrice intumescente

Le bouclier se forme dans une phase semi-liquide qui coïncide avec la formation des gaz et l'expansion de la surface, puis il se solidifie ensuite en une couche multicellulaire rigide. L'efficacité d'un système intumescent dépend de sa capacité à gonfler et à développer une structure multicellulaire. Le gonflement est dû à la diffusion lente des gaz de dégradation du système dans une matrice charbonnée partiellement dégradée. Lors de ce phénomène d'intumescence, l'étude de la viscosité est donc essentielle: si la matrice dégradée est trop liquide, les gaz ne sont pas piégés et diffusent facilement pour alimenter la flamme. Si au contraire la matrice dégradée est trop visqueuse, l'augmentation de pression entraînée par le dégagement de produits gazeux peut conduire à l'apparition de fissures permettant la diffusion d'oxygène ainsi qu'un échange de chaleur et de matière entre la flamme et le polymère. Il est également important de caractériser la résistance mécanique de la structure développée car celle-ci doit conserver ses propriétés protectrices même sous l'action de contraintes externes telle que l'impact d'une flamme issue du jet-fire. Enfin, il faut bien sûr caractériser les systèmes intumescents selon leur capacité de résistance au feu. Pour cela des tests normés ont été développés avec des courbes temps/température spécifiques aux feux d'hydrocarbures. Cependant aucun de ces tests ne prenait en compte l'aspect dynamique du jet-fire avec l'impact de la flamme sur la structure. Ainsi un nouveau test a récemment été développé par des industriels et normé en 2007 pour déterminer la résistance aux feux propulsés des matériaux de protection passive contre l'incendie.

Ce test à grande échelle réalisé sur nos quatre formulations intumescentes a permis de déterminer quatre comportements spécifiques face à l'impact d'une flamme et aux conditions extrêmes de température (Figure 2). Sous les contraintes thermiques et mécaniques du jet-fire IF-1 réagit et développe un bouclier très dur et résistant à l'impact. Cependant ce bouclier est peu expansé et n'apporte pas une isolation suffisante du substrat au point le plus chaud, localisé sur le haut de la partie centrale.

Par contre la seconde formulation intumescente (IF-2) gonfle suffisamment sur toute la surface de la plaque d'essai. Mais le bouclier expansé présente une très faible résistance mécanique et est détruit sous l'impact du jet-fire et de la pression inhérente. L'utilisation d'un grillage pour renforcer la structure expansée et pour maintenir en place la protection apporte une amélioration significative et permet de meilleures performances face au jet-fire.

Ensuite la formulation intumescente IF-3 est présentée comme un compromis entre les deux premières formulations. Elle doit permettre une bonne expansion pour isoler suffisamment et une résistance mécanique face au jet-fire, néanmoins l'utilisation du grillage renforçant est toujours nécessaire. La structure protectrice résiste donc à la pression et isole la plaque métallique des températures extrêmes, mais lors du test on observe un écoulement de la peinture sur les faces latérales de la plaque laissant non protégées de larges zones. Ainsi le point faible d'IF-3 est observé à un endroit où ni IF-1 ni IF-2 ne se sont révélées sensibles.

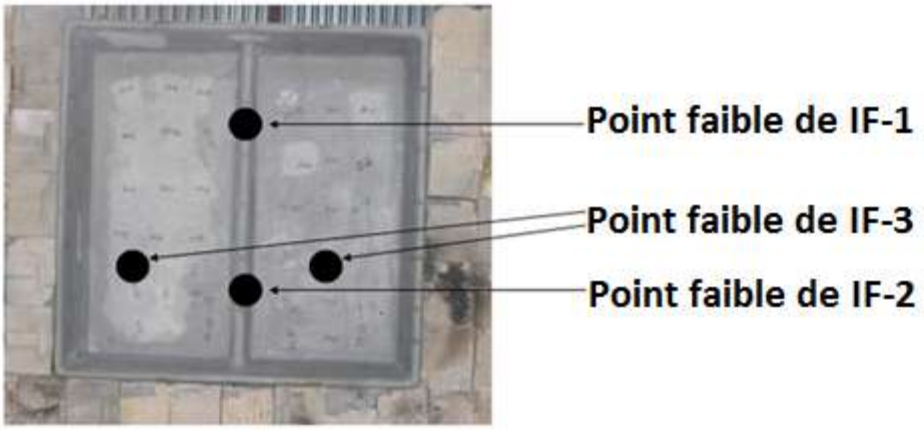

Figure 2 : Mise en évidence des zones de point faible pour IF-1, IF-2 et IF-3

Enfin IF-4 échoue au test de résistance aux feux propulsés par manque d'adhésion, la structure expansée ayant révélé de grandes alvéoles creuses à l'interface métal/revêtement. Ces alvéoles permettent ainsi le passage des flammes et de la chaleur.

Dans ce travail, nous avons donc tenté d'expliquer ces quatre comportements très différents en s'intéressant aux propriétés physiques et aux évolutions chimiques de ces revêtements intumescents. Les propriétés du 1er revêtement (IF-1) ont été particulièrement étudiées par Maude Jimenez dans ses travaux de thèse qui a pu mettre en évidence l'effet de l'acide borique sur les propriétés viscoélastiques et le mécanisme de dégradation d'IF-1. De manière similaire nous nous sommes donc intéressés aux trois autres formulations, sachant que la source de carbone est respectivement la résine époxyde seule dans IF-2, la résine époxyde et le pentaérythritol dans IF-3, la résine époxyde et le dipentaérythritol dans IF-4.

Tout d'abord l'étude des propriétés mécaniques (mesure de la résistance du char en compression lorsqu'il subit une contrainte normale) à l'aide d'un rhéomètre plan-plan utilisé de manière originale selon une technique développée au laboratoire ont permis de confirmer la différence existant entre IF-1 développant un bouclier peu expansé mais résistant et les trois autres formulations, qui gonflent beaucoup mais qui présentent une faible résistance à la contrainte. Une raison avancée pour expliquer cette différence est la présence de fibres silicates et d'acide borique dans IF-1 (Maude Jimenez a clairement montré l'effet de ces ingrédients sur les propriétés mécaniques du bouclier intumescent). Ensuite un effet de la source de carbone a été démontré sur l'évolution de la viscosité apparente des systèmes en fonction de la température (ici nous mesurons une viscosité apparente pour nous permettre de quantifier dans des conditions expérimentales données les propriétés d'écoulement de nos matériaux). En effet, le pentaérythritol provoque un déplacement vers les basses températures du pic de viscosité observé lors du phénomène d'intumescence. Ainsi le minimum de viscosité est observé respectivement vers 270°C pour IF-3 et vers 360°C pour les 3 autres formulations (Figure 3).

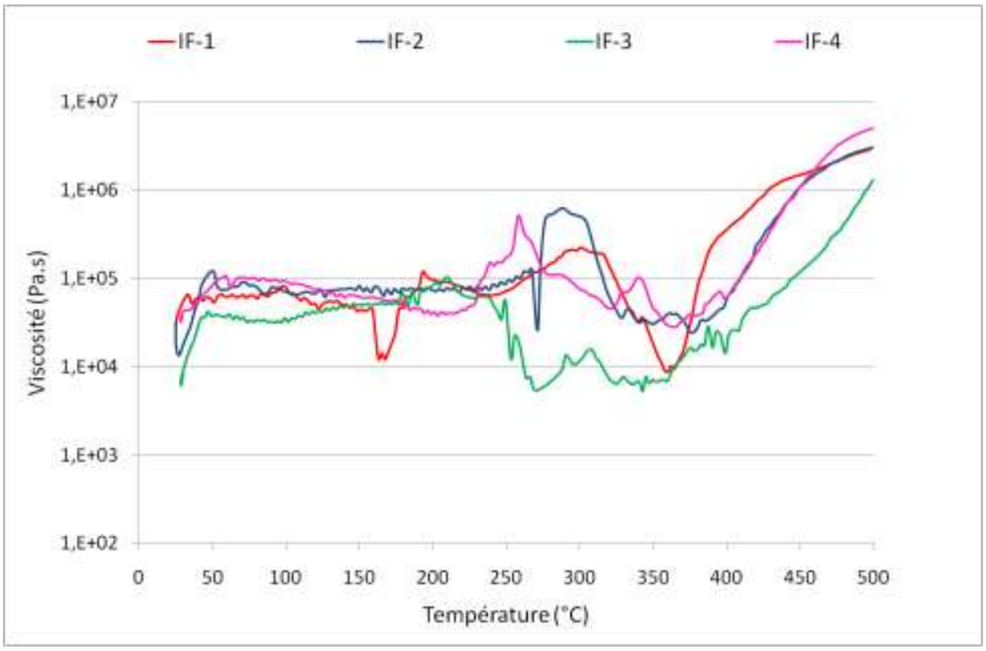

Figure 3 : Evolution de la viscosité en fonction de la température pour IF-1, IF-2, IF-3 et IF-4

Ce comportement viscoélastique particulier de IF-3 est clairement attribué au PER comme le montre le comportement de IF-4 où le PER a été remplacé par du dipentaérythritol. Ce large éventail de température où la viscosité du système est faible est avancé comme explication à l'échec d'IF-3 au test de résistance de jet-fire et l'utilisation d'IF-4 plutôt qu'IF-3 permet de résoudre partiellement ce problème.

De plus l'effet de la source de carbone a également été étudié par une approche chimique. En effet, des analyses chimiques par diffraction des rayons X et RMN à l'état solide des noyaux ^{13}C et ^{31}P ont été réalisées à différentes températures caractéristiques de la dégradation des formulations intumescentes afin de comprendre leur processus d'intumescence. Des mécanismes de dégradation ont été proposés pour les 3 formulations IF-2, IF-3 et IF-4 en fonction de leurs particularités. Quelque soit la source de carbone, nous avons démontré que l'APP réagissait dans un premier temps avec la source de carbone pour former une structure charbonnée et des composés phosphorés issus de sa dégradation. Ces produits de dégradation et de réaction de l'APP présentent une réactivité importante avec de nombreux composés thermiquement stable et présents dans les formulations intumescentes. Lors de la dégradation thermique de nos formulations, nous observons ainsi une réaction entre ces composés à base de phosphore et le dioxyde de titane TiO_2 pour donner une structure cristalline de pyrophosphate de titane TiP_2O_7. D'après la littérature, cette structure apporte des améliorations en termes de résistance mécanique et de performance au feu du bouclier développé. De plus, nous avons mis en évidence que la source de carbone intervient sur la température à laquelle les réactions se déroulent. En effet nous avons montré que l'évolution chimique du revêtement à base de dipentaérythritol était accélérée, la réactivité entre l'APP et le dipentaérythritol est supérieure à celle entre l'APP et le PER ou entre l'APP et le réseau époxyde. Cela se traduit par la formation de la structure protectrice et du TiP_2O_7 à plus basses températures comme on peut le voir sur les diffractogrammes à 600°C des trois formulations intumescentes (Figure 4).

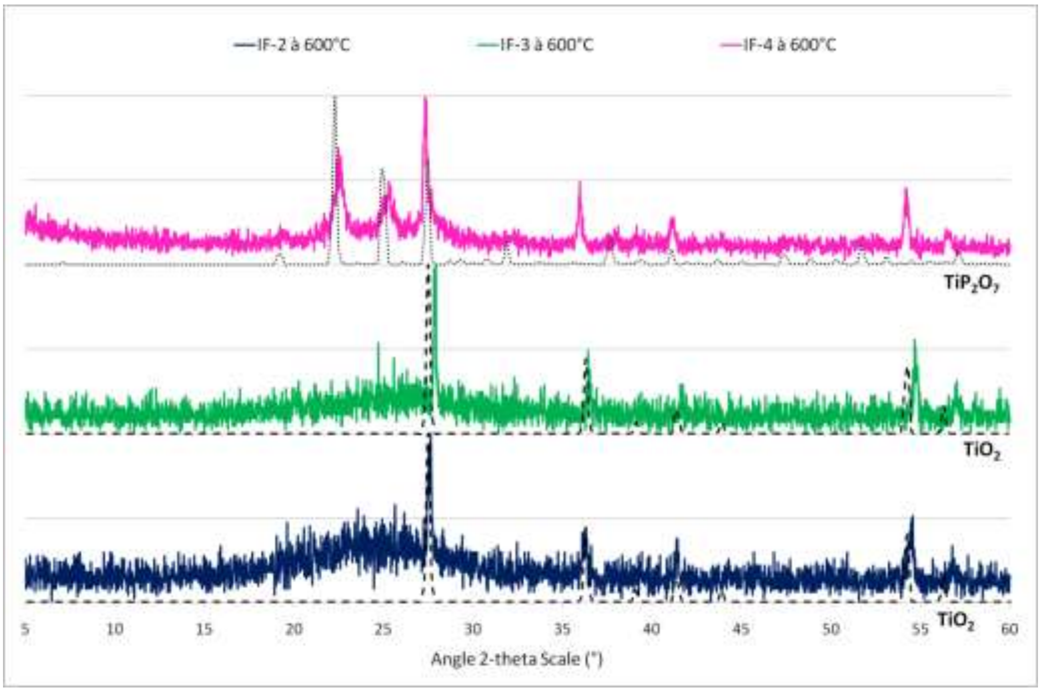

Figure 4 : Diffractogrammes des residus des trois formulations intumescentes après un traitement thermique à 600°C

Ainsi l'influence de la source de carbone est démontrée. Même si le mécanisme de dégradation est similaire quelque soit la source de carbone utilisée (résine époxyde, pentaérythritol et dipentaérythritol) les étapes « clés » de formation de la structure protectrice et du TiP_2O_7 se déroulent à des températures moins élevées en présence de dipentaérythritol. Ce mécanisme a également été mis en évidence lors des tests de résistance au feu et la formation précoce de la structure cristalline à base de titane pourrait expliquer les meilleures performances observées lors d'un test dans des conditions de feu d'hydrocarbures (norme ISO 834) (Figure 5).

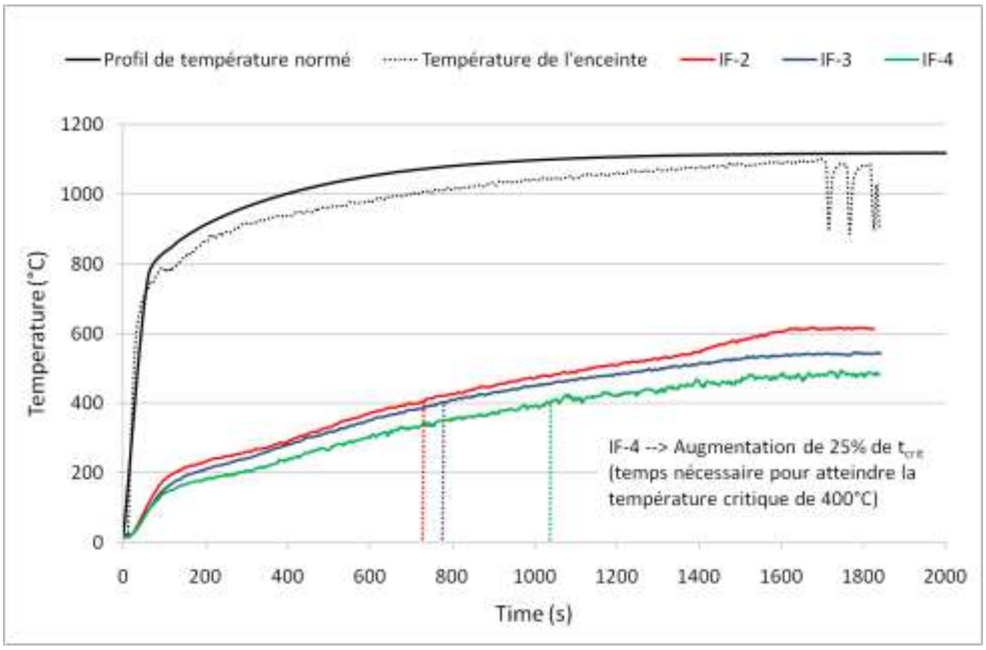

Figure 5 : Profils de température relevées au dos de plaque d'acier revêtue de peintures intumescentes IF-2, IF-3 et IF-4 dans des conditions specifieés par la norme ISO 834- Feu d'hydrocarbures

Enfin et puisque la réalisation de test à grande échelle est financièrement coûteuse et ne permet pas l'évaluation de nombreuses formulations, nous avons dans un dernier chapitre développé un test imitant les conditions d'un jet-fire à l'échelle laboratoire. En associant un cône irradiant pour apporter la contribution radiative présente lors d'un jet-fire et un jet d'air pour l'aspect dynamique et la quantité de mouvement, nous avons construit un dispositif expérimental pour tester nos formulations intumescentes dans des conditions de températures et de pression permettant des corrélations satisfaisantes entre le test de résistance à grande échelle et à l'échelle laboratoire. En effet après une phase d'optimisation des paramètres, nous avons réussi à obtenir des comportements de nos peintures facilement identifiables. Quelque soit les conditions de test, IF-1 présente le même comportement, développant un bouclier peu expansé mais résistant. Nous retrouvons ainsi les conclusions du test à grande échelle d'IF-1. Concernant IF-2 et IF-3, la résistance mécanique de la structure est également mise en cause à l'échelle réduite puisque le revêtement est « soufflé » par le jet d'air dès le premier impact. De la même façon que lors du test normé, l'utilisation de grillage renforçant a permis de maintenir une protection et de retarder l'augmentation de température. Enfin la substitution de PER par le dipentaérythritol a été étudiée en comparant le comportement d'IF-3 et d'IF-4 : le test réalisé sur IF-4 a montré des différences significatives avec celui d'IF-3, une couche résiduelle résistante est formée en présence de dipentaérythritol permettant une protection substantielle du substrat.

Ainsi durant cette thèse, trois approches ont été suivies pour étudier et expliquer le comportement des peintures intumescentes destinées à la protection de plateformes offshores et susceptibles de subir un jet-fire. Une approche physique tout d'abord qui nous a permis de mettre en avant l'importance de la résistance mécanique et du comportement viscoélastique des peintures intumescentes. L'influence du PER sur la viscosité a été évalué et son effet négatif a obligé la substitution du PER par du dipentaérythritol dans la formulation. Une approche chimique a ensuite permis de mettre en avant un mécanisme de dégradation pour chaque formulation avec la formation d'une structure protectrice et d'un composé cristallin (TiP_2O_7) bénéfique pour les performances feu des revêtements. Le dipentaérythritol joue également un rôle important sur l'aspect chimique des formulations puisqu'il présente une meilleure réactivité avec l'APP que le PER ou la résine époxyde, permettant aux étapes « clés » du mécanisme de se réaliser à plus faible température. Enfin une approche expérimentale nous a amené à développer un test à l'échelle laboratoire pour simuler les conditions d'un « jet-fire » et étudier les comportements des formulations intumescentes.

General Introduction

In 1988, Occidental's Piper Alpha platform (United Kingdom) was destroyed by explosion and fire and 167 workers were killed in the blaze. 17 years later, on Mumbai High North platform (India), a support vessel collided with the structural framework, ruptured a riser causing a major fire which destroyed the platform and killed 11 persons. In spite of advancement and progress in fire protection, these dramatic events, picked on a too long list, have widely opened the mind about fire hazards possible on offshore platforms. Moreover several key lessons have been learnt following each accident. All major disasters lead to a tightening of regulations and to the development of new technology. The protection of steel framework against fire has notably become an important issue in the construction industry. Protection of residential or commercial building has been regulated since several years but it is only after 1988 and Piper Alpha disaster that characteristics of the offshore platforms have been taken into account to propose new fire tests and new materials.

Usual cellulosic fire tests have been substituted by more severe hydrocarbon tests. Use of active and passive fire proofing have been required and thanks to their properties, intumescent coatings (intumescence means the formation of an expanded carbonaceous char upon heating) have become one of the easiest and one of the most efficient ways to protect steel structure against fire. The coating has the ability to expand by a factor of 40 or more upon heat exposure that effectively leads to the protection of the substrate against rapid increase of temperature, thereby maintaining the structural integrity of the building.

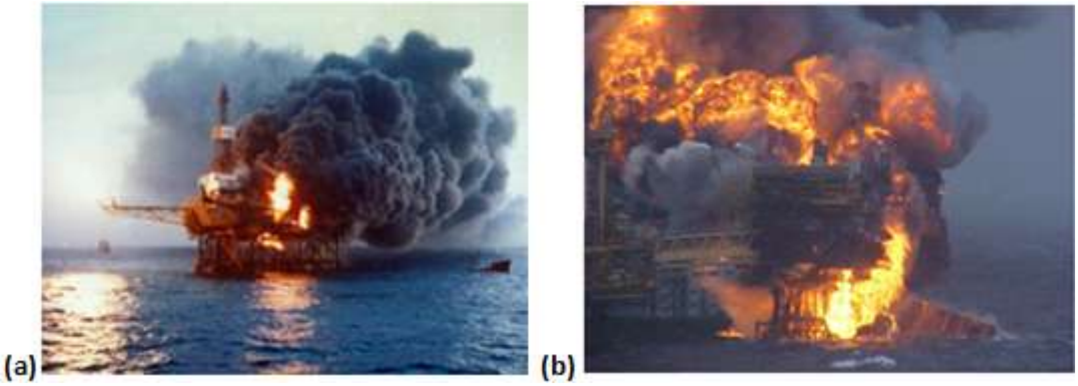

Figure 6 : Pictures from Piper Alpha disaster (a) and Mumbai accident (b)

In this context, this dissertation, divided in five parts, is based on the study of an epoxy based intumescent coating, applied on offshore platforms. These coatings have to ensure protection of steel in case of "jet-fires", which means that it has to resist to very severe conditions combining extremely high heating (fire) and high momentum (velocity of the jet).

The first chapter of this Ph-D work proposes a state of the art focused on the specific fire hazards that can occur on offshore platforms and on the new solutions developed to struggle against them and avoid human and materials losses. Different hydrocarbon fire situations will be detailed, as pool fires or fireballs but it is jet-fires that will catch particularly our attention because of its severity and consequence on steel structure. Jet-fires represent an important fire risk in offshore installations and potential jet-fires may vary with respect to flame length, heat flux and velocities. We propose thus to study jet-fire taken into account these parameters. Then in a second section of this state of the art, we will deal with the means developed to limit jet-fire effect and obviously the intumescent coatings. They are designed to perform under severe conditions and to maintain the steel integrity for up to three hours when the temperature of the surroundings is in excess of 1100°C. Their performances are tested using fire test, classically based on time temperature curves. We will comment typical fire scenario. Furthermore, we will treat of a specific fire test, developed to simulate jet-fire and to determine the resistance of passive fire protection materials facing to high load resulting from a gas line rupture on an offshore oil rig.

The second chapter is also dedicated to jet-fires and particularly to the standard developed by the Health and Safety Executive to determine the efficiency of the passive fire protection coating facing to jet-fire conditions: OTI 95654 Jet-fire resistance - Test of passive fire protection materials. After a description of the experimental settings and the parameters used for severe conditions, we will detail the results exhibited by the four intumescent formulations that have been investigated in this work. Their weaknesses will be highlighted by a thermal behaviour and illustrated by an investigation of the specimen after test.

Physical and chemical properties of the intumescent coatings will be then respectively investigated on **a third and fourth chapter**. Indeed, the efficiency of the char is closely related to the physical behaviours, namely its ability to expand and the visco-elastic properties of the melted degraded matrix during the intumescent process. The swelling of intumescent coating is due to the slow diffusion of the evolved degradation gases released into the degraded matrix. The importance of the visco-elastic properties of this layer is then crucial since it would affect the porosity and the expansion of the resulting char. The toughness of the char will also be determined thanks to an original test based on a rheological approach.
In the fourth chapter, we will report the complete investigation of the selected intumescent formulations using a chemical approach investigating their degradation pathway. Preliminary analyses on mixtures of the additives contained in the coating have first been carried out. At the end of this chapter, we will expect to propose a mechanism of degradation for our formulations, highlighting the main particularities and the role played by the ingredients and their interactions. Knowing the chemical and physical properties of the coating (Chapters III and IV), our goal will be to explain their behaviour facing the jet-fire exposed on the second chapter.

Finally, the evaluation of coatings in hydrocarbon and jet-fire test regimes is both expensive and time consuming and the companies involved in the research and development of fire protection coatings are looking to reducing these costs by developing high throughput screening using small scale fire tests. Another objective of this PhD work is to examine whether the performance in large scale industrial fire tests can be correlated with parameters of the intumescent coating measured using labscale tools. Therefore **the last chapter** of this report (Chapter V) will talk about the development of a novel labscale tests permitting to predict the behaviour of intumescent formulations for the jet-fire test.

Chapter I: State of the art

A century ago, steel was a comparatively unusual building material, mass production of steel did not begin until 1855 and then it took several decades before it became popular as a building material [1]. However, steel is today a much appreciated building material all over the world and is used in a vast array of different types of buildings; from huge sport arenas to offshore platforms. World steel demand has increased steadily since 1999, but this increase has been accelerating since 2002 and represents around 50 million tonnes more per year. This strong surge in steel consumption is the result of the dramatic acceleration of domestic steel demand in China (Figure 7).

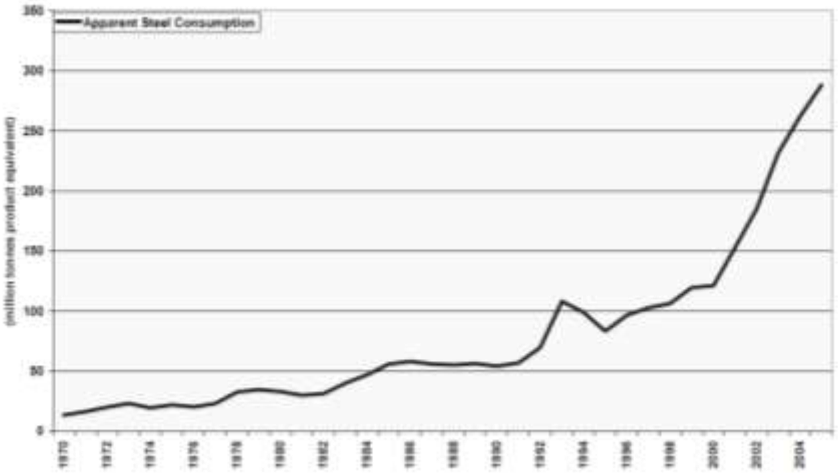

Figure 7 : China apparent steel consumption [1]

The selection of structural steel as a building's framing system brings numerous benefits to a project. All other materials are measured against the standard of structural steel and structural steel is still the material of first choice [2]. These benefits include economic approach with speed of construction, lower project costs or readily availability but also more technical ones. Structural steel is a non-combustible material (M-0 rating). It exhibits a large standard strength in both compression and tension. Moreover structural steel, long considered the premier green construction material, is continuing to improve its environmentally friendly position by reducing greenhouse carbons emissions (-37.7% between 1990 and 2003) [2]. At the same time, the industry remains the world leader in the use of recycled material, with recycled content now accounting for 95% of the structural steel produced.

However, structural steel has some disadvantages. Most steel are susceptible to corrosion when freely exposed to air and water, and therefore must be covered periodically with anti-corroding paints. The use of weathering steels, however, in suitable applications tends to eliminate this cost. Furthermore, steel is sensitive to heat and fire since it is an excellent heat conductor. Although structural parts are incombustible, their strength is detrimentally reduced at elevated temperatures reaching in fires. The major focus has been on the tensile and strength properties of the steels at high temperature [3]. Steel begins to lose most of its structural properties from 550°C that is defined as critical temperature. The critical temperature of steel is defined as the temperature at which the materials loses up to 50% of its strength and can no longer support the design load, that being the maximum load permitted by the structural provisions of the building codes [4]. Yield strength is the stress at which material strain changes from elastic deformation to plastic deformation, causing it to deform permanently. In Figure 8, the ratio between yield strength at temperature θ and the yield strength at ambient is plotted versus temperature θ, we remark that ratio decreases from 400°C and reaches 0.5 at 550°C.

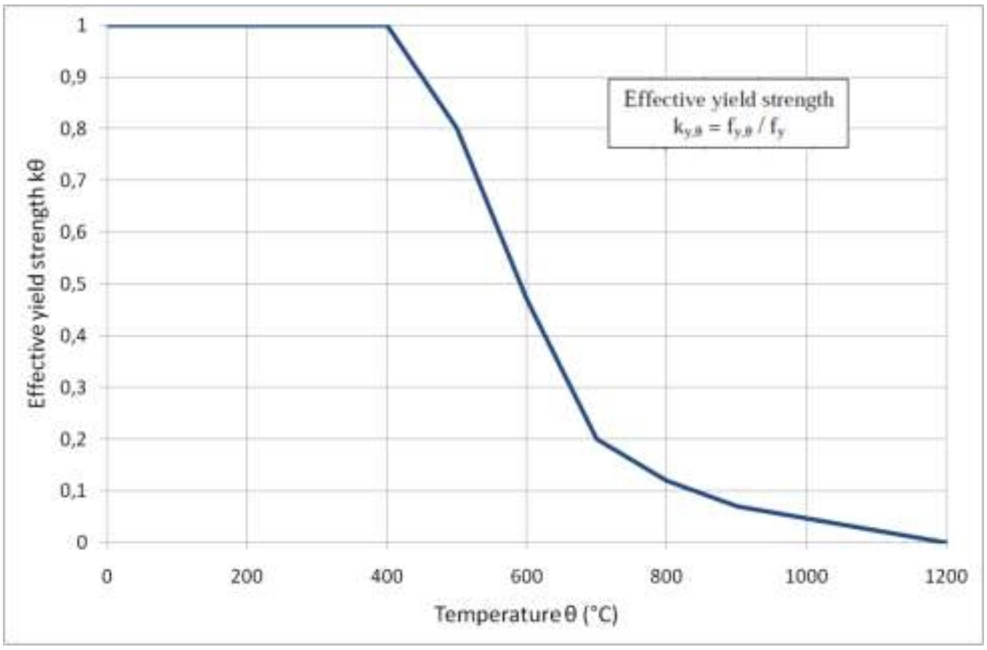

Figure 8 : Reduction factors for steel strength and stiffness at elevated temperatures [5]

This point must be taken into consideration by architects and solutions must be developed in accordance with the structural steel and the locations of the structure. Indeed, regulations and requirements are not the same for a residential, a commercial building or an offshore platform where risks are maximum.

Our study is based on materials used for offshore platforms.

The first part of this chapter describes the different risk on offshore platform sites. Offshore quantitative risk assessments have historically been complex and costly, but here we try to introduce the main fire risks that could occur in offshore and we focus on jet-fire that appears as the most severe fire scenario. Its properties and its parameters are investigated to understand the different modes of heat transfer occurring during the test and to propose potential safety solutions.

Then the second part deals with the several ways existing for the protection of steel and the particular requirements for offshore platforms. These systems are called "passive fireproofing materials", which means insulating systems designed to decrease the heat transfer from a fire to the structure being protected. Currently, the intumescent coating based on epoxy resin appears as the best mean to protect steel framework which requires high protection against fuel fires and to resist the strong conditions as fuel fires or jet-fires occurring in offshore platforms, we will detail thus their action and their characteristics in this part.

I. Offshore fire risk assessment

Offshore oil and gas platforms are well known for their compact geometry, high degree of congestion, limited ventilation and difficult escape routes. A study carried by the UK Health and Safety Executive showed that process and structural failure incidents account for almost 80% of the risk to personnel offshore. Potential risks offshore include: blowouts, riser and process leaks, fires, explosions, vessel collisions, helicopter accidents, dropped objects, structural failures, and capsizing. An examination of incidents such as Piper Alpha in the North Sea and the P-36 production semi-submersible off Brazil reveals that most offshore incidents are in fact process-related and a small mishap under such conditions can quickly escalate into a catastrophe. However, among all the accidental process-related events occurring offshore, fire is the most frequently reported [6-8].

I. 1. Specific fire scenario on offshore platforms

This section considers the physical fires types that, in the light of the identified fire event, need to be appraised in terms of harm. Fire events on offshore result always from a hydrocarbon escape. This loss of hydrocarbon containment can arise from mechanical failure, damage or procedural failures. The leakage rates and their duration greatly influence the nature and extent of a fire. Consequently, offshore hydrocarbon fires can have varied characteristics and encompass a very extensive range of size, fires might also be preceded by an explosion causing damage to structures, process plant or fire protection systems and thereby affect the extent of fire development. The fire events and their ranges had arrived by considering what could be released, where and under what conditions and the possible event following the release. To do this, the following information is desirable:

- The range of flammable hydrocarbons on offshore facilities
- How they arrive, are stored and leave
- Where they are processed/stored/used
- Typical transfer/process/storage conditions, pressure and temperatures
- Typical releases for each category of material, release rates and the inventory at risk
- Possible events following release

Based on these considerations above, three main classes of fire events can be defined and characterized.

A pool fire is a turbulent diffusion fire burning above a pool of vaporizing hydrocarbon fuel where the fuel vapor has negligible initial momentum. The probability of occurrence of pool fires on offshore platforms is high due to continuous handling of heavy hydrocarbons onboard. Liquid fuel released accidentally during overfilling of storage tanks, rupture of pipes and tanks etc., forms a pool on the surface, vaporizes, and upon ignition, results in a pool fire. Consequence models for pool fires in open spaces have been well-documented over the past few years [9-11]. A key feature of these fires is that there is a degree of feedback between the fire and the fuel in that, to a greater or lesser extent, heat transfer back from the fire to the pool influences or even controls the rate of evaporation and hence the fire size and other characteristics. The prime variable other than fuel type that influences the fire characteristics is the pool size. Wind effects are also significant in deciding certain parameters such as flame drag, flame tilt and flame length [6].The condition of the substrate may also be influential via heat transfer into the pool liquid. The hazard consequence of pool fires are pool spread, flame extent and geometry and external thermal radiation from combustion products. These parameters determine the potential harm of this kind of fires.

A jet-fire is a turbulent diffusion flame resulting from the combustion of a fuel continuously released with some significant momentum in a particular direction. Jet-fires represent a significant element of risk associated with major incidents on offshore installations, with the fuels ranging from light flammable gases to two-phase crude oil releases. Consequently to their particularities and to its severity, jet-fire will be fully developed in a specific section.

A fireball (Figure 9) is a rapid turbulent combustion of fuel, usually in the form of a rising and expanding radiant ball of flame. When a fire such as a pool or jet fire impinges on a vessel containing pressure-liquefied gas, the pressure in the vessel rises and the vessel wall weakens. This can eventually lead to catastrophic failure of the vessel with the release of the entire inventory. This phenomenon is known as a boiling liquid expanding vapor explosion (BLEVE). In such releases, the liquefied gas released to the atmosphere flashes due to the sudden pressure drop. If the released material is flammable, it will ignite; in addition to missile and blast hazards, there is thus a thermal radiation hazard from the fireball produced.

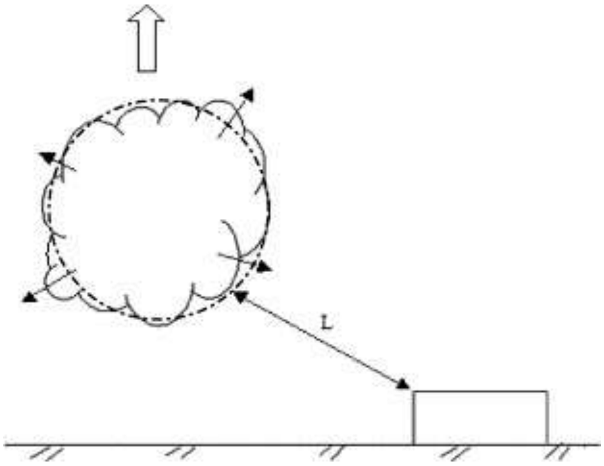

Figure 9 : Flame geometry for an expanding, rising fireball [6]

It is this thermal radiation, which dominates in the near field. Although the duration of the heat pulse from a fireball is typically of the order of 10–20 seconds, the damage potential is high due to the fireball's massive surface emissive power. Large-scale experiments carried out by Roberts et al. [12] with propane as the fuel, measured a maximum average surface emissive power ranging from 270 to 333kW/m^2 . The engulfment of structures in a fireball is generally immediately catastrophic to life. The hazard consequences of fireballs that determine their potential for harm are size, rise duration and radiation of the phenomena.

To conclude about fire types that can happen on offshore site, obviously these classes overlap and offshore fire events might be a combination of these fire types. Consequently risks and harms are again increased. In addition with the close proximity of personnel and the difficulties of escape, hazard and unfortunately dramatic issues with human losses cannot be eliminated to these industrial facilities.

I. 2. An overview of the nature of hydrocarbon jet-fire

Jet-fire has its own specific properties:
"A Jet-fire is **a turbulent diffusion flame** resulting from the combustion of **a fuel continuously released** with some significant momentum **in a particular range of directions**."[13]

This is one of the most used definitions of jet-fire and it is focused on the continuity of the gas flow, the important momentum and the direction of the impingement without mentioning intensity, severity torching, high velocities or localised impact, in spite of the strong association done with jet-fire in some publications [14].

Jet-fires represent a significant element of risk associated with major incidents on offshore installations, with the fuels ranging from light flammable gases to two-phase crude oil releases. This can lead to structural, storage vessel, and pipe-work failures, and can cause further escalation of the event (i.e. domino effect). A recent study by Gómez-Mares et al. [15] reports that approximately 50% of the recorded cases of jet-fires are followed by additional severe events. This is an extremely important factor because it means that the scale of an accident may increase considerably when a jet-fire occurs. For example, the riser failure which occurred during the Piper Alpha Incident in 1988 [16], contributed to the collapse of the platform and a major loss of life.

Prior to the Piper Alpha incident, there was little public domain information concerning the quantification of fire hazards possible on offshore platforms and the incident led to the project of a technical report coordinated by the Steel Construction Institute and by UK Health and Safety Executive [13]. This report contains an appraisal of the knowledge and ability to predict the hazards consequence of a jet-fire. It permits also to determine the physical characteristics and the key feature of such phenomenon.

I. 2. a) Jet-fire length

There is a considerable body of literature on the geometry of jet flames [17-24]. The geometry of a jet-fire is important in predicting radiation from the flame and the possibility of flame impingement on nearby facilities. The most important geometric parameter is the flame length. The flame length is the distance from the release point to the defined end of the flame. Whatever the scale is, the definition is not modified and its determination is easily available. An internet site [25] allows even to calculate it based on several parameters and using a sophisticated formula commented below.

But its precision is linked with the circumstances taken into account the release conditions and jet-fire size can be primarily related to the heat released. For gaseous releases, this is related to the size of the leak (hole diameter) and the pressure (which may vary as a function of time). For non-gaseous fuels, the liquid content results in relatively higher release rates for a given aperture and pressure compared to gaseous releases and, when the release is two-phase (such as may arise from a relatively long pipe connected to a storage vessel containing a liquid above its boiling point), estimates the release rate is non-trivial.

$$L = A * Q^{b} \qquad \textbf{\textit{(Eq.1)}}$$

Where L is the flame length, in m and Q is the net heat released by combustion, in MW. A and b are constant

A first correlation (Eq. 1) can be used to present reasonable predictions in spite of its simplicity. Several studies [18, 19, 26] have optimized it and adapted it, by changing A and b values, to represent sonic and subsonic release for a range of gaseous fuels and a large range of stack diameters between 500 and 800mm. For example Figure 10 shows jet-fire lengths for a range of fuels plotted against the net heat released by combustion. It exhibits good fit with empirical values of A and b.

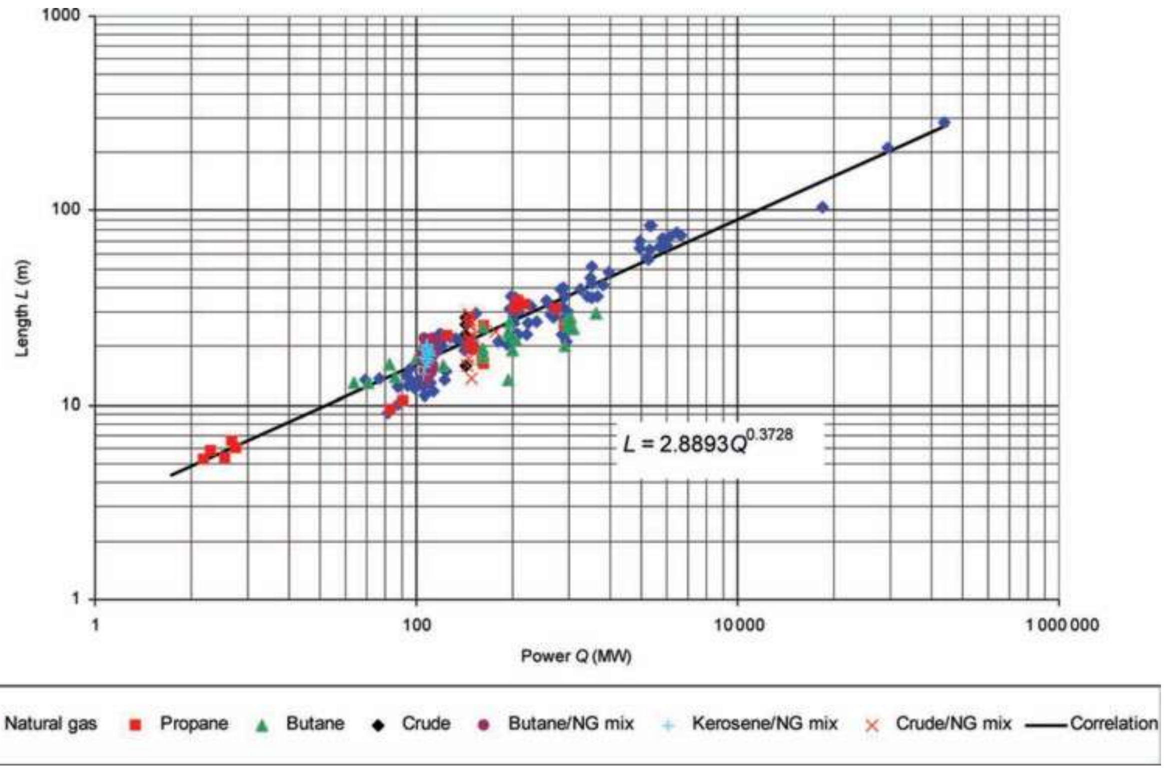

Figure 10 : Jet-fire lengths versus heat released for different hydrocarbons [27]

Other correlations more sophisticated and asking more information not easily available have been also developed. The well known model of Hawthorne et al. [22] (Eq.1) is for instance used to predict the distance, L, from the orifice to the visible flame tip on the internet website mentioned above. Hawthorne et al. [22] take the turbulent mixing and buoyancy processes at the end of the flame into account but in the other hand neglect the jet exit conditions contrary to previous formula. So the ratio of moles of reactants to products and the stoichiometry of the gas mixing seem to play a role on the length of the flame and the latter is thus measured as a distance where mixing has reduced the fuel concentration to stoichiometric:

$$L = B + \frac{5.3D}{C_T}\left[\frac{T_F}{T_N}\cdot\frac{1}{a_T}\left(C_T + (1 - C_T)\frac{M_S}{M_N}\right)\right]^{1/2} \qquad \textbf{(Eq.2)}$$

Where B is the flame lift-off distance, m
D is the source hole diameter,
C_T is the molar concentration of fuel in the stoichiometric mixture
T_F and T_N are respectively the temperature of the flame and this of the vapour leaving the hole, in K
a_T is the ratio of moles of reactants to products
M_S/M_N is the ratio of the molecular weight of the surroundings atmosphere to that of the gas issuing from the nozzle.

A new notion of flame distance is also introduced here; it is the lift-off distance. Indeed jet flames are generally lifted i.e. the base of the flame is not attached to the release point

(Figure 11). This occurs because of the high velocities, strain rates and the richness of the fuel near the source make it difficult to maintain a flame. The actual lift off position is defined either as the point at which a blue gaseous flame appears or the point further downstream at which yellow sooty flame first appears.

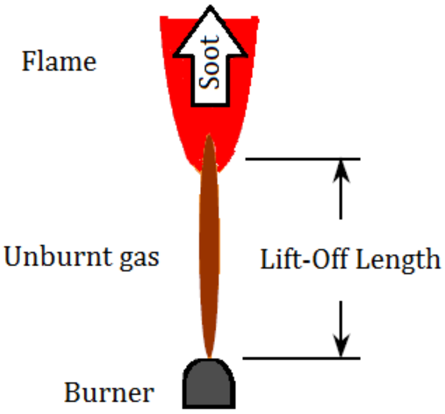

Figure 11: Flame and lift-off diagrams

These correlations give us information about the length of a perfect flame issued of the ignition of a gas release. However, some limitations must be underlined. Indeed ignition of discharges of fluids in open surroundings does not necessarily produce stable jet flames. The discharge conditions can be such that flames cannot burn back to form a steady flame. Whether or not a stable jet-fire will arise following the releases of a pressurized hydrocarbon will depend principally upon the nature of the fuel, the size of the hole from which the release occurs and the geometry of the surroundings. In practice [27] this means that most small leaks will be inherently unstable and will not support a flame without some form of flame stabilization, such as the presence of another fire in the vicinity or any impact onto a pipe-work, vessels or the surrounding structure. However, in the highly congested environment offshore, impact within a short distance is very likely, and hence small leaks are most likely to stabilize on the nearest point of impact. Apart from providing flame stabilization, impact onto an obstacle may modify the shape of the jet-fire. Objects which are smaller than the flame half-width at the point of impact are unlikely to modify the shape or length of the flame to any great extent. However, impact onto a large vessel may significantly shorten the jet-fire, and impact onto a wall or roof could transform the jet into a radial wall jet where the location and direction of the fire is determined by the surface onto which it impacts and its distance from the release point.

Other limitations of the flame length determination are the influence of wind for external jet-fire. Indeed, in a crosswind, the flame lengths shorten highly due to an additional mixing and buoyancy. These effects are not as well identified and characterized as in still air, but empirically flames from subsonic gaseous releases are quite wind and buoyancy affected beyond the early momentum dominated region of the flame. Air entrainment in low velocity jet-fire is not particularly efficient; they are therefore comparatively long, sooty and radiant. Some studies include these effects by adding a factor inside the expressions [28] (Eq.3):

$$L = L_0\left(0.51\times e^{-0.4V} + 0.49\right) \qquad \textbf{(Eq.3)}$$

Where L is the wind-affected flame length measured in m in a straight line from the release point to the flame tip

L_0 is the still air flame length, in m

V is the wind speed in m.s^{-1}

Therefore introducing as the most important parameter of the jet-fire, the flame length appears as a characteristics widely influenced obviously by the size of fuel leakages and also by the surroundings. If the first effect is directly link with the accident degree (a wider source hole cause a high release of fuel and thus a large powerful flame), the other parameters highlight once again the high risks occurring on offshore platforms, due to the highly congested environment offshore that reinforce the flame and the random wind effect.

I. 2. b) Radiative and convective heat contribution

The thermal load to an engulfed object in a jet-fire will be a combination of radiative load and convective load.

The radiative behaviour of jet flames is very varied and complex [13]. Radiation from a jet flame arises from hot soot particles and gases. In most of the offshore jet flames, radiation from soot dominates. However, in many sonic natural gas flames the soot radiation will be quite small compared to the molecular emission from CO_2 and H_2O vapour. The directionality of jet-fires provides the possibility of direct flame impingement onto surroundings structures or targets. So this is a supplementary source of serious hazard to offshore facilities. In literature, we find several studies about nature and extent of impingements and the resulting heat fluxes. But as for radiation, a problem appears with the soot radiation, the molecular radiation and their ratio. Clearly, the total heat flux which is imparted to an engulfed object will vary over the surface of the object. In addition, the relative proportions of convective and radiative heat flux will vary over the surface, with the highest convective component likely to be experienced close to the point of impact of a flame where the highest velocities occur, whereas the highest radiative heat load will be experienced where the more radiative part of the flame (usually towards the end of the flame) is viewed by the object.

Figure 12 shows total heat fluxes experienced by a horizontal cylinder (pipe) impacted by a horizontal high pressure gas jet-fire [29]. The cylindrical surface is presented flat by cutting along the rear. Several configurations can be observed:

- (a) When the pipe was located at 21m (towards the end of the flame) the maximum heat fluxes were experienced at the point of impact on the front of the pipe.

- (b) At 15m the heat loads were relatively uniform around the pipe.
- (c) But at 9m, the heat loads were greatest to the rear of the pipe due to radiation from the tail of the flame.

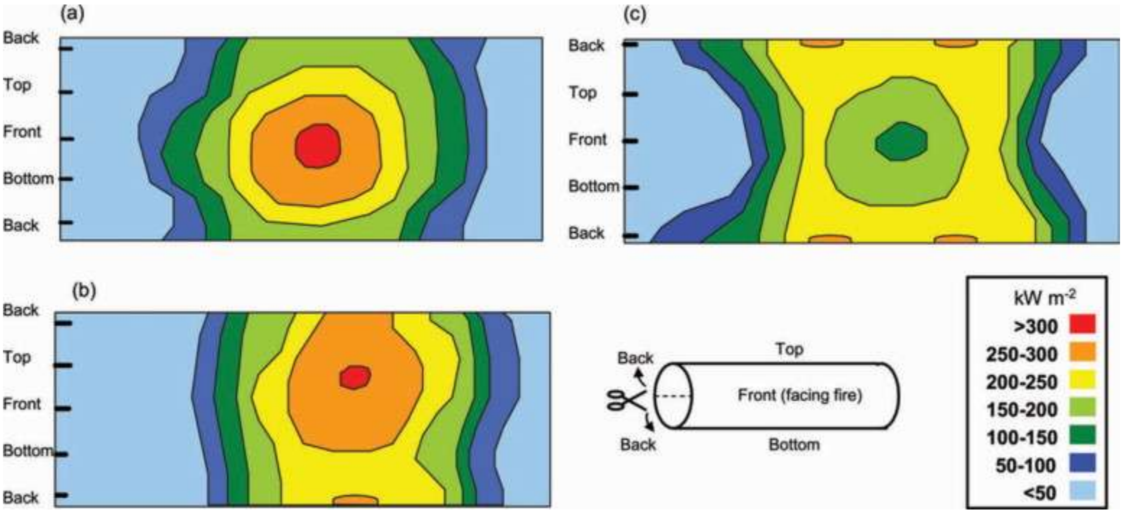

Figure 12 : Variation of total heat flux over the surface of a pipe according to distance from the flame source: (a) pipe at 21m; (b) pipe at 15m; (c) pipe at 9m [27]

As the more radiative part of the flame is closer to the tail, this can result in the highest overall heat fluxes being experienced on the rear surface of an engulfed object which may seem counter-intuitive. Other tests with subsonic methane jet flames [30] and subsonic [30] and sonic [31] gaseous propane flames at different flow rates and exit velocities have presented similar results and allow to conclude to the non-local impingement of the jet-fire, that increase again the harm of this phenomena. Indeed, temperature measurements [32] along a pipeline positioned close to the source show that the rear of the tubular target received the greater incident flux as evidenced by the greater temperatures, shown in the Figure 13.

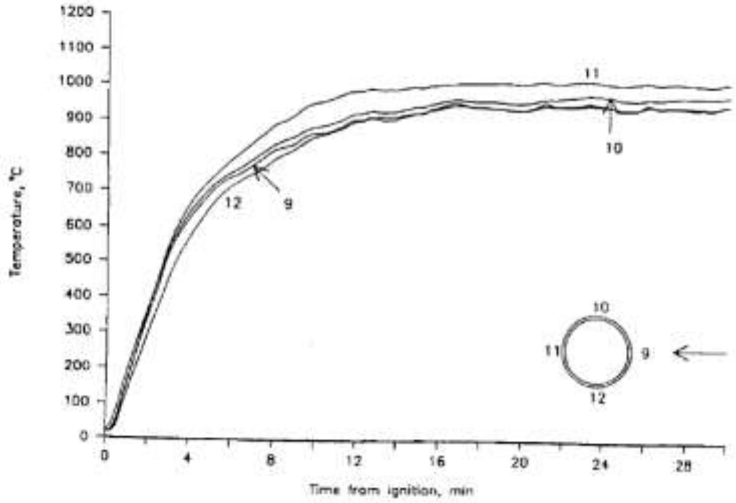

Figure 13 : Temperatures versus time at different locations of a pipe engulfed by jet-fire [13]

As noted above, the combustion process within a natural gas jet-fire is relatively efficient and produces little soot (carbon). Consequently, these flames are not as luminous as higher hydrocarbon flames. The net result is that the radiative heat transfer to the surroundings is lower than for comparable higher hydrocarbon jet-fires. This is reflected in the fraction of heat radiated, F, for such fires as can be seen in Figure 14 (F is defined as ratio between energy released as radiation from the flame surface and net energy of combustion). As can be seen, F increases with carbon number (from natural gas to crude oil), reflecting the increased radiative emissions from soot within the higher hydrocarbon jet-fires.

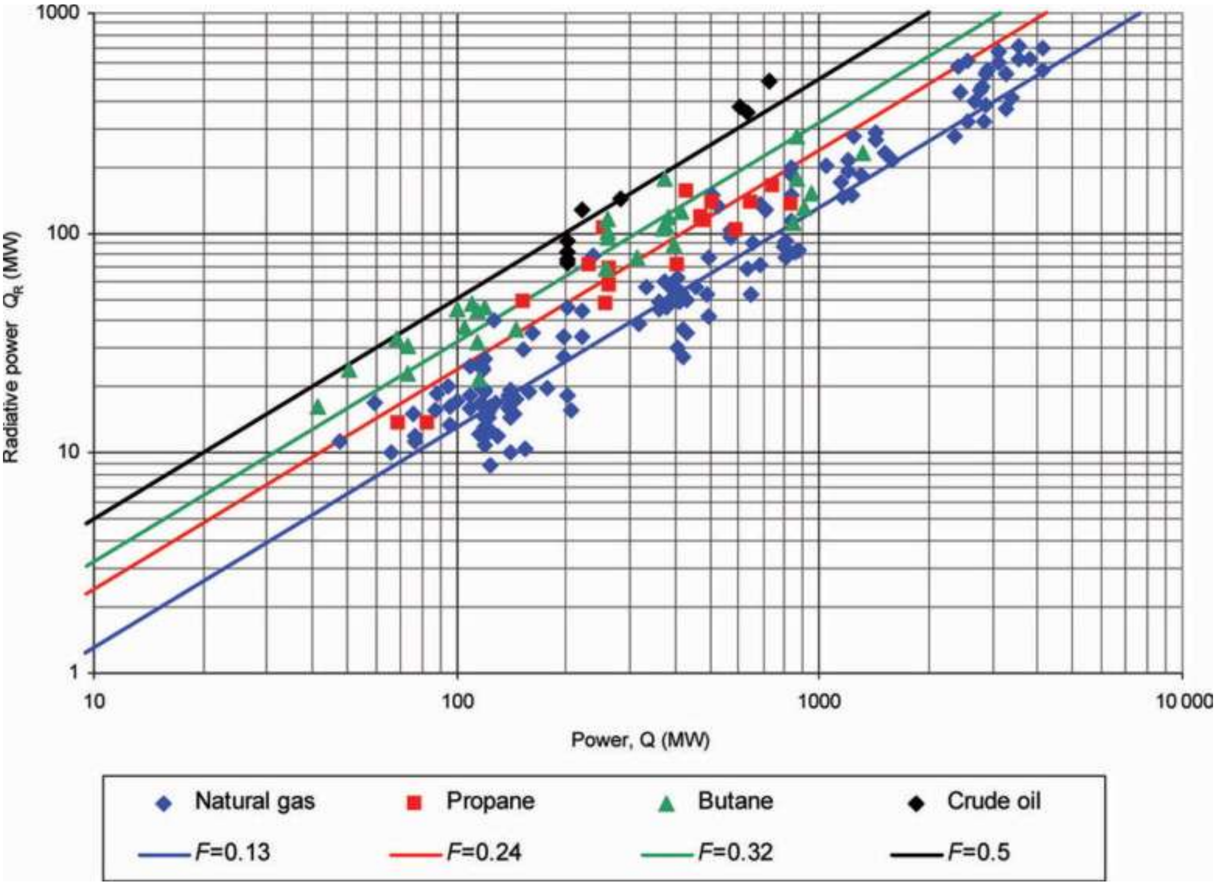

Figure 14 : Fraction of radiative power versus total power observed for jet-fire with different hydrocarbons [27]

Due to the radiant soot emissions, the radiative heat transfer from higher hydrocarbon jet-fires is generally greater than that from natural gas flames and the generally lower velocities arising from flashing liquid releases (such as propane or butane) result in a lower convective flux to engulfed objects. For the rear surface of an engulfed object, Figure 15 shows that the fraction of the heat flux which is radiative increases from about 0.5 for natural gas to about 0.8 for fuels containing a large proportion of higher hydrocarbons [33-36].

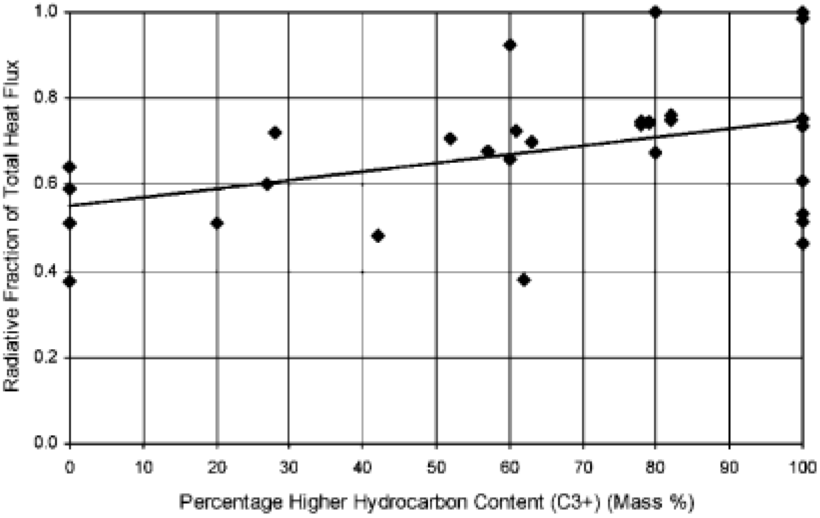

Figure 15 : Radiative heat flux as a fraction of total heat flux versus hydrocarbon content for an engulfed object for a jet-fire [27]

Different authors report also several correlations between F factor and the jet exit velocity [19, 28, 37]. In the case of a pressurized gas–liquid mixture (such as ‘live’ crude oil), the high gas velocities may still occur and result in a high convective contribution, whilst the higher hydrocarbon content maintains a high radiative contribution; making these type of jet-fires a ‘worst case’ in terms of total heat flux to engulfed obstacles [27].

Finally, the next section describes the high fire risk assessment on offshore platforms. Increased by the locations, fire risk on offshore is mainly caused by an accident and lead always to materials collapse and always to human losses. The dramatic Piper Alpha accident has a strong influence on this assessment and great efforts have been made to draw up this hazard identification. Hydrocarbon leaks and subsequent fire and/or explosions are the main threats to offshore explorations and production of hydrocarbon oil and gas, with fire kinds as pool fires, fireballs, or cloud fires. But the jet-fire represents the worst fire risk in offshore installations. In a jet-fire assessment, the two important parameters are the flame dimensions, the thermal radiation heat flux and velocities field around the flame. The convective heat transfer rate can be very high increasing by velocities and impingement and leading to rapid failure of objects engulfed by the flame envelope. Thermal radiation outside the flame envelope can also lead to equipment failure caused by rapid increase of heat flux.

Therefore, due to these severe conditions occurring on offshore platforms, solutions must be provided not to avoid unavoidable accident but to reduce consequences of fire event and safe structure and obviously people.

II. Key requirements for offshore protection

Several ways exist for the fire protection of steel. There are two categories of prevention and control of fires; passive protection and active control and protection. Active 'protection' consists of several systems that may require human intervention to initiate. These include water deluge, foam systems, sprinklers, monitors, inert systems, fire extinguishers. Passive fire protection (PFP) is defined as “a coating, cladding or free-standing system which, in the event of a fire, will provide thermal protection to restrict the rate at which heat is transmitted to the object or area being protected” [38].

In most cases passive fire protection materials exhibit successful results when they are used in conjunction with “active” systems. Passive fire protection is the primary measure integrated within the constructional fabric of a structural steel to raise the fire resistance of the structure and to maintain the fundamental requirements of structural stability. However their use on offshore platforms requires additional severe properties that must be kept in mind.

Therefore, after a global description of the different passive systems in a first part of this section, we will detail in a second one the key parameters required by intumescent coatings based on epoxy resin to comply with the jet-fire resistance since this kind of PFP is widely used on offshore platforms. Then in a third part we will introduce the different methods existing to evaluate their performance and their efficiency for maintaining steel integrity and for reducing damage on offshore installations.

II. 1. Passive fire protection

The main property of passive fire protection systems used for steel is the ability to maintain the steel structure at temperature below 550°C, which is considered as the critical temperature for structural steel, above which, it is in jeopardy of losing its strength, leading to collapse.

Different methods can be used to improve fire protection of steel and the main classes of passive fireproofing materials used are cementitious products, fibrous materials, composites and intumescent materials. Early in the previous century [39], encasements in concrete, brick, clay tiles, lath and plaster, and similar materials were commonly used for this purpose. Now, less expensive forms of protection have been developed, such as cementitious coatings and sprayed of mineral fibres, which can be applied directly on the steel members

[40]. Furthermore intumescent paints are available in Europe for over 25 years, although these materials have been known for centuries [41].

Cementitious products include concrete, gunite, lightweight vermiculite based mixes, gypsum, calcium silicate and magnesium oxychloride. All cementitious fireproofing materials protect the steel in two ways. Firstly, they contain trapped moisture which is released upon heating and keep the steel temperature around 100°C until all the water is evolved. Secondly, the product acts as a thermal insulator [42]. Moreover, these materials are essentially inorganic and therefore do not burn. No additional smoke or toxic fumes are produced in a fire which makes them suitable for internal use in living quarters and work areas [43].

Advantages of these materials are that they have an attractive appearance, are usually hard and durable, relatively cheap, and easy to install or repair. The cementitious materials can be sprayed (Gunite, vermiculite-cement, magnesium oxychloride, etc.) or supplied as panels (Gypsum, plaster, calcium silicate, etc.), which are fixed to the structure with either steel wire or nailed to a timber cradle [44].

However, although they offer reasonable protection, the traditional cementitious based materials have been found in a number of instances not to give satisfactory performance in the highly corrosive offshore environment and, consequently, because of this and also because of its weight, have been largely replaced by epoxy intumescent systems suitable for hydrocarbon jet-fires [45].

Fibrous materials include boards and blankets of mineral wool and ceramic fibres. They are particularly used as passive fireproofing systems when thermal insulation is an additional requirement. Inorganic binders that do not burn out during the initial stages of the fire are recommended [46]. Mineral wool is commercialized to resist to 850°C and ceramic fibre to 1150°C [47]. As ceramic fibre is more expensive than mineral wool they are often used in combination. Mineral wool fibres can be sprayed with an adhesive to provide protection to structural steelwork. Mineral Wool insulation and fire protection products can be used in all types of buildings. It is also used in critical applications in offshore oilrigs and petrochemical refineries as it protects against hydrocarbon fires [48]. The main disadvantage is that fibrous materials absorb water easily, they are therefore recommended for internal use only except where they can be effectively clad with metal sheeting. Some of these materials have also recently been shown to be having human health and safety implications, so their use is increasingly restricted.

Composite fire protection panels are produced with various types of materials from different fire resistant classes. Panels may consist of a metallic cladding, often stainless steel, a cementitious board (typically plaster or gypsum) and mineral or ceramic fibres in between. These panels may resist cellulosic or hydrocarbon fires as required. They are generally fixed to structural members with steel binding wire or bolted to a supported frame or cradle.

These three first technologies are currently used to protect structural steel from fire and heat. However, in this dissertation the building that should be protected is offshore platforms, sensitive to very aggressive conditions, namely corrosion, chemical attacks and potential powerful fires. Therefore, although traditional cementitious fireproofing materials are known for their low cost and ease of installation, they do not resist to corrosion and aggressive weathering conditions. They do neither resist to jet-fires, which is an essential requirement in the petrochemical industry and cannot be used for protecting offshore platforms [45]. Then similar disadvantages can be drawn about the fibrous materials, in addition with the sensitivity to water and their use on offshore platforms is not extended.

On the other hand, **intumescent materials** are widely used in passive fire protection systems, where potential pathways for the spread of flames and fumes, such as conduits, wall openings and ventilation grilles can be protected with fire retardant products. An intumescent material is one that undergoes a chemical change when exposed to heat or flames, becoming viscous then forming expanding bubbles that harden into a dense, heat insulating and multi-cellular char. Consequently, as shown by an increasing market supplied by several companies, intumescent systems are the current better technology for the protection of offshore platforms. Intumescent coatings are generally epoxy based and are delivered to the site in drums to be sprayed or hand applied [42]. Intumescent epoxy materials have been recognised as the best means of saving lives and limiting damage when hydrocarbon fires hit offshore platforms [49]. Therefore the rest of this state of art deals with the study of different commercial thick intumescent coatings in terms of thermal, chemical or physical properties.

II. 2. Epoxy based intumescent coatings

The increasing acceptance of the benefits of epoxy intumescent fireproofing materials has resulted in much increased uses, particularly offshore, of this type of product in recent years [50].

Epoxies are thermosetting materials and consist in a two-component mixture composed of a prepolymer and a hardener. Thermosets are, due to the irreversible curing reaction, rigid three dimensional cross-linked plastics [51]. Due to their two components implementation and the properties of the cross-linked structure [52], epoxy-based thermosets are choice elements for varying the characteristics of the end products following a quasi-infinite variety of recipes [53]. Globally, after curing, epoxies have satisfactory intrinsic mechanical properties such as suitable weather, chemical and thermal resistance [54]. In addition, different methods have been studied to modify their network structure and to improve these properties. One of the most important parameters controlling the network structure is the crosslink density and could be determined by differential scanning calorimetry and modified by changing the prepolymer chain length [52]. Furthermore, thanks to an appropriate selection of formulation chemistry (i.e. not only epoxy prepolymer and hardener but also catalysts, additives, impact modifiers, etc.), a wide range of properties and behaviours, required for numerous applications, can be provided to epoxy resins [55]. So, the many applications of epoxy resins have focused attention on these materials since the beginning of their commercial use by the end of the 1930's [56]. Epoxies are applied for moulding compounds, surface coating and painting materials, composites, microelectronic encapsulated materials, printed circuit boards, adhesives, etc [53, 54]. Epoxy resins are used in many industrial applications in which stiff, high glass transition temperature, low creep and high heat resistant materials are required [57]. All these technical advantages justify their higher cost in comparison with other thermosetting materials [58].

The versatility of these resins is due to the instability of the epoxy group. Thanks to its great nucleophilicity, this ring can be opened by reacting with different compounds like polysulfides, polyamides, aromatic and aliphatic amines and anhydrides [56, 59]. Groβ et al. [60] have shown that the nucleophilicity of the functional groups is the determining parameter in curing of epoxy resins in order to provide different mechanical, chemical and physical properties. The presence of polar groups on the polymer backbone allows good adhesion to metal substrates and the cured epoxy resin shows high resistance to abrasion, moisture, thermal shock and vibration damage. High tensile and compressive strengths can be obtained and weather resistance is excellent, even if they show a poor resistance to UV exposure.

There are two main categories of epoxy resins, namely the glycidyl epoxy, and non-glycidyl epoxy resins. The glycidyl epoxies are further classified as glycidyl-ether, glycidyl-ester and glycidyl-amine. They are prepared by polycondensation between a dihydroxy compound, a dibasic acid or a diamine and epichlorhydrin. Glycidyl-ether epoxies such as diglycidyl ether of Bisphenol A (DGEBA) are the most commonly used epoxies [51]. The non-glycidyl epoxies are either aliphatic or cycloaliphatic epoxy resins, and are formed by peroxidation.

The most studied coatings use a diglycidylether of Bisphenol A (DGEBA). It is synthesized by reaction between bisphenol A and epichlorohydrin (Figure 16). DGEBA provides several properties to the epoxy coating according to the polymerization degree [51], namely adhesive properties, corrosion of hydrolysis sites [61].

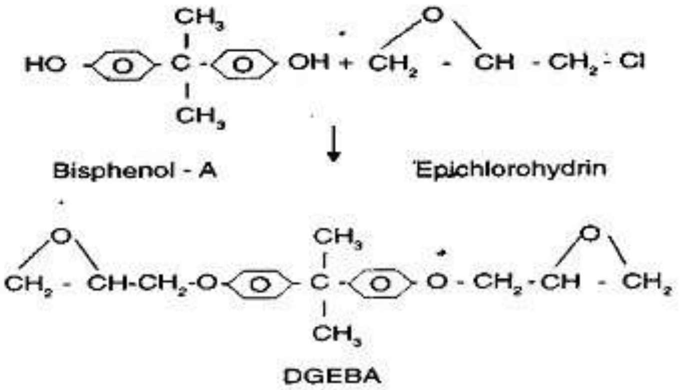

Figure 16 : Reaction and formula of DGEBA [62]

In order to convert epoxy resins from DGEBA to a hard and rigid network, a hardener or curing agent is necessary. Amines are the most commonly used curing agents for epoxy cure [63]. Primary and secondary amines are highly reactive with epoxies. Tertiary amines are generally used as catalysts, commonly known as accelerators for the cure reaction. Otherwise polyaminoamide can also been used as hardener.

The curing process is a chemical reaction in which the epoxy groups react with a secondary amine to form a hydroxyl group and to reduce the amine to a primary one (Figure 17).

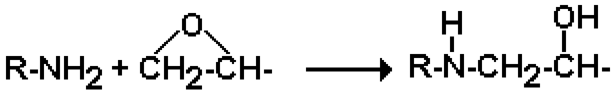

Figure 17 : Reduction of the primary amine and opening of the epoxy ring

Then in a second step the reaction continues with the reaction of the amine with another epoxy group. So a three dimensional network is formed, containing ternary amine and framework issued of DGEBA (Figure 18, Figure 19).

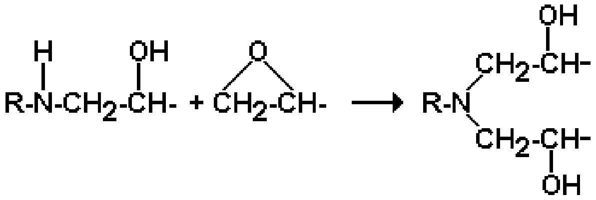

Figure 18 : Formation of a 3D-network

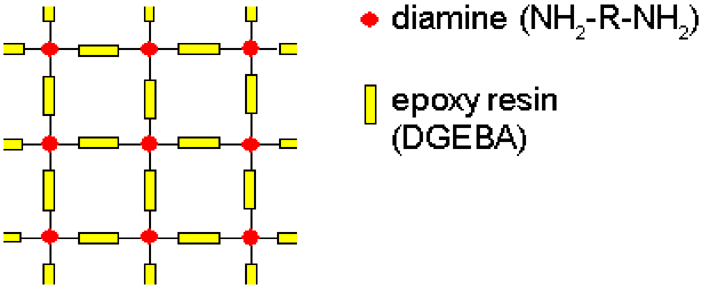

Figure 19 : Schematic representation of the reticulated network between epoxy resin and hardener

However, this hard material does not exhibit fire retardant properties and need additives and/or chemical modifications in order to develop an acceptable reaction to fire [54]. Indeed epoxy resins are used in many industrial applications, but flammability of this resin type is a major limitation in areas requiring high flame retardance. The approach chosen to improve the flame retardance of composites has been to add flame retardants and smoke suppressants to the resin [64-66]. However, the addition of some flame retardants could significantly decrease the mechanical properties of polymers [67-69] and must consequently be used with care in order to maintain with respectable ratio intrinsic properties of epoxy resin.

Intumescent coating acts as a thermal barrier for construction materials during fire hazards. The coating has the ability to expand by a factor of 40 or more during heat exposure that effectively leads to the protection of the substrate against rapid increase of temperature, thereby maintaining the structural integrity of the building. Most of the published information on intumescent coatings is in the patent literature while little is reported on the chemical-physical mechanism of intumescence [70-74]. The first intumescent coating has been patented in 1938 [75].

The primary focus of research on intumescent coatings is to identify the combination of ingredients that results in a coating that develops a controlled volume of cohesive and insulative char when the system is exposed to a fire (Figure 20) and a system that also provides all the protection and other properties required of a high quality coating.

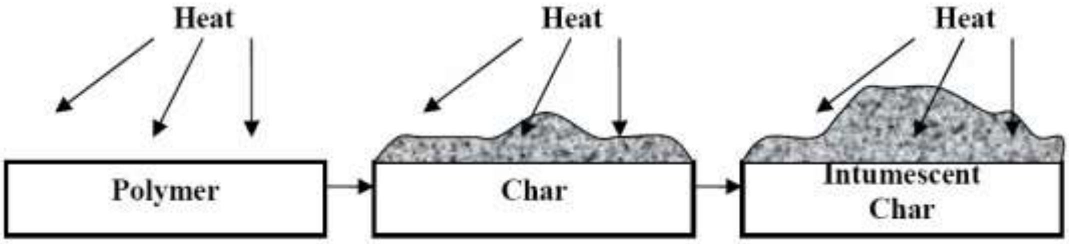

Figure 20 :Formation of intumescent char

In 1970, Vandersall [76] published a detailed paper describing the usual and efficient elements of intumescent coatings. He stated “A quality intumescent paint cannot be visually differentiated from a conventional paint. It provides the protective, serviceable and aesthetic properties of the non fire-retardant system. However, when heated above its critical temperature, the film begins to melt, to bubble and to swell, forming a thick, non-flammable, multi-cellular insulative barrier which affords protection for the substrate.” So the goal of intumescent additives is to provide fire protection without altering other properties.

Vandersall [76] classified the chemical compounds of intumescent systems in three categories:

- A carbonisation agent, this means a carbon-rich polyhydric compound: starch and polyhydric alcohols are mostly used. The number of carbons will influence the amount of char formed whereas the number of hydroxyls will determine the rate of char formation. In the studied intumescent epoxy coating, the polymer itself acts as the carbonific agent.
- An acid source: an inorganic acid, either free or formed in situ from a precursor during heating.
- A foaming agent: usually halogenated or nitrogenated compounds, which also evolve copious quantities of non-flammable gases.

Similarly, Jones et al. [77] defined as carbonific the compounds in intumescent formulations that act as a carbon source for char formation and spumific those which evolve gaseous products and induce foaming.

Numerous papers have tried to describe the possible mechanism leading to intumescence [74, 76, 78, 79]. It is generally accepted that first, the acid source breaks down to yield a mineral acid. This takes part in the dehydration of the carbonisation agent to yield the carbon char and finally, the blowing agent decomposes to yield gaseous products. The latter causes the char to swell and hence provides an insulating multi-cellular protective layer. This shield limits the heat transfer from the substrate to the heat source, resulting in a conservation of the underlying material. The presence of a compound in each of the above three classes does not by itself ensure intumescent behaviour of the mixture. In fact, a series of chemical and physical processes must occur in an appropriate sequence, while the temperature increases, to produce the intumescence phenomenon.

Examples of the components from the different categories are shown in Table 2.

Table 2 : Examples of components playing a role in intumescent coatings [79, 80]

Inorganic acid source	Carbonisation compounds
- Acids (phosphoric, boric, sulphuric) - Ammonium salts (Phosphate, polyphosphates, sulphates, halides, etc.) - Amine/amide phosphates (Urea, Guanylurea, Melamine phosphate, etc.) - Organophosphorus compounds (Tricresyl phosphate, alkyl phosphate, haloalkyl phosphate).	Starch Dextrin Sorbitol Pentaerythritol Polymers Phenol-formaldehyde resins Methylol melamine
Foaming compounds	**Amines/amides**
Chlorinated paraffins Tetrachlorophtalic resins Melamine	Urea Urea-formaldehyde resins Dicyandiamide Melamine Polyamides

Classical and efficient intumescent formulations use ammonium polyphosphate as acid source and foaming agent and pentaerythritol as carbon source [81-83]. Used on epoxy resin based coating at different ratios, this fire retardant mixture alters degradation characteristics of the materials by increasing the residual mass and the char yield [84, 85]. The incorporation of the APP/PER system in the resin provides also the convenient mechanical and thermal properties to the protective shield: high flexibility and heat diffusion abilities [86]. Its mechanism of degradation is widely studied and now well known. At 200°C, APP reacts with PER to yield ortho- and pyro- phosphate species, via a hydrolysis reaction (Figure 21). At this step, the first P-O-C bonds have been formed; the key of the efficiency of the coating will be to keep these bonds, providing beneficial properties to the insulative structure.

Figure 21 : Hydrolysis of ammonium polyphosphate

Then the phosphor ester formed can undergo a ring closing esterification, in which water and ammonia is released [87]. A succession of these and similar reactions results in a char consisting of mainly carbon (Figure 22), but also small amounts of oxygen, phosphorus, and nitrogen atoms [70]. Besides, the binder takes part in the control of the char expansion and ensures a uniform foamed structure [88].

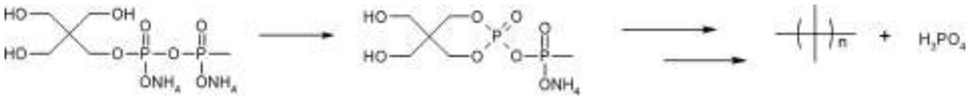

Figure 22 : Ring closing esterification of the phosphor ester and subsequent reduction to a carbon network

The formation of the effective char occurs via a semi-liquid phase, which coincides with gas formation and expansion of the surface [89]. Gases released from the degradation of the intumescent material, and in particular of the blowing agent, have to be trapped and to diffuse slowly in the highly viscous melt degraded material in order to create a layer with appropriate morphological properties as shown in Figure 23.

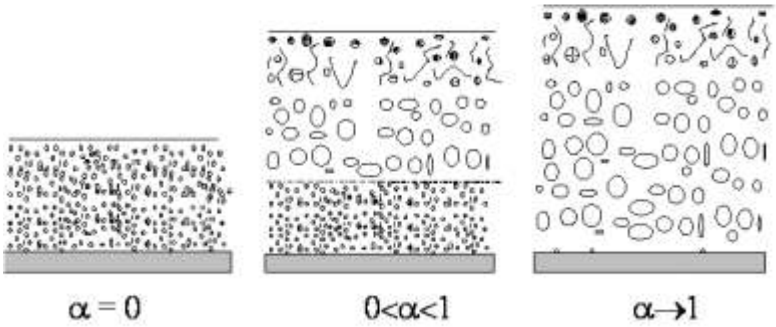

Figure 23 : Development of intumescence (α= conversion degree)

The viscosity of the degraded matrix in the blowing phase is, as a consequence, a critical factor [90, 91] and the different components of the intumescent formulation can modify this visco-elastic behaviour. If the degraded matrix has a too low viscosity, easy diffusion of gases takes place and the gases will not be trapped but rather escape to feed the flame. If the viscosity is too high, there can be formation of some cracks which allow the oxygen to diffuse into the char and which could increase the heat transfer from surface to substrate. Hence the efficiency of the protective layer may decrease. Moreover, several previous studies have shown good correlation between the different steps of the intumescent process and the dynamic properties (expansion and apparent complex viscosity) of the formed char using thermal scanning rheometer measurements on different intumescent materials [90, 92-94]. Applied on intumescent coatings based on epoxy resin, Jimenez [95, 96] showed that viscosity and swelling are linked as the expansion takes place because of the decrease in the viscosity of the degrading material combined with the release of volatile degradation products. In this study, Jimenez showed also the modification and the synergistic effect provided by the different intumescent additives on the visco-elastic properties and the swelling abilities of the materials. The degradation of the thermoset resin at about 350°C creates an important decrease of viscosity detrimental to development of an efficient intumescent shield. Boric acid and APP seems to be the key additives to reduce this fall of viscosity and to allow a high expansion and a char with a good mechanical resistance.

Furthermore, another important parameter that also has to be taken into account is the mechanical strength of the intumescent char. This factor is significant because in the conditions of fire, char destruction can proceed not only by means of ablation and heterogeneous surface burning but also by means of an external influence such as wind, mechanical action of the fire or convective air flows. This aspect appears as a key parameter especially after describing the jet-fire phenomenon in the previous section and knowing the location where our intumescent formulations are applied. A consideration of the mechanical stability of intumescent char appeared first in the technical literature in discussions about the nature of bonds which provide char stability [70].

A simple criterion [97, 98] was subsequently proposed for the mechanical stability of the intumescent char: mechanical properties of foams depend both on the structure, porosity and mechanical properties of the foam material; it is assumed that chemical structure is one of the main factors affecting mechanical stability. Moreover, physical structure data (such as thickness of the walls inside the char cap, micro-density of the char, density of the char material) should also been taken into consideration. Finally, mechanical stability probably depends on the direction of external perturbation and its type (direct, rotation, vibration). The question for intumescent chars is why and how this perturbation is distributed through the char cap, from the surface layer and up to "frozen" pyrolysis zone. This distribution depends on the char porosity and, to a less extent, on the chemical structure.

Reshetnikov et al. used a "Structurometer ST-1", developed at the Moscow State Food Academy, to measure the force required to destroy the char [98]. The samples were first pyrolysed and then a destructive force was applied to the sample. It was concluded that one of the main factors influencing the mechanical stability is the char porosity: the smaller the pore size the better the char strength. A similar method was developed in our laboratory at Lille University [93] in recent years, using the Thermal Scanning Rheometer. The main interest of our approach is that the measurement of the destruction force is made directly after swelling of the sample, at high temperature, working as an "in situ" experiment. This is particularly important in the case of jet fires, as the char has to resist very aggressive conditions, such as explosions, violent wind.

As a summary based on a careful review of the literature, we may establish parameters required by the intumescent structure to provide an efficient protection:

- The flame retardancy of modified polymeric materials does not only depend on the thermal stability of the constituent elements, but also on their rate of degradation, rate of char formation and the amount of residual char [99].
- The performance is determined by the kinetics of the charring process and the exact timing of the expansion of the char. If it takes place too early after dehydration, the char is ineffective and non-insulative. If the expansion occurs too late, the char hardens before swelling [93].

- The efficiency of intumescent systems depends on the thermo-physical properties of foamed char [100].
- The efficiency of the char is closely related to its ability to expand and form a multi-cellular structure and consequently to its physical properties during the intumescent process. One of the main aspects of intumescent char physical structure is its uniformity and its porosity [88].
- A high mechanical stability promoting by a highly cross-linked structure is also required for the foamed char to resist to fire conditions [97]. This last property is even considered as the most important because of the aggressive conditions occurring for a jet-fire event.

To conclude, this section has described the main fire retardants used in epoxy resin focusing on the intumescent systems which are the most appropriate to provide fire protection in offshore platform applications. The selection of intumescent flame retardant for a material is then governed by the chemical and physical properties of the whole material and its degradation characteristics. We have introduced APP and PER as convenient intumescent additives for epoxy resin and drawn up the main properties required to such system. These materials introduced above are materials designed to protect offshore platforms and their properties are thus developed in agreement with focus on the mechanical resistance and the thermal insulation. Indeed, fire events possible on offshore platforms can be described as powerful fire and jet-fire resistance requires high stability and resistance facing to impingement. Consequently, the physical properties introduced for intumescent coatings must be considered above all as fundamental for fire protection of offshore platforms and will be developed in a following chapter.

II. 3. Fire tests specified for offshore fire protection

II. 3. a) Fire tests based on furnace conditions

There are no internationally accepted rules for fire safety of offshore constructions. Instead there are many national and corporation standards. Required levels of protection are normally specified in terms of time and temperature on the basis of one or more criteria, which may include statutory requirements, design considerations and insurance cost implications. The duration is established by a time rating which is determined by testing in accordance with an approved standard specifying a time / temperature curve (Figure 24).

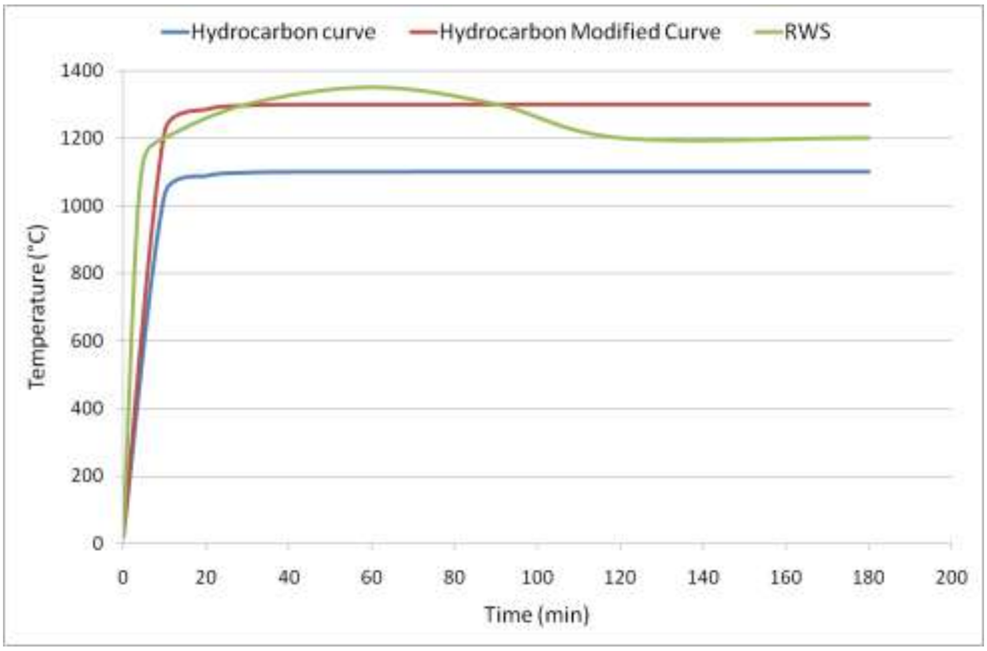

Figure 24 : Standard fire test curves used for materials applied on offshore platforms

The **hydrocarbon test curve** (UL 1709) [101] is meant to duplicate or to be indicative of the rapid temperature rise seen when a hydrocarbon fuel such as oil or natural gas burns: the temperature rises rapidly to 900°C within 4 minutes and significantly higher overall temperatures are reached (between 1100°C and 1200°C). This hydrocarbon fire test curve, developed by the Mobil Oil Company in the early 1970's and adopted by a number of organisations and in particular Underwriters laboratories, UK Dept. Of Energy, BSI, ISO and the Norwegian Petroleum Directorate is now a common test method for high risk environments such as petrochemical complexes and offshore platforms.

Derived from the above-mentioned hydrocarbon curve, the French regulators asked for a modified version, the so called **hydrocarbon modified curve (HCM)**. The maximum temperature of the HCM curve is 1300°C instead of the 1100°C for standard hydrocarbon curve. However, the temperature gradient in the first few minutes of the HCM fire is as severe as all hydrocarbon based fires. This test has been developed to consider jet-fire scenarios in which leaking high pressure hydrocarbon gases ignite to produce intense, erosive jet flames that can reach speeds of 150 metres per second.

The **RWS** (Rijkst Water Staat) **curve** [102] was developed by the Ministry of Transport in the Netherlands. This curve is based on the assumption that in a worst case scenario, a fuel, oil or petrol tanker fire with a fire load of 300MW could occur, lasting up to 120 minutes. The RWS curve was based on the results of testing carried out by TNO Centre for Fire Research in the Netherlands in 1979. The difference between the RWS and the hydrocarbon curve is that the latter is based on the temperatures that are expected from a fire occurring within a relatively open space, where some dissipation of the heat occurs, whereas the RWS curve is based on temperature you find when a fire occurs in an enclosed area, such as a tunnel, where there is little or no chance of heat dissipating into the surrounding atmosphere. The RWS curve simulates the initial rapid growth of a fire using a petroleum tanker as the source, and the gradual drop in temperatures to be expected as the fuel load is burnt off.

The standards listed above are the most commonly used standards. However, it is generally recognized that the conditions in the standard and hydrocarbon furnace tests do not represent the characteristics such as heat flux and erosion found in full scale high velocities jet-fires. After the explosion and fire on Piper Alpha, Lord Cullen [16] highlighted it is clearly desirable that any fire test used must be realistic. Any information provided by the test must be useful to the chemists/industrial about the probable behaviour of the fire barrier in real hydrocarbon fire conditions. With increasing reliance being placed on passive fire protection materials offshore and the realisation that in many areas jet-fires pose the most onerous threat, the need for a jet-fire test is now widely accepted.

II. 3. b) Jet-fire resistance test

An initial project, denominated OTI 95634 [103] has been developed jointly by the UK Health and Safety Executive and the Norwegian Petroleum Directorate for using predominantly on offshore installations. This jet-fire test (Figure 25) was designed to determine how various objects and passive fire protection materials perform when exposed to this fire scenario. The test impinges a high-speed stream of ignited propane fuel onto a substrate. The propane is delivered at a rate of 0.3kg/s and can consume 1 tonne of fuel per test. Since 2007, this project is become an international standard [104] that determines the resistance to jet-fires of passive fire protection materials.

The method provides an indication of how passive fire protection materials perform in a jet-fire that may occur for example, in petrochemical installations. It aims to simulate the thermal and mechanical loads imparted to passive fire protection material by large scale jet-fires resulting from high-pressure releases of flammable gas, pressure liquefied gas or flashing liquid fuels. Jet-fires give rise to high convective and radiative heat fluxes as well as high erosive forces.

Figure 25 : Jet-fire resistance test in progress on an intumescent coating

To generate both types of heat flux in sufficient quantity, a 0.3 kg/second sonic release of gas is aimed into a hollow chamber, producing a fire ball with an extended tail. The flame thickness is thereby increased and hence so is the heat radiated to the test specimen. Propane is used as the fuel since it has a greater propensity to form soot than natural gas and can therefore produce a flame of higher luminosity. High erosive forces are generated by release of the sonic velocity gas jet 1 meter from specimen (bulkhead) surface. The propane vapour issues from a tapered, converging nozzle of length 200mm, inlet diameter 52mm and outlet diameter 17.8mm (Figure 26).

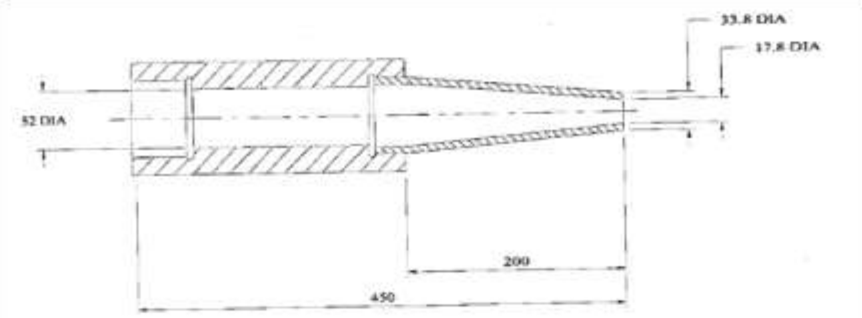

Figure 26 : Jet nozzle used for jet-fire resistance test [103]

The nozzle is aimed horizontally and normal to the rear wall of the test specimen. The tip of the nozzle is located 1.00m from the front surface of the test specimen and with its centre on quarter of the height of the test specimen above the inner surface of the test specimen's base (Figure 27). The average heat flux is approximately 240kW/m² and the maximum heat flux 300 kW/m². The heat fluxes are highest in the upper part of the chamber and lowest in the corners and at the jet impact zone, as already mentioned in the previous section.

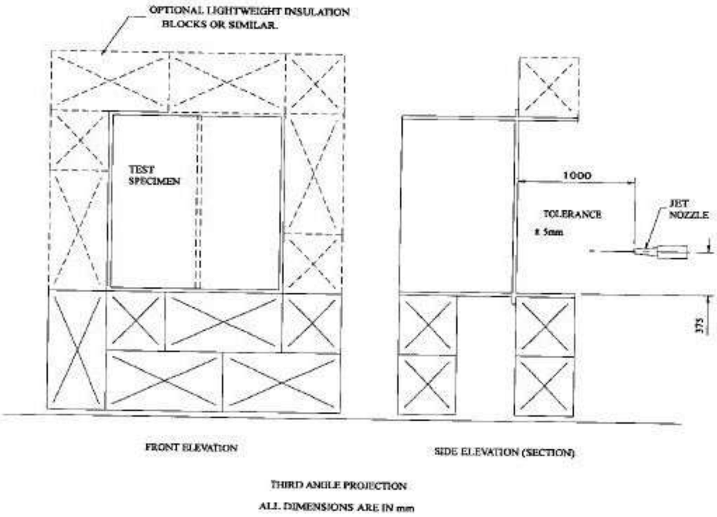

Figure 27 : Layout of test facility with steelwork test specimen used for evaluating protective fire materials [103]

Four different versions (panel, planar steelwork, structural steelwork and tubular section tests) of the test procedure can be used according to the materials under consideration. The structural steelwork test specimen is constituted of an open fronted bow, with the addition of a central flange (also named web, and note it is this name which appears on the different figures), with passive fire protection as described on Figure 28. The structural steelwork test should be used to represent the application of passive fire protection material to steelwork with corners or edge features, for example "I" beams.

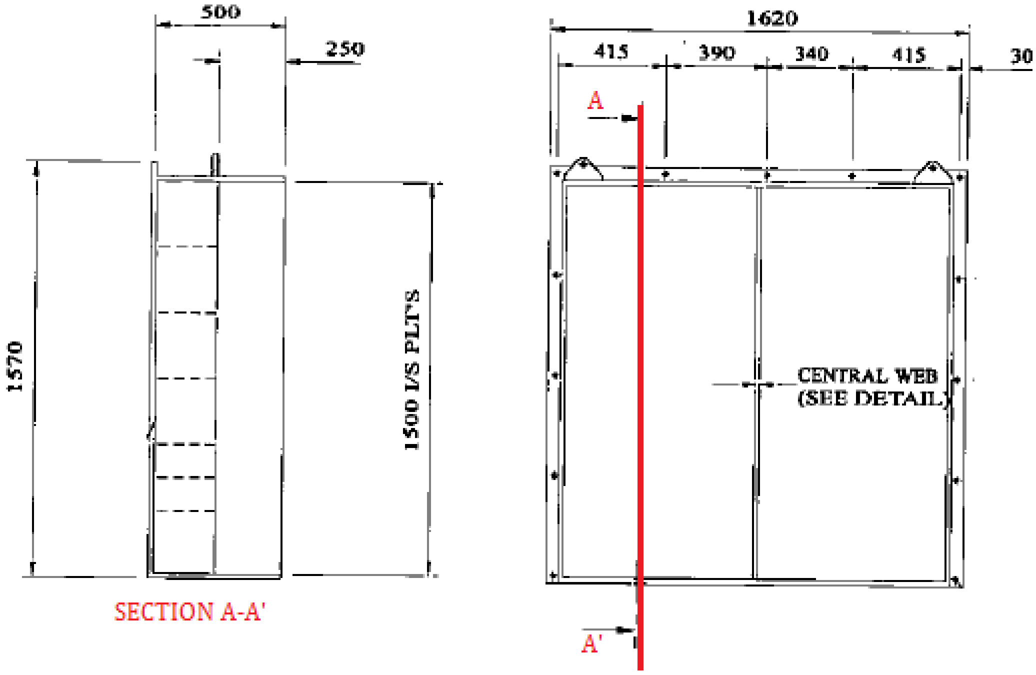

Figure 28 : Construction of structural steelwork test specimen with a central flange [103]

The test duration can be defined in either a specified period of exposure to the jet-fire or the period required to reach a specified maximum temperature. The test specimen is fixed to the rear box and the assembly is mounted on lightweight concrete blocks approximately 1.0 m from the ground. The test specimens are instrumented with type K thermocouples (Figure 29). They are fastened to the back of the rear wall by drilling and peeing or other equivalent methods while sheathed ones are inserted into the central flange.

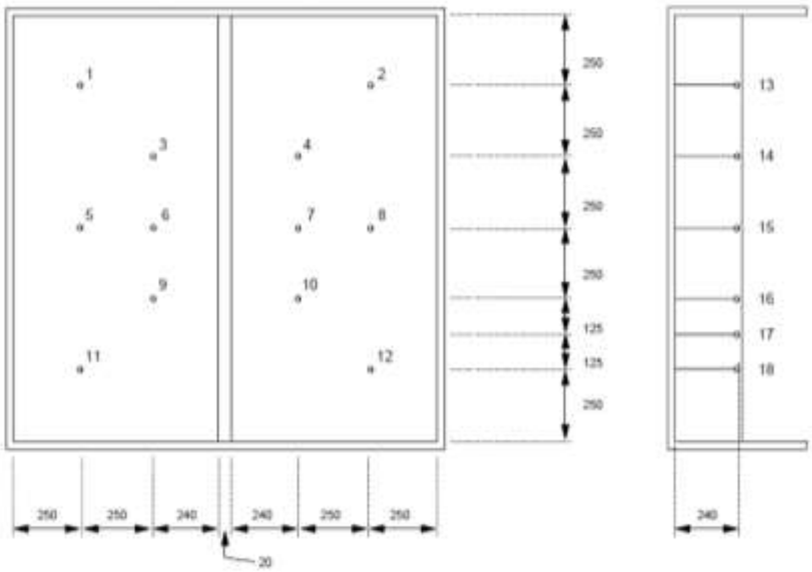

Figure 29 : Thermocouple positions for structural steelwork test specimen [103]

Little information is currently available about this standard because of the date of publication. However some new passive fire protection materials has proven to be capable of resisting to jet-fire for 90 (rating J-90) or 120 minutes (rating J-120) according to this standard. For instance Chartek 7 is an epoxy intumescent fire protection system featuring excellent jet-fire resistance for up to two hours [105], Benarx is also a patented jet and hydrocarbon fire-rated epoxy fire protection material that is tested and certified up to two hours [106].

III. Conclusions

This current state of the art is based on the hazards onboard offshore platforms. Indeed, the slightest incident on such locations can quickly become the worst accident. The nature of their operation (extraction of volatile substances sometimes under extreme pressure in a hostile environment) means risk, accidents, and tragedies occasionally occur following by pool fires or fireball. But the worst scenario that can occur on offshore platforms is most probably the jet-fire. A jet-fire is a turbulent diffusion flame resulting from the combustion of a fuel continuously released with high momentum in a particular direction. The convective heat transfer rate can be very high increasing by velocities and impingement and leading to rapid failure of objects engulfed by the flame envelope. Thermal radiation outside the flame envelope can also lead to equipment failure caused by rapid increase of heat flux. Such events are cause of worst accident.

Therefore, new technology has been developed to be specially adapted to fire protection of offshore platforms. If the oldest insulative methods such as cementitious products or fibrous materials do not prove great efficiency in the aggressive offshore conditions, intumescent epoxy coatings have proven to be efficient protection against hydrocarbon fires of offshore oilrigs and petrochemical refineries. Thanks to fire retardant additives, we have so detailed the intumescent process and the key parameters required to promote an efficient protection. Ammonium polyphosphate combined with pentaerythritol appears as the most used and the most efficient intumescent mixture that exhibits the satisfying properties with a sufficient swelling rate, an ability to dissipate heat and a great mechanical stability facing to severe conditions.

The efficiency of epoxy coating is then evaluated by different fire test. Firstly hydrocarbon fire test are carried out in a furnace environment under time/temperature conditions specified by relevant curves then evaluated by the jet-fire resistance test. Recently standardized, this test focuses on the thermal and mechanical loads and provides an indication of how passive fire protection materials perform in a jet-fire. It leads to 'J' ratings for given length of time. However, a rapid survey of the open literature have shown that the most of the papers reports comprehensive studies about the jet fire test itself but no work report as far as we know, detailed studies about jet fire test on steel protected with intumescent coating. Nevertheless, both these tests are essential since they give a good simulation of a real fire, all our work in this study will so be based on the behaviours of the intumescent coatings facing to jet-fire.

That's why in the next chapter, we will comment the results obtained by four different intumescent coatings evaluated at the jet-fire resistance test based on the parameter discussed above.

Chapter II: Evaluation of the efficiency of the intumescent coatings facing to jet-fire

The previous chapter has reviewed the different methods to protect steel framework and notably offshore platforms. We have also focused on the standardized tests able to measure the efficiency of an intumescent coating undergoing fire corresponding to different scenarios, from hydrocarbon fires to most hazardous jet-fires. The purpose of this work is intumescent coating protecting offshore platforms and the associated fire scenario is the jet-fire. Usually thick intumescent coatings are firstly evaluated in large furnace test in agreement with standard UL 1709 [101]. If they pass it, they are then evaluated by the jet-fire resistance test of passive fire protection materials OTI 95634 [103] or ISO 22899 [104].

Furthermore, several properties of the char have been mentioned in the literature. The previous state of art shows desirable properties from the point of view of flame retardant performance: mechanical strength and integrity, adherence of the coating on the steel plates, porosity and of course abilities to limit heat and mass transfer in order to protect the substrate. The efficiency of an intumescent coating depends thus mainly on the quality of the char produced during burning and degradation.

This chapter examines the fire behaviour of four intumescent coatings according to the OTI 95634 report [103]. In a first part, the characteristics of the four intumescent coatings will be presented, highlighting the main active components responsible for the intumescent process and whose action has detailed in the first chapter. Then details and settings of the jet-fire resistance test will be commented according to the requirements and setup specified by the standard. Finally, the results exhibited by the intumescent formulations will be fully discussed.

I. Materials and experimental techniques

I. 1. Materials

This entire dissertation is based on the study of four different epoxy-based intumescent coatings. The whole formulations are divided into two parts:

- The part A containing the prepolymer and others components
- The part B containing the curing agent (an amide) and others components.

Both parts are stored separately, mixed just before the application of the coating on the substrate at different ratio (Table 3) and cured at ambient temperature over a 48h period.

Table 3 : Ratio between the two parts used to prepare the intumescent coatings

Intumescent coating	Ratio Part A/Part B
IF-1	2.44/1
IF-2	2.49/1
IF-3	2.31/1
IF-4	2.31/1

Among these four formulations, some ingredients are common. For the four grades of intumescent coatings, the prepolymer is the same: a DGEBA type liquid prepolymer DER 311 from Dow Chemicals while the curing agent is a polyaminoamide. In addition, fire retardant additives play an important role; different grades of ammonium polyphosphate have been used according to the formulations. The coated ammonium polyphosphate used in the IF-1 formulation is a blended mixture of ammonium polyphosphate (APP) (Figure 30), and tris-(2-hydroxyethyl)isocyanurate (THEIC) (Figure 31) commercialized as IFR 36 from Clariant [105]. APP is an acid source yielding to phosphoric acid upon heating, reacting with THEIC and epoxy and leading to the formation of an intumescent structure.

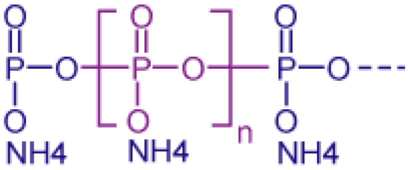

Figure 30 : Formula of APP, n>1000

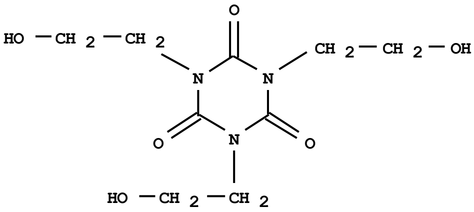

Figure 31 : Formula of THEIC

On the three other formulations an uncoated ammonium polyphosphate (Figure 30), Exolit AP422 from Clariant, is added as both acid source and blowing agent (because of the release of ammonia) [76]. In addition, the carbon source is played respectively by the epoxy resin on IF-2, by pentaerythritol (PER) added to epoxy resin on IF-3 and by dipentaerythritol (dPER) added on epoxy resin on IF-4 (Figure 32). Note that epoxy resin can also play a role of char former in IF-3 and IF-4 formulations.

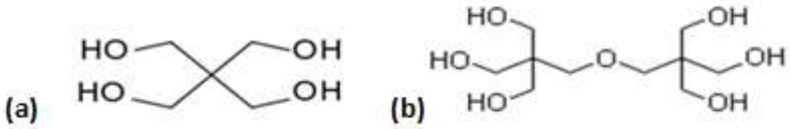

Figure 32 : Formula of pentaerythritol (a) and dipentaerythritol (b)

Furthermore, classical additives used on paint formulations have been added: pigments, surfactant, and mineral fillers but the exact formulations of the four coatings are not known. However TiO_2 is used on IF-2, IF-3 and IF-4 and could play a role for the chemical pathway. The main active ingredients of the intumescent formulations are reported in Table 4, highlighting the main differences between the coatings.

Table 4 : Comparison between the active ingredients of 4 formulations

Intumescent coating	Polymeric matrix	Acid source	Carbon source	Blowing agent
IF-1	DGEBA prepolymer + polyaminoamide	Coated APP + Boric acid	Epoxy resin + THEIC from coated APP	APP
IF-2	DGEBA prepolymer + polyaminoamide	APP	Epoxy resin	APP
IF-3	DGEBA prepolymer + polyaminoamide	APP	Epoxy resin + PER	APP
IF-4	DGEBA prepolymer + polyaminoamide	APP	Epoxy resin + dPER	APP

In addition, the use of mesh in intumescent coating provides an additional reinforcement of the barrier formed when burning. This is crucial when the coating is exposed to high pressure during the test as in the case of the jet-fire resistance test. The efficiency of this reinforcement has been demonstrated in the case of the most fragile coatings as IF-2 and IF-

3 whereas its effect is not significant for a robust coating as IF-1 (see discussion in the next sections). Mesh (Figure 33) comprises alternating strands of carbon and glass fibre, woven together with polyester thread running in one direction. Each component is used with an accurate objective:

- The polyester melts at 140°C leaving the strands of carbon and glass fibre free to move as the intumescent shield expands.
- The glass fibres melt at about 400°C, it is used to make it easier to handle.
- Finally, the carbon fibres exhibit a high thermal stability and should be preserved through a standard hydrocarbon fire test but, it cannot resist prolonged exposure to the pressures involved in a jet-fire test.

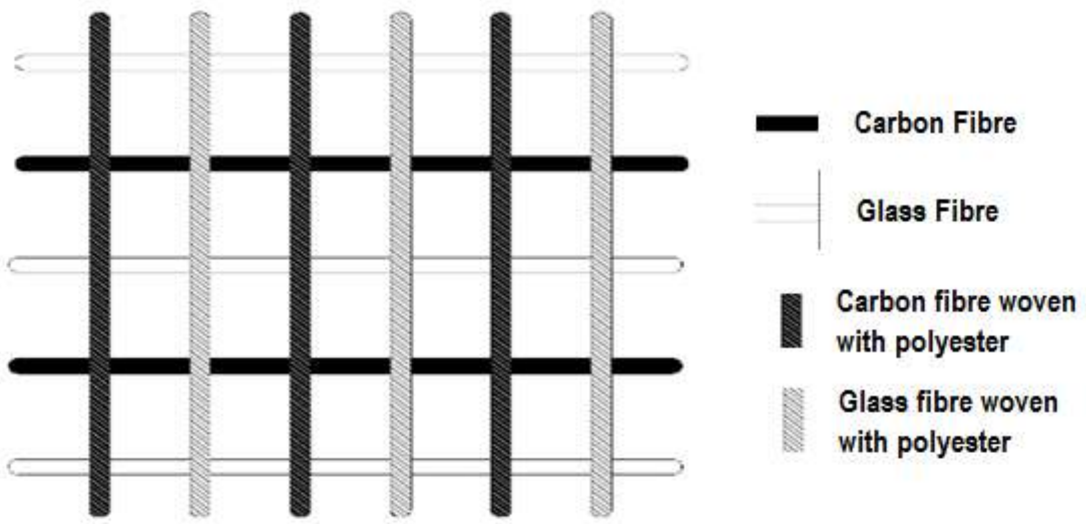

Figure 33 : Structure of mesh with carbon and glass fibre

I. 2. Jet-fire resistance test

The different formulations labelled IF-1, IF-2, IF-3 and IF-4 have been evaluated in the conditions of a jet-fire according to the recommendations established by the Health and Safety Executive [103] and already described in the first chapter. This test permits to determine properties of passive fire protection materials. It is designed to give an indication of how well passive fire protection materials will perform in a jet-fire. In spite of smaller dimensions than typical offshore or plant structures, the thermal and mechanical stresses imparted to the passive fire protection materials by large-scale jet-fires resulting from high-pressure releases of natural gas have been shown to be similar as those from the jet-fire defined in this procedure.

The structural steelwork test specimen is constituted of an open fronted box divided into two back faces with the addition of a central flange. To describe test panel, we will refer thus to back faces (right and left hand sides) and to central flange. For testing passive fire protection materials applied as coating, the structural steelwork specimens shall have passive fire protection material applied directly to all inside surfaces according to the standard specifications. However, in the case of IF-2 and IF-3, some tests have been carried out on panel where only the central flange is coated by intumescent formulations. This adaptation of the experimental setup has been motivated by the properties of the coatings and the low mechanical resistance exhibited by these two formulations. Thanks to these settings, we have focused our investigation in the zones where the pressure is maximal and where the coatings should not resist and cause the test failure.

In the jet-fire test, the fuel is commercial propane, delivered as vapour without a liquid fraction at a steady state rate of 0.30±0.05kg/s. The tip of the nozzle is located 1.00m from the front surface of the test specimen and with its centre on quarter of the height of the test specimen above the inner surface of the test specimen's base.

Temperature measurements are carried out on specified positions thanks to type K thermocouples. The thickness of the passive fire protection material shall be also measured at each thermocouples position. To locate event on the test specimen, we refer thus to thermocouple positions.

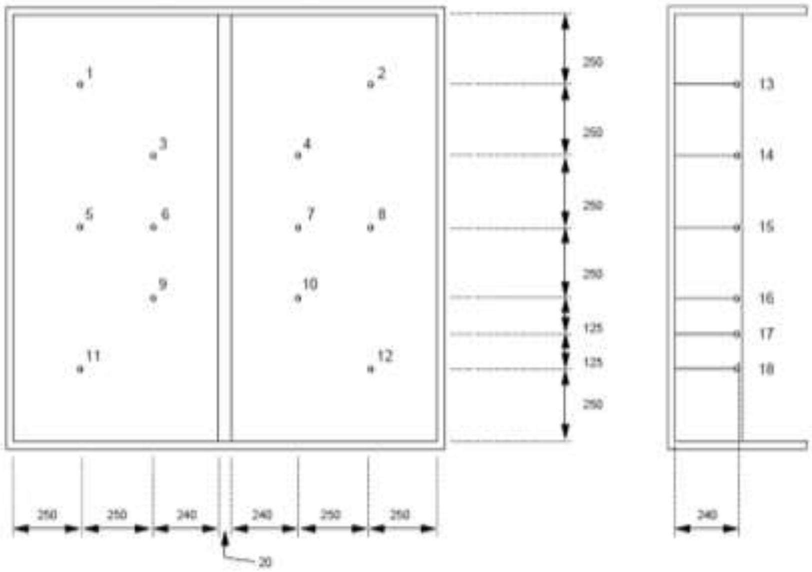

Figure 34 : Thermocouple positions for structural steelwork test specimen

Finally, the test duration is defined as the period required to reach the specified maximum temperature chosen for metallic substrate (i.e. 400°C). The test is over when two thermocouples have reached this temperature.

II. Large-scale jet-fire test evaluation

In accordance with all these recommendations and instructions described in the previous section, the different coatings have been tested according to the OTI jet-fire test. Results must provide a reliable representation of the behaviour of different coatings facing to jet-fire and give a certification for the coatings, useful for knowing its good application on offshore platforms and for marketing commercializing the formulation as a jet-fire rated intumescent paint.

Results exhibited by the four intumescent formulations described above appear as our starting point to explain and to understand the behaviour of the formulations. It is expect to get important information to detect their weaknesses in order to enhance their properties and consequently their fire performance. As mentioned in the state of the art, we will focus on determining governing parameters required for developing efficient coatings.

II. 1. Intumescent formulation 1

This part describes a jet-fire resistance test lasting 62 minutes on a structural steelwork test specimen protected with the passive fire protection materials IF-1 with an average thickness of 9.7mm.

During test, the flame engulfed the specimen making it difficult to see the coated surfaces very clearly through the flame. Nevertheless, some remarks can be stated during the test:

- After 5 minutes from the start of the test, pieces of coating were seen to detach from the surface of the specimen, particularly on the central flange in line with the release point.
- After 10 minutes from the start of the test, cracks appeared in the coating on different locations and pieces of coating became detached from the bottom surface of the box.
- After 30 minutes from the start of the test, pieces of the coating were displaced from the top left hand side of the back face.
- After 40 minutes from the start of the test, flames could be seen getting behind the top surface coating on the right hand side of the box.

After cooling the test specimen, a first description of the char can be made (Figure 35). In spite of high temperature, coating is not completely reacted all along the panel. Indeed, we can distinguish two kinds of zones:

- A first one where the coating is completely reacted and where a protective char is formed. This zone corresponds to hottest zone (one single thickness measurement is available and reported in Figure 37 ; 0mm is reported in Figure 36 about non-reacted coating thickness).
- A second zone where a deep layer remains non-expanded because of insulation and low temperature (two thickness measurements are thus available, on the surface corresponding to formed char and in deep corresponding to non-reacted coating).

In addition, there is a circular region of dark, sooty coating on the left hand side of the flange, extending on to the flange. This circular region is centred approximately 400mm above the bottom of the back box and has a radius of around 200mm. This zone is clearly viewable in Figure 35 and corresponds to the region where the propane jet impinges on the specimen.

Figure 35 : Pictures taken after jet-fire test of IF-1

To highlight the reaction of the coating and the char formation, we must detail the progress of the development of the coating. Figure 36 reports the thickness of partially reacted coating (here we mean the formation of an expanded char), where no char formation has occurred, knowing that the initial thickness was around 10mm. The coating on the front and sides of the top two thirds of the flange have completely reacted (0mm non-reacted coating remaining); on the remaining third the coating has partially reacted with no char formation (4mm). On the back face of the specimen, the coating has partially reacted, with between 20% and 80% of the original thickness remaining, apart from a small area on the bottom right hand side which has fully reacted. The reaction of the coating can be directly link with the surface temperature and we suggest that the flange is the hottest location while on the back face convective effect and flame circulation on the box may cold down the coating and prevent its complete reaction.

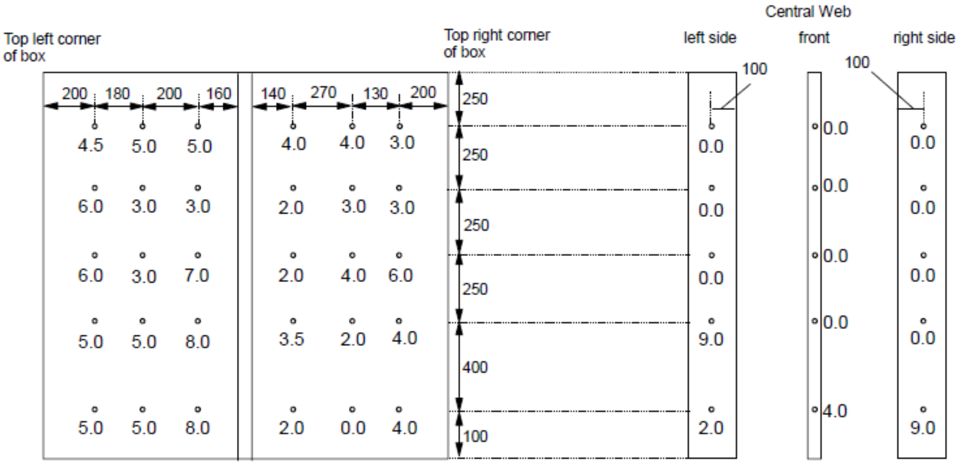

Thickness measurement positions viewed from open side of box.
Locations of measurements are approximate. All measurements in mm.

Figure 36 : Thickness of non-reacted coating remaining at various locations after jet-fire test on IF-1

In correlation with the reaction of the coating, the char thicknesses are reported on Figure 37. It is noteworthy that char thickness is well uniform all along the back plate and on the sides of the flange in spite of partially reaction: mean thickness is around 40mm. However, these different measurements allow to observe the destruction of the protective intumescent layer on the front of the central flange. Indeed a low thickness is detected on the middle of the central flange front (6mm) that can be caused by the flame erosion and the fragility of the char issued of the complete reaction.

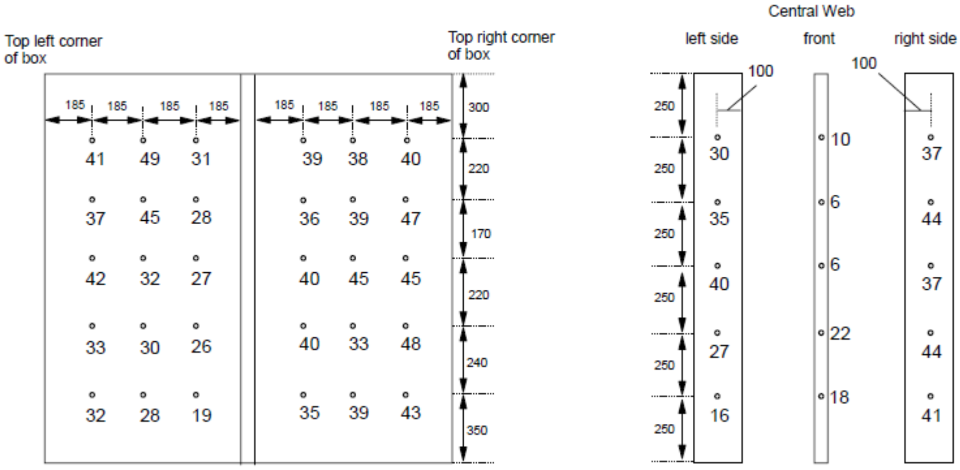

Thickness measurement positions viewed from open side of box.
Locations of measurements are approximate. All measurements in mm.

Figure 37 : Thickness of char at various locations after jet-fire test on IF-1

Consequently, regarding the behaviour of the coating facing to temperature and flames, end of the test occurs when two thermocouples have reached 400°C, two times must thus be highlighted:

- At 48 minutes, when the first thermocouple reaches 400°C: thermocouple at position 14 on the top of the central flange (Figure 29).
- At the end of the test (62 minutes) when a second thermocouple reaches 400°C and the propane flow ends: thermocouple at position 15 on the centre of the central flange (Figure 29).

On the right side of the back face of the box (Figure 38), the temperatures are measured by six thermocouples and begin to increase linearly from 100 seconds after the ignition to the end of the test. The temperature rise is then approximately linear at all positions to reach a maximum temperature of 206°C after 48 minutes (when the thermocouple 14 reaches 400°C) and a temperature of 228°C at the termination of the test.

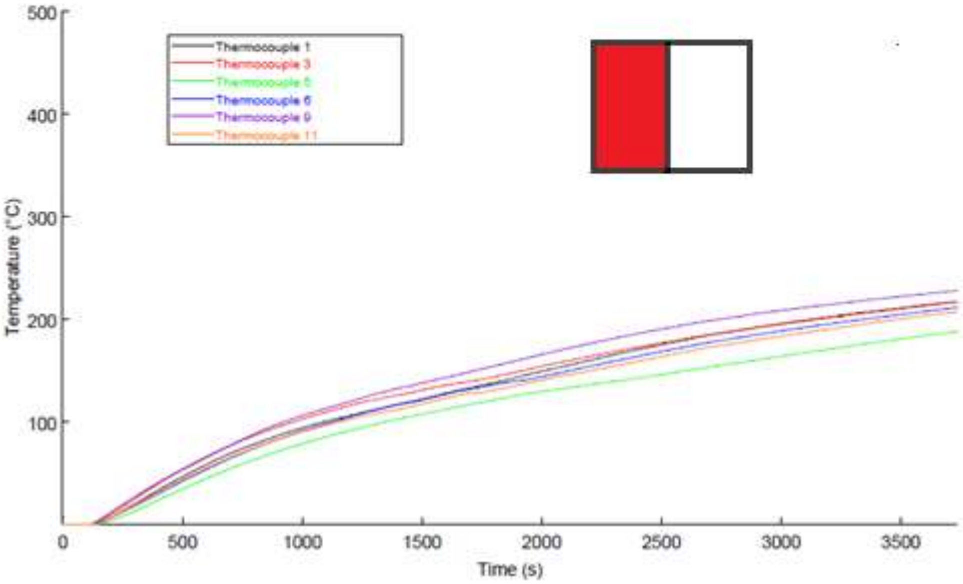

Figure 38 : Temperature measured versus time on the right side of the box (in red on panel schema) for jet-fire test on IF-1

Similarly, on the left side of the back face of the box (Figure 39), the temperatures are measured by six thermocouples and begin to increase linearly from 120 seconds after the ignition to the end of the test. The temperature rise is then approximately linear at all positions to reach a maximum temperature of 200°C after 48.5 minutes.

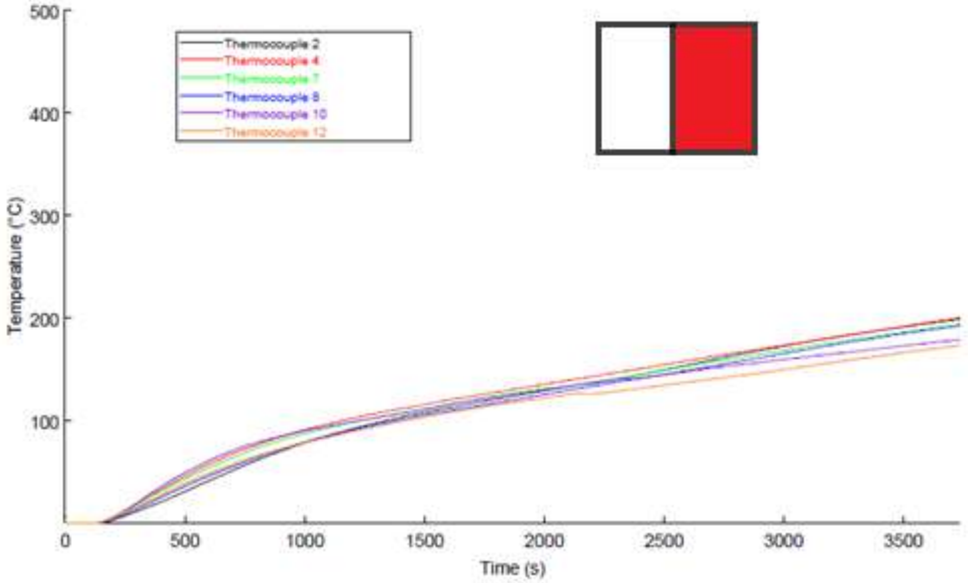

Figure 39 : Temperature measured versus time on the left side of the box (in red on panel schema) for jet-fire test on IF-1

Therefore, temperatures on back face are controlled thanks to the protection of a partially reacted hard coating. Then temperatures on the central flange have also been investigated thanks to five thermocouples. The inspection of the coating has already shown that the reaction is complete yielding to char formation and the thermal protection is consequently less efficient than on the rest of the panel due to the destruction of a part of the char on the central flange front. Indeed the temperature evolutions are presented Figure 40 and the maximum temperature measured on the specimen during the test is 484°C at thermocouple position 14 located on the flange where the coating is thinner.

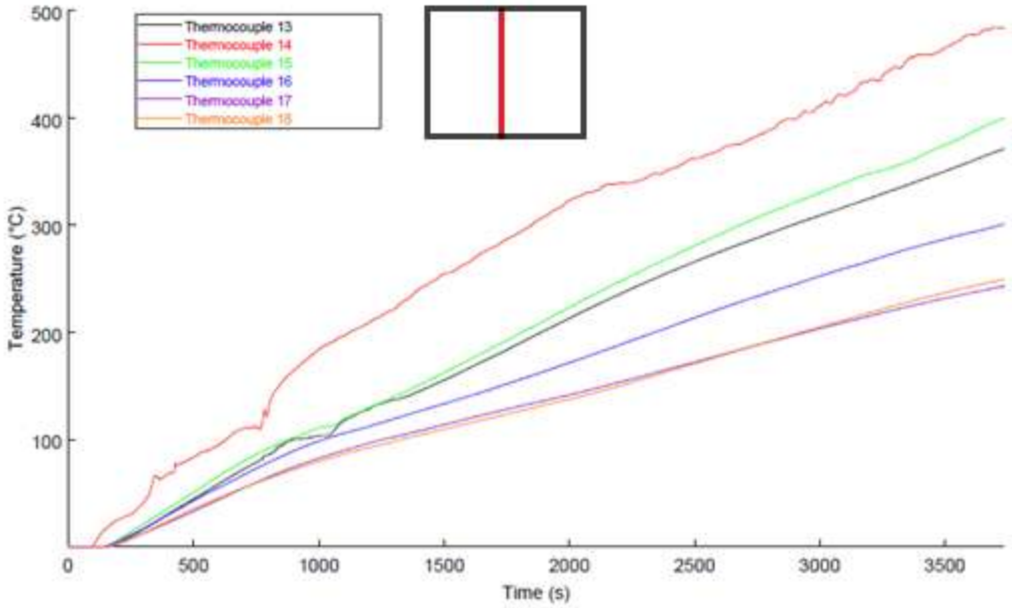

Figure 40 : Temperature measured versus time on the central flange (in red on panel schema) for jet-fire test on IF-1

So, the structural steelwork test specimen, coated with a single layer of IF-1 was subjected to a propane jet-fire with an average mass flow rate of 0.30kg.s^{-1} for a period of approximately 62 minutes. The thermocouples at position 14 displayed significantly higher temperatures throughout the test than the other 17 thermocouples. The test was not terminated until a second thermocouple (at position 15 on the central flange) reached a temperature of 400°C but the cause of failure appears as clearly the hot conditions on the flange and the bad efficiency of the protection on this location where heat flux is maximal. A reason advanced to explain this failure is the low expansion of the coating associated to not appropriate thermo-physical properties (e.g. heat conductivity) and thus its failure at the hottest point where low expanded protection is not sufficient to insulate metallic substrate.

II. 2. Intumescent formulation 2

Similar experiments in accordance with the Health and Safety Executive document OTI 95634 have been carried out with intumescent formulation 2 used with mesh located at a nominal depth of 7mm. The test is undertaken on panel box with central flange but only the flange is coated in the passive fire protective material because we suspect this flange to be subjected to higher temperature and higher pressure. The PFP material thickness has been made at the positions specified in standards on the flange and the global average coating thickness is 10.8. The flange is instrumented with 6 thermocouples to monitor the specimen temperature positioned on the flange (position 13 to 18 specified by OTI 95634 standard in accordance with Figure 29).

During the test, the flame engulfed the specimen making it difficult to see the coated surfaces very clearly through the flame (same behaviour as for IF-1). The test is over when successively the temperature at position 15 and then at position 17 reached a value of 400°C approximately after 35 minutes.

Following the completion of the test, the specimen was allowed to cool down. After this time a detailed inspection was carried out (Figure 41). The coating on the specimen had fully reacted, no coating remain without being expanded. There was a section of the flange in the region where the propane jet impacted on the specimen that had no coating present. The coating on the rest of flange has fully reacted and remained intact on the top.

Figure 41 : Pictures taken after jet-fire test of IF-2

The description of the flange is shown schematically in Figure 42. The coating on the upper portion of the flange has reacted but remained intact. There are areas where the top layer of the coating has been removed but the mesh and the coating beneath the mesh is in place and continues to insulate steel to flames. The mesh has lifted 130mm from the flange on the left hand side of the flange (as viewed facing the front of the box). A 170mm width band where the propane jet impacts on the specimen has no coating present and constitutes a non protected zone for steel.

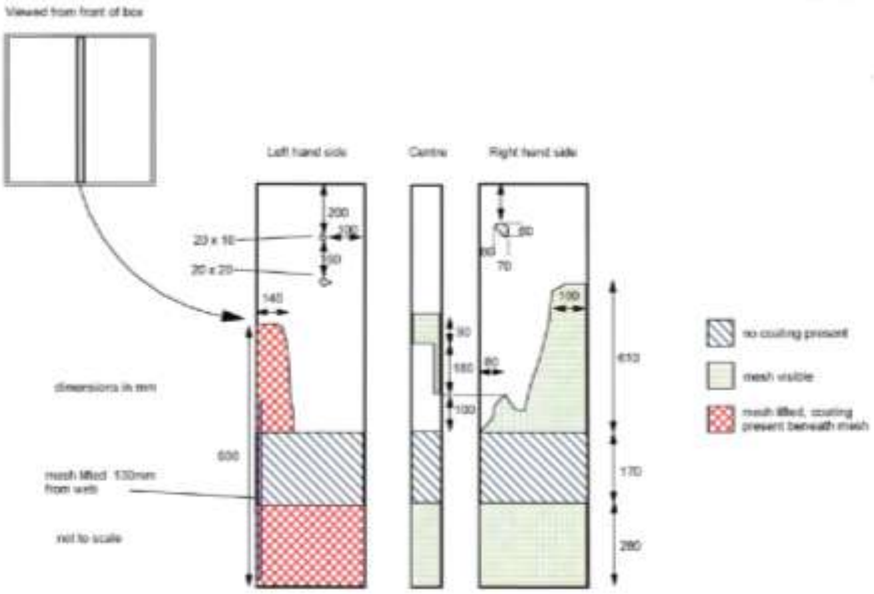

Figure 42 : Schematic diagram showing fire damage to the flange after jet-fire test on IF-2

Temperature profiles can be gathered for 6 thermocouples at equivalent position all along the flange (position 13 to 18 from the top to the bottom). On the flange, plots of temperature variation with time are presented in Figure 43. Several behaviours can be determined in accordance with aspect of the coating after test.

- Firstly, at all positions, the temperature rise increases steadily throughout the test up to approximately 1500 seconds.
- After approximately 1500 seconds, the temperatures measured at thermocouple positions 13, 14 and 15 continue to rise approximately linearly; these measurements correspond to the top of the flange where coating is still intact after test. At others positions, temperatures continue to increase but the rate of temperature reduces until approximately 2800 seconds, 2000 seconds and 3000 seconds respectively for position 16, 17 and 18.
- Furthermore, after these respective times, thermocouple measurements exhibit an chaotic evolution. These rapidly changing rates of temperature rise measured at thermocouples 16 to 18 can most likely be attributed to the breakdown of the passive fire protection coating due to erosion from the propane jet.

The test has been terminated when the temperature measured at thermocouple position 17 exceeds 400°C.

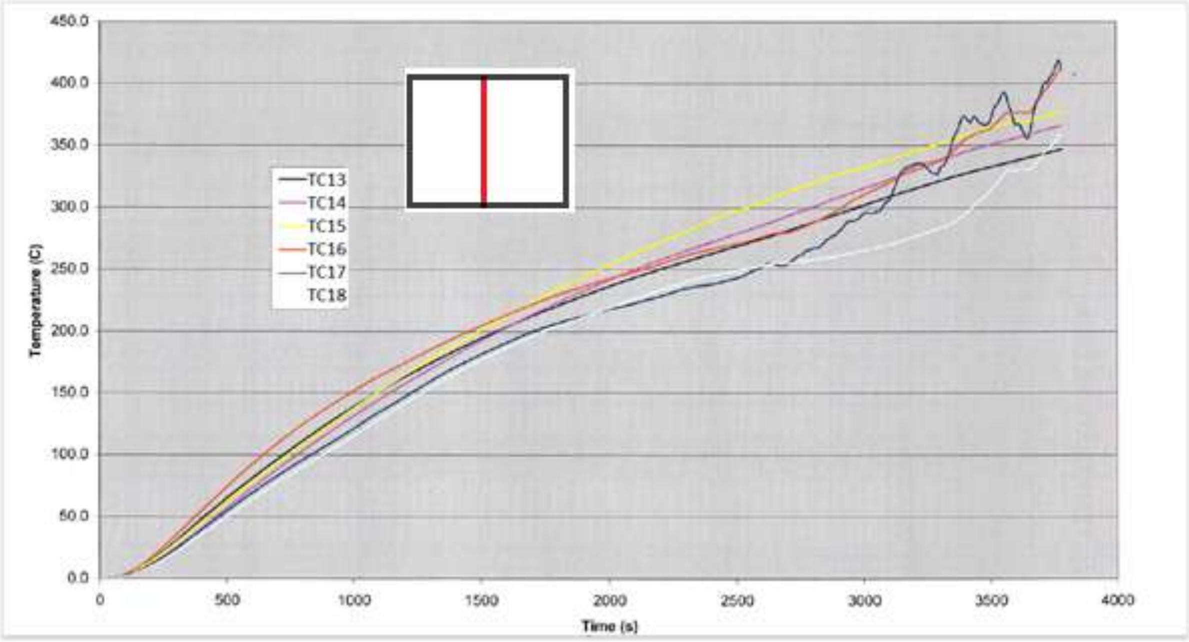

Figure 43 : Temperature measured versus time on the central flange (in red on panel schema) for jet-fire test on IF-2

The flange coated with a layer of IF-2, with an initial thickness of 10.8mm and with a steel mesh at a nominal depth of 7mm, was subjected to a propane jet-fire for a period of approximately 35 minutes. Temperatures on the test specimen increased throughout the test and the maximum temperature rise measured at the termination of the test was 410°C at thermocouple position 17, located directly where jet impacts. After test the coating is intact on the top half of the specimen and is significantly eroded on the bottom half of the specimen with no coating present in the area of impact of the propane jet, highlighting clearly the low mechanical resistance of the developed coating facing to jet pressure and impact.

II. 3. Intumescent formulation 3

About the intumescent formulation 3, jet-fire tests have been carried out in two steps. Indeed, because the formulation of IF-2 and IF-3 are very close, a first test has been carried out only with the flange coated by the passive fire protective material including a mesh, similarly to the previous one introduced for IF-2 (in agreement with OTI specifications except that only central flange is coated by intumescent paint). This first test should permit an observation of the char after test and determine the mechanical resistance of the coating directly facing to the jet impact. Then a second test describes a jet-fire resistance test on a completely coated panel box with IF-3 reinforced by mesh composed of a hybrid carbon and glass fibre and mounted in a steel box.

Some remarks can be stated during the test:

- From the start of the test, there were flakes of material blasted from the surface of the flange. Pieces are smaller in size than for the intumescent formulation 2.
- Approximately 10 minutes from the start of the test, flakes continues to be ejected from the flange upon impact. There is erosion of the coating in the region of jet impact and some erosion of the rear wall of the specimen.
- Approximately 25 minutes from the start of the test, although being not easy to discern due to flame, horizontal cracks appear to be developing where the jet is impacting the flange and just above where the jet is impacting the flange.

Following the completion of the test, the specimen was allowed to cool and then a detailed inspection is carried out and is viewable schematically on Figure 44. The coating on the specimen had fully reacted. There was a section of the flange in the region where the propane jet impacted on the specimen that had no coating present. The coating on the upper portion of the flange had fully reacted and remained intact on the flange. This area of the test specimen was coloured black from the top to about 290mm from the top of the specimen with the remainder of the test specimen coloured white/grey (Figure 45).

There were areas where the top layer of the coating had been removed but the mesh and the coating beneath the mesh were in place. At the bottom right hand side of the test specimen, the coating was pushed away from the metal surface.

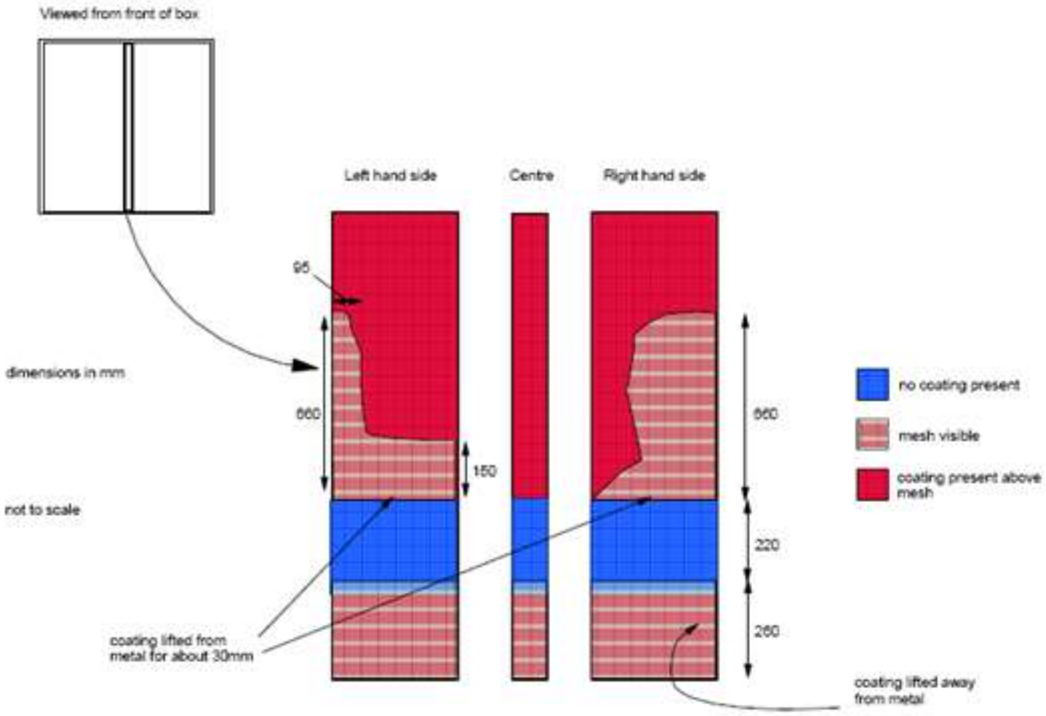

Figure 44 : Schematic diagram showing fire damage to the flange after jet-fire test on IF-3

Figure 45 shows the flange immediately after the jet-fire test. It was apparent at this point that the char close to the jet impingement has been eroded away, whereas at other parts of the flange the char looks intact. The general appearance of the breakdown of the material and the subsequent char showed similar trends both sides of the flange. The surface of the top part of the flange is characterised by blackened intumesced char, lower down the char is grey / white, followed by an area of detachment where no material appears present and at the bottom most part of the flange of the char is white in colour and has almost completely detached. Cracking is clearly visible at the top of the flange where the char is black or grey in surface appearance although the char integrity appears good.

Figure 45 : Pictures taken after jet-fire test of IF-3

Upon destructive inspection, it is apparent that the char on the flange sides is hard and compact and is difficult to damage (Figure 46). Removal of char from the around cracks showed that these were only surface deep, suggesting that material ejected from the flange during test in the early stages is from the surface. Where the surface appearance is black, the char is not all eroded, the char is extremely compact and hard enough to resist. Where the surface is grey, all the char above the mesh is mostly eroded either to a point just above the mesh or flush with the mesh. The char below the mesh is still hard and dense in nature and resistant to damage.

Figure 46 : Pictures exhibiting the density and the hardness of IF-3 after jet-fire test

In accordance with the setup of this test, temperatures are only reported on positions 13 to 18 (Figure 47), corresponding to thermocouples of the flange and placed where the thermal failure occurs generally.

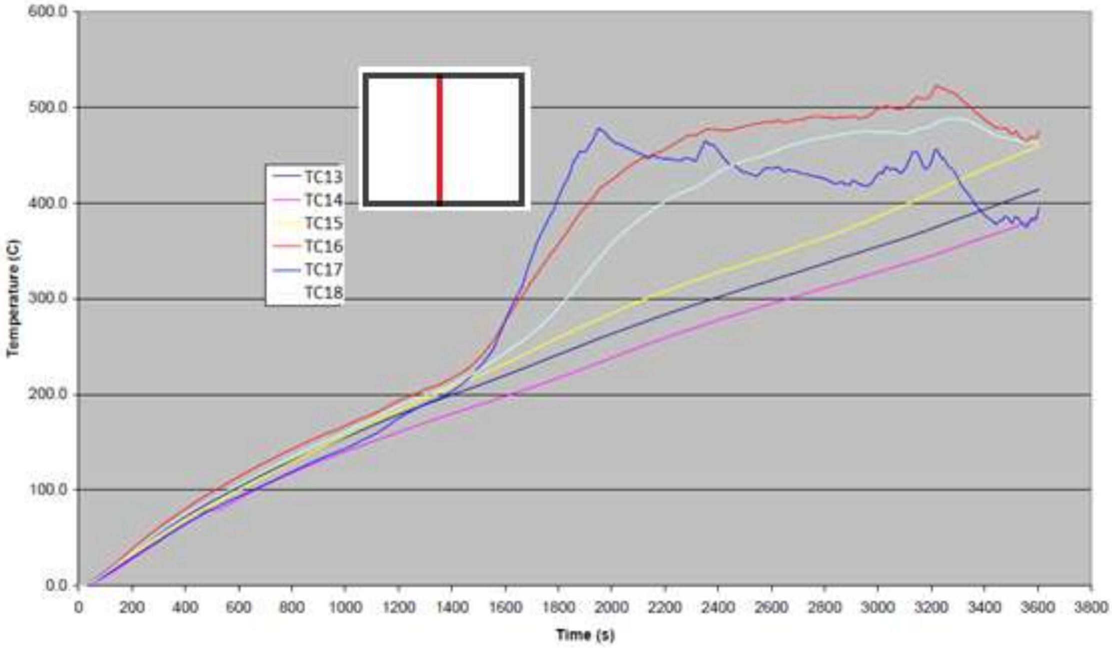

Figure 47 : Temperature measured versus time on the central flange (in red on panel schema) for jet-fire test on IF-3 not reinforced by mesh

Increases in temperature are clearly seen at all positions in the period approximately 5 to 10 seconds after the start of the test. From the graph, at 25 minutes there is a rapid increase in temperature which is believed to be detachment of material around thermocouple positions 16 and 17 then at 18. Failure occurs at 30 minutes where the jet impinges the flange and thermocouples positioned at 17 then at 16 measure temperature above 400°C.

As for a previous test with intumescent formulation 2, thermocouple 14 is lower in temperature throughout the test which seems to be typical of the circulation properties of the jet around the box.

Finally, the behaviour of IF-3 exhibits some similarities with the results exposed with IF-2: the failure describing by this first test shows a lower mechanical resistance of the char where jet impacts.

Furthermore, an additional jet-fire test on a completely coated box has been carried out using mesh to reinforce the intumesced structure and maintain coating in place. Effects are clearly viewable and beneficial to the resistance to coating. Indeed on the area of the previous observed detachment, the thickness and mesh placement have given a good improvement of resisting the jet-fire test for 60 minutes and a nonattendance of detachment. By investigating the char aspect and notably the central flange, mesh reinforcement permits to keep a residual layer on steel under the mesh. So the zone where usually no coating is present disappears to be substituted by a zone where the residual resistant layer continues to protect steel substrate as viewable on Figure 48.

Figure 48 : Aspect of the flange reinforced by mesh after jet-fire test on IF-3

Consequently to the presence of this residual layer, temperature profiles taken on flange positions do not exhibit high temperature and do not cause failure of the test. Indeed, Figure 49 shows a smooth increase of the temperature all along the flange. The temperature rise is approximately linear at all positions to reach a maximum temperature of 190°C at the end of the test.

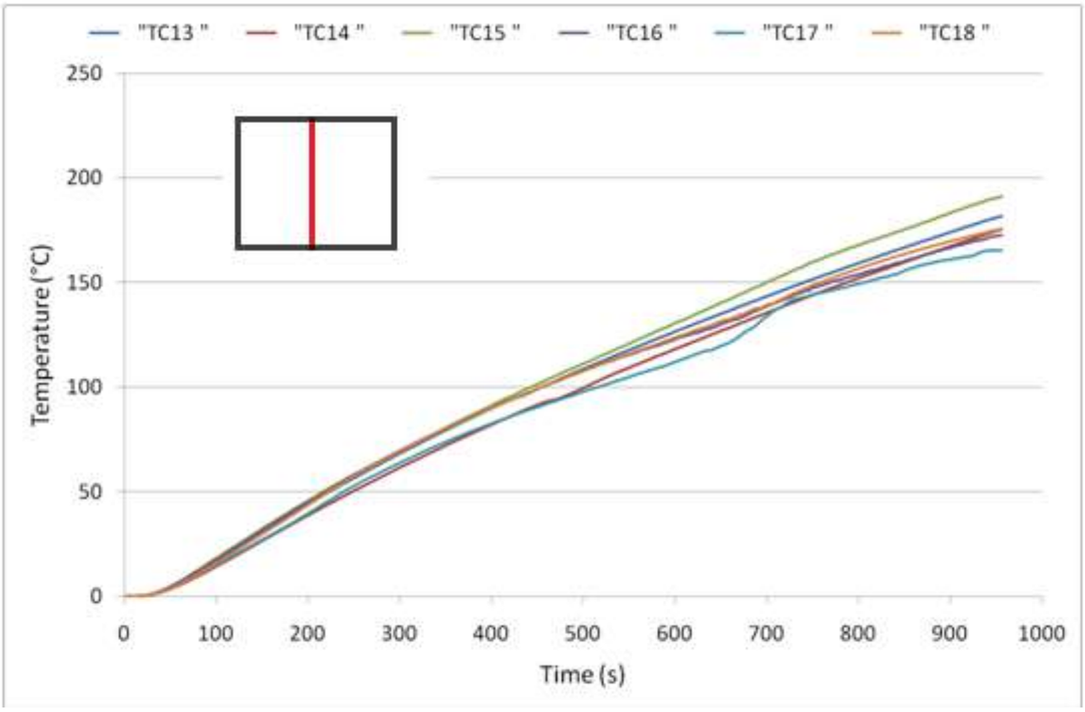

Figure 49 : Temperature measured versus time on the central flange (in red on panel schema) for jet-fire test on IF-2 reinforced by mesh

The end of the test has been determined by the increase of temperature on the back face. Indeed, intumescent formulation 3 failure occurs on the back face of the box, an area where neither IF-1 nor IF-2 fail. The temperature increase occurs on thermocouple 9 positioned at box back face Figure 50. Increases in temperature are perceptible at all positions in the period approximately 5 to 10 seconds after the start of the test. The temperature rise increased steadily throughout the test up to approximately 500 seconds from the start of the test for all the thermocouples and for the duration of the test for thermocouples at positions 1 to 9 (all placed on the top of the back face). After approximately 500 seconds the temperature measured at thermocouple positions 9 increased at a higher rate to a temperature in excess of 400°C after 11 minutes. Quickly this high temperature is conducted to thermocouples positions 10 and 11 and the test is terminated when the second thermocouple reaches 400°C: at position 11 after 13 minutes. Thanks to these thermocouples positions (Figure 29), a zone of failure can be delimited on the bottom of the back face.

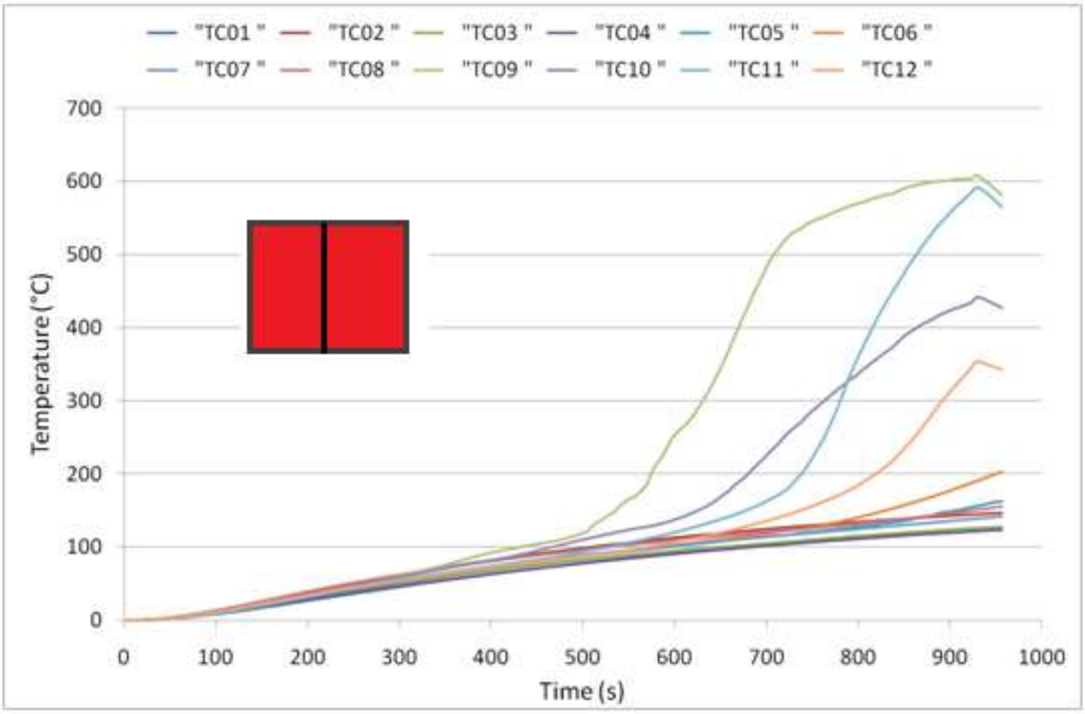

Figure 50 : Temperature measured versus time on back face of the box (in red on panel schema) for jet-fire test on IF-2 reinforced by mesh

Char inspection after cooling of the box exhibits two large zones on the back bow where flowing char has been discovered leading to bad protection of the substrate and premature failure. The destructive flow pattern of the jet should cause a shearing force and intumescent formulation 3 seems to be highly susceptible to damage from such an action.

Figure 51 : Pictures taken after second jet-fire test on IF-3 reinforced with mesh

Finally, the material resists to the jet-fire test for 13 minutes prior to failure. The material at the top of the flange gave close to 60 minutes prior to reaching 400°C nevertheless failure occurs early on a zone where neither IF-1 nor IF-2 fail. Overall, the material exceeds intumescent formulation 2 performance but is inferior to intumescent formulation 1. Intumescent formulation 3 is characterised as evolving a char of dual layers. The char at the heated surface is similar to the char produced by intumescent formulation 2, i.e. with a low density and a porous char with large hollow cells while the char at the substrate is much harder, denser and less flexible; approaching the structure of char produced by intumescent formulation 1. Therefore, the intumescent formulation 3 can be thought of as a compromise between the char properties of intumescent formulation 1 and intumescent formulation 2 (Figure 52).

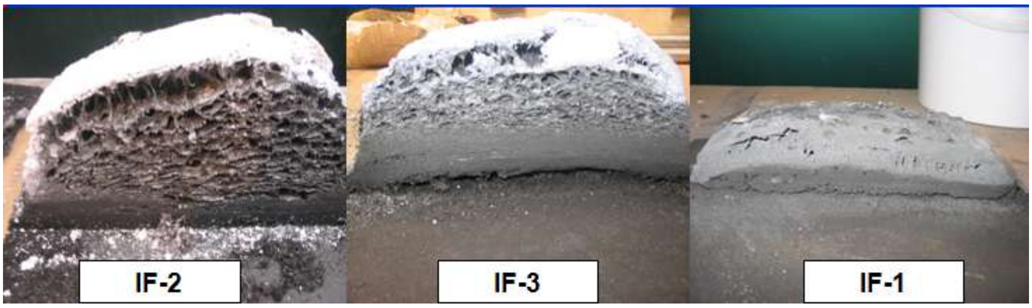

Figure 52 : Investigation of chars produced by the intumescent formulations (IF-1, IF-2 and IF-3) after jet-fire resistance test

II. 4. Intumescent formulation 4

The fourth intumescent formulation has been evaluated on a structural steelwork test specimen with central flange. The entire panel surface has been coated by the PFP material (back faces + central flange) according to the jet-fire resistance test.

At first sight, the char formation is significantly different to that of IF-3. Its inspection after cooling of the box reveals sever damage on the back faces (Figure 53) and the presence of large voids present at the steel/char interface (Figure 54). This bad contact between substrate and coating causes a bad adhesion and that the jet had a route behind the char to peel back.

Figure 53 : Pictures taken after jet-fire test of IF-4

Figure 54 : Char from IF-4 after jet-fire test exhibiting large voids close to metallic substrate

Another significant difference is the appearance of large cracks all long the thickness of the char. They should be caused by the inflexibility of the char and either by the impinging jet on the surface layer or by the build up of spumifics and the pressure from the inner layer.

Its behaviour is so consequently modified and first conclusions can be established in accordance with the temperature evolution (Figure 55).

- Up to 40 minutes, char stays intact.
- Then after 40 minutes, it is noticed that a section of char was going to peel off in the bottom left hand corner of the box.
- After 41 minutes, we observe an increase in amount of smoke produced by the coating reaction.
- After 45 minutes, an intense increase of temperature is observed in thermocouples 7 and 9 then in thermocouples 10.

- Finally 5 minutes later at 51 minutes after the gas release, failure of the specimen occurs when temperature exceeds 400°C in thermocouples 10 and 9.

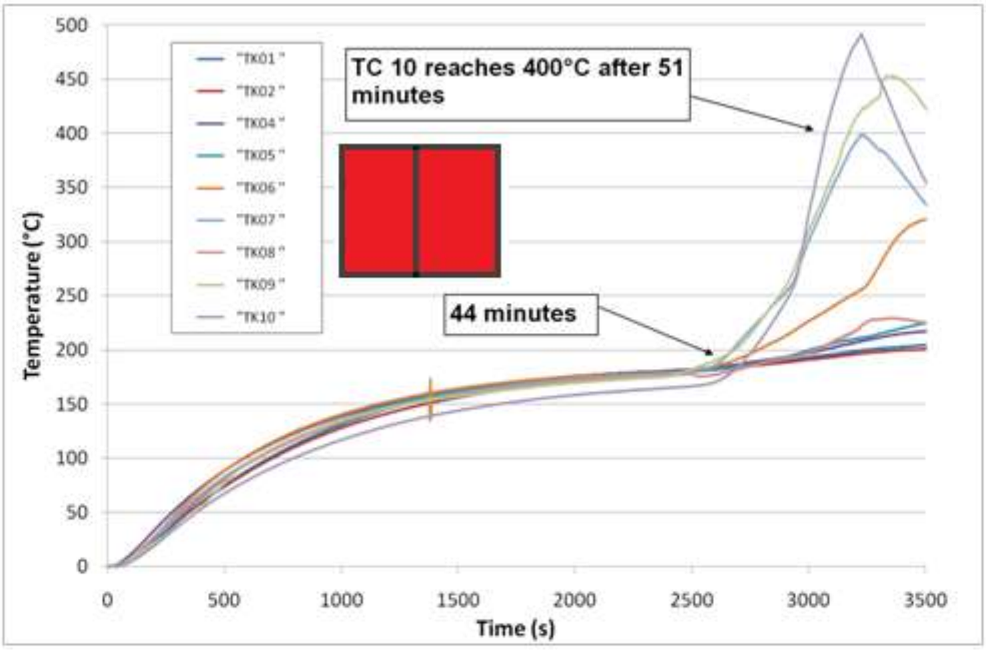

Figure 55 : Temperature measured versus time on the back face (in red on panel schema) for jet-fire test on IF-4

This failure can directly be linked to large voids observed with the post inspection of the char and the flame that can be engulfed close to the metallic substrate. Causes of failure seem to be a bad adhesion and the build-up of spumific components on the lower layer of the char leading to vacuum zone and cracks all along the thickness.

III. Conclusions and discussion about the jet-fire behaviours

To resume, each intumescent formulations exhibit different failures (Figure 56) and regarding those different failures, some explanations can be suggested highlighting the different swelling abilities or the mechanical resistance (Table 5).

Table 5 : Comparative sum-up of the different beahviours exhibited by the four intumescent formulations for large-scale jet-fire resistance test

Intumescent coatings	Test conditions	Time of failure	Position of failure	Explanations of the failure
IF-1	Entire panel coated No mesh reinforcement	62 minutes	Top of the central flange (hottest point)	Bad insulation due to a low expansion
IF-2	Only flange coated Mesh reinforcement	35 minutes	Bottom of the central flange (flame impact)	Bad resistance to jet-fire impact
IF-3 (first try)	Only flange coated Mesh reinforcement	30 minutes	Bottom of the central flange (flame impact)	Bad resistance to jet-fire impact
IF-3 (2nd try)	Entire panel coated Mesh reinforcement	13 minutes	Bottom of the back faces	Bad protection caused by flowing of char
IF-4	Entire panel coated	51 minutes	Back faces	Bad adhesion to steel substrate causing voids

Obviously, intumescent formulation 1 produces a very hard and not flexible char that does not expand very much. As it does not expand enough, it fails at the hottest part of the box due to lack of insulation. Experimental data given by thermocouples all along the test and in the state of the art about fire tests have permitted to determine the heat phenomenon that takes place for jet-fire and to localise the hottest point in the top third of the flange front. Temperature distribution is consistent with the direct observation of the char after test and correlates the lowest swelling of the specimen with the hottest point of the panel.

Even if no report is available in this chapter, jet-fire resistance test has been carried out on a structural panel box completely coated by IF-2 (back faces and central flange) and has confirmed the test conclusions and the behaviours of IF-2. Intumescent formulation 2 failure occurs on flange edge where the flame impacts. The char made from this product seems not to be sufficiently resistant and is destroyed by the pressure due to the flame impact. Reinforcement provided by inclusion of mesh system before testing can permit a great improvement of the mechanical resistance. Nevertheless, results commented above show a resistance weakness of IF-2 directly linked with the impact and pressure of the flame: no damage is detected and reaction of the coating is completed whatever the position on the panel except on the bottom of the flange front, where jet impacts.

Then intumescent formulation 3 has been tested as a compromise between the two first coatings and should solve swelling and mechanical weaknesses. Indeed char issued from IF-3 appears as strong enough to resist on edge of flange and exhibit an expanded insulative char. However its failure occurs on the back face of the box: an area where neither intumescent formulation 1 nor intumescent formulation 2 fail. This failure seems due to the destructive flow pattern of the jet and the shearing force highly susceptible to damage IF-3 on the back face.

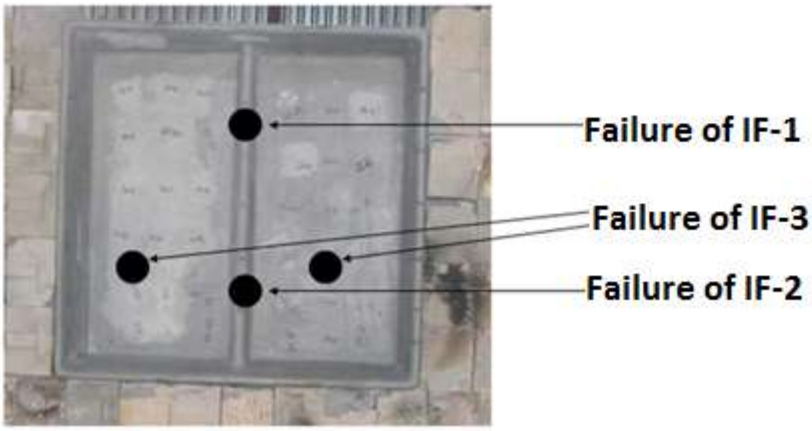

Figure 56 : Zones of failure on jet-fire test according to the intumescent formulations

Finally, intumescent formulation 4, based on a slight modification of IF-3, introduces also a new type of failure caused by appearance of large voids at the steel/coating interface. These large voids permit the engulfment of flame near substrate leading to an increase of temperature and a non protection of the steel. Nevertheless, we can report an improvement about the time of failure between IF-3 and IF-4 in accordance with their behaviour: expansion of the large voids occurs later than the flowing of the char observed with IF-3.

Therefore, we have shown that the four intumescent coatings exhibit different behaviours for jet-fire test. Some of these failures are self explanatory with the investigation of the char aspect. Low swelling abilities of IF-1, low mechanical resistance of IF-2 or viscosity evolution of IF-3 are clearly implicated, but some questions remain. Furthermore, in spite of all these interesting results and observations, jet-fire tests and, to a least extent, hydrocarbon fire tests are very expensive and time consuming. Pieces of information about the coating behaviours are so limited and the possibilities of testing a large number of formulations are reduced. New approaches to study the intumescent coatings and to determine their fire efficiency must be developed at small scale to reduce cost and to make easier access to substantial experimental data. Nevertheless, the different phenomena that take place during these kinds of tests are not always well-known and their extrapolations from large to small scale are risky. Therefore, the development of such experimental setup must be undertaken with care and with accuracy and will be described in the last chapter.

Our work in the next chapters will be so to understand these behaviours at laboratory scale. The range of small scale tests should give us a large number of results concerning different characteristics of the intumescent coatings. But before introducing a small scale fire test, we have focused our study on the fundamental determination of the physical and chemical properties that may be responsible for the jet-fire performances. Currently, swelling abilities and mechanical resistance are parameters easily available thanks to experimental tools developed previously in our laboratory and that have already proven their efficiency to characterize intumescent systems [95, 107]. Therefore, the physical approach developed in the next chapter to study the key properties of the intumescent formulations should permit to understand further the behaviours of the coating in fire conditions.

Chapter III: Physical behaviours of intumescent coatings

This chapter deals with the study of the dynamic behaviour of four intumescent coatings based on epoxy resin, designed for offshore platforms and described on the previous chapter. Consequently, it means that these coatings have to provide protection on the steel over a long time period and they also have to resist to aggressive conditions (i.e. severe hydrocarbon fires).

The state of art about intumescent formulations introduced on the first chapter has highlighted the crucial properties required to develop efficient coatings in terms of fire protection: mechanical strength and integrity, cohesion and adherence, porosity. We have also widely focused on visco-elastic properties exhibited by the partially degraded and melted materials during the intumescent process. If the degraded matrix has a too low viscosity upon heating, easy diffusion of gases takes place and the gases will not be trapped but rather escape to feed the flame. If the viscosity is too high, there can be formation of some cracks which allow the oxygen to diffuse into the char and thus decrease the efficiency of the protective layer. As a consequence, the measurement of the apparent viscosity using a classical rheometer should give information about the ability of complex systems will behave upon heating (flowing of the condensed matter, expansion of the structure measuring both the apparent viscosity and the gap between the plates of the rheometer).

Taken into account the different failures exhibited by the four coatings at large-scale jet-fire test described in the previous chapter, we have suggested failure of IF-1 because of its low expansion, failure of IF-2 because of its poor mechanical resistance, failure of IF-3 because of its rheological properties (flowing of the char) and failure of IF-4 because of its poor adhesion to substrate. That is why, after description of the experimental apparatus used to study in details these properties, we will discuss the results and the consequence on the quality of the char obtained during burning and on the resulting efficiency of an intumescent coating.

I. Experimental apparatus

I. 1. Materials

The materials used in the experiments below have been previously described on the chapter II (Section I.1 – page 68) but main components can be briefly reminded.

- IF-1 contains boric acid that plays a crucial role on the degradation mechanism and also a carbon source blended with APP coated by THEIC [105].
- The formulations of the three other coatings (IF-2, IF-3 and IF-4) are similar. One noticeable difference is the change of carbon source used in each formulation. Carbon source in IF-2 is played by the thermosetting resin (no additional incorporation of a specific char former), a DGEBA type epoxy resin while on IF-3 and IF-4 a specific components is added on formulation respectively pentaerythritol for IF-3 and dipentaerythritol for IF-4.
- Others additives usually used on paint formulations have been added: pigments, surfactant and mineral fillers but their compositions are unknown.

I. 2. Complex viscosity and expansion measurements

Visco-elastic measurements were carried out in order to evaluate the rheological behaviour of the system when the temperature increases. The rheological studies are based on the use of Thermal Scanning rheometer TSR Rheometric Scientific ARES-20A, in a parallel plate configuration. This apparatus allows an original approach of the study of the physical behaviour of an intumescent coating as both the apparent viscosity and the swelling can be simultaneously measured as a function of temperature and/or time.

In order to measure the viscosity and the expansion, sample pellets (Ø = 25mm, thickness = 3mm) are positioned between the two plates (Figure 57). The sample pellets were produced by casting the coating between PTFE plates and after curing for 24 hours at ambient temperature.

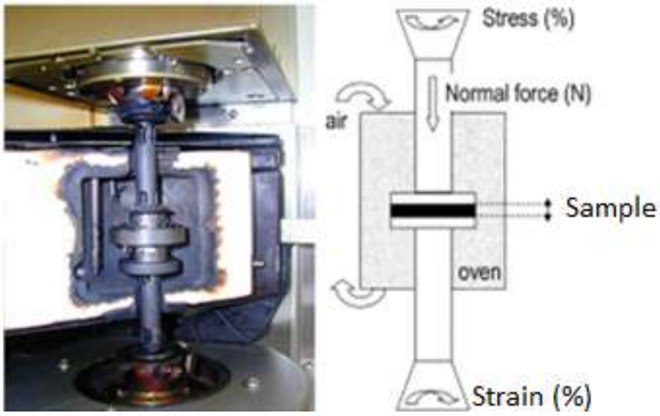

Figure 57 : Dynamic visco-elastic measurements in a parallel-plate rheometer

Testing is carried out using a "Dynamic Temperature Ramp Test" with a heating rate of 10°C/min in the range 25-500°C, a strain of 1% and a constant normal force of 100N (200Pa) or 200N (400 Pa) according to the tested sample (Table 6). Indeed, the four formulations exhibit different mechanical resistance, IF-1 appears as very strong and compact whereas IF-2, IF-3 and IF-4 are relatively "fragile". Hence, two experimental protocols must be used to characterize reliably intumescent formulations. The first ones for "strong" coatings has been developed for IF-1 and validated by a previous study [96]. This study has compared the behaviour of intumescent formulations (notably IF-1) using different laboratory analyses (notably rheometer) and has correlated thanks to Principal Component Analysis the laboratory and large-scale furnace test results. Results suggest excellent correlation between the different techniques. The second protocol is derived from the first one, except that the normal force is reduced in order not to destruct the char.

Table 6 : Experimental protocols used to reach visco-elastic properties

		Protocol for fragile coatings	Protocol for strong coatings
Thermal program	**Initial Temperature**	25°C	25°C
	Ramp Rate	10°C/min	10°C/min
	Final Temperature	500°C	500°C
Sampling time		1s	1s
Strain		1%	1%
Normal force		100N (200Pa)	200N (400Pa)
Sensitivity		10g	20g

This test leads to the apparent complex viscosity values and allows the measurement of the swelling corresponding to the gap between plates. The test is a measurement of the ability of the coating to expand in spite of the load applied upon it during the intumescence. So the degree of expansion is related to the strength of the developing char [88]. Furthermore, knowing the behaviour of the formulations for jet-fire test and notably ones of IF-3, this test provide us information about the visco-elastic behaviour of formulation and could explain the potential flow of materials observed at high temperature.

I. 3. Mechanical resistance of the char

Mechanical resistance is evaluated using TSR Rheometric Scientific ARES-20A as we did for measuring viscosity and swelling (see above) but with a specific test protocol. Samples are also 25mm-sized pellets but thinner than ones for viscosity measurements: h = 1mm instead of 3mm in order to reduce the final size of the sample after free swelling and allow reliable measurements between plates. At t = 0 s, the sample is put into the furnace heated at 500°C, without applying any strain (the upper plate is not in contact with the sample) as shown in Figure 58. This allows the sample to intumesce without any constraint. After 5 minutes when swelling is completed, the upper plate is then brought into contact with the intumesced material and the gap between the plates is reduced linearly (0.02mm/sec).

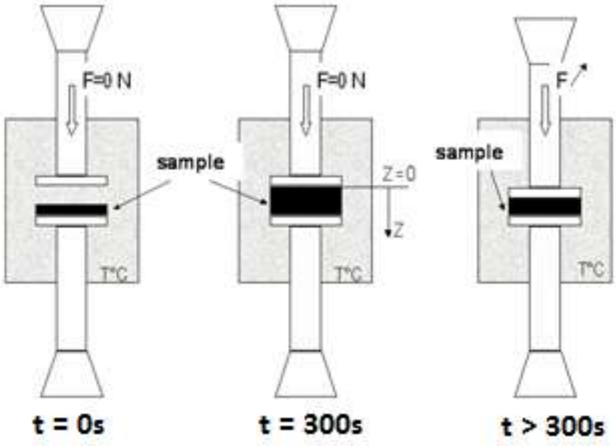

Figure 58 : Measurement of the char strength in a parallel-plate rheometer

The force is followed as a function of the gap between the two plates. The upper plate used in this experiment has a diameter of 5mm in order to increase the pressure on the whole sample and to ensure complete destruction of the char.

I. 4. Swelling abilities

To measure swelling abilities and complete the results obtained by rheological experiments, we have followed using image analysis the development of the char and we have calculated the relative swelling in pure radiative conditions. We have so carried out experiments on squared panels of intumescent coatings (5x5 cm², thickness = 2mm) under mass loss conical heater at two different external heat fluxes (35 and 50kW/m²) following the protocol shown on Figure 59. The experimental set-up was designed to shoot a mass loss calorimeter experiment using an infrared camera.

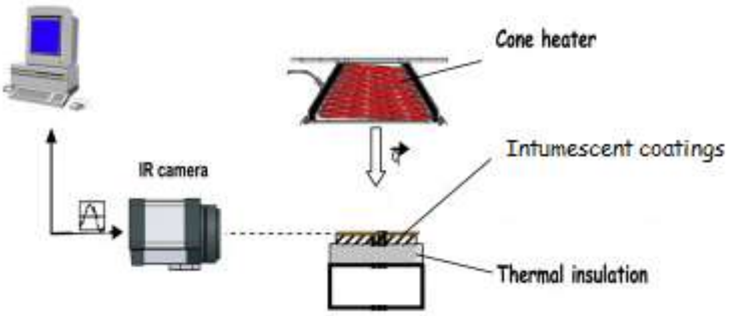

Figure 59 : Experimental set-up for measuring the swelling during a mass loss experiment using infrared camera

Although no information about temperature will be investigated, the use of infrared camera provides some benefits. Indeed the infrared camera allows to get clear images with a greater contrast to make image analysis than traditional camera. Typical infrared images at the beginning of the experiment and at the maximum of expansion of the intumescent coating are shown in Figure 60.

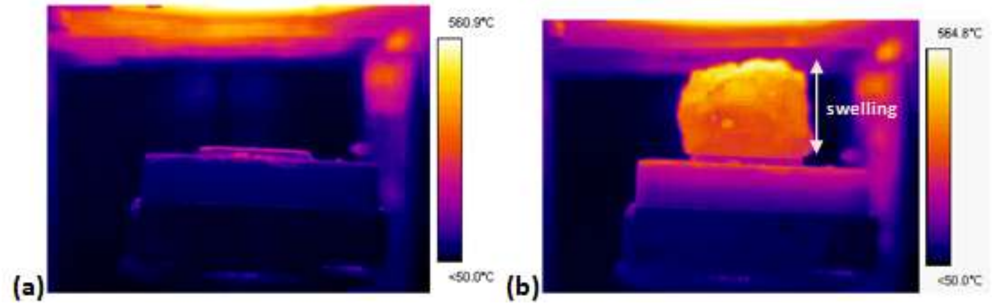

Figure 60 : IR images of an intumescent coating on steel plate upon heating at t=0s (a) and at the maximum of expansion (b)

Using image analysis in dynamic conditions (from a movie), swelling of the intumescent can be measured and quantified (see the arrow on Figure 60). In this approach, it is assumed during calculation on images that the expansion is homogeneous and occurs in one dimension. Typical curve exhibits a sigmoidal shape showing first a rapid development of intumescence and second a pseudo-steady state at longer times (Figure 61). The benefit of this approach is to get a quantitative phenomenological model which might be included in further modeling.

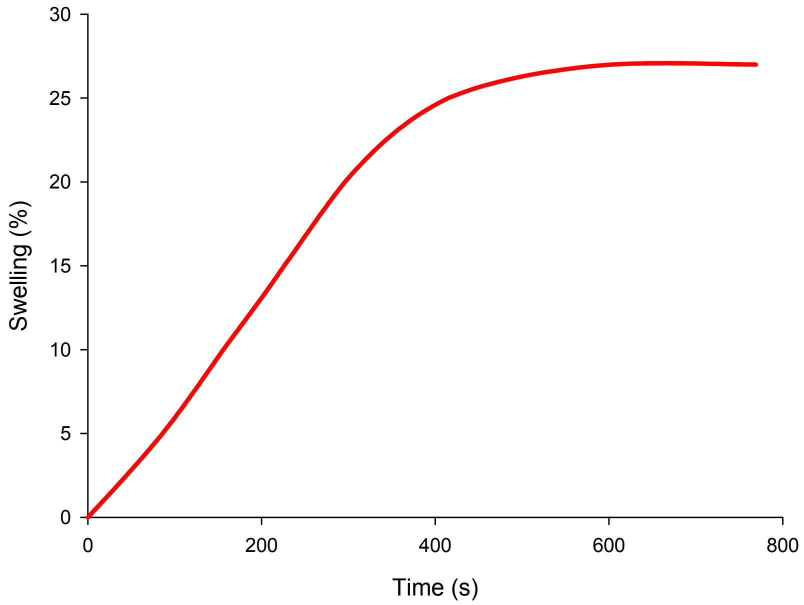

Figure 61 : Typical relative expansion as a function of time of an intumescent formulations during a mass loss calorimeter experiment (external heat flux = 35 kW/m²)

I. 5. Thermal stability

Thermo-gravimetric analyses were carried out at 10°C/min under synthetic air (flow rate = 100mL/min, Air Liquide grade), using a TA SDT Q-600. The samples (approx. 10mg) in powder form were placed in open alumina pans, using gold sheets in order to avoid reactions of the phosphorus species of the coating with alumina.

II. Results and discussion

II. 1. Visco-elastic measurements

As introduced in the previous section and discussed in the state of art, apparent viscosity measurements and swelling abilities are important characteristics of our intumescent formulations and have been widely correlated with the fire behaviour [90]. Here they can be estimated simultaneously with an only one experiment.

II. 1. a) Precaution to use rheological tool to characterize intumescent coatings

Before investigating the apparent viscosity changes of the intumescent systems, the behavior of the epoxy resin must be studied. Its evolution of the apparent viscosity must firstly be correlated with thermal stability of the systems (Figure 62). Before 300°C, the material is not degraded, the system is a solid tri-dimensional reticulated network thus the viscosity values have not physical signification. Then the main step of degradation of the resin, which loses 80% of its mass, occurs between 300 and 460°C while the apparent viscosity measurements of the epoxy resin show an important decrease in the temperature range [330-350°C] with a minimum at 350°C. At 350°C, the material has the aspect of a black viscous paste. We can so link these two phenomena. The degradation of the resin causes the decrease of the crosslink density and therefore a decrease of the apparent viscosity. The material is quite totally degraded at 500°C. The high viscosity can then be explained by the carbonization of the material.

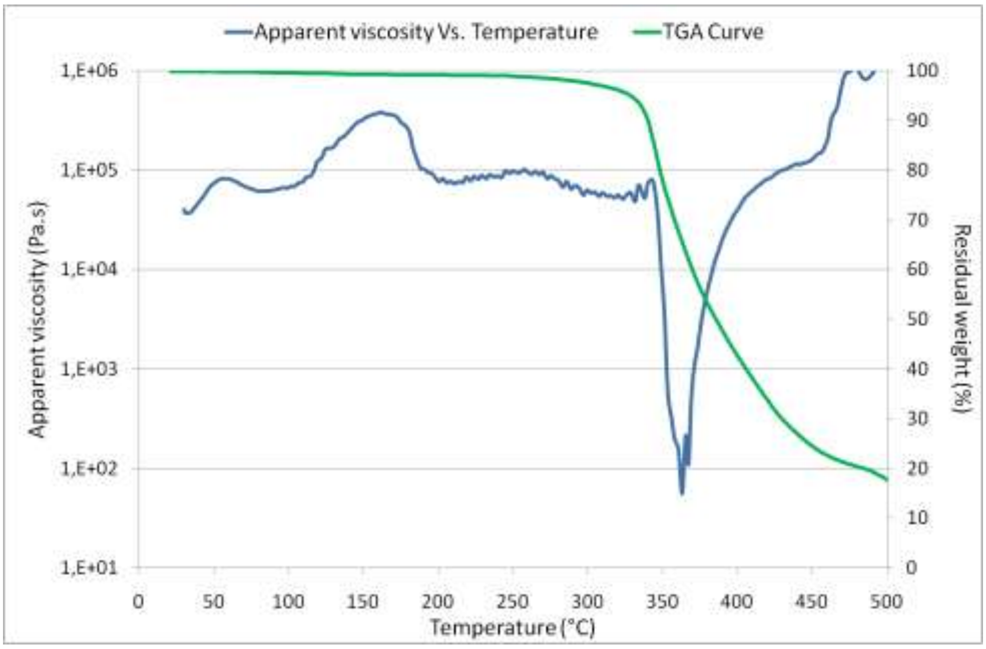

Figure 62: Correlation between viscosity changes (F=100N) and thermal degradation of the system

So, use of rheometer and investigation of apparent viscosity change give interesting information but must be interpreted correctly. No physical interpretation is possible before the onset of the degradation. Once the degradation has begun, we can reach the measurement of an apparent viscosity values. This approach may then be used to characterize the behaviour of an intumescent coating.

II. 1. b) Results of IF-1 and role of the intumescent additives

First work has been done at our laboratory only with IF-1. It provides reliable correlations between viscosity and swelling and highlights the effects of active components of the formulations such as APP or boric acid [95]. The four systems are a thermoset resin based on a DGEBA prepolymer and an amide, a thermoset resin mixed with boric acid, a thermoset resin mixed with the APP derivative and IF-1 (intumescent formulation based on epoxy resin and containing both boric acid and APP). Its study shows how to use a rheometer to characterize the behaviour of intumescent formulations.

Figure 63 compares the thermal stability of the four systems while Figure 64 compares their apparent viscosity changes.

When boric acid is added to the resin, a first degradation step is viewable between 100 and 170°C due to dehydration of H_3BO_3 [105]. This first step of degradation has consequence on the viscosity changes because we can detect a quick variation of the viscosity around 150°C. Moreover, the apparent viscosity shows also a decreasing peak but over a larger range of temperature [300-390°C] compared with [330-360°C] in the case of the epoxy resin alone.

When APP is incorporated into the resin, the TGA curves show evidence that the main degradation step occurs at a lower temperature than epoxy resin alone. As a consequence of this early degradation, the apparent viscosity measurements decrease at lower temperature (290°C) and in a larger temperature range [290-370°C] when APP is added to the thermoset resin.

When both additives are combined into IF-1, there is a first variation of the apparent viscosity measured around 150°C due to H_3BO_3 dehydration. Then a small decrease of viscosity is viewable at 330°C and could be correlated with the slow degradation of IF-1 between 250°C and 500°C. The observations show the formation of a pasty intumescent shield from 330°C. The intumescent additives reduce the fall of viscosity due to degradation of the polymeric matrix forming a carbonaceous coating and permit trapping of gases inside this coating. Jimenez [105] explains the behaviour of commercial formulation IF-1 investigating mixtures based on the main components of the formulations (epoxy resin, APP and boric acid). She showed the role of particular additives and notably silicate fillers which should reinforce the char and limit the viscosity decrease.

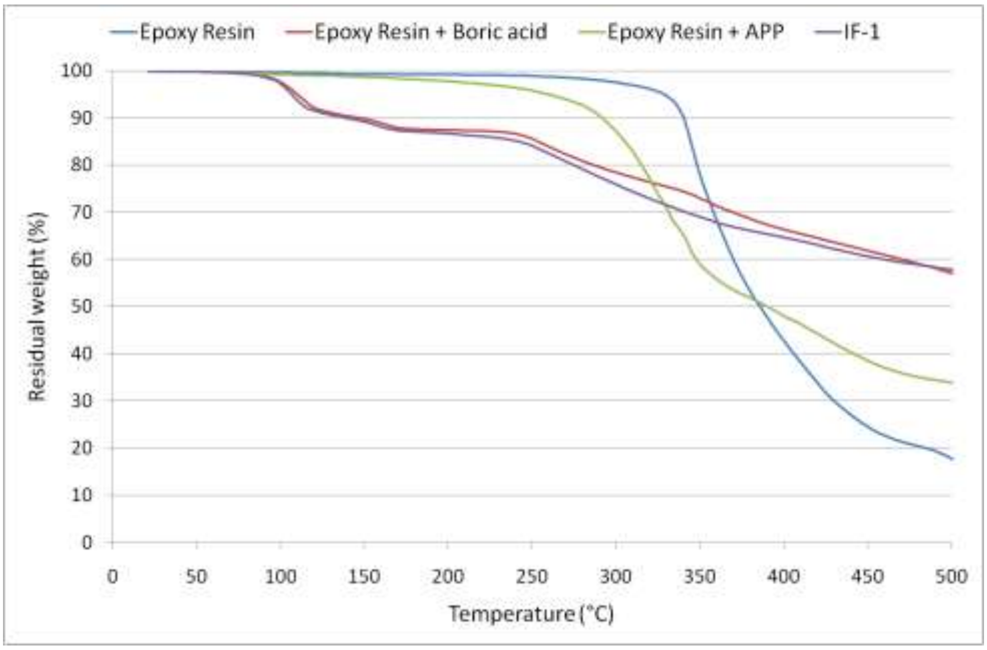

Figure 63 : TGA Curves of the four systems

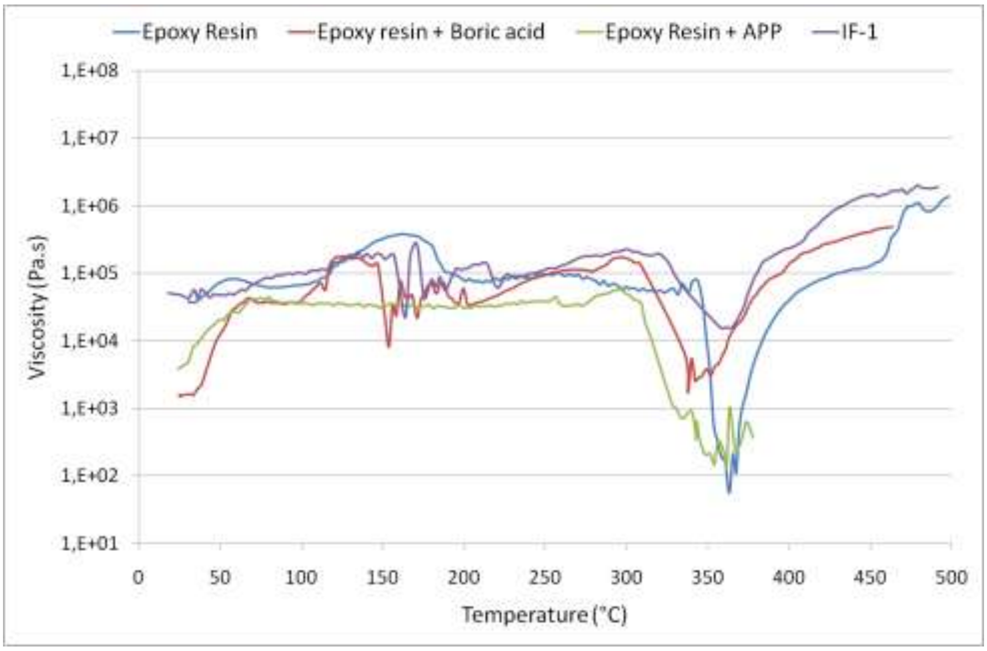

Figure 64 : Viscosity measuremant versus temperature for epoxy resin alone with boric acid, with APP and with both (F=200N)

Then, the swelling abilities of the same formulations are compared on Figure 65.

Expansion of the thermoset resin is significantly increased when the APP derivative is added. APP additive degrades to yield ammonia above 200°C [108] and the expansion is attributed both to ammonia and to the evolution of volatile degradation products, which are trapped in the structure. APP incorporated into the resin leads to intumescence.

Similarly, boric acid causes the intumescent formulation to swell from 140°C. It was proposed that the formation of B_2O_3 due to the dehydration of the boric acid leads to the formation of an intumesced material [95].

The presence of both boric acid and the APP derivative in the intumescent formulation (IF-1) leads to a higher expansion (180%) while the main decrease of viscosity is the lowest. The residue obtained is solid and dense. It is noteworthy that the swelling (main step) starts at 300°C suggesting that the expansion takes place because of the relatively low viscosity of the char combined with the release of volatile degradation products. As the peak of viscosity of the intumescent formulation is the smallest, the swelling is the highest because the decomposition gases can slowly diffuse into the matrix, providing high expansion and avoiding escape (either from cracks in the case of too high viscosity or as bubbles in the case of too low viscosity) to feed the flame.

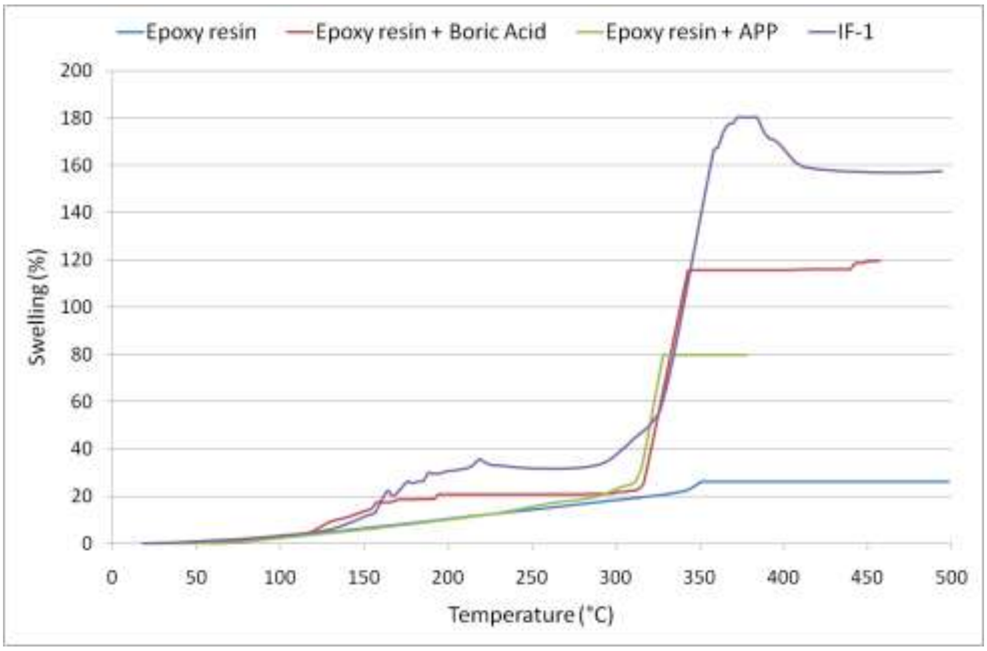

Figure 65 : Swelling abilities versus temperature for epoxy resin alone with boric acid, with APP and with both

Finally, this short study based on IF-1 and its components illustrate the role of each intumescent ingredient on the swelling abilities and on the visco-elastic properties of the systems. Rheological approach is also described as an efficient tool to characterize the intumescent formulations as soon as the degradation occurs. This method is so validated and can be used to study the three other formulations

II. 1. c) Visco-elastic measurements and swelling abilities of IF-2, IF-3 and IF-4

Figure 66 compares the apparent complex viscosity of the three intumescent formulations IF-2, IF-3 and IF-4 measured with a normal force of 100N (instead of 200N because of the fragility of the intumescent structure from these coatings).

By observing TG curves of these intumescent formulations (Figure 67), we detect that degradation begins at 200°C. Therefore, all values taken before 200°C have no physical signification. Up to this temperature, the viscosity measurements can be investigated. All formulations exhibit profile with a quick viscosity decrease attributed to matrix degradation and gases diffusion then with a viscosity increase characteristics of the stiffening of the structure by carbonization process [90, 95]. In spite of these common phenomena, the profiles versus temperature are widely different according to the intumescent coatings.

Indeed, viscosity measurements for IF-2 show a decrease at 300°C to reach an apparent viscosity minimum of 2.5×10^4Pa.s at 370°C. So, the temperature range where the viscosity is relatively low is [300-400°C]. On the contrary, the behaviour exhibited by IF-3 is widely different. The apparent viscosity decreases from 220°C and the values have remained very low (around 5×10^3Pa.s) for a wider temperature range [220-430°C]. Finally the profile of IF-4 is close to that of IF-2, the apparent viscosity decrease at 270°C to reach apparent viscosity minimum of 2.9×10^4Pa.s at 360°C. The temperature range where relatively viscosity is low is between 270°C and 400°C for the three formulations.

Therefore, among the three formulations, we can observe two main different behaviours. In one hand, IF-2 and IF-4 exhibit a small viscosity decrease and a narrow temperature range where the apparent viscosity remains relatively low. In the other hand, the profile of IF-3 is specific with a quick viscosity decrease at lower temperature and a wide temperature range from 220°C to 430°C with low viscosity. To explain these visco-elastic behaviour differences, we suspect obviously the different carbon sources. Indeed, the main difference between IF-2, IF-3 and IF-4 is the carbon source used for intumescent process with epoxy resin on IF-2, epoxy resin and pentaerythritol on IF-3 and epoxy resin and dipentaerythritol on IF-4. The pentaerythritol is mainly suspected to cause the low viscosity of IF-3.

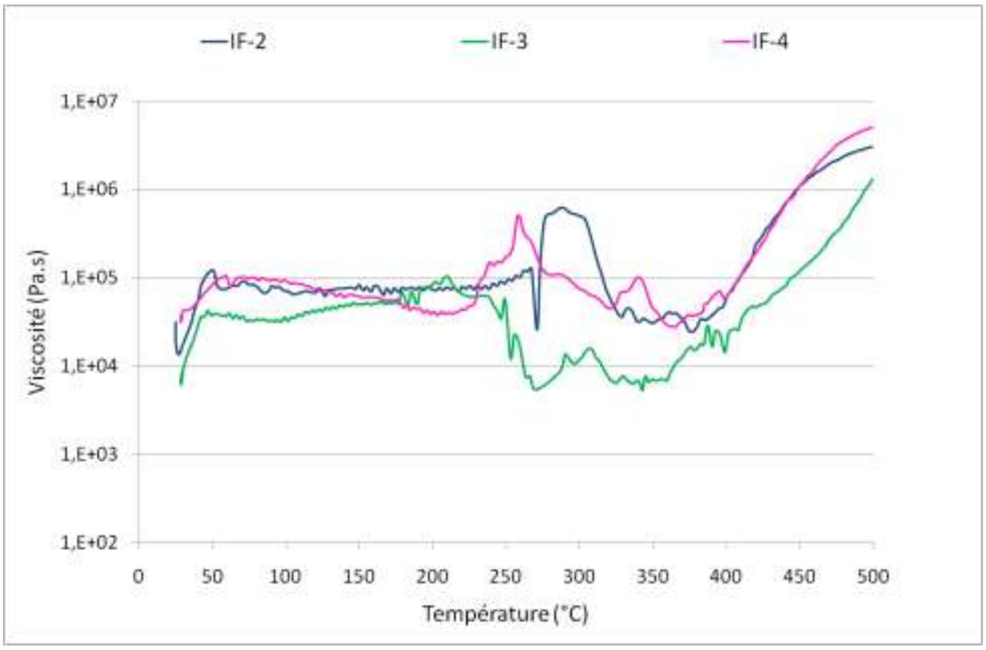

Figure 66 : Viscosity versus temperature for IF-1, IF-2, IF-3 and IF-4 (F=100N)

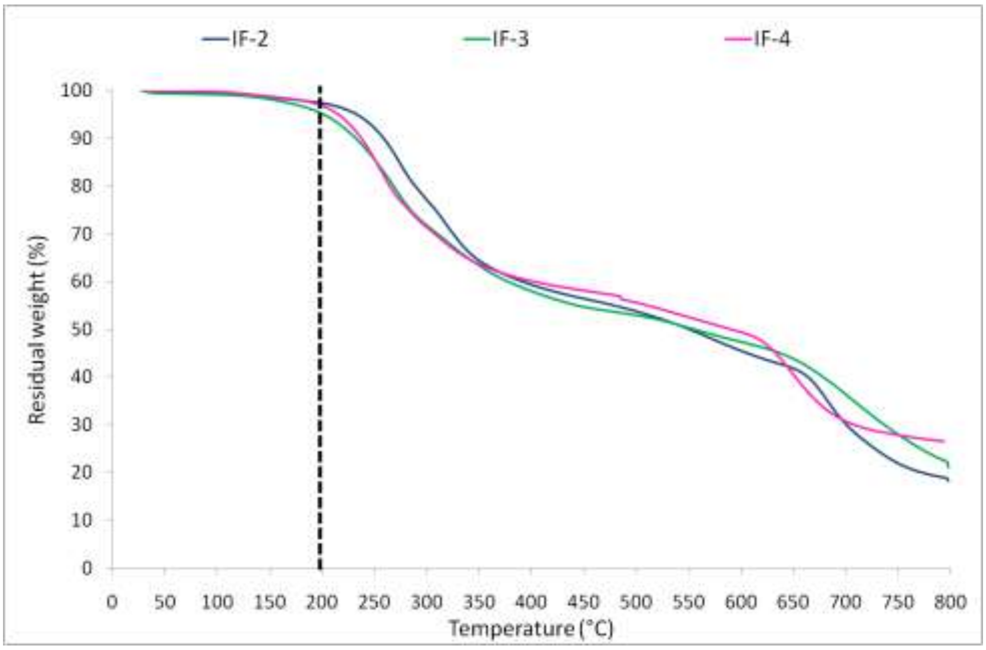

Figure 67 : TGA curves of the intumescent formulations in air at 10°C/min

About the expansion, we have previously seen that it is attributed to the evolution of volatile degradation products, which are trapped in the structure. Thanks to the Figure 68 and to the Table 7, we observe that expansion measurements are correlated with viscosity changes. Indeed, it is noteworthy that swelling starts at temperature where the decrease in viscosity is observed, suggesting that the expansion takes place because of a concomitant gases release and decrease in the viscosity of the material. Similarly the swelling period corresponds to the temperature range where the viscosity is low.

We can also remark a correlation between the maximal swelling and the minimum of viscosity: the lowest the minimum viscosity, the highest the swelling. With a viscosity minimum around $5x10^3$Pa.s, IF-3 exhibits a higher swelling with a rate above 150% while IF-4 swells only to 110%. This reduction in swelling observed between IF-3 and IF-4 can be explained by the carbon donor used and especially by the ratio between of OH groups and C groups. Indeed, the crucial parameter for a carbon source yielding high expansion is the ratio between OH groups and C groups [83]. Therefore, the pentaerythritol is the compound most rich in hydroxyl groups per carbon groups (4 OH per 5 C for PER and 6 OH per 10 C) and its presence in IF-3 can explain the best swelling rate exhibited by IF-3. Moreover, due to its viscosity decrease at lower temperature, intumescent period of IF-3 occurs at lower temperature and for a wider temperature range [210–290°C].

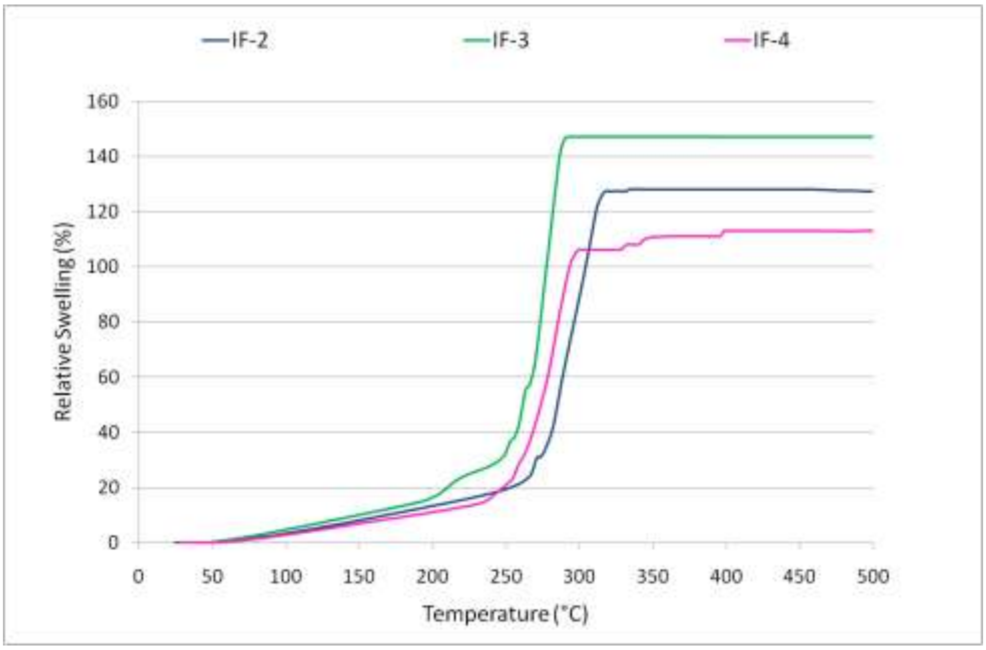

Figure 68 : Swelling versus temperature for IF-1, IF-2, IF-3 and IF-4 measured in the rheometer

Table 7 : Swelling temperature range

Intumescent Formulation	Temperature where viscosity decreases	Swelling temperature range (°C)
IF-2	300°C	[250 - 315]
IF-3	220°C	[210 - 290]
IF-4	270°C	[245 - 300]

Therefore, the investigation of the intumescence with a rheological tool allows to underline some characteristics of the formulations. The effect of the carbon source is notably determined by comparison between IF-2, IF-3 and IF-4. Pentaerythritol causes a decrease of the apparent viscosity at lower temperature (220°C). As a consequence, swelling and intumescence process starts earlier for IF-3. Substitution of PER by dipentaerythritol in IF-4 allows to modify this behaviour. IF-4 behaves at high temperature similarly than IF-2 with viscosity values around $2.5\text{x}10^4$Pa.s between 300 and 400°C. The role of the carbon donor in intumescent coatings and these effect on the visco-elastic behaviours have been also reported by Andersson et al. [109]. Indeed, they have studied apparent viscosity profiles of formulations containing pentaerythritol, dipentaerythritol and tripentaerythritol and they showed that the formulation with pentaerythritol starts its intumescent process at a lower temperature over a wider temperature range than the formulations with dipentaerythritol and tripentaerythritol.

These observations and explanations must be directly linked with the behaviour of the coatings observed during jet-fire resistance test. Indeed, IF-3 exhibits phenomena of char flowing that occur on the back faces and that have firstly been explained by the rheological issue. Indeed, we have just shown that apparent melt phase viscosity of IF-3 is minimum for a broad temperature range [210-290°C] and that the development of an expanded structure occurs at lower temperature. However, the char does not seem very resistant and flows under the pressure and the temperature of the flame. The char of IF-2 is so subjected to severe aggressions and cannot withstand for a too long time to high velocity jet. On the contrary, in similar conditions, IF-4 exhibits better performance in agreement with the visco-elastic change observed between IF-3 and IF-4. Use of dipentaerythritol would so be more desirable than pentaerythritol in coatings for an application in severe conditions in order to limit the potential flowing and cracking and the early destruction of the protective shield.

II. 2. Mechanical resistance of the formulations

When viscosity varies during the temperature range of intumescence process, the internal structure of the charred material is also modified. It is this structure that governs the character of the intumescent shield and the efficiency of its protection. Indeed, if the shield becomes too hard, the creation and propagation of cracks leading to a rapid degradation of the material occurs. If a char has a good structural, morphological and heat insulative properties but is easily destroyed under a mechanical action, its efficiency is totally lost in the turbulent regime of combustion. The mechanical strength of the char is considered as particularly important in the case of jet-fires while the char has to resist very aggressive conditions, such as explosions, violent wind, and impact of the flame.

Figure 69 presents the destruction force of the carbonaceous char plotted against the distance between the plates for the four coatings at 500°C. At first sight, we can divide the coatings into two categories: IF-1 appears as a more robust and more resistant char than the three others.

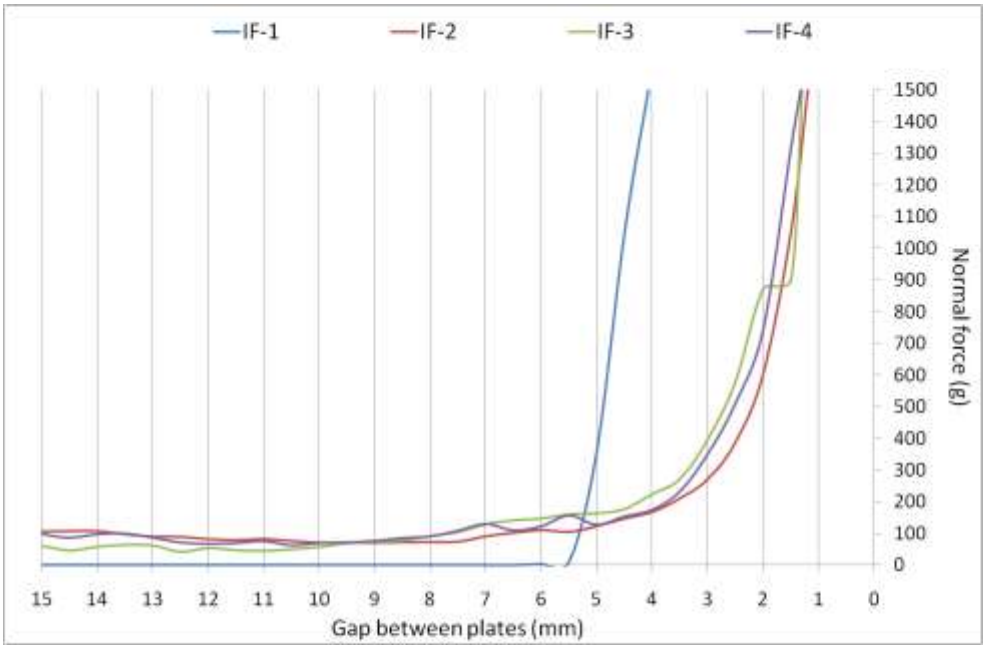

Figure 69 : Mechanical resistance measured at 500°C for char issued from IF-1, IF-2, IF-3 and IF-4

The curves corresponding to IF-2, IF-3 and IF-4 are similar: the char is not mechanically resistant and a very low force is sufficient to destroy it. It is only when the gap between the plates reaches 3mm that the force increases. This can be explained by the fact that the residue has been strongly compressed.

The curve corresponding to IF-1 exhibits a complete different behaviour compared to the three others. When gap between plates is higher than 6 mm, the measured normal force is low while for 6mm, the force begins to vary and increases quickly which means that the char is harder. It is because of the presence of boric acid which provides better mechanical resistance and the presence of mineral fibres and silicates [95, 105].

Globally, the mechanical resistance curves underline the worst resistance of IF-2, IF-3 and IF-4 by comparison with IF-1. This parameter have been commented in the state of the art as primordial to maintain an efficient char facing to fire strain and are subjected to be cause of IF-2 failure for jet-fire resistance test. Indeed, protective structure developed from IF-2 and IF-3 does not resist where the jet impacts i.e. where pressure is maximal.

To confirm the difference between the mechanical resistances of the coatings, we can visually observe the internal structure exhibited by the char after reaction and development (Figure 70). Intumescent development takes place in rheometer at 500°C for 5 minutes without any strain, similarly to the first phase of the experimental protocol used to evaluate the mechanical resistance (before destruction between the two plates).

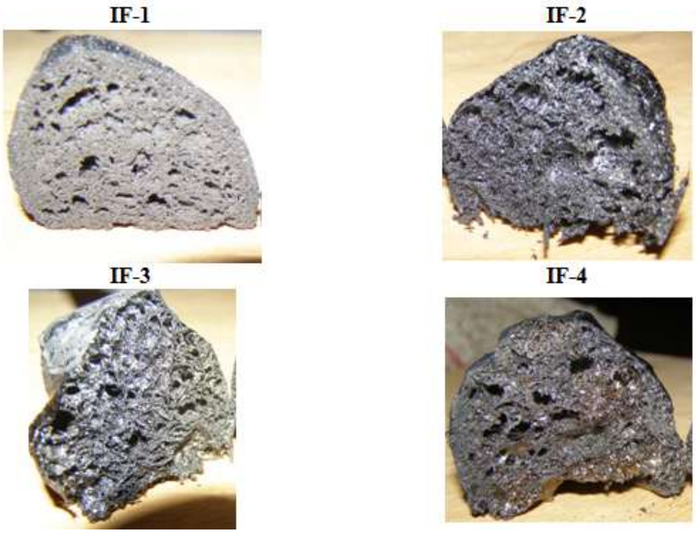

Figure 70 : Comparative aspects of the four chars after 5 minutes of free development in rheometer furnace at 500°C

Useful information has been obtained thanks to the previous pictures to explain the behaviour of the sample (mechanical resistance and swelling). Indeed IF-1 exhibits an internal structure that is compact and that keep the initial form with few tiny cells in agreement with the conclusions suggested by mechanical resistance curve. A high density could explain the high resistance of the char. On the contrary, morphologies of the char resulting from IF-2, IF-3 and IF-4 exhibit large voids that could weaken the structure. An additional difference is thus underlined thanks to the internal structure of the char. It is a compact and carbonised char issued from IF-1 whereas the three others demonstrate a porous and fibrous structure as the mechanical resistance experiments let firstly suggest.

II. 3. Swelling abilities of the coatings

As we mention in the previous section, experiments made with rheometer need application of a normal force to obtain reliable measurements. However, the application of this normal force prevents the free development of the coating and obviously modifies the abilities of the coatings to expand. An investigation of the swelling with variation of the normal force illustrates clearly this effect and shows the effects on all coatings (Figure 71).

Figure 71 shows results on IF-2 and shows that swelling abilities vary from 400% to 150% according to the normal force applied on the char. We can also note the fragility of the developed char when normal force is 400N. From 300°C, the measurement of the swelling is erratic and decreases from 150 to 50% due to the crash of the intumesced structure by the upper plate.

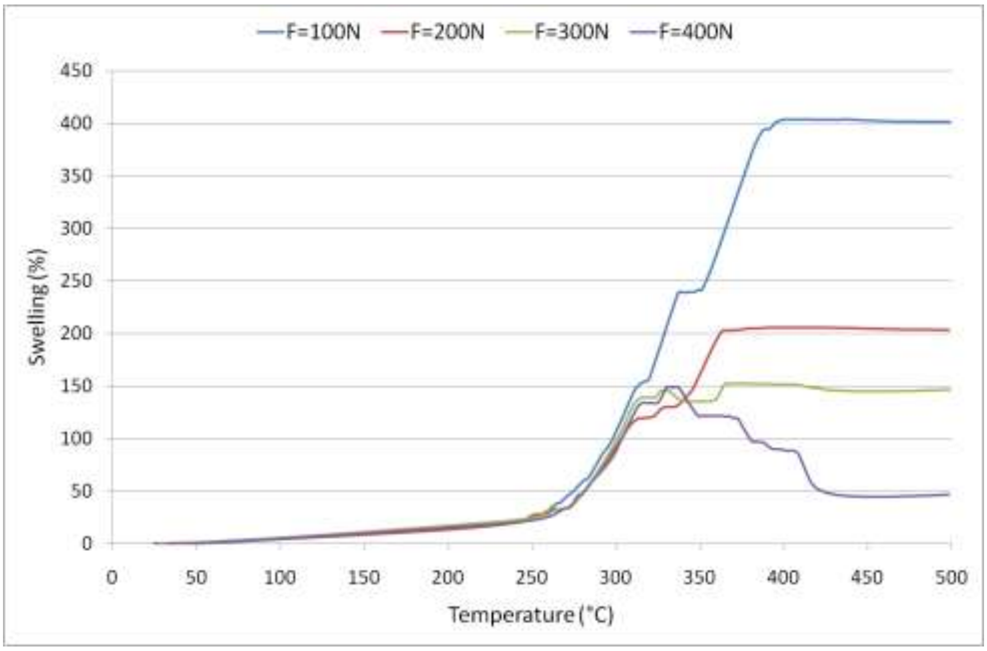

Figure 71 : Influence of the normal force applied by rheometer plates on swelling abilities of coatings (here results of IF-2 are exposed)

Therefore, a new experimental setup has been developed to get a reliable measurement of the swelling without strain. With this protocol, only the three fragile coatings have been analysed because IF-1 is sufficiently robust to swell in rheometer with normal force. Results of IF-2, IF-3 and IF-4 are investigated at two external heat fluxes: 35kW/m² that corresponds to simulation of a fire in development and 50kW/m² that corresponds to the simulation of a developed fire with pre-flashover phenomena [110, 111].

About IF-2 (Figure 72), we can observe the influence of the heat flux applied on the swelling abilities. Under a high heat flux, the expansion of IF-2 is higher at 50kW/m² than at 35kW/m². Without strain, IF-2 exhibits a swelling ratio of 900% at 35kW/m² and 1200% at 50kW/m². Even if the heat conditions are different in rheometer furnace (convective heat at 500°C) and under heat fluxes (radiation), we can compare the two measurements of swelling, respectively done on rheometer (130% viewable on Figure 68) or in cone calorimeter. This comparison allows to clearly show the limitation of swelling caused by the normal force and the strain applied during rheological experiments.

Other change caused by the heat flux variation is the speed of development. Indeed, we can have a rough estimation of this parameter by comparing the slope of the swelling curve. Clearly, we observe a faster development at high heat flux because at the beginning of the test IF-2 growths by 950% in 100 seconds under a 50kW/m² heat flux while it growths only at 450% during the same time at 35kW/m². This quicker growth at high heat flux can be explained by the degradation rate of the material. Indeed, we can assume that material degradation is higher at high heat flux and causes then an important release of volatile products i.e. an important amount of gases trapped into the swollen structure.

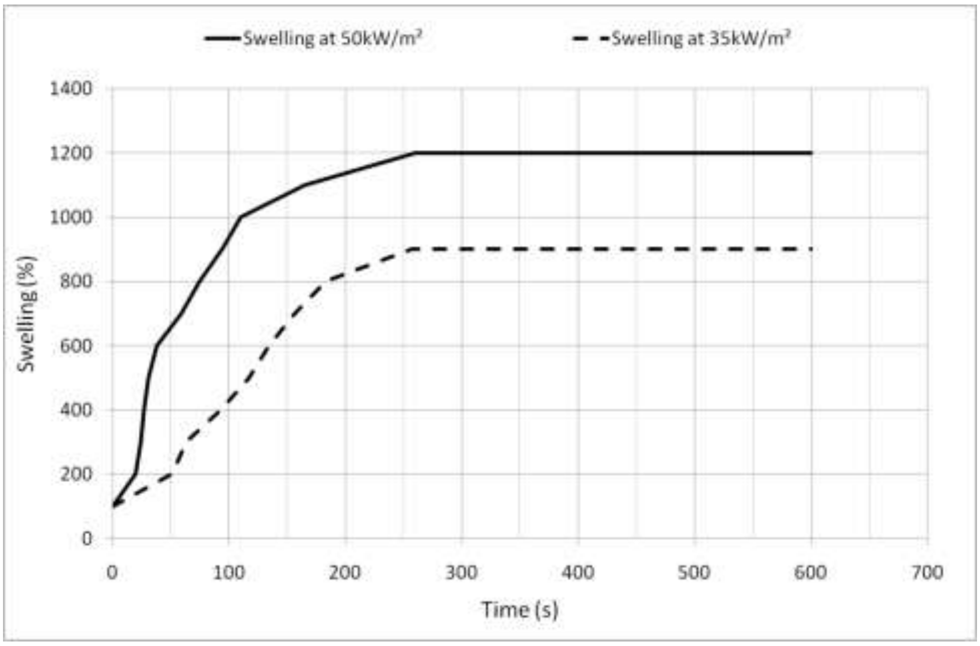

Figure 72 : Expansion measurements of IF-2 exposed to conical heater at two different heat fluxes

Same experiments have been carried out on IF-3. The trends, clearly viewable and exposed with IF-2 in Figure 72, are however more difficult to be stated with IF-3. Indeed, in Figure 73, we observe that the expansion of the char versus heat flux appears very close: the swelling ratio of IF-3 at the end of the test is around 1000% whatever the heat flux. We can however determine a slight difference in terms of swelling speed because the shield develops faster at high heat flux: the complete expansion is reached after 150 seconds at 50kW/m² versus 250 seconds at 35kW/m². It is also noteworthy that time needed to reach the complete development of char at 50kW/m² in the case of IF-3 (i.e. 1000% after 160s) is lower than for a char from IF-2 (i.e. 1200% after 250s). So the behaviour of IF-3 permits to put quickly in place a structure in severe conditions and consequently to provide a protection earlier than IF-2. This information is in agreement with the early intumescent process caused by PER and highlighted by previous rheological experiments.

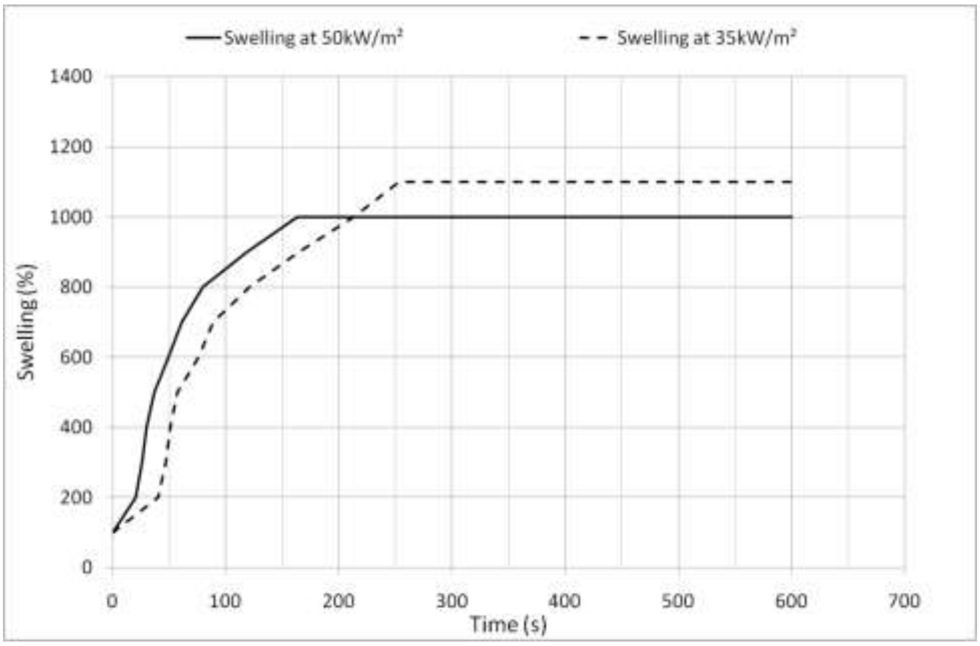

Figure 73 : Expansion measurements of IF-3 exposed to conical heater at two different heat fluxes

Substitution of PER by dipentaerythritol is the main difference between IF-3 and IF-4. We have already observed the consequence of this modification on visco-elastic properties and swelling abilities on the previous section. However, normal force modified our measurements and no conclusion could be reliably drawn.

On Figure 74, we observe the development of the char issued from IF-4 at 50kW/m² and at 35kW/m². Effect of the heat flux is easily viewable on the speed of development, but less evident on the final swelling. Indeed, whatever the heat flux, a swelling of around 700% is reached by the sample. Nevertheless, the steady state is obtained after 150 seconds at 50kW/m² while it occurs after 300 seconds at 35kW/m². The speed of development can be estimated at 650% per 100 seconds at 50kW/m² and at 350% per 100 seconds at 35kW/m². So we note that this speed is lower than in the case of IF-3. This low expansion and this slow speed of development confirm the effect of dipentaerythritol compared from pentaerythritol. Indeed, we have already enounced that the ratio of OH groups is strongly linked to swelling abilities. Consequently use of dipentaerythritol instead of PER in intumescent formulations causes a decrease of the swelling abilities and slows down the growth of the intumescent shield rate because PER has a higher ratio of hydroxyl group than dipentaerythritol.

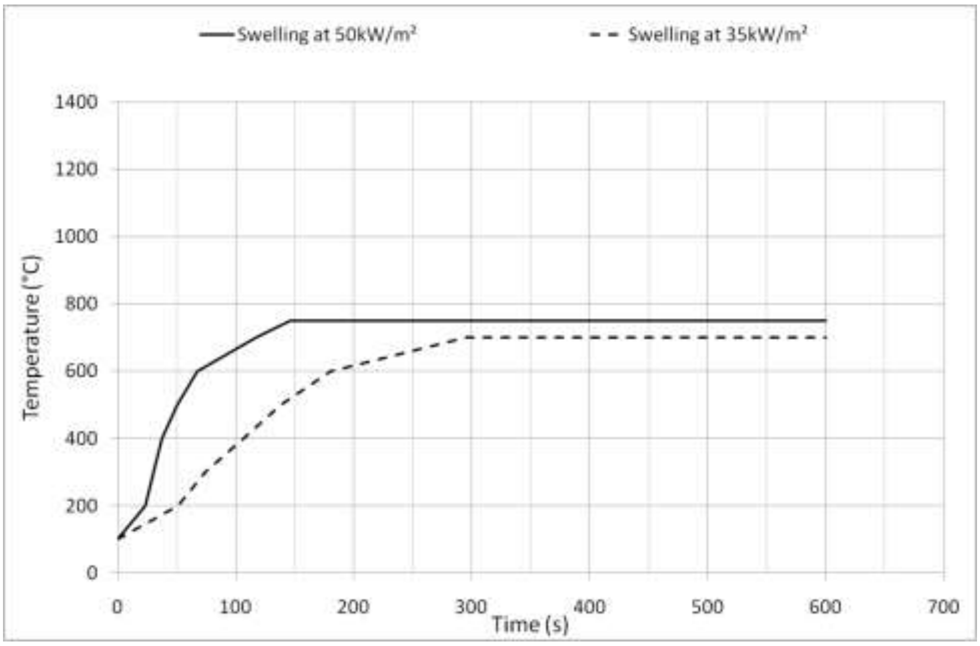

Figure 74 : Expansion measurements of IF-4 exposed to conical heater at two different heat fluxes

To resume about swelling abilities (Table 8), we can firstly remark the effect that is caused by normal force and strain applied by plates on rheological measurements. Even if the heat phenomena that take place in the two devices are different (convection in rheometer furnace and pure radiation in cone calorimeter), a direct comparison of the values shows clearly the limitation implying by the strain. Hence, we have defined a ratio between the swelling abilities measured without normal force and the ones measured with normal force in order to highlight the sensitivity of the char to strain. Higher the ratio, more the char would be affected by strain. Even if the accuracy of this parameter has not been determined, we can obtain some interesting information about the mechanical resistance of the coating. Indeed, when we take into account the swelling at 35kW/m², no significant difference is observed. Whatever the coating, the calculated ratios exhibit values in a narrow range. At low heat flux, the specificities of the formulations and their differences cannot be underlined. On the contrary, at 50kW/m², IF-2 appears clearly as the most sensitive char to strain whereas IF-3 and IF-4 still exhibits values close to the ones at 35kW/m². Thanks to this experimental parameter, we have so underlined the weakness of IF-2 responsible for its failure during jet-fire resistance test.

Table 8 : Swelling abilities obtained with and without normal force and ratio between the two measurements to quantify sensitivity to the normal force

	Measurements with normal force	Measurements at 35kW/m²	Ratio at 35kW/m² (Col.2/Col.1)	Measurements at 50kW/m²	Ratio at 50kW/m² (Col.4/Col.1)
IF-1	140%	-	**-**	-	**-**
IF-2	130%	900%	**6.9**	1200%	**9,2**
IF-3	150%	1100%	**7.3**	1000%	**6.6**
IF-4	110%	700%	**6.3**	750%	**6.8**

Second, with this experimental setup, the effect of substitution of PER (IF-3) by dipentaerythritol (IF-4) is also viewable. Indeed, thanks to PER, IF-3 develops its intumescent shield quicker than IF-4 containing dipentaerythritol. Moreover, IF-4 exhibits a lower swelling rate than IF-3 whatever the heat flux. This can be explained by a lower ratio of OH groups in dipentaerythritol than in PER.

III. Conclusions about physical properties

Thanks to these different experiments, we have determined some fundamental physical properties of intumescent coatings which are known to play an important role to build a performing coating. Indeed investigations in the state of the art have demonstrated that the viscosity of the degraded matrix, the swelling abilities of the formulation and the mechanical resistance of the developed structure are critical factors.

About our four intumescent coatings, we have firstly shown significant differences in terms of viscosity provided by carbon sources (epoxy resin alone or with PER or with dipentaerythritol according to the formulations). Indeed, PER causes the shift of the viscosity decrease at lower temperature (270°C) in IF-3. Consequently swelling and intumescence process begin also at lower temperature for IF-3. Substitution of PER by dipentaerythritol (IF-4) allows to modify the behaviour of IF-3 to a behaviour close to that of IF-2. Indeed, IF-4 exhibits a viscosity decrease and begins to swell at higher temperature than IF-3 and we suspect this modification to provide better fire properties to IF-4 than to IF-3. These results must be linked with the behaviours observed for jet-fire tests. Indeed, the IF-3 failure and the flowing of char observed for jet-fire test can be partially explained by the visco-elastic properties. Indeed, we can suggest that phenomenon of flowing that occurs on the back faces can be the consequence of a too low viscosity of the melt phase, as observed at 220°C in our rheological experiments. In similar conditions in jet-fire test, IF-4 presents a better performance because this flowing disappears in agreement with the change observed for rheological experiments with our coatings and in literature when PER is substituted by dipentaerythritol.

The mechanical resistance is also a crucial parameter for an efficient protective shield and this parameter could explain the failure of IF-2 and IF-3 without mesh. Our experiments allow to conclude that IF-1 is the most robust and dense char, its char appears as not sensitive to any strain. Presence of boric acid and a high content of silicate in IF-1 explain this property and have been well studied by Jimenez [105]. On the contrary, the three other coatings do not exhibit any resistance facing to the least force applied on the top of the char during experiments carried out in the rheometer. This sensitivity to strain is shown by experiments in rheometer to evaluate the mechanical resistance but also by comparing the swelling abilities of the coatings in rheometer and in free conditions. Indeed a new experimental setup has been developed and it permits to reach the swelling abilities in radiative conditions without application of normal force. This methodology highlights the limitations of the expansion implying by any strain on coatings. Thanks to an empirical parameter (ratio between the two swelling measurements with and without normal force), we have determined that IF-2 and IF-3 are the most sensitive coating to strain. This confirms thus previous results observed for IF-2 and for IF-3 during jet-fire test resistance that fail in the impact zone where pressure is maximal and where no coating resists to impact.

Therefore, physical approach provides us interesting information about the intumescent process. Some conclusions target the role of boric acid and the effect of the carbon sources on the visco-elastic behaviours or on the mechanical resistance of the formulations. Strongly linked with the efficiency of the char of these mixtures, these properties have been shown by physical approach but could be explained by the investigation of the chemical evolution that takes place inside these formulations. That is why the next chapter is dedicated to the chemical approach of the intumescent process focused on the role of the carbon source and the slight differences known inside IF-2, IF-3 and IF-4.

Chapter IV: Chemical approach of the intumescent process

Intumescent coatings are designed to maintain the steel integrity under severe conditions. As discussed in Chapter I, we know that intumescent formulations are generally based on three "active" ingredients:

- A carbon source (polyols such as PER or dipentaerythritol) to provide carbons needed to form the carbonaceous structure,
- An acid source (usually ammonium polyphosphate APP) to dehydrate the carbon source from an accurate temperature or in presence of flames.
- A blowing agent producing non-flammable gases that cause expansion of the carbonaceous structure.

APP-PER systems have been widely studied and their mechanism of action has been elucidated [70] and detailed in the state of the art. Several synergisms have also been observed with APP and notably combination of APP with boron compounds (e.g. H_3BO_3, Zinc Borate…) and TiO_2 (ingredients widely used in intumescent paints notably in our formulations). The reactivity of APP with boron derivatives has shown to be beneficial in terms of thermal stability and fire protection in intumescent paints [74, 112] because of the formation of borophosphates. On the contrary with TiO_2, the formation of TiP_2O_7 (reaction between phosphate and TiO_2) is less investigated and conclusions are opposite: some papers [85, 113] conclude to a beneficial contribution of the interaction between APP and TiO_2 in terms of mechanical properties and fire performance while others [114] do not report any benefit. One of the purposes of this section will thus be to investigate the reactivity of APP with TiO_2 in each formulation and to clarify the potential benefit of such reaction.

In addition the results for jet-fire test (Chapter II) and first investigations of the physical behaviours (Chapter III) have underlined the influence of the carbon source and notably the effect of the substitution of PER by dipentaerythritol. We have shown that carbon source could allow a shift of the temperature range where intumescent process occurs, PER based systems developing their intumescence at lower temperature than dipentaerythritol based ones. So the second purpose of this chapter will be to investigate the chemical changes of the systems due to use of different carbon sources and to elucidate the role of each carbon donor.

To carry out these investigations, in a first step, basic mixtures based on active components in our intumescent formulations have been studied. This preliminary investigation should provide some information about the mechanism of degradation of the intumescent formulations, the respective role of the carbon sources and the effect of TiO_2. To determine the chemical degradation pathways, we have first studied the thermal stability of the mixtures then by using relevant techniques, we have analysed the residues of mixtures after a 3 hours of heat treatment at a characteristic temperature of the intumescent process.

In a second step, a similar approach has been followed to study IF-2, IF-3 and IF-4 in order to highlight the interaction and the reactivity between the different components in presence of the resin and of others ingredients such as silicates for example. IF-1 is excluded of this study because its formulation is widely different since it contains boric acid. The effect of boric acid has already been observed on physical properties in the previous chapter and the chemical investigation is reported in details in the literature [74, 105]. As a conclusion, we should propose a chemical degradation pathway for IF-2, IF-3 and IF-4.

I. Materials and experimental details

I. 1. Material

A complete presentation of the intumescent formulations has been made at the beginning of the second chapter. Nevertheless, it is useful to remind the main active components.

The investigation is based on the study of three different epoxy based intumescent coatings, IF-2, IF-3 and IF-4. On the three formulations an ammonium polyphosphate, AP422 from Clariant, is added as both acid source and blowing agent (because of the release of ammonia) [76]. In addition the carbon source is played respectively by the epoxy resin on IF-2, by both epoxy resin and pentaerythritol (PER) on IF-3 and by both epoxy resin and dipentaerythritol (dPER) on IF-4 (Table 9). Furthermore, additives used on paint formulations have been added (pigments, surfactant and mineral fillers) but the exact composition of the coatings are not known. One of these additives will be investigated: TiO_2 that is suspected to play a role in the chemical degradation pathway of the systems.

Table 9 : Comparison between the active ingredients of 3 formulations

Intumescent coating	Polymeric matrix	Acid source	Carbon source	Blowing agent
IF-2	DGEBA epoxy resin	APP	Epoxy resin	APP
IF-3	DGEBA epoxy resin	APP	Epoxy resin + PER	APP
IF-4	DGEBA epoxy resin	APP	Epoxy resin + dPER	APP

First, to focus our investigation on intumescent process we have carried out experiments with basic mixtures containing the “active” ingredients of intumescence. The systems studied are mixtures based respectively on APP-Epoxy, APP-PER and APP-dPER containing or not TiO_2. Ratios (Table 10) between these different components have been chosen according to those used in intumescent formulations.

Table 10 : APP/Carbon source/TiO_2 ratio of the basic mixtures

Composition	APP	Epoxy Resin	PER	dPER	TiO_2
APP/Epoxy	60	40	-	-	-
APP/Epoxy/TiO_2	56	36	-	-	8
APP/PER	60	-	40	-	-
APP/PER/TiO_2	56	-	36	-	8
APP/dPER	60	-	-	40	-
APP/dPER/TiO_2	56	-	-	36	8

Our investigations have been so carried out firstly on six basic mixtures that could provide a first idea about the chemical degradation mechanism of the complete intumescent formulations. Indeed, the use of three carbon sources represents the main (known) difference observed on IF-2, IF-3 and IF-4.

I. 2. Thermal stability

Thermo-gravimetric analyses were carried out at 10°C/min under synthetic air (flow rate = 100mL/min, Air Liquide grade), using a TA SDT Q-600. The samples (approx. 10mg) in powder form were placed in open alumina pans, using gold sheets in order to avoid reactions of the phosphorus species of the coating with alumina.

In order to determine whether a potential increase or decrease in the thermal stability happens between the studied ingredients, the weight difference curves between experimental and calculated TGA curves were computed as follows [72]:

- $W_{intu}(T)$: values of weight given by the TGA curve of the intumescent ingredients (APP + Carbon source),
- $W_{TiO2}(T)$: values of weight given by the TGA curve of TiO_2,
- $W_{exp}(T)$: values of weight given by the TGA curve of the basic mixture (APP + Carbon source + TiO_2),
- $W_{the}(T)$: theoretical TGA curve computed by linear combination between the values of weight given by the TGA curve of the intumescent mixtures and TiO_2: $W_{the}(T) = x.W_{TiO2}(T)+(1-x).W_{intu}(T)$ where x is the content of TiO_2 in the mixtures.
- $\Delta W(T) = W_{exp}(T)-W_{the}(T)$: weight difference curve.

Therefore, the $\Delta W(T)$ curves allow us to show a potential increase or decrease in the thermal stability of the system due to the presence of TiO_2.

I. 3. Heat treatment

Thanks to the thermo-gravimetric curves, we are then able to determine five characteristic temperatures (heat treatment temperature: HTT) in order to simulate the evolution of the intumescence structure. Heat treatments have been carried out under synthetic air in tubular furnace following the temperature-time program shown in Figure 75.

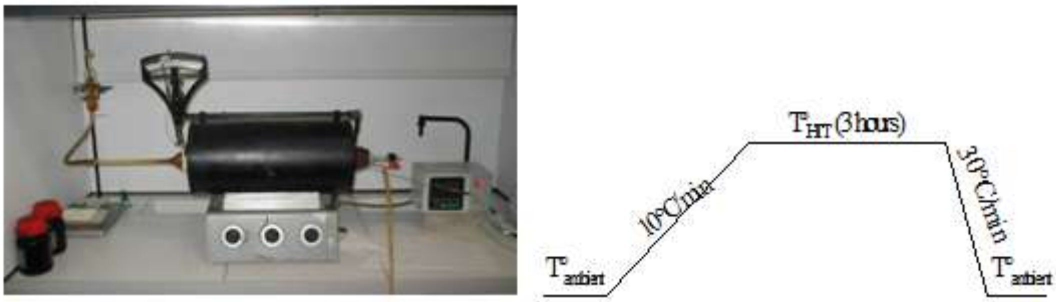

Figure 75 : Experimental setup and temperature profile of the heat treatment in tubular furnace

The coatings are heat treated for three hours at these specific temperatures in a tubular furnace and the products are then grinded as powder in order to carry out chemical analyses. The heat treated residues are then analysed by XRD and solid state NMR.

I. 4. X-Ray diffraction

The X-Ray diffraction (XRD) analyses allow us to characterize the crystallized products in the char. Samples have been analyzed to investigate the structure of the intumescent char and its composition.

XRD spectra were recorded in the [5°–60°] 2-theta angle range using a Bruker AXS D8 diffractometer with radiation Cu K_{α} ($\lambda_{(Cu\ K\alpha)}$ = 1,5418 Å) in configuration 2θ/θ. The acquisition parameters were as follows: a step of 0.02°, a step time of 2 s. The data are analysed using the diffraction patterns of Inorganic Crystal Structure Database (ICSD).

The ICSD is a comprehensive collection of crystal structure entries for inorganic materials, produced by Fachinformationszentrum Karlsruhe, Germany, and the National Institute of Standards and Technology, US. ICSD includes records of all inorganic crystal structures with atomic coordinates published since 1913. The data base contains more than 70 000 record.

I. 5. Solid state NMR

The high-resolution solid-state NMR spectroscopy was performed using a Bruker Avance II 100 and a Bruker Avance II 400 spectrometer at a spinning speed of 5kHz and of 10kHz respectively (exception are mentioned when results are presented). Bruker probe heads equipped with 7mm (Bruker 100) and with 4mm (Bruker 400) MAS (Magic Angle Spinning) assembly were used.

The low abundance of some atoms compared to the protons leads to poor absorption of the radiofrequency pulse in a FT-NMR experiment. This limitation can be overcome by exciting the protons in a sample followed by a sequence of two series of long-time pulses which make the protons and the other nuclei resonate at the same frequency. The latter is called the "Hartman-Hahn" condition and the process is called "Cross-polarization" (CP). The time of cross-polarization is called the "contact time". Cross-polarization leads to a large enhancement of the excitation of the nuclei. The large number of protons in the sample however interferes with the decay of the isolated nuclei due to weak interactions of the spins. This dampening of the signal can be removed by a strong radio frequency signal which essentially holds the protons in a highly resonating state so they are not capable of absorbing resonance from the nuclei. This is called "^{1}H Dipolar Decoupling (DD)".

^{13}C NMR measurements were performed at 100.8 MHz (9.4 T) with CP-MAS-DD. All spectra were acquired with contact times of 1ms and a repetition time of 5s was used for all the samples. Typically, 1024 scans (or 2048 for samples heat-treated at high temperature) were necessary to obtain spectra with good signal to noise ratio. Tetramethylsilane was used as the reference.

^{31}P NMR measurements were performed at 40.5 MHz (2.35 T) using MAS. A repetition time of 120s was used for all samples. H_3PO_4 in aqueous solution (85 %) was used as reference.

II. Basic mixtures based on intumescent ingredients and TiO_2

II. 1. Thermal stability

II. 1. a) Basic mixtures based on APP and different carbon sources

First step of this study investigates the influence of the carbon source on the thermal stability of the systems without TiO_2. In Figure 76, we observe the thermal stabilities of each component.

From the TGA curves, it can be seen that APP has no weight loss before 300°C. The mechanism of degradation of pure APP has been widely investigated [76, 87]. The weight loss around 20% over the range of 290 – 500°C is attributed to APP decomposition releasing NH_3 and H_2O. The weight loss over the range 500 – 650 °C can be attributed to the sublimation of P_2O_5 [115]. The residual weight is 20% at 800°C.

The three carbon sources exhibit different behaviours. The degradation of pentaerythritol occurs between 220 and 300°C. The weight loss is mainly due to PER dehydrating, then dehydrogenizing and charring. Similarly, dipentaerythritol begins to degrade at 300°C and is almost completely degraded at 400°C (a first degradation step can be observed before 300°C corresponding to degradation of around 5% of PER contained in commercial dipentaerythritol). Then after 400°C, the degradation rate is slower until 570°C, this last step should correspond to the rupture of C-O-C bond. Finally, the degradation of the epoxy resin occurs in two main steps: a first step between 300 and 460 °C, corresponding to a weight loss of 80% and a second step between 460 and 600°C leading to the total degradation of the resin. The mechanism of thermal degradation of the cured epoxy resin has been studied by different authors. According to Grassie et al. [116], the weakest points in the cross-linked resin network should be the N-C and the O-CH_2 bonds. However, the high concentration of hydroxyl groups in the cured resin favours localised intra-molecular hydrogen bonding which would promote dehydration as it has been found in other studies [117, 118]. In the other hand, Keenan and Smith [118] postulated that primary degradation occurs at the N-C_6H_5 bond and most likely at the C_6H_5-$C(CH_3)_2$-C_6H_5 bonds by homolytic rupture to produce free radicals. Complex secondary reactions then occur to lead to the formation of small molecules such as phenols or cresols found during degradation of cured epoxy

Finally, titanium dioxide exhibits no weight loss up to 800°C and is thermally stable.

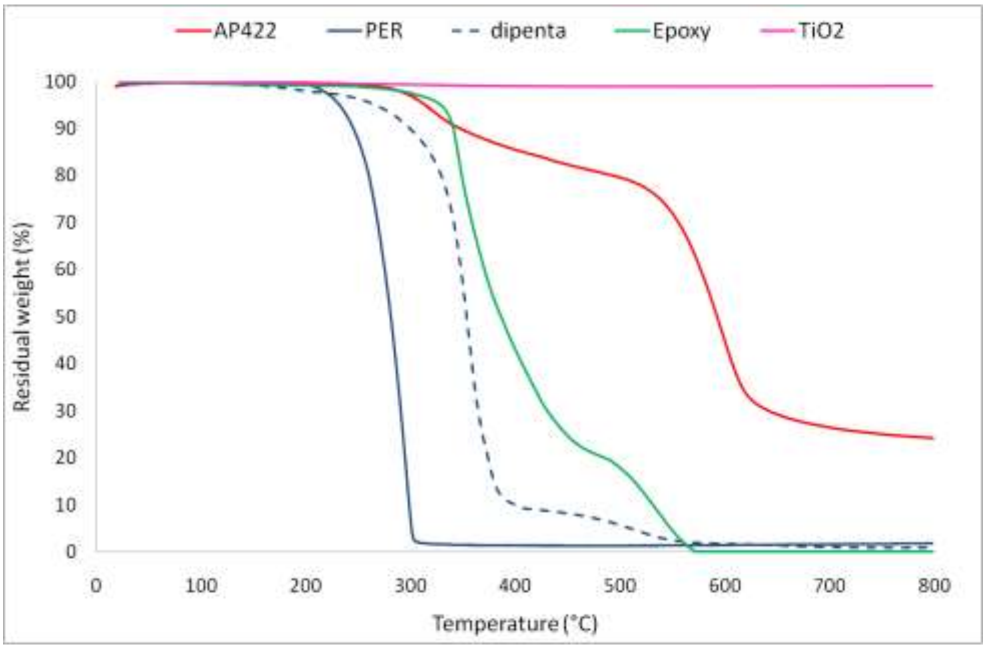

Figure 76 : TGA curves of the pure components in air at 10°C/min

The thermal stability of the basic mixtures without TiO_2 is reported in Figure 77. Whatever the composition, degradations occur in three main steps:

- Between 200 and 400°C, two degradation steps occur successively. The determined temperatures of degradation are correlated with those observed on the TGA curves of pure products (Figure 76) because we observe degradation of APP/PER from 190°C, APP/dPER from 205°C and APP/Epoxy from 250°C. Those temperatures are close to the respective degradation onset of pure carbon sources.
- The last step, which could be attributed to the oxidation of the formed char, occurs at higher temperature (between 600 and 700°C) that is significantly different according to the carbon source: the degradations of APP/PER and APP/dPER begin at lower temperature than that of APP/Epoxy.

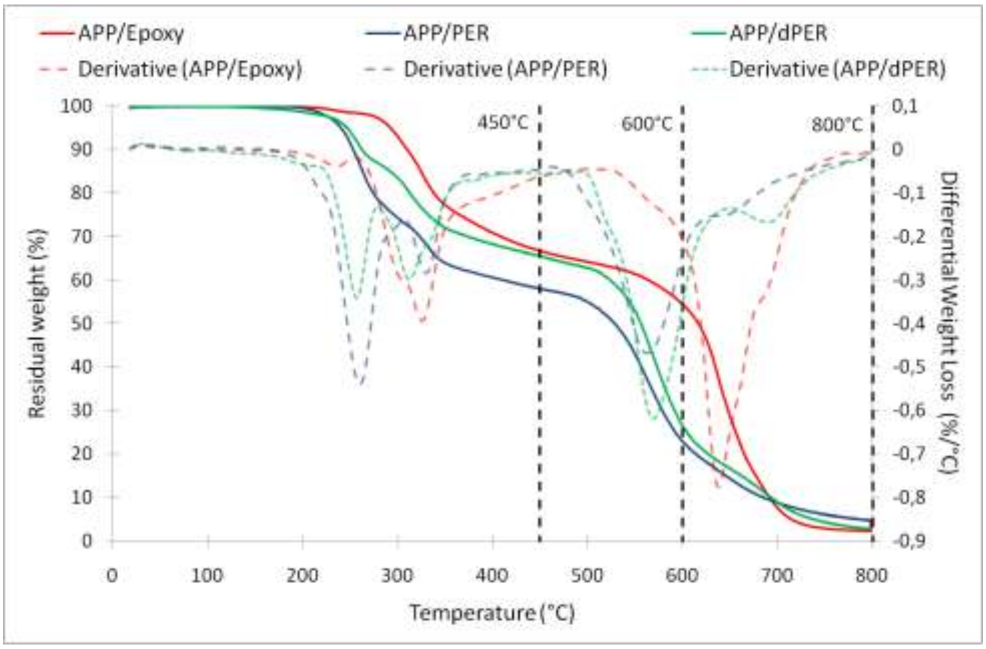

Figure 77 : TGA and derivative TGA curves of the mixtures based on APP and carbon sources in air at 10°C/min

Regarding the curves, it is obvious that APP/PER is the less stable, APP/Epoxy exhibits the higher thermal stability and the behaviour of APP with dipentaerythritol seems to be intermediate. This stability ranking is in agreement with those of carbon sources but results also of an interaction between the two different components. Indeed, literature [86, 119] reports that APP and PER react together at 200°C: phosphoric ester bonds are formed first by alcoholysis of the polyphosphate chain, then alcoholysis and/or esterification leads to cyclic pentaerythritol phosphate structures inserted in the polyphosphate chains. Similarly, first step of APP/dPER degradation occurs on temperature range from 250 to 350°C, in agreement with dPER TG curve. We could assume that similar interactions/reactions occurs between dipentaerythritol and APP. The increase of the temperature at which the interaction happens could be explained because the dehydration ability of the dimer is lower than the one of pentaerythritol (lower ratio of hydroxyl sites compared to carbons). Finally, APP and cured epoxy resin react together at 320°C. The high temperature of reaction can also be explained by the high temperature of degradation of epoxy resin (viewable on Figure 76) and by the lower reactivity of epoxy chain with APP.

The residue obtained after those first steps of degradation is more stable in the case of dipentaerythritol and epoxy resin than in the case of PER. Finally, the last step of degradation (oxidation) occurs at similar temperature (from 550°C to 600°C) for APP/PER and APP/dPER while it is delayed for APP/Epoxy from 600°C to 700°C. This difference of temperature of oxidation could provide information about the sensitivity of the char to oxidation. The char resulting from the mixture between APP and epoxy is less sensitive to oxidation than the two other char. Nevertheless, the final residual weight is very close whatever the mixtures compositions.

Thanks to this investigation about thermal stability, three heat treatment temperatures can lead to interesting information and further analysis at those temperatures should be carried out. Those temperatures are:

- T=450°C, the evolutions of APP/Epoxy and APP/dPER seem to be similar with a residual weight (RW) of 65% whereas APP/PER is more degraded (RW=55%).
- T=600°C, the mixtures between APP and PER or dipentaerythritol present a RW=25% whereas the residue of the APP/Epoxy system is around 60%.
- T=800°C, whatever the carbon source, the degradation is almost completed and the residual mass is lower than 5%.

Therefore, carbon sources used on these mixtures exhibit different thermal behaviours and cause change on thermal stability of the mixtures. Among the three main steps of degradation, we can observe that at low temperature epoxy resin improves the stability of the mixtures, by comparison with PER and dipentaerythritol. This improvement is also viewable at high temperature because the onset temperature of last step is also increased of 100°C with epoxy resin, without modifying the final residual weight.

II. 1. b) Basic mixtures based on APP, different carbon sources and TiO_2

In addition to these mixtures and to study the influence of TiO_2 and the potential reactivity between phosphorus-based components and titanium dioxide, TGA curves of APP/Carbon source/TiO_2 systems have been carried out. The modification of the thermal stability is investigated comparing the theoretical and the experimental TGA curves according to the method described in the experimental section of this chapter.

For APP/Epoxy/TiO_2 mixtures (Figure 78), we do not observe any difference between the experimental and the calculated curves up to 620°C, evidencing that no interaction between TiO_2 and APP/Epoxy occurs until this temperature. On the contrary, after 620°C, a significant improvement is viewable and lead to the assumption that a reaction between TiO_2 and the degradation products of APP/Epoxy occurs leading to the formation of a thermally stable residue.

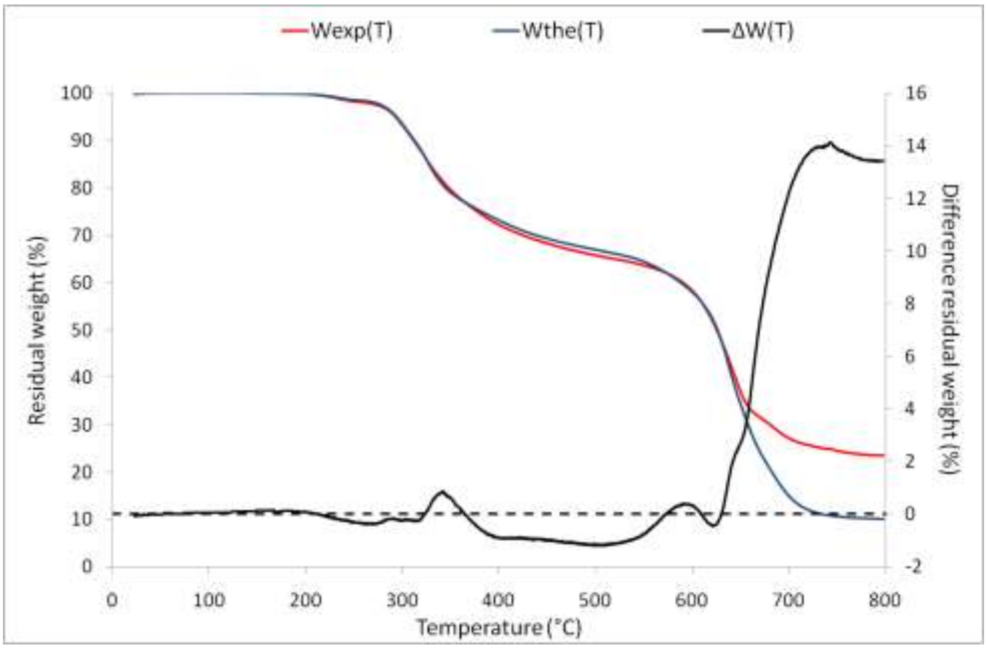

Figure 78 : TGA and difference weight loss curves of APP/Epoxy resin/TiO_2 in air at 10°C/min

At the contrary, in the case of APP/PER/TiO_2 mixtures (Figure 79), a large stabilization is observed from 220°C up to 800°C. This effect is mainly observable between 500 and 800°C (between 220°C and 500°C, the difference of residual weight is only 3%). Thus, it can be concluded that, as observed in the case of epoxy resin, the stabilization provided by TiO_2 occurs at high temperature when a reaction between TiO_2 and products of a first step of degradation between APP and PER could take place.

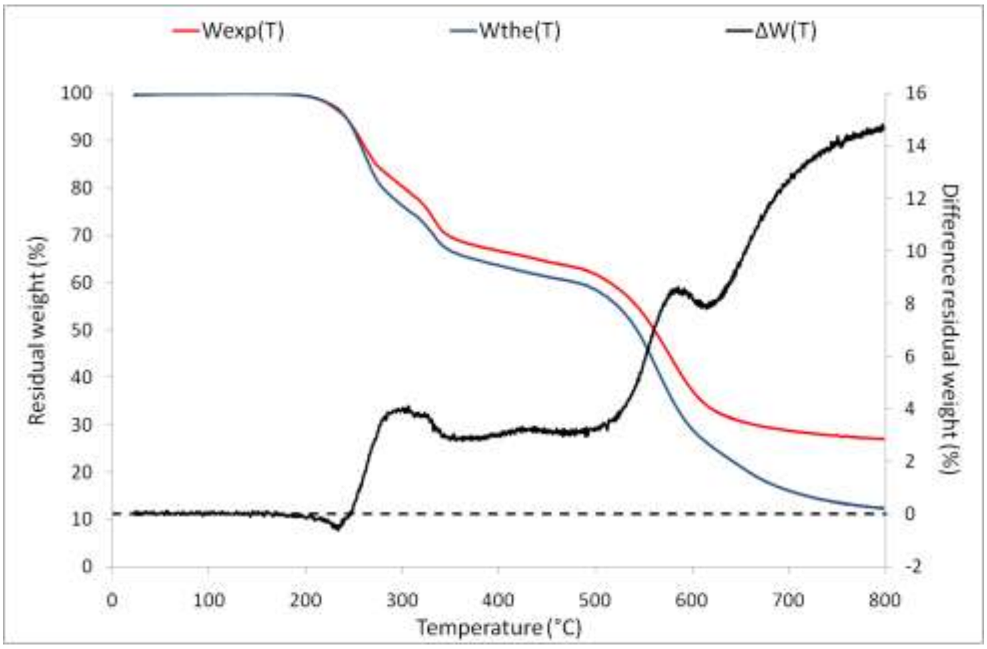

Figure 79 : TGA and difference weight loss curve of APP/PER/TiO_2 in air at 10°C/min

Finally, the behaviour of APP/dPER/TiO_2 (Figure 80) is similar to that of APP/PER/TiO_2. No interaction is detected up to 500°C. At higher temperature, a large stabilization is observed and it suggests a reaction between TiO_2 and degradation products of APP and/or APP/dPER.

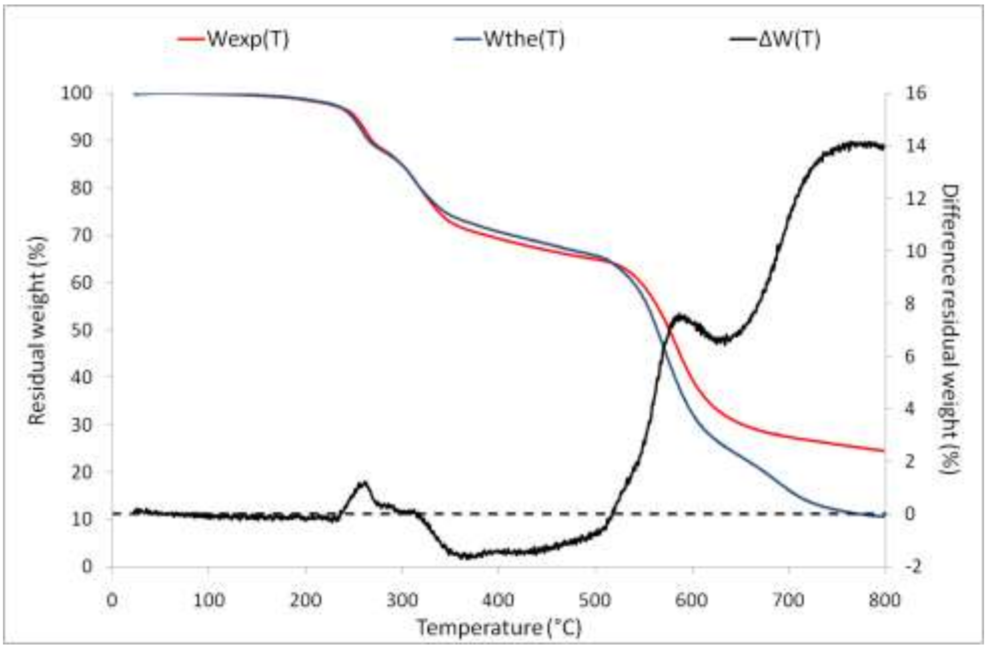

Figure 80 : TGA and difference weight loss curve of APP/dPER/TiO_2 in air at 10°C/min

About the effect of TiO_2, whatever the carbon source we cannot observe any significant modification on the difference weight loss curves consequently to the addition of TiO_2 up to 500°C for PER and dPER mixtures (up to 600°C for APP/Epoxy/TiO_2). However, from this temperature, a significant stabilisation is observed and potential interaction and/or reaction is suggested between TiO_2 and the products issued from the APP-carbon sources degradation. Thanks to TiO_2, the residual weight of the mixtures at 800°C is doubled, going from around 10% (corresponding to thermally stable TiO_2) to 20% (attributed to a thermally stable products based on titanium derivatives).

II. 2. X-Ray diffraction analyses of the residue

In order to go further in the understanding of the above observed phenomenon (thermal stabilisation at high temperature), APP/Carbon sources mixtures and APP/carbon source/TiO_2 mixtures have been heat treated at T = 450°C for 3 hours in a tubular furnace in oxidative conditions, according to the profile exposed in Figure 75. This temperature has been chosen in order to observe products resulting from the interaction between TiO_2 and the degradation products of APP-Carbon sources. Indeed, even if this interaction between components has been detected in TGA curves from 500°C (or 600°C), previous investigations lead in the laboratory have shown a kinetic difference between a degradation in tubular furnace (isotherm heat treatment for three hours) and a dynamic degradation in TGA device (rate of 10°C/min). We can thus assume empirically that step of degradation observed from

500°C in TGA curves occurs at lower temperature after three hour-heat treatment in tubular furnace. The residues have then been analyzed using adapted spectroscopic tools.

II. 2. a) Basic mixtures based on APP and different carbon sources

The first analytical tool used to identify the product is X-Ray diffraction. Whatever the carbon source, diffractograms of residue after heat treatment at 450°C (Figure 81) are similar. The residues exhibit a charred structure and their spectra exhibit a broad band (centred on $2\theta = 22–23°$) suggesting the formation of an amorphous product containing carbons [112, 120]. It is well recognized that the carbon structure obtained when the intumescent process occurs is poorly organized [74, 121]. It could also be noted that at this temperature APP (a crystallised compound) is no more observed. It is not surprising according to the TGA curve of the APP reported in Figure 76 demonstrating that the weight loss at this temperature is around 20%. Indeed, at this temperature APP decomposes firstly to yield polyphosphoric acid and evolving ammonia (first step of the TGA curve), then between 360 and 420 C, the polyphosphoric acid reacts with the carbonaceous compound to form a phospho-carbonaceous structure, namely char [122].

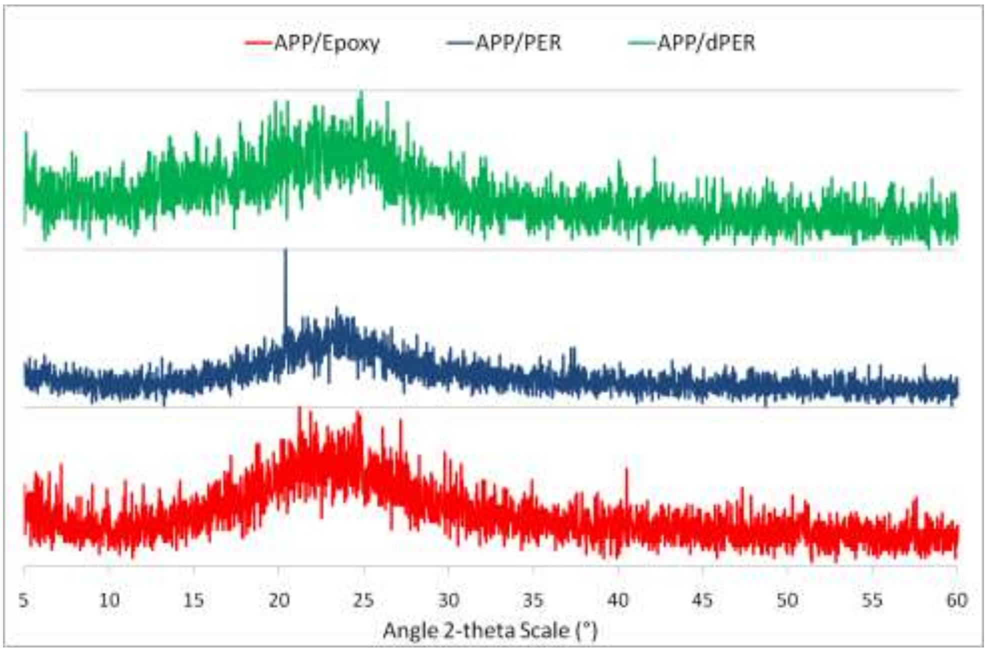

Figure 81 : X-Ray diffractograms of basic mixtures APP/Carbon source after heat treatment at T=450°C

II. 2. b) Basic mixtures based on APP, different carbon sources and TiO_2

When TiO_2 is added in the mixture, the behaviour of the ternary systems differs from one system to another (Figure 82). Indeed, after heat treatment at T = 450°C, a well-defined diffractogram for the two mixtures composed by APP/Epoxy/TiO_2 and APP/PER/TiO_2 is observed. This well-defined diffractogram may be attributed to the presence of TiP_2O_7 [114, 123, 124], whereas peaks of TiO_2 are not viewable anymore thanks to direct comparison with Figure 83. As a consequence, it can be proposed that a reaction between APP and/or its degradation products and TiO_2 leading to the formation of TiP_2O_7 occurs at high temperature. In other hand, the addition of TiO_2 in APP/dPER system does not lead to the formation of titanium pyrophosphate since only a broad band centred around 2theta=22° is viewable. This diffractogram is similar to the one obtained previously when the APP/dPER system was heat treated without TiO_2.

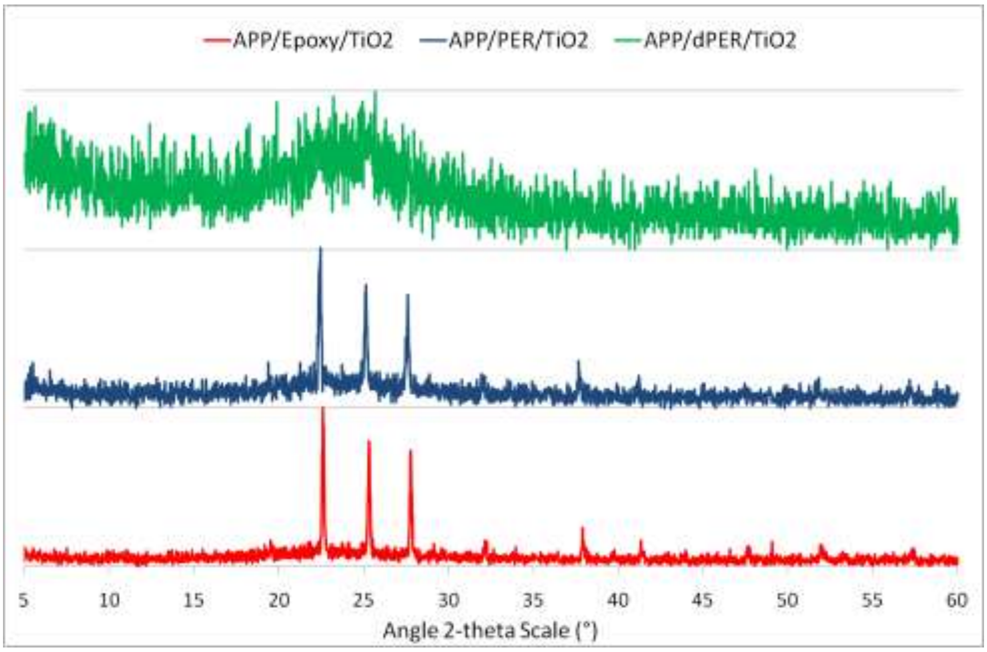

Figure 82 : X-Ray diffractograms of the ternary systems APP/Carbon source/TiO_2 after heat treatment at T=450°C

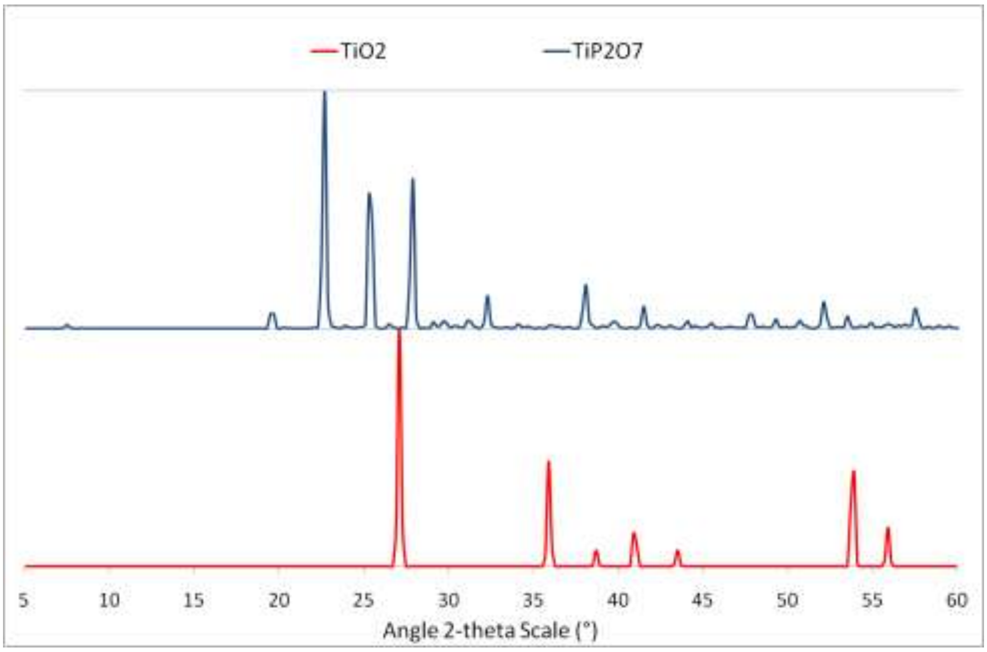

Figure 83 : X-Ray diffractograms of TiO_2 (red) and TiP_2O_7 (blue)

The X-Ray diffraction analyses demonstrate that TiO_2 modifies the chemical evolution of the basic mixtures based on APP/Epoxy and APP/PER. The product resulting from a reaction between TiO_2 and APP or its degradation products was identified as TiP_2O_7. This reaction does not occur before T = 450°C when the carbon source used in the mixture is dipentaerythritol. In order to go further in the understanding, ^{13}C NMR and ^{31}P NMR analyses were used to follow the changes respectively of the carbon structure and of the phosphorus species present in the char.

II. 3. ^{13}C NMR spectra of the residue

II. 3. a) Basic mixtures based on APP and different carbon sources

The CP/DD-MAS ^{13}C spectroscopy is a powerful tool to characterize the carbonaceous materials and, thus, to confirm the hypothesis proposed from the previous X-Ray diffractograms. The ^{13}C NMR spectra of the binary systems are presented in Figure 84. They exhibit a broad band centred at 130ppm. The broadness of the band implies the presence of several non-magnetically equivalent carbons [74, 86]. Thus, it may be assumed that a not well-organized structure is observed. This result is in good agreement with the data obtained from X-Ray diffraction analyses that demonstrate that an amorphous structure is obtained. Moreover, the chemical shift of this band leads us to assign the carbon present in the char to unsaturated C=C bonds mainly present in aromatic and polyaromatic species [125]. Furthermore, oxidation of the char can also be proposed since the large band present an overlap between 150 and 170ppm, in particular in the case of APP/Epoxy and APP/PER.

In addition, we can distinguish a small band between 0 and 50ppm on the spectra of the APP/PER and of the APP/dPER mixtures. This band can be assigned to aliphatic carbons from polyol derivatives even if the high temperature suggests its degradation.

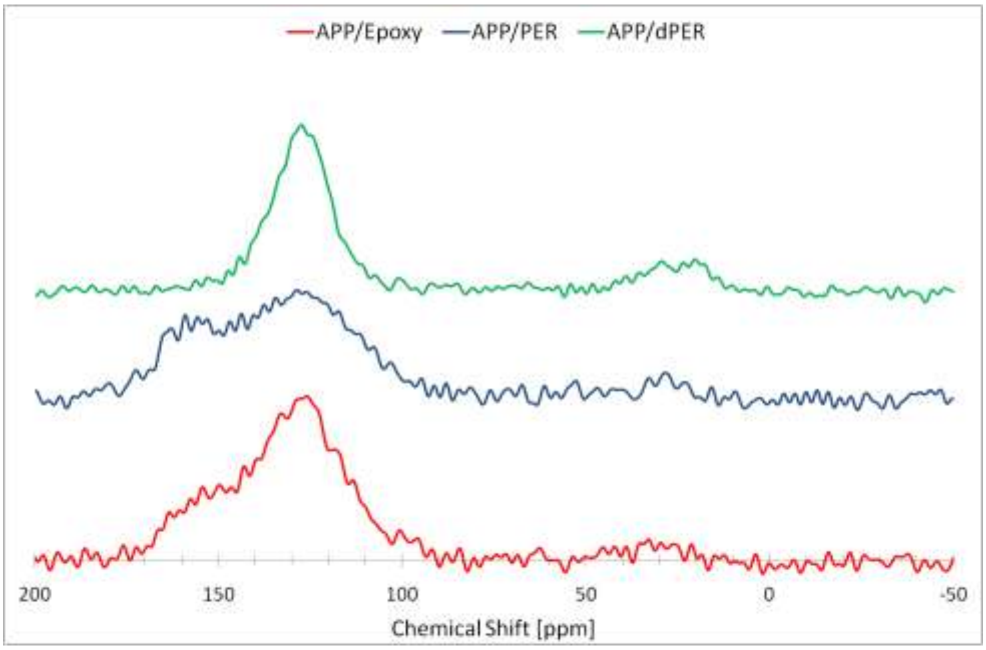

Figure 84 : ^{13}C NMR spectra of the binary systems APP/Carbon source after heat treatment at T=450°C

Whatever the carbon source used in the binary systems (APP/carbon source), the residues obtained after heat treatment at 450°C present a carbonaceous structure (aromatic/polyaromatic stacks that is partially oxidised).

II. 3. b) Basic mixtures based on APP, different carbon sources and TiO_2

Figure 85 reports the ^{13}C NMR spectra of the ternary basic mixtures after heat treatment at T = 450°C. Similarly, to the results obtained in the case of the binary system, a broad band centred at 130ppm is observed for the three carbon sources demonstrating that part of the carbon is included in amorphous aromatic/polyaromatic condensed structure. In the case of APP/Epoxy and APP/dPER, the spectra obtained with and without TiO_2 are more or less similar even if their broadness is higher with TiO_2, above all for APP/dPER/TiO_2 compared to APP/dPER. However, the spectrum of the residue obtained from APP/PER/TiO_2 shows, in addition to the band at 130ppm, additional broad band (with three main peaks) centred at 30ppm that can be assigned to aliphatic carbons. This band is not observed in the case of the binary system without TiO_2 and the presence of aliphatic carbons on mixtures at this temperature is surprising because at 450°C PER is totally degraded. This band can attributed to alkyl carbon type $–CH_2-$ [125]. So, not attributed to PER, such aliphatic groups could be yielded during the degradation mechanism and the formation of the protective structure and trapped in the polyaromatic shield. We could suspect a modification of the degradation mechanism causing not only the formation of an intumescent structure but also aliphatic species thermally stable and trapped into the structure.

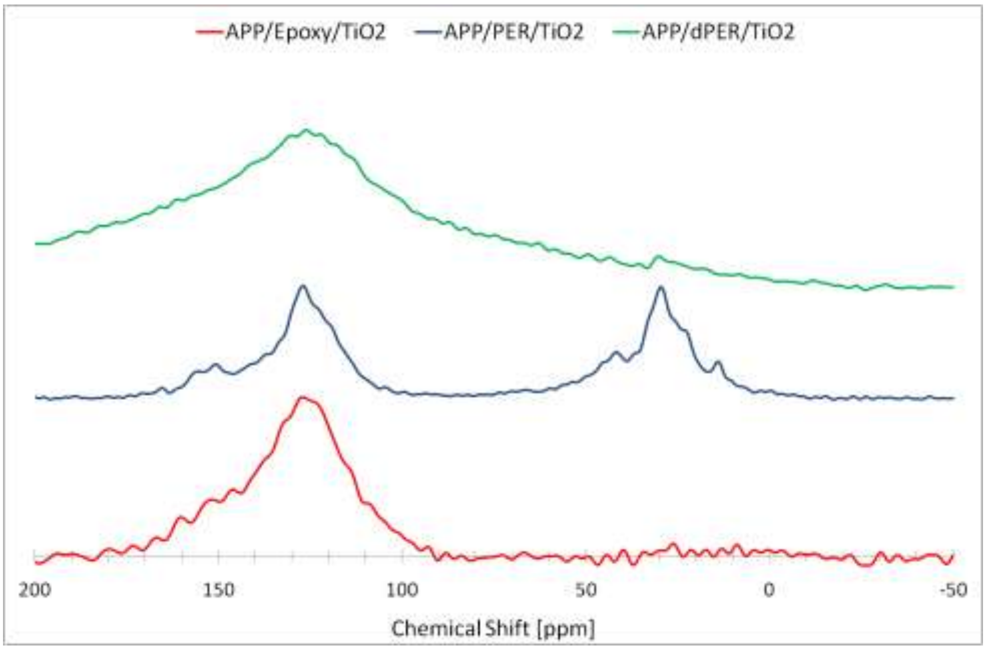

Figure 85 : ^{13}C NMR spectra of the ternary systems APP/Carbon source/TiO_2 after heat treatment at T=450°C

Therefore, ^{13}C solid-state NMR highlights the formation of the carbonaceous char at 450°C. Whatever the composition of the mixtures, the characteristics broadband centred at 130ppm is observed, demonstrating the development of the condensed structure composed of aromatic and polyaromatic species, these species can be partially oxidized in particular in the case of char resulting from the degradation of APP/Epoxy and of APP/PER that appear more oxidized than char of APP/dPER.

Concerning TiO_2, this additive does not modify the global mechanism of degradation for two systems: APP/dPER and APP/Epoxy. However, we could suspect with APP/PER/TiO_2 that stable aliphatic carbons are yielded during the degradation and trapped into the structure. Indeed, ^{13}C NMR allows us to demonstrate the formation of the carbonaceous structure from 450°C whatever the composition with and without TiO_2. This carbonaceous structure is mainly composed of aromatic and polyaromatic species (mixed with aliphatic carbons for APP/PER/TiO_2) and is issued from a reaction between APP and carbon source that occurs before 450°C.

II. 4. ^{31}P NMR spectra of the residue

II. 4. a) Basic mixtures based on APP and different carbon sources

^{31}P NMR is finally used in order to investigate both the amorphous and crystallised phosphorus species present in the residual char of the basic mixtures. Indeed, even if X-Ray diffraction analyses demonstrate the formation of TiP_2O_7, it does not give information, regarding the amorphous phosphorus-containing products present in the residue and it is well recognised that intumescent char can contain amorphous phosphate-based compounds [74, 86].

Figure 86 and Figure 87 report the ^{31}P NMR spectra of the basic mixtures respectively without and with TiO_2. In the case of APP/Epoxy and APP/PER, the residues obtained after heat treatment exhibit a large band centred around 2ppm. This band can be assigned to phosphoric acid [86, 88, 121, 126-128]. But in the case of APP/dPER, the spectrum is noisier and the band is shifted to 0ppm. We can attribute it to orthophosphate species linked to aliphatic carbons previously determined by ^{13}C NMR in Figure 84. Indeed APP degrades to form ortho-phosphoric and pyro-phosphoric acids. Moreover, in the case of APP/PER (clearly viewable) and of APP/dPER (detected among a noisy spectrum), a large band centred around -52ppm is observed and may be attributed to cross-linked phosphates and/or branched polyphosphoric acid [129-131] which are in an intermediate state between APP degradation and formation of phosphorus oxides P_4O_{10}.

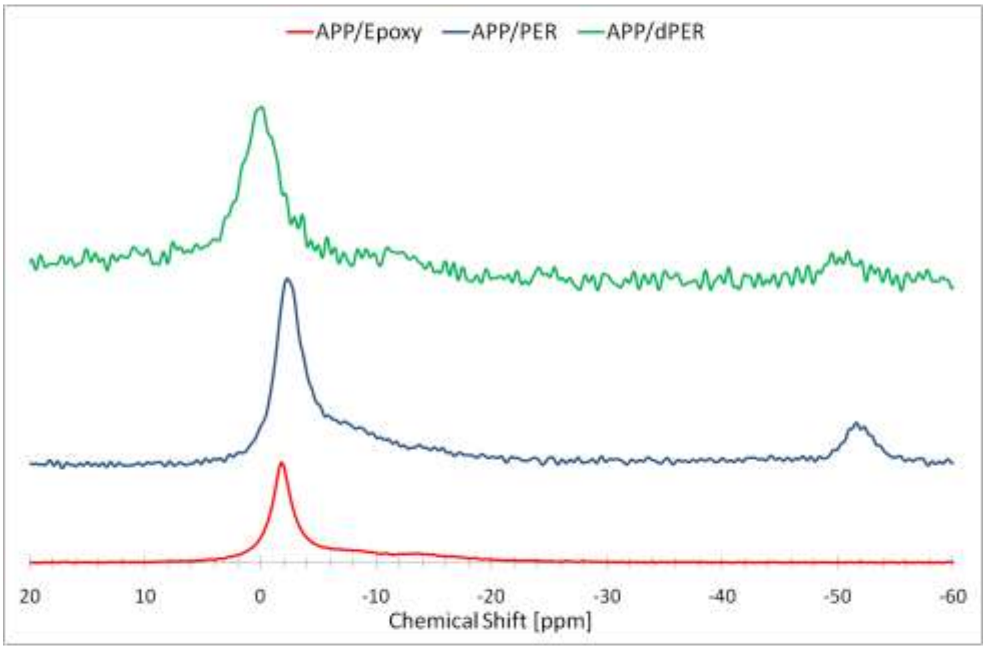

Figure 86 : ^{31}P NMR spectra of the binary systems APP/Carbon source after heat treatment at T=450°C

II. 4. b) Basic mixtures based on APP, different carbon sources and TiO_2

When TiO_2, is added in the basic mixture, the degradation pathway of the formulations is different. For APP/Epoxy/TiO_2, a large peak centred at around 0ppm and a collection of bands between -40 and -50ppm is observed. According to the previous XRD spectrum and literature [85, 114], this collection of bands could be attributed to TiP_2O_7 whereas the large peak at 0ppm is still assigned to phosphoric acid. For APP/PER/TiO_2, only TiP_2O_7 is viewable with a collection of bands between -40 and -50ppm. No peak is detectable at 0ppm and thus it suggests that no phosphoric acid or orthophosphate species are present. However knowing the initial content (56% of APP i.e. 17% of phosphorus and 8% of TiO_2 i.e. 5% of titanium), we calculate that phosphorus components are in excess in the mixtures. So we can suggest that not only TiP_2O_7 derivatives is formed but also branched polyphosphoric acid is, viewable in the same chemical shift range [131]. Finally, with dipentaerythritol, bands are observed between 0 and -20ppm whereas a large and not well-defined band is observed between -40 and -50ppm. The first set of peaks is usually detected in the case of intumescent systems. Bands at 0ppm can be attributed to phosphoric acid (similarly to band observed for APP/Epoxy/TiO_2) while band at -10ppm is attributed to ortho- and pyro-phosphate species linked to aromatic carbons and/or to pyrophosphate species, [86, 127]. Then the large band centred around -45ppm can be attributed to titanium pyrophosphate, probably in a glassy structure because of the broadness of the band not. Those results are in good agreement with the X-Ray diffraction analysis (Figure 82).

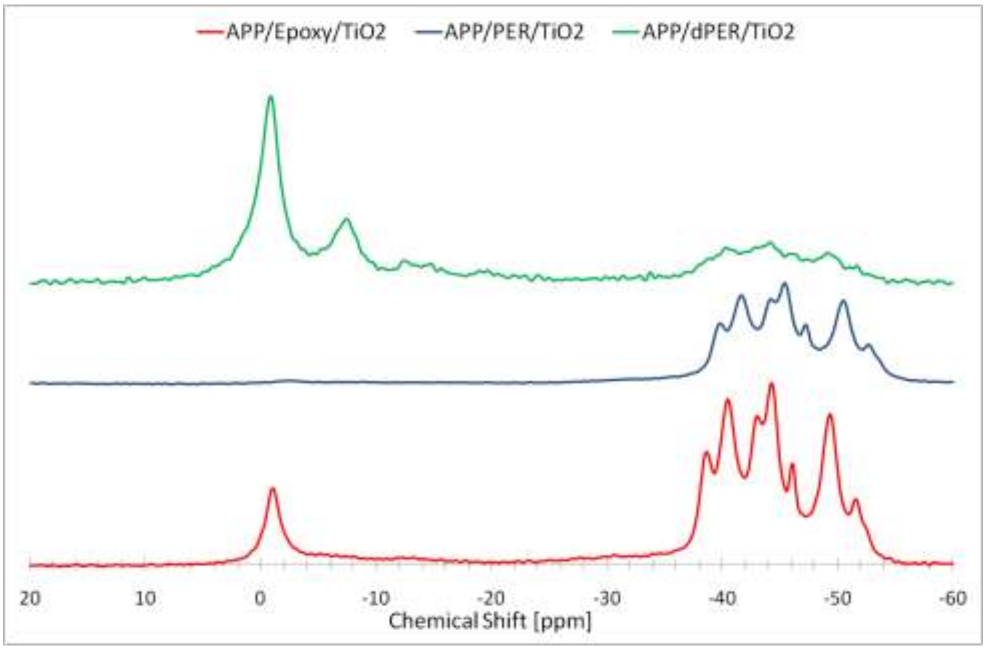

Figure 87 : ^{31}P NMR spectra of the ternary systems APP/Carbon source/TiO_2 after heat treatment at T=450°C

II. 5. Discussion and conclusion

Those results lead us to propose two different chemical degradation pathways:

- (1) either the APP degrades leading to the formation of phosphoric acid, the acid reacts with the carbon source leading to a phospho-carbonaceous structure that degrades and further reacts with TiO_2 leading to titanium pyrophosphate embedded in a degraded phosphorus and carbon containing matrix.

$$APP \rightarrow Phosphoric\ acid \xrightarrow{Carbon\ source} Phosphocarbonaceous\ structure \xrightarrow{TiO_2} TiP_2O_7$$

- (2) or the APP degrades leading to the phosphoric acid and competitive reactions between the acid and the carbon source or TiO_2 occur leading to the formation either of a phospho-carbonaceous structure and/or of TiP_2O_7.

$$APP \rightarrow Phosphoric\ acid \xrightarrow{Two\ competitive\ reactions} \begin{cases} Phosphorcarbonaceous\ structure \\ and \\ TiP_2O_7 \end{cases}$$

It may be proposed that depending on the carbon source used in the system, the first or the second pathway could occur and thus the influence of the titanium dioxide will be different. TiO_2 can react with ammonium polyphosphate (or its derivate products) to form TiP_2O_7, a ceramic-like compound at high temperature [113]. This ceramic-like material is suspected to enhance the properties of the char structure and to protect the substrate against fire [85]. Indeed the TiP_2O_7 structure consists of TiO_6 octahedra and PO_4 tetrahedra sharing corners in a three-dimensional network [123] and the Ti-O-Ti structure can better resist to oxidation and can improve the thermal stability of the intumescent coating at middle and later stage of a fire [113].

Second in the case of PER, we suspect TiO_2 to slightly modify the degradation mechanism of the APP/PER mixture. Indeed, while with epoxy resin or dipentaerythritol, we observe a degradation of the aliphatic carbons and an aromatization of the residues, with PER and TiO_2, thermally stable aliphatic carbons seems to be formed and trapped in the carbonaceous structure. Moreover, stabilization of the system by TiO_2 could explain the absence of phosphoric acid and why we detect only TiP_20_7 at high temperature.

In order to go further in the understanding and to demonstrate that the effect observed in the basic mixtures can also be detected in the complete intumescent formulations, similar analyses of heat treated intumescent formulations will then been investigated following the same protocol.

III. Chemistry and reactivity of the complete intumescent formulations

The same experiments and the same techniques as those described in the first section of this chapter are carried out on the complete intumescent formulations in order to highlight the interaction and the reactivity between the different components of the complete formulations. The objective is to propose a chemical degradation pathway for each intumescent formulation.

III. 1. Thermal stability of the intumescent formulations

The thermo-gravimetric curves of the four intumescent formulations in air are presented in Figure 88 and their derivatives in Figure 89. Thanks to these graphs, we can determine the different steps of degradation of each formulation and compare the stability of the different intumescent coatings versus temperature in thermo-oxidative conditions.

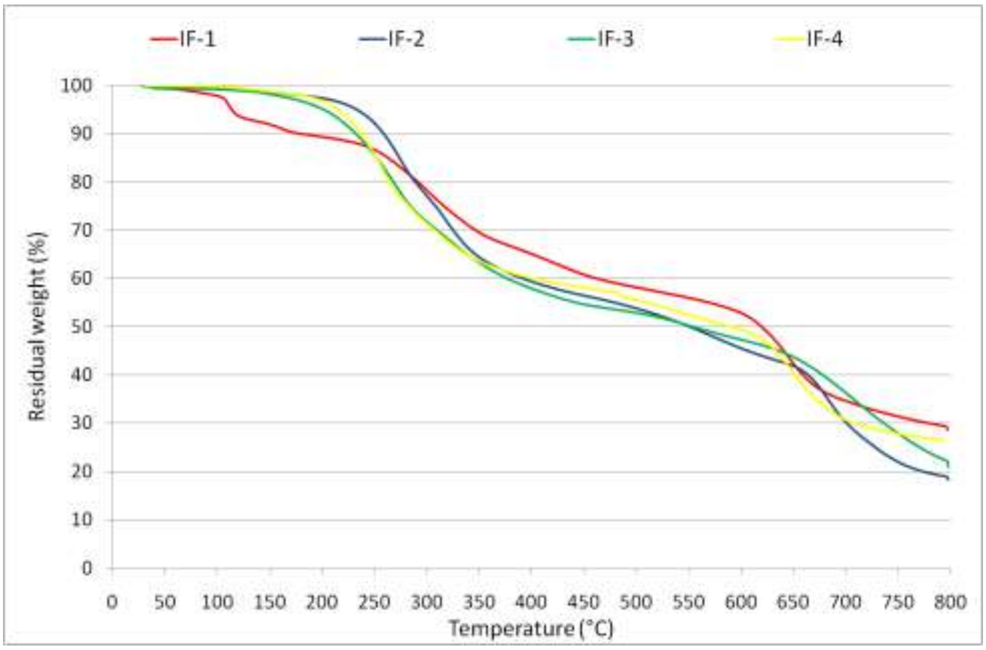

Figure 88 : TGA curves of the intumescent formulations in air at 10°C/min

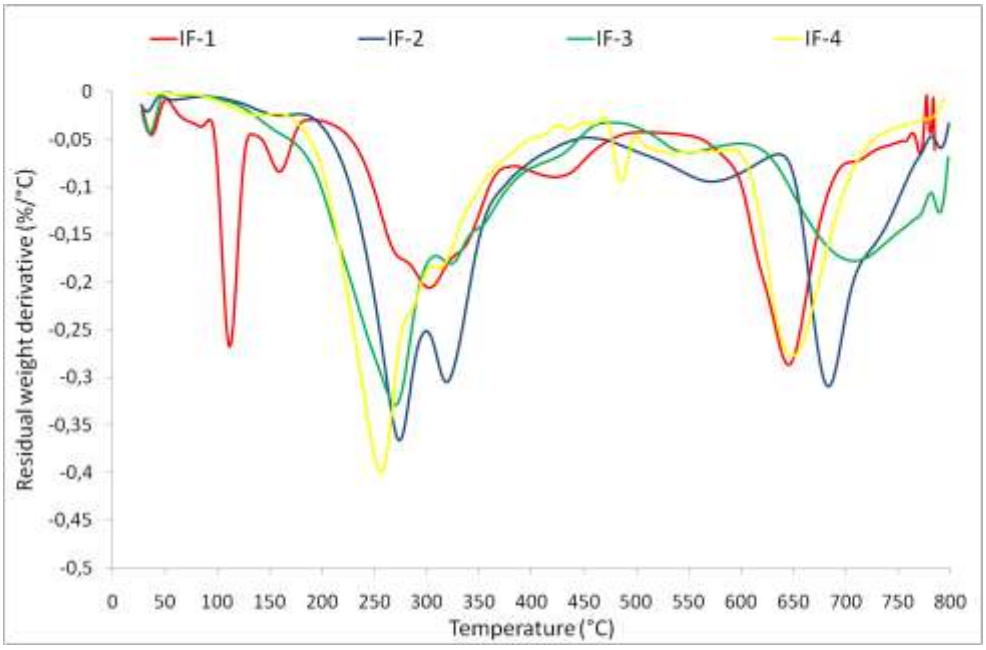

Figure 89 : Derivative TGA curves of the intumescent formulations in air at 10°C/min

Firstly, the mechanism of degradation of IF-1 is well known and exhibits four main degradation step as described in a previous work [105]. Two overlapped steps are observed between 100 and 200°C corresponding to a weight loss of about 10% and to the degradation of boric acid. Indeed H_3BO_3 successively dehydrates into metaboric acid and then into boron oxide:

$$H_3BO_3 \overset{\Delta}{\rightarrow} H_2O + HBO_2$$
$$2HBO_2 \overset{\Delta}{\rightarrow} H_2O + B_2O_3$$

A third step occurs between 180 and 500°C, corresponding to a weight loss of about 35%. Boron oxide and phosphoric acid obtained from APP degradation react together to yield borophosphates BPO_4 and as boron has been added in excess compared to phosphorus, some B_2O_3 remain at 600°C.

$$\text{Coated APP} + B_2O_3 \xrightarrow{250-400°C} BPO_4 + B_2O_3 + char$$

Then, a fourth step, occurring between 500 and 800°C, leads to a final residue of about 30% of the initial weight. This step is attributed to degradation of different fillers contained in IF-1 and to the oxidation of the char.

This mechanism of degradation has been well-defined and the performance of the intumescent formulation has been successfully correlated with the formation of borophosphates. However, the three other formulations do not contain boron components and borophosphate formation become thus impossible. Therefore, the goal of the next investigations is to determine a chemical degradation pathway for the three other coatings.

Regarding those coatings, we can note that, except the degradation of boric acid (100-180°C), the two other steps of degradation occur in the same range of temperature: from 200 to 400°C concerning the main step and oxidation of the transient char is observed after 600°C. Nevertheless, some differences provide us additional information. First, the stability of IF-2 is higher since its degradation begins at 200°C while the mass losses of IF-3 and IF-4 become significant respectively from 170°C and from 180°C. This highest stability of IF-2 could be explained by the addition of respectively PER and dipentaerythritol in IF-3 and IF-4 that causes degradation at lower temperature as observed with basic mixtures: thermal stability of APP/Epoxy is higher than APP/PER and APP/dPER (Figure 77). Moreover, we could note that the oxidative degradation at high temperature of IF-2 and IF-4 is faster than IF-3. Contrary to the basic mixtures where APP/Epoxy residue was less sensitive to oxidation than the two others, it is the IF-3 (with PER) that seems to be the less sensitive to oxidation and that exhibits the highest stability. Consequently, at 800°C, the thermal degradation of IF-3 is not completed and continues above 800°C.

Thanks to these TGA curves highlighting the thermal stability of the formulations (Figure 90), five temperatures have been chosen corresponding to characteristic steps of the intumescence process:

- At 250°C, boric acid is completely degraded while degradation of the three other coatings starts.
- At 300°C, the rate of degradation is maximal.
- At 450°C, the degradation rate is slow, a transient material is obtained.
- The fourth temperature (600°C) corresponds to the material just before its last degradation step attributed to oxidation.
- At 800°C, a relatively stable residue is formed for the coatings, except for IF-3. An additional higher temperature (900°C) has been added to investigate the evolution of this intumescent formulation.

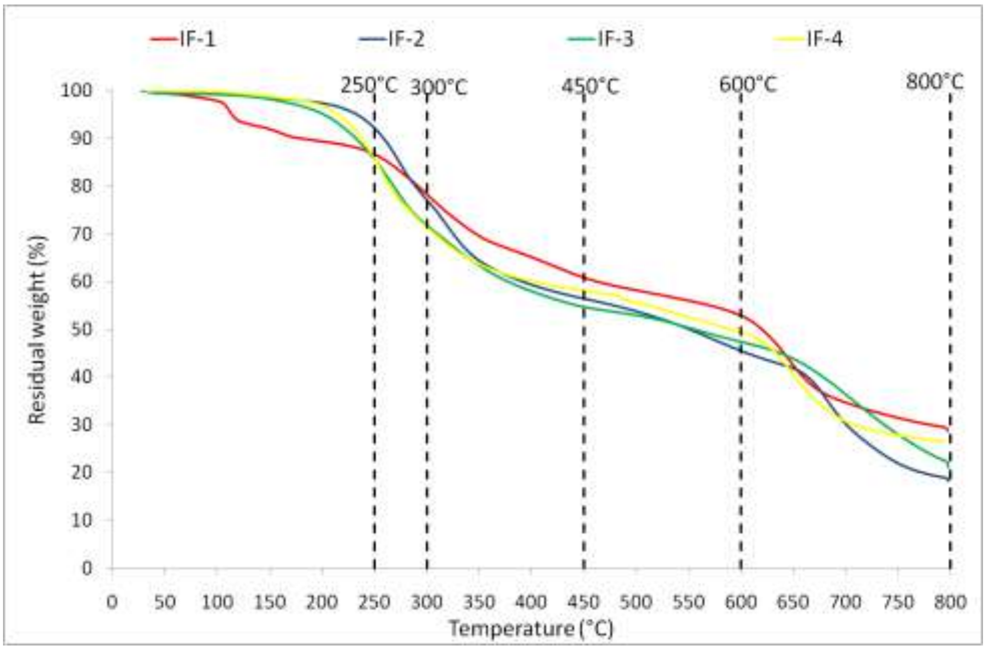

Figure 90 : Determination of the five characteristic temperatures

According to these temperatures, the intumescent coatings are heat treated for three hours in a tubular furnace (m = 5g) and the residues are analysed using adapted spectroscopic analyses.

III. 2. Mechanism of degradation of intumescent formulation 2

III. 2. a) Investigation of the structure of the intumescent system by X-Ray diffraction

Figure 91 reports the X-Ray diffraction patterns of IF-2 and of its residue obtained after heat treatment at the previously defined characteristic temperatures.

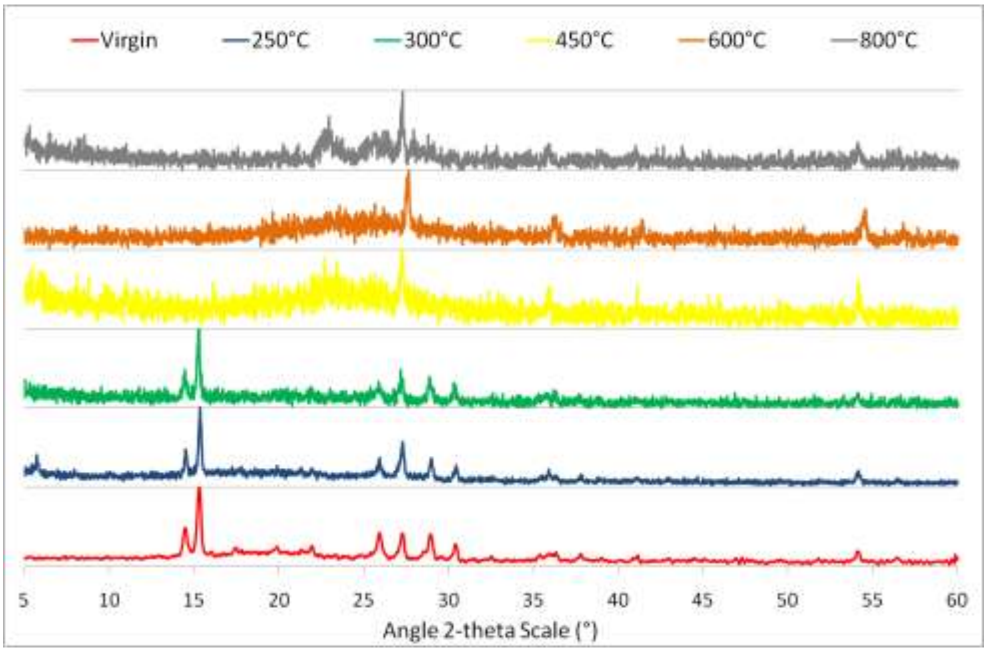

Figure 91 : X-Ray diffraction patterns of IF-2 and of its residues at several characteristic temperatures

From ambient temperature to 300°C, mainly APP and TiO_2 are detected (see Figure 92 for comparison) with two intense peaks around 15° and four peaks between 25 and 30°. Then from 450°C and at higher temperatures, diffractograms become noisy due to the carbonisation of the system and progressive loss of its crystallinity. Whereas TiO_2 is still detected (peaks at 27, 36 and 54°), APP is no longer observed. The disappearance of the characteristic peaks of APP can be explained by its reaction with epoxy resin and the formation of a carbonaceous structure as previously observed in TGA curves of APP/Epoxy (Figure 77) and of IF-2 (Figure 88) showing a step of degradation of systems between 300 and 450°C. This observation is also in agreement with literature [76, 79] that reports reactivity of APP with carbon source around 300°C and with the degradation of the epoxy resin in the same temperature range (Figure 76). So we can suggest that in this temperature range [300 – 450°C] the intumescent process occurs as already observed by rheological experiments as swelling is important from 300°C. In addition, we detect since 450°C the progressive growth of a large band between 20 and 25° that can be attributed to amorphous carbons [120] mainly present in char.

Finally, for a heat treatment at 800°C, TiO_2 is still detected but three additional peaks at 23, 25 and 27° appear and can be assigned to TiP_2O_7 (Figure 82). ^{31}P NMR spectra are necessary to confirm those species because of the low resolution of XRD diffractogram.

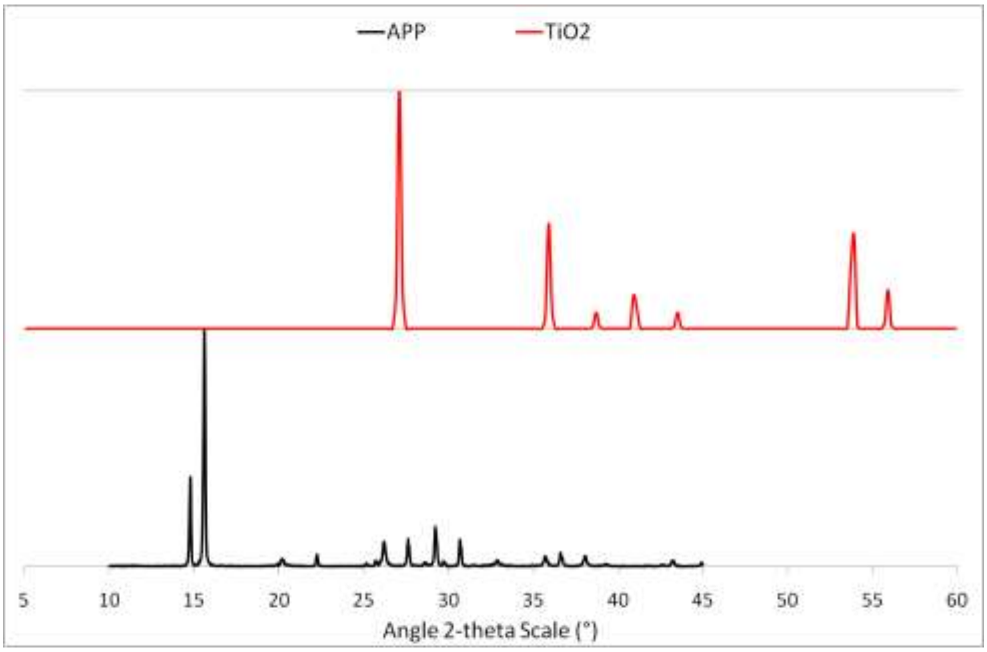

Figure 92 : X-Ray diffractograms of APP and of TiO_2

III. 2. b) Investigation of the evolution of the carbon structure in the intumescent system by ^{13}C solid-state NMR

The ^{13}C NMR spectra of IF-2 and of its residue obtained after heat treatment at the previously defined characteristic temperatures are reported on Figure 93. Only heat treatments up to 450°C have been reported because additional analyses do not present further information. At higher temperature, spectra are similar to that at 450°C, exhibiting a broad band centred at 130ppm with a low signal to noise ratio.

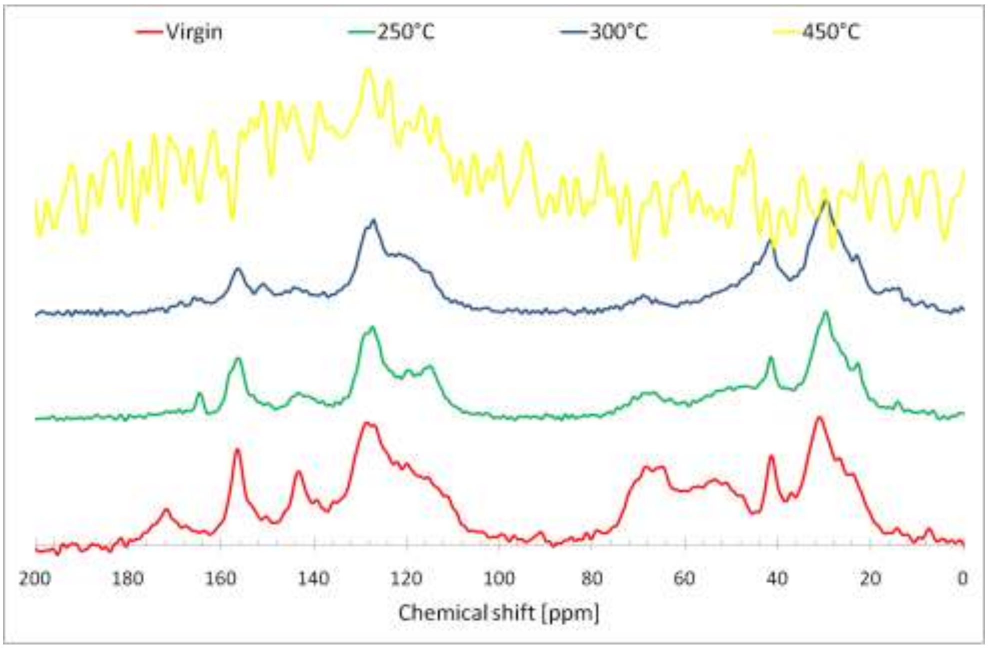

Figure 93 : ^{13}C NMR spectra of IF-2 and of its residues at several characteristic temperatures

From ambient temperature to 300°C, the three first spectra exhibit a signal that is mainly characteristic of the epoxy resin (see Figure 94 to comparison). Indeed, we assume that, as far as we know the formulations, IF-2 does not contain other carbon elements, except DGEBA type resin and amide hardener with unknown carbonyl chains [59, 132]. This assumption is confirmed by spectra at low temperature where no more additional peaks have been detected thanks to ^{13}C NMR. Thanks to these spectra, we can however remark that two bands detected at 70ppm and at 170ppm have intensities that decrease progressively with temperature. At 170ppm, band is attributed to carbons from carbonyl group of the hardener and has disappeared at 250°C. At 70ppm, band corresponding to CH_2-O sites (C3 and C10 from epoxy network) decreases up to 300°C. This intensity decrease should be caused by a scission of this bond in the epoxy chain and thus the formation of ϕ–OH. Then we suggest that APP could react with hydrolyzed epoxy resin and form of P-O-C bonds with aromatic carbons (C4 and C7) whose bands decrease up to 300°C.

Then the spectrum of the material heat treated at higher temperature (T > 300°C) only shows a noisy signal. The temperature of 300°C could be classified as “a critical temperature” for the intumescent development. Indeed, as previously demonstrated this temperature corresponds to the temperature range where the sample swells (observed during rheological experiments) and corresponds to the beginning of the APP degradation and its reaction with the carbon source (observed thanks TGA curves and X-Ray diffractograms).

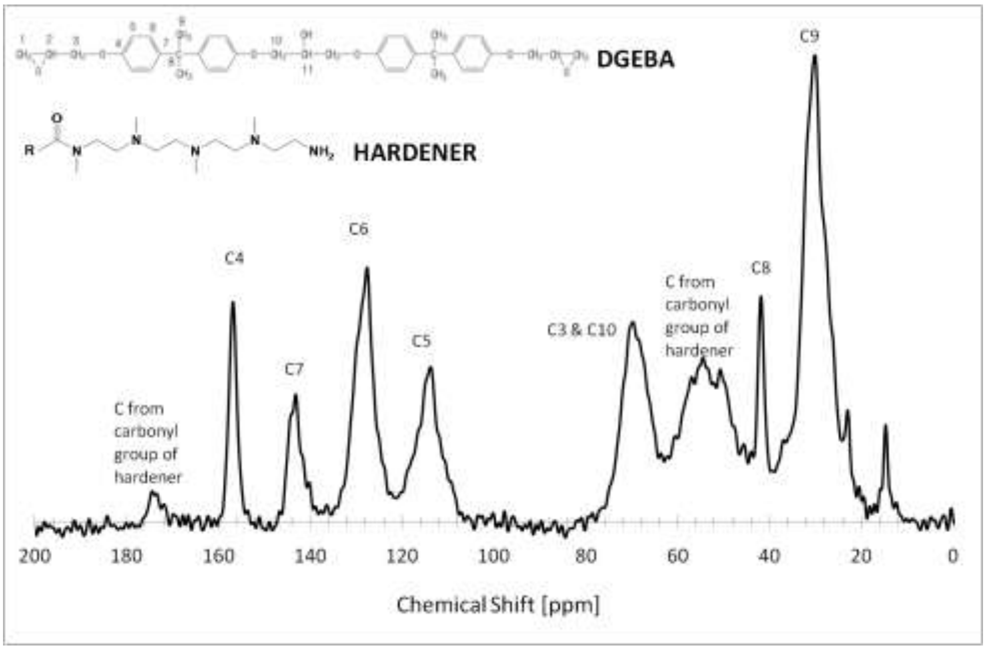

Figure 94 : ^{13}C NMR spectrum of the thermoset cured resin

III. 2. c) Investigation of the evolution of the phosphorus components in the intumescent system by ^{31}P solid-state NMR

Finally, the ^{31}P NMR spectra of IF-2 and of its residue obtained after heat treatment at the previously defined characteristic temperatures are reported on Figure 95. ^{31}P NMR appears as the spectroscopic tool of choice since it provides information regarding the evolution of the phosphorus containing compounds that are observed in the intumescent shield along the heat treatment.

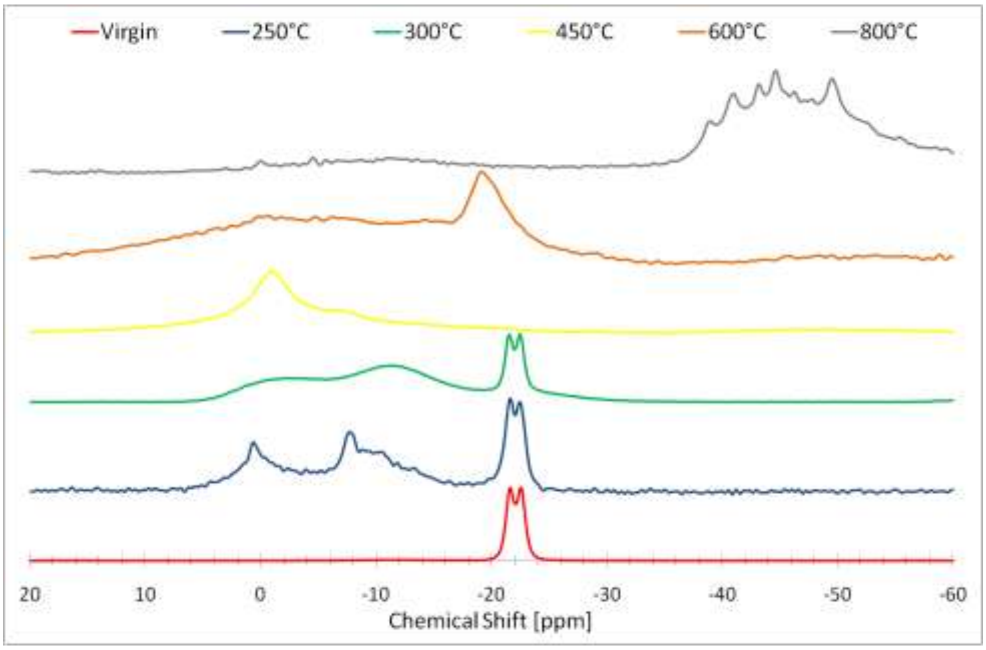

Figure 95 : ^{31}P NMR spectrum of IF-2 and of its residues at several characteristic temperatures

On Figure 95, the spectra of the residues heat treated up to 300°C show a double band at -22 and -24ppm which is attributed to the central group of polyphosphates in ammonium polyphosphate. In that temperature range, we observe broad bands centred at 0ppm and at -10ppm attributed respectively to phosphoric acid or orthophosphates linked to aliphatic carbons and orthophosphates linked to aromatic carbons. These two bands are caused by the degradation of APP and its reaction with the carbon source. Indeed APP degradation leads to the formation of phosphoric and/or pyrophosphoric acids via a hydrolysis reaction that may react on –OH sites of hydrolyzed epoxy resin, as suggesting after ^{13}C NMR investigation, to form P-O-C bridges.

At higher temperature, (T = 450°C), a broad band centred around 0ppm and presenting shoulder at δ = -8ppm is observed. At this temperature, the degradation of the APP is complete, phosphoric acid has been mainly detected (band at 0ppm) but they remain also ortho- and pyrophosphate linked to aromatic groups from epoxy resin degradation (band at -8ppm).This last band should confirm the formation of thermally stable P-O-C bonds [128].

The spectrum of the residue collected after a heat treatment of 600°C shows a broad band between 0 and -25ppm with a singlet at δ = -20ppm. The singlet at -20ppm is assigned to polyphosphoric acid often observed in degradation of intumescent systems [90], but the non complete knowledge of the formulation prevent us to conclude accurately. Broad and low intense bands between 0 and -25ppm could also be attributed to ortho- and pyro-phosphate resulting from APP. Lastly, at T = 800°C, a collection of bands similar to those observed in the case of the basic mixtures and attributed to TiP_2O_7 is detected. It is thus demonstrated that at higher temperature the formation of titanium pyrophosphate occurs also in the case of IF-2 similarly to observation made with APP/Epoxy/TiO_2 basic mixture.

To conclude, when epoxy resin is used as a single acid source, IF-2 exhibit a mechanism of degradation leading to the formation of titanium pyrophosphate. Nevertheless, several steps can be determined to yield crystalline structure. Firstly, APP and epoxy resin may react together, via a scission of CH_2-O bonds. This reaction permits the formation of a phospho-carbonaceous structure from 450°C. Then TiO_2, observed up to 600°C, reacts with phosphorus components to product TiP_2O_7 at 800°C, causing therefore scission of P-O-C bonds.

III. 3. Mechanism of degradation of intumescent formulation 3

A similar approach than the first one used for IF-2 was used to investigate the mechanism of degradation of IF-3. The focus is nevertheless on the influence of PER and the consequence of this modification between the two formulations. Furthermore as already mentioned with investigation of the thermal stability, last oxidation of IF-3 is not completed at 800°C. We have so added a higher heat-treatment temperature (900°C) to investigate the chemical changes of this intumescent system.

III. 3. a) Investigation of the structure of the intumescent system by X-Ray diffraction

Figure 96 reports the X-Ray diffraction patterns of IF-3 and of its residues obtained after heat treatment at the previously defined characteristic temperatures.

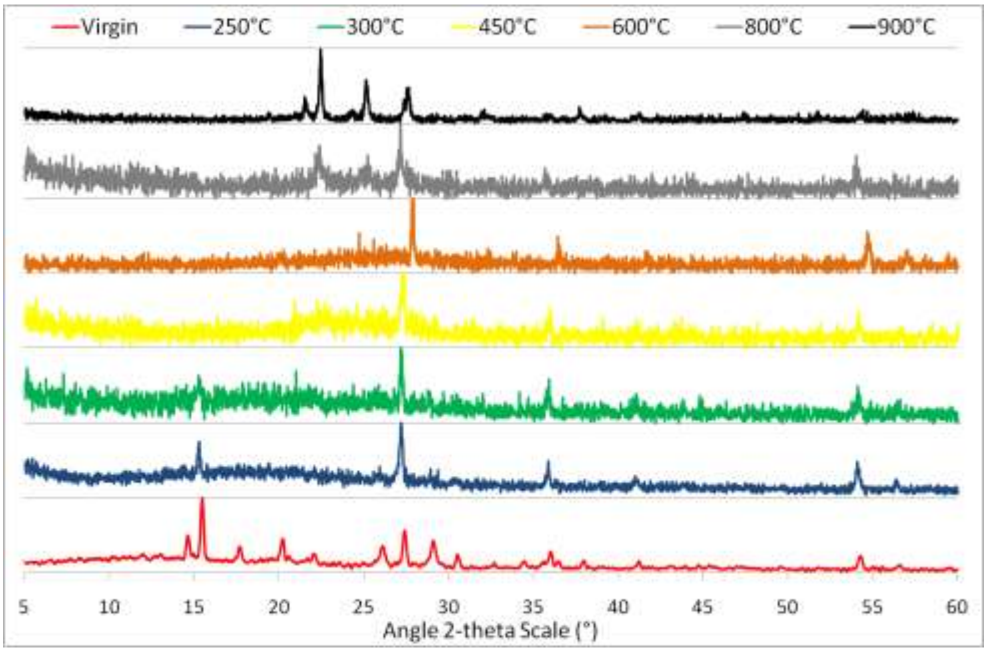

Figure 96 : X-Ray diffraction patterns of IF-3 and of its residues at several characteristic temperatures

Similarly, to IF-2, the first component that we can detect by X-Ray diffraction at low temperature is APP with intense peaks. However while we are able to detect it from ambient to 300°C for IF-2, the peaks attributed to APP have already disappeared at 250°C for IF-3 and only TiO_2 is clearly viewable at 300°C. Therefore it seems that addition of PER causes the degradation of APP and/or its reaction with PER as suggested elsewhere at lower temperature [127, 133]. This degradation at lower temperature is also in agreement with the TG curve of IF-3 where the onset temperature appears lower than those of IF-2 (Figure 89). Consequently at 300°C, IF-3 exhibits only a noisy spectrum where TiO_2 peaks are still viewable (at 27, 35 and 54°) because of the intumescent process and of the carbonization. This carbonization and the development of an intumescent structure containing amorphous carbons cause the appearance of a broad band between 20 and 25° as observed with IF-2 from 300°C. It can thus be assumed that the phospho-carbonaceous structure characteristic of the intumescent shield should be formed at lower temperature when PER is used as co-carbon source with epoxy resin.

Then up to 800°C, we observe noisy signal. At 800°C, similarly to what occurs in IF-2, we detect appearance of three peaks at 23, 25 and 27° assigned to TiP_2O_7 (Figure 82) whose crystallisation is in progress. Indeed, for a heat treatment of 900°C, we observe a well-defined spectrum highlighting the formation of well crystallized TiP_2O_7. Diffractograms of complete formulations become as well-defined as those of basic mixtures and reveal the formation of a more crystallized structure that literature [113] qualifies as a ceramic-like material enhancing the char structure and protecting the substrate. ^{31}P NMR spectrum will confirm the presence of such specie.

III. 3. b) Investigation of the evolution of the carbon structure in the intumescent system by ^{13}C solid-state NMR

The ^{13}C NMR spectra of IF-3 and of its residue obtained after heat treatment at the previously defined characteristic temperatures are reported on Figure 97. Once again, only heat treatments up to 450°C have been reported because additional analyses do not present further information except a broad band centred at 130ppm among a noisy signal.

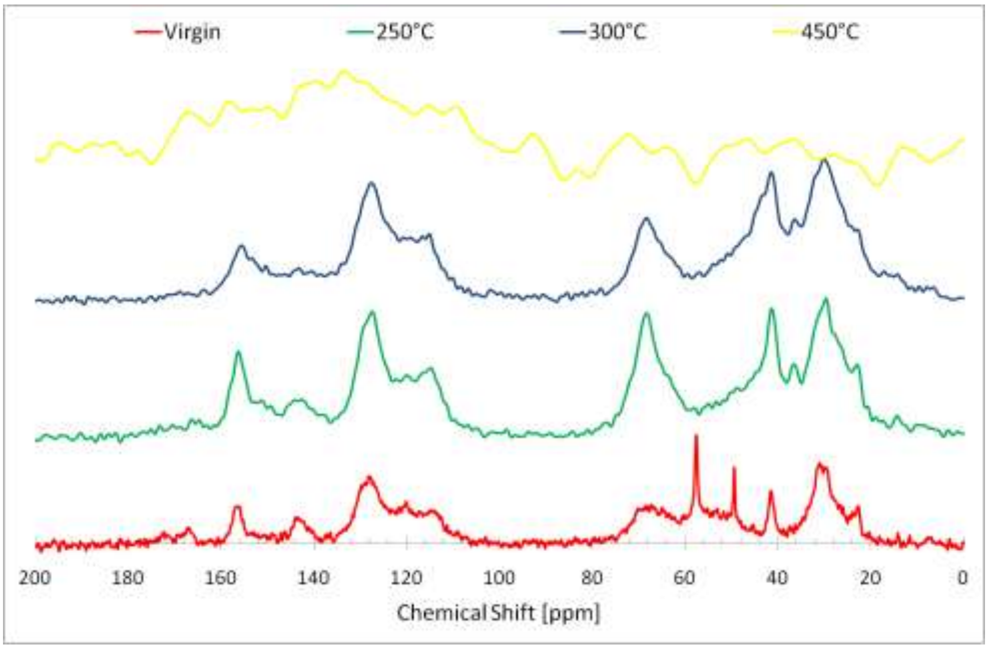

Figure 97 : ^{13}C NMR spectra of IF-3 and of its residues at several characteristic temperatures

The first difference provides by ^{13}C NMR is the detection of PER at ambient temperature with two bands at 50 and 58ppm (Figure 98).

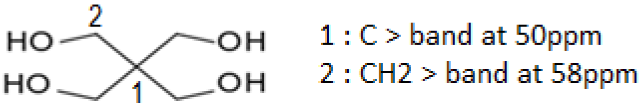

Figure 98 : Assignment of bands on ^{13}C NMR spectrum of PER

We note that when the material is heat treated at low temperature (250°C), PER has already reacted or degraded as suggested by the disappearance of its two bands and the conclusions drawn using the TG curve of pure products (Figure 76). The epoxy resin degrades in a second step because the “signature” of the epoxy resin is observed until a heat treatment of 300°C in the case of IF-3. It should also be underlined that the band at around 70ppm (band corresponding to CH_2-O sites in epoxy network - Figure 94) does not decrease up to 300°C when the carbonization due to intumescent process occurs and a consequent noisy spectrum is observed. It is thus possible to assume that in presence of PER, the APP or its degradation products react with PER rather than with the epoxy resin. The transient residue should thus present a different structure comparing IF-2 and IF-3.

Previous works with basic mixtures and several papers [119, 133, 134] report this interaction between APP and PER, showing that upon heating APP and PER together phosphoric ester bonds are formed first by alcoholysis of the polyphosphate chain around 280°C. The formed phosphor-ester can then undergo a ring closing esterification and a reduction to a phospho-carbonaceous network. This second step could be viewable from 450°C when spectrum of the material exhibits only a noisy signal. Similarly, to IF-2, this phenomenon may be attributed to the aromatic and polyaromatic carbons forming the structural shield.

III. 3. c) Investigation of the evolution of the phosphorus components in the intumescent system by ^{31}P solid-state NMR

Finally, the ^{31}P NMR spectra of IF-3 and of its residue obtained after heat treatment at the previously defined characteristic temperatures are reported on Figure 99.

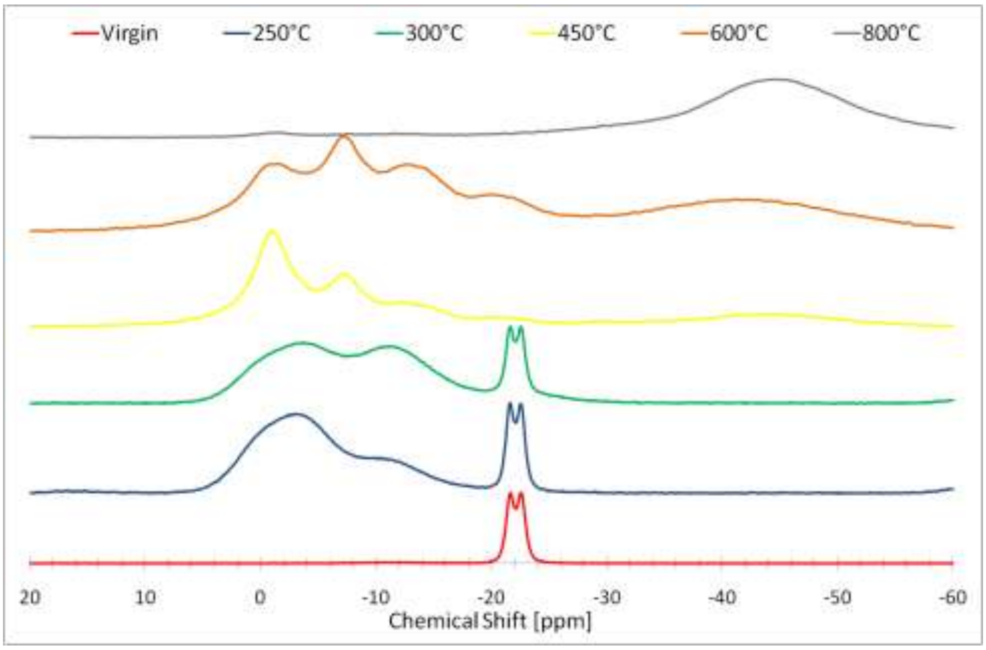

Figure 99 : ^{31}P NMR spectra of IF-3 and of its residues at several characteristic temperatures

In the case of IF-3, APP is detected up to 300°C. This is demonstrated by the double bands at -22 and -24ppm while we have suspected its degradation at lower temperature drawn on the disappearance of characteristic peaks at 15° on X-Ray diffractograms (Figure 96). This apparent discordance can be explained by a loss of the crystallinity of APP which gives no signal by XRD. But this sustained detection of APP at 300°C confirms also a similar evolution of IF-2 and IF-3. Indeed the degradation of IF-3 begins from 250°C since additional bands appear after a heat treatment at this temperature. At 250°C and 300°C, we detect two bands at -4 and -12ppm that are attributed respectively to ortho-phosphates PO_4 in R_3PO_4 (R being an alkyl group) and to either PO_4 in $R'R_3PO_4$ (with R' being an aromatic group whereas R is an alkyl group) or to pyro-phosphates ($R_4P_2O_4$). At higher heat treatment temperature (450°C), we can distinguish three bands in the region [-1 to -20ppm]. Even if it is difficult to attribute accurately each one, it may be reasonably assumed that these bands correspond respectively to orthophosphate and/or phosphoric acid (-1ppm), to pyrophosphates groups (at -7ppm) and to orthophosphate in Φ_2RPO_4 around -15ppm.

Then from 450°C, a broad band between -40 and -50ppm is also observed. This chemical shift range corresponds to the range where TiP_2O_7 is observed. It can be reasonably assumed that non-crystallised titanium pyrophosphate is formed at this temperature because we cannot detect it with X-Ray diffraction. Lastly, it can be noticed that whatever the heat treatment (≤800°C), no evidence of crystallised TiP_2O_7 is found as we do not observe any well-defined collection of bands between -40 and -50ppm at the contrary of the results obtained in the case of the basic mixture APP/PER/TiO_2 (Figure 87). This result is however in agreement with the results obtained from the X-Ray diffraction analyses at 800°C that do not show clear evidence of the formation of titanium pyrophosphate except only a progressive outline of the three peaks at 23, 25 and 27° that suggests its formation at higher temperature.

Nevertheless, it appears that when PER is added as co-carbon source with epoxy resin on intumescent formulation, it is the additive (PER) that plays mainly the role of carbon source and that react faster with APP. In the other hand, epoxy network is distinguished up to 300°C without reacting with APP because their characteristic bands are not modified up to 450°C (even at 70ppm where APP usually react with epoxy network in the case of IF-2). This change of carbon source could modify the chemical pathway of IF-3 compared to IF-2. We assume that the residue obtained after reaction between APP and carbon source should exhibit a different structure based on ortho- and pyro-phosphates. Then titanium pyrophosphate is suggested at 800°C and well detected at 900°C. So we remark that main difference between IF-2 and IF-3 could be the temperature where TiP_2O_7 is crystallized. In spite of degradation at lower temperature, PER and intermediate residue seem to delay its formation at higher temperature.

III. 4. Mechanism of degradation of intumescent formulation 4

Due to their similarities, investigation of IF-4 will be done in direct comparison with IF-3. Indeed, PER is completely substituted by dipentaerythritol in order to modify the visco-elastic behaviour of the coating. We have already shown that this modification causes a shift of the viscosity decrease and the observed behaviour is close to the one of IF-1 or IF-2.

However, a decrease of the swelling abilities was also noted. Aim of this investigation is to study the chemical changes of the system.

III. 4. a) Investigation of the structure of the intumescent system by X-Ray diffraction

Figure 100 reports the X-Ray diffraction patterns of IF-4 and of its residue obtained after heat treatment at the previously defined characteristic temperatures.

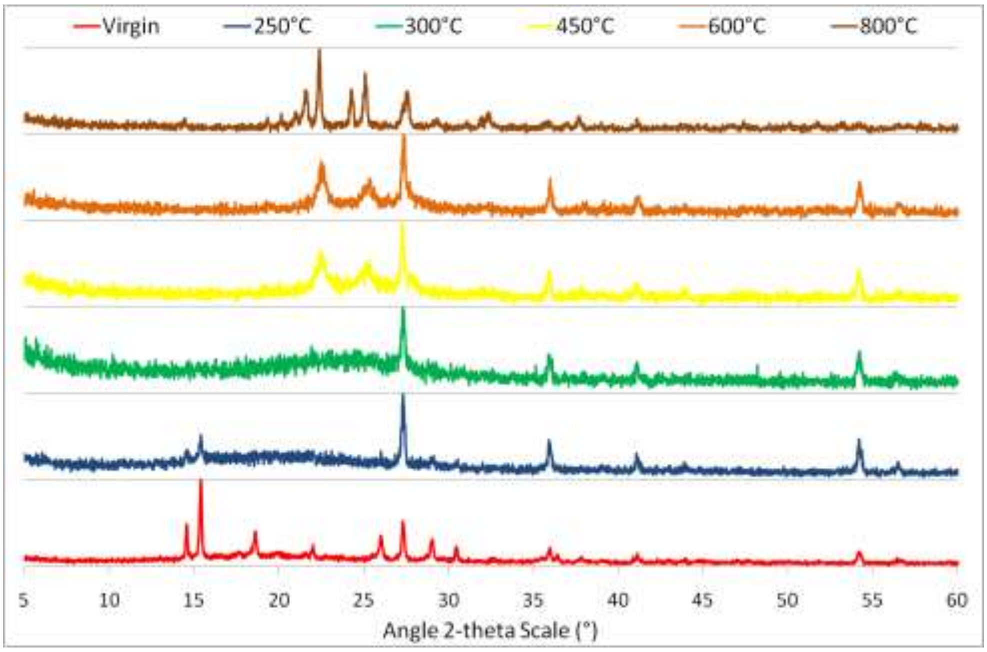

Figure 100 : X-Ray diffraction patterns of IF-4 and of its residues at several characteristic temperatures

Firstly, we observe that patterns of IF-4 (Figure 100) are less noisy than those obtained for IF-3 (Figure 96). It can thus be proposed that since X-Ray diffraction analysis is sensitive to the crystallized components, the crystallinity of the charring system resulting from IF-4 decomposition is higher than that observed for IF-3.

At ambient temperature, similarly to what observed for previous coatings, the pattern of the complete intumescent formulation exhibits mainly the bands that are characteristic of APP and TiO_2 (Figure 83). The characteristic peaks of APP disappear partially after a heat treatment at 250°C whereas the peaks attributed to TiO_2 (an intense peak at 27° and two low peaks around 36 and 54°) are observed up to 600°C for IF-4. Then, the degradation of APP is complete at 300°C. We observe the degradation of APP at lower temperature similarly to IF-3 while APP is still detected at 300°C for IF-2. Consequently, it may be proposed that PER and dipentaerythritol exhibit a higher reactivity with APP than epoxy resin. This difference can be explained by the mechanism occurring in each formulation. With PER or dipentaerythritol, we assume that esterification reaction occurs while with epoxy resin we have shown that a first bond scission from epoxy network is needed to form ϕ–OH sites and then a reaction with APP could occur. The phospho-carbonaceous structure resulting from the degradation of APP and characteristic of the intumescent shield should be formed at lower temperature when dipentaerythritol is used as co-carbon source with epoxy resin in the complete formulations.

Following the degradation of APP, from 450°C, we detect directly the formation of TiP_2O_7, demonstrated by the presence of three intense diffraction peaks between 2theta = 20 and 30°. These peaks are detected up to a heat treatment of 800°C. Moreover, the X-Ray diffraction pattern of IF-4 heat treated at 800°C is very well-defined and presents some additional peaks particularly at 22° and 24°. Due to unknown formulation and in spite of investigation using ICSD database, we cannot attribute these peaks. Therefore, as a first conclusion, X-Ray diffraction analyses show that whereas IF-3 and IF-4 both degrade with the subsequent formation of TiP_2O_7, the temperature range in which this reaction occurs is very different. Indeed, TiP_2O_7 may be suspected from 800°C for IF-3 (with pentaerythritol) whereas it is clearly observable from 450°C in IF-4 (when PER is substituted by dipentaerythritol).

III. 4. b) Investigation of the evolution of the carbon structure in the intumescent system by ^{13}C solid-state NMR

Thanks to the ^{13}C NMR spectra of IF-4 and of its residue obtained after heat treatments (Figure 101), we should confirm the chemical pathway discussed above and the formation of the potential carbonaceous structure. Once again, only heat treatments up to 450°C have been reported because analyses at higher temperature do not present additional information and any new change in system.

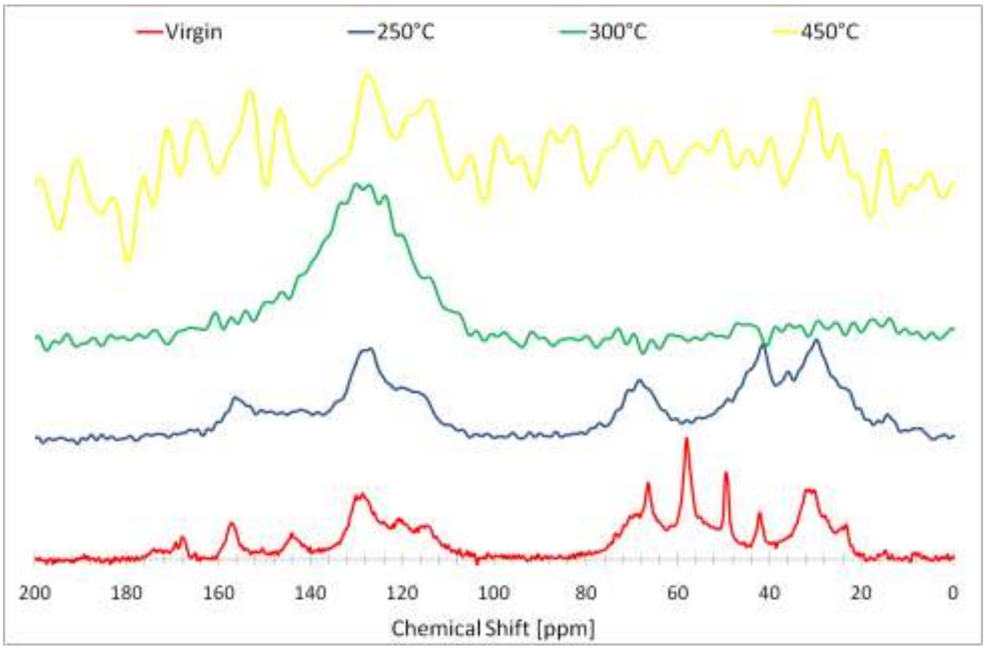

Figure 101 : ^{13}C NMR spectra of IF-4 and of its residues at several characteristic temperatures

On the spectra at ambient temperature, we mainly detect bands attributed to epoxy resin by direct comparison with Figure 94. Moreover, typical bands attributed to dipentaerythritol (narrow and intense bands at 50, 58 and 66ppm) are also detected (Figure 102).

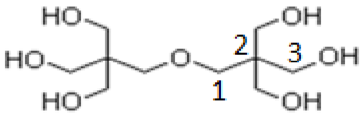

1 : CH2 > band at 66ppm
2 : CH2 > band at 50ppm
3 : C > band at 58ppm

Figure 102 : Assignment of bands on ^{13}C NMR spectrum of dipentaerythritol

When the material is heat treated at low temperature (250°C), the dipentaerythritol degrades shown by the disappearance of peaks attributed to dipentaerythritol. This observation suggests a reaction of dipentaerythritol or of it degradation products and similarly to what happens with PER (disappearance of bands at 250°C) we assume an esterification reaction of dipentaerythritol by APP to form phosphoric ester bonds. Furthermore this reaction is correlated by the degradation of APP at 250°C (lower temperature than those observed with IF-2 or IF-3) determined using the X-Ray diffraction patterns. In parallel, we can note that the epoxy resin does not degrade up to 300°C. So if we consider that both epoxy resin and PER are used as carbon source in the intumescent formulation, we can observe that APP reacts preferentially with PER (disappearance of its bands) than with epoxy resin (whose bands are remaining at 250°C). Thus we can assume that reactivity of PER with APP is higher than ones of epoxy resin with APP and that the activation energy required to such reaction is lower for PER with APP than for epoxy resin with APP.

At 300°C, degradation of the matrix is also observed because only a large band centred at around 130ppm is detected. This broad band is characteristic of intumescent coating and implies the presence of several non-magnetically equivalent carbons. This band can be assigned to several types of aromatic and polyaromatic species which can be partially oxidized. It suggests the condensation of aromatic species to polyaromatic species. This broadening may also be explained by the fact that a disorganized structure is created. At higher heat treatment temperature (T = 450°C), the signal is very noisy, similarly that we have already observed for IF-2 and IF-3.

III. 4. c) Investigation of the evolution of the phosphorus components in the intumescent system by ^{31}P solid-state NMR

The chemical change of phosphorus components should also be highlighted by ^{31}P NMR. The different spectra of IF-4 and of its residue obtained after heat treatments are introduced on Figure 103.

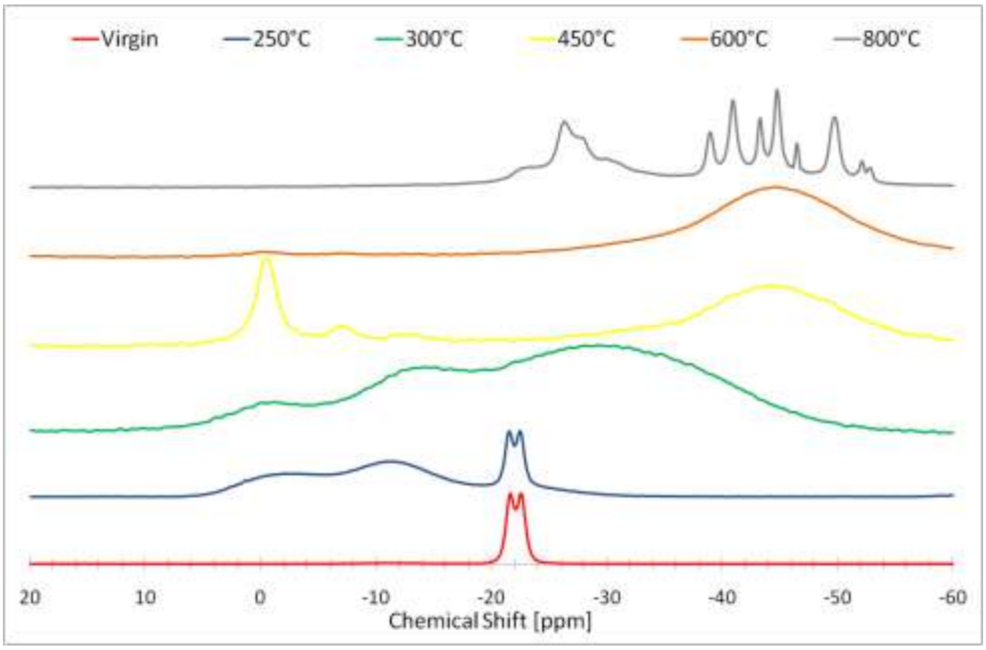

Figure 103 : ^{31}P NMR spectra of IF-4 and of its residues at several characteristic temperatures

The main phosphorus component that we detect and that degrades is APP shown by its double band at -22 and -24ppm. However while we detect this double band up to 300°C for IF-2 (Figure 95) and IF-3 (Figure 99), when dipentaerythritol substitutes PER, band disappears and APP degrades completely before 300°C. From 250°C, several broad bands centred at 0 and -10ppm assigned to orthophosphates issued from APP degradation and its reaction with the carbon source. It is also noteworthy that at T = 300°C, the two broad bands centred at 0 and -10ppm are still observed whereas another broad band centred at -30ppm appears. This band was observed neither in the case of IF-2, nor in the case of IF-3 but it is well recognized that this band appears when an intumescent system degrades [129, 131]. This band may be attributed to condensed phosphate/polyphosphate species.

At 450°C, we can also see a broad band around -40 and -50ppm, similar to that viewable on the spectrum of the residue of IF-3 at 800°C. This band could be similarly attributed to non-crystallised TiP_2O_7. This is in agreement with the XRD pattern at the same temperature (450°C) showing large bands attributed to titanium pyrophosphate. Once again, we can note the lower temperature at which this phenomenon occurs. By increasing the temperature treatment up to 800°C, this band transforms progressively. The bands are more and more well-defined. At 800 °C, a well-defined spectrum exhibiting a collection of bands between -40 and -50ppm, similarly to what we observe with the basic mixtures (Figure 87) and attributed to TiP_2O_7. In addition a broad band is detected at -30ppm but, similarly to peaks observed by X-Ray diffraction, we cannot assign it because the composition of the formulations are not completely known.

Therefore, X-Ray diffraction and NMR analyses carried out on IF-4 show that TiP_2O_7 is formed from 450°C. Similar reaction as that with PER may firstly be assumed between dipentaerythritol and APP to form a phosphorus ester at 250°C then a phospho-carbonaceous structure at 300°C. However, reaction between phosphorus component and TiO_2 occurs at lower temperature than with PER. Indeed, we detect TiP_2O_7 from 450°C instead of 600°C and their bands are well defined at 800°C instead of 900°C. It evidences that dipentaerythritol speeds up the evolution of the system without modifying the global chemical pathway observed with PER leading to a well-crystallized TiP_2O_7 formation.

III. 5. Discussion and conclusion

III. 5. a) Influence of the carbon source on the chemical pathway and the formation of TiP_2O_7

In order to highlight the effect of the carbon source, we have carried out investigation on three intumescent formulations which contain three different carbon sources: epoxy resin for IF-2, PER and epoxy resin for IF-3 and dipentaerythritol and epoxy resin for IF-4. In the previous chapter, we have underlined the nature of the carbon source on visco-elastic behaviours and on swelling abilities of the intumescent coatings. Thanks to this current chapter, some differences have been highlighted about the chemical changes that take place on the different intumescent systems thanks to the different carbon sources.

Firstly, we have demonstrated that epoxy resin could play the role of carbon source on IF-2 as well as other polyols but only when no other char former is present. Indeed when PER or dipentaerythritol is added, no reaction between epoxy resin and acid source (APP) is detected (or at higher temperatures). Nevertheless, the chemical pathway of IF-2 and the reaction between APP and epoxy resin suggest formation of TiP_2O_7 similarly to what occurs with PER and dipentaerythritol. Then, whatever the carbon source, the TiP_2O_7 formation is observed at high temperature. However, effect of the carbon source can be observed by comparing the temperature where the steps of degradation occur as carbon source seem to shift the temperature where APP degrades or when TiP_2O_7 is formed. To corroborate this change of temperature in the pathway, we can compare the different systems at different characteristic temperatures of their degradation.

Firstly, at 300°C, we observe in Figure 104 that APP is completely degraded on IF-4 while it is still detected for the two other coatings, IF-2 and IF-3 evidenced by the double bands at -22 and -24ppm of APP. So thanks to ^{31}P NMR we can suppose a degradation/reaction of APP at lower temperature with dipentaerythritol than with PER or epoxy resin. The reactivity of the carbon source with APP plays an important role for the esterification reactions and we suppose that it is better with dipentaerythritol. This first step yields to the development of a protective shield but also intermediate products containing residues of APP.

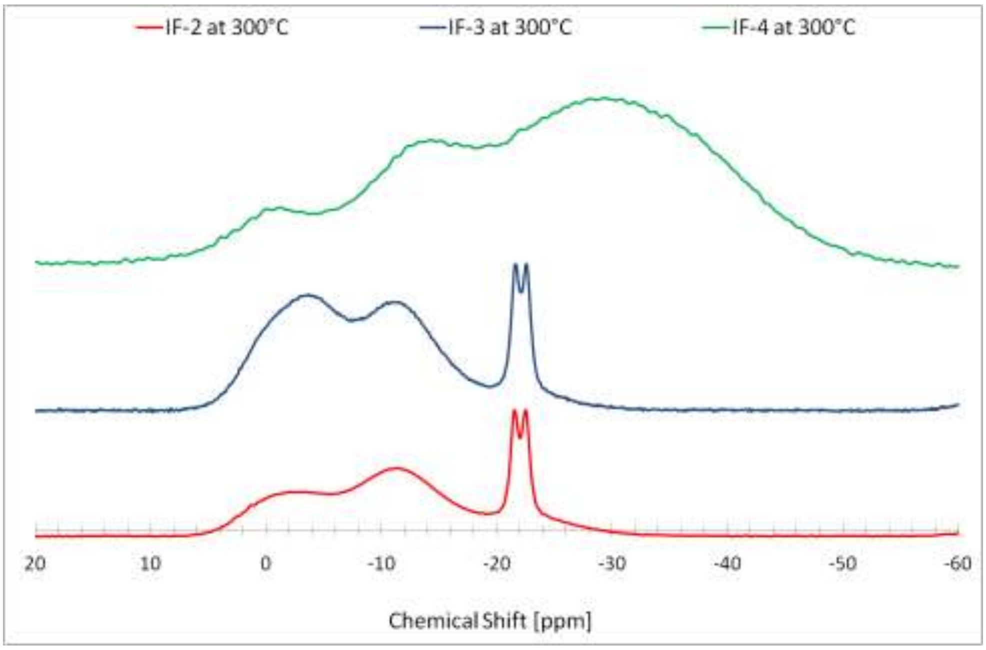

Figure 104 : Comparative ^{31}P NMR spectra of residues of IF-2, IF-3 and IF-4 at 300°C

Even if the structure of the intermediate phosphorus products could be different according to the carbon source, we have shown that these phosphorus based compounds react then with TiO_2 to form TiP_2O_7. Figure 105 shows the evolution of the phosphorus components at 450°C. The delay highlighted about the comparative analyses of IF-3 and IF-4 is prolonged at this temperature corresponding to the reaction between phosphorus components and TiO_2. Indeed, for IF-4 we have already detected a broad band between -40 and -50ppm, which suggests TiP_2O_7 formation. This same band can also be observed with difficulties on spectra of IF-3 but is less intense (highlighting the delay in terms of degradation) and is not viewable for IF-2.

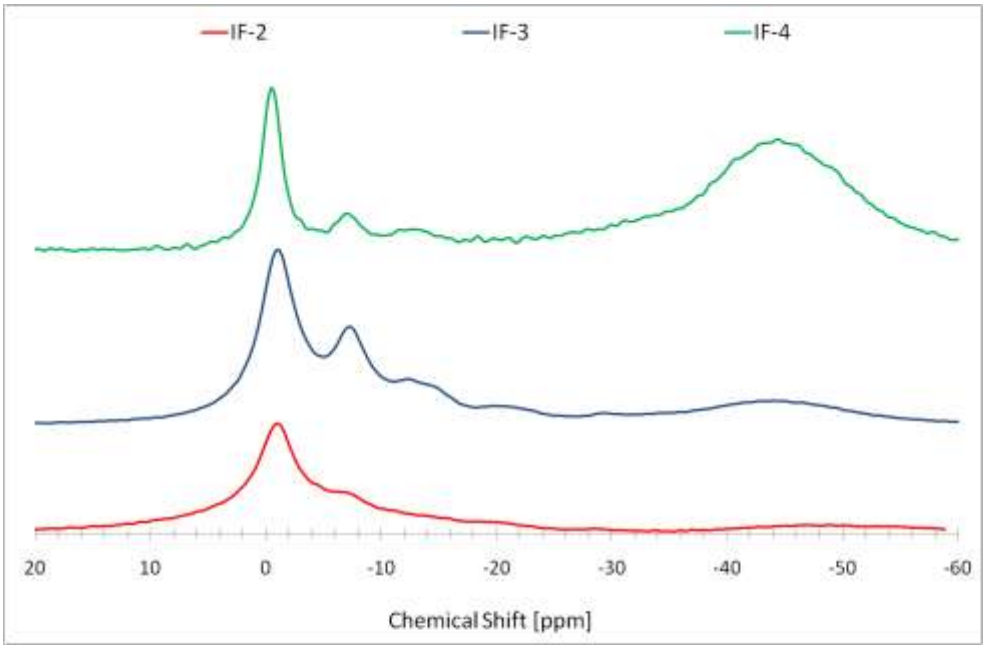

Figure 105 : Comparative ^{31}P NMR spectra of residues of IF-2, IF-3 and IF-4 at 450°C

Lastly, X-Ray diffraction pattern of the final residue obtained from IF-2 at 800°C, IF-3 at 800°C and 900°C and IF-4 at 800°C can be compared on Figure 106. The diffraction patterns in particular those of IF-3 at 900°C and IF-4 at 800°C show similar bands in spite of the difference of temperature. The peaks attributed to TiP_2O_7 are clearly observed in both cases whereas for IF-2 and for IF-3 at 800°C the formation of TiP_2O_7 can only be suspected.

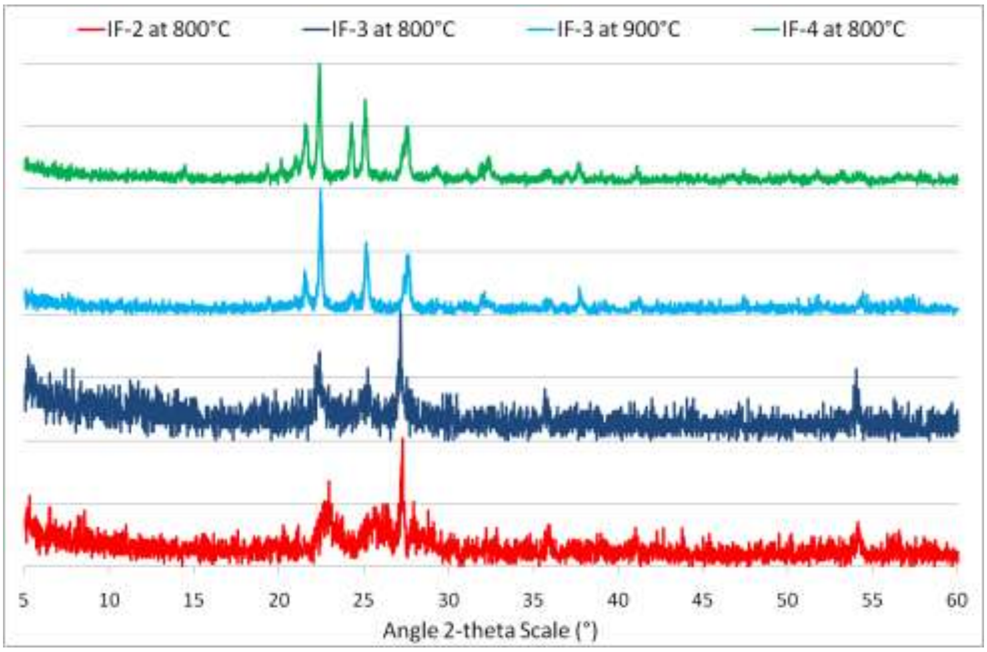

Figure 106 : Highlights of TiP_2O_7 formation at different temperature according to the coating

Therefore, these last X-Ray diffractions and other NMR analyses carried out on the three studied coatings show that whatever the carbon sources used, titanium pyrophosphate is formed. However, the temperature range at which it is formed is different. Concluding a systematic investigation of the evolution of the coatings, the chemical approach of the three coatings highlights the importance of the carbon source and also the role played by TiO_2 on the different formulations. In the study of basic mixtures based on APP, different carbon sources (epoxy resin, pentaerythritol and dipentaerythritol) and TiO_2, we have demonstrated the formation of TiP_2O_7 for the three coatings. The titanium pyrophosphate is the product of a reaction between TiO_2 and the phosphorus components issued from the reaction between APP and different carbon sources. Indeed, APP first degrades into ortho- and pyro-phosphate as evidenced by solid state ^{31}P NMR and then its degradation products react with TiO_2 to yield TiP_2O_7. However, we should note that the temperature range in which this reaction occurs is different according to the carbon source used. Indeed, TiP_2O_7 can hardly be detected from 800°C for IF-3 whereas it is observable from 450°C for IF-4 in diffractogram with three peaks between 20 and 30°. For IF-2 without additional carbon source added to the formulation, epoxy resin alone plays a similar role leading to the formation of TiP_2O_7 at around 800°C.

Consequently, it may be proposed that the use of dipentaerythritol instead of PER or epoxy resin allows to increase the reactivity of APP with the carbon source and thus leads to the formation of TiP_2O_7 at lower temperature, notably. Furthermore, we suspect this crystalline structure to provide a better fire performance to the intumescent coating. Consequently, the formation of such structure at lower temperature and the shift of the chemical pathway could explain the different behaviour of IF-4 for jet-fire test and could be a benefit chemical change for fire protection.

III. 5. b) Chemical investigation of residues from jet-fire resistance test - Correlation with proposed chemical pathways

To correlate further these observations with the performance of the coating at the jet-fire test, we have analysed by X-Ray diffraction residues obtained from the jet-fire resistance tests described on the second chapter. Only IF-2 and IF-4 analyses have been done because they were the only residue available.

On IF-2 char resulting from the large scale jet-fire test (Figure 107), three zones can be distinguished on the piece of char. From the surface to the steel/coating interface, we observe respectively an upper layer that is dense and compact (thickness = 2cm), then on the middle this part exhibits large vacuum with lot of bubbles, and finally near steel another thinner layer (1cm) that is dense and compact.

Figure 107 : Piece of IF-2 char from large scale jet-fire test

So we have analysed these three samples taken on the piece of char of large scale jet-fire test (Figure 108). On large scale test, peaks characteristics of TiP_2O_7 is detected whatever the layer of the sample analysed. In the upper layer, sharp peaks (attributed to TiP_2O_7 or TiO_2) are superimposed on a broad band characteristic of amorphous carbons. Amorphous carbons are mainly located in the upper layer because on the two other samples (middle and inner layer), all bands viewable on the diffractograms are sharp and can be attributed to TiP_2O_7 or TiO_2. Indeed the internal structure of the char seems to be mainly formed with crystalline components and the detection of titanium pyrophosphate is more and more well defined when the layer is deep. We suggest thus a high concentration of carbons on the surface and furthermore presence of TiP_2O_7 all along the depth of the char.

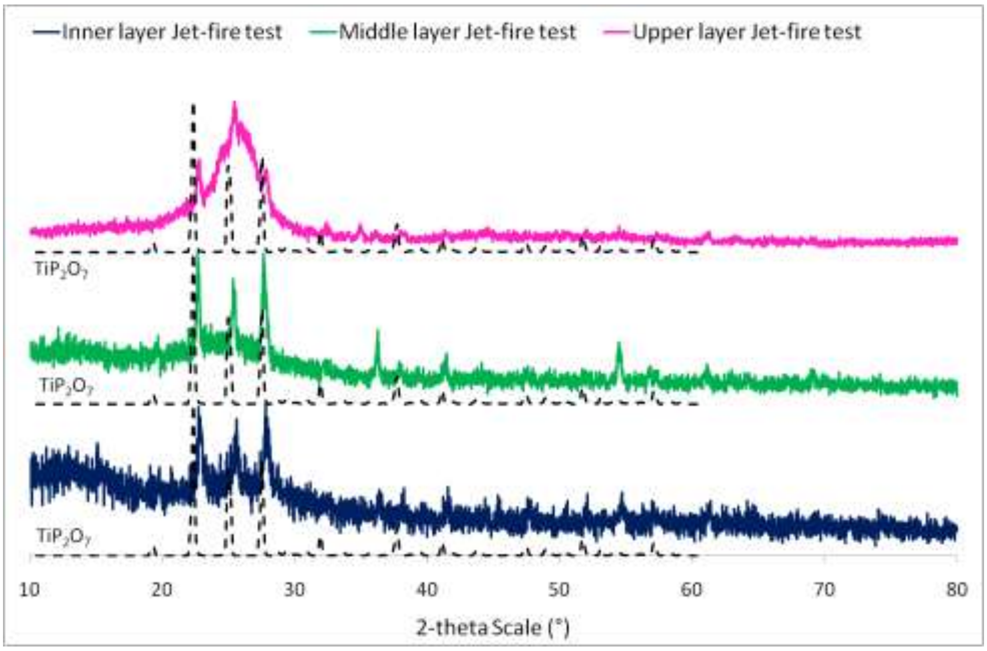

Figure 108 : X-Ray diffractograms of IF-2 residues from jet-fire resistance test

On IF-4 char, it is easier to distinguish two zones on the piece of char (Figure 109). From the surface to the steel/coating interface, we observe respectively a 1cm top layer that peels off for the jet-fire test and a harder and more compact second part with a thickness of 3cm. We have however obtained three samples by dividing into two sections the wide layer near substrate.

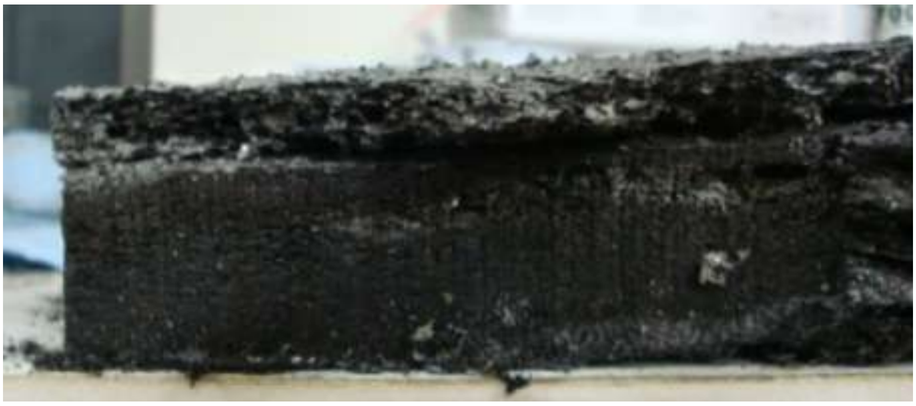

Figure 109 : Piece of IF-4 char from large scale jet-fire test

We have analysed these three samples (Figure 110). On the surface, we find again a broad peak at 27° attributed to amorphous carbons, their presence at the surface to yield to carbonaceous structure is underlined. Overlapped with this broad band, other bands appearing at 25° could be attributed to TiP_2O_7. On deeper layers, TiP_2O_7 could be also detected on the middle of the sample and bands of TiO_2 are present on the basis of the residue, where temperature is lower. Because of thermal protection and temperature gradient, TiP_2O_7 is less and less present from the surface to the depth of the coating.

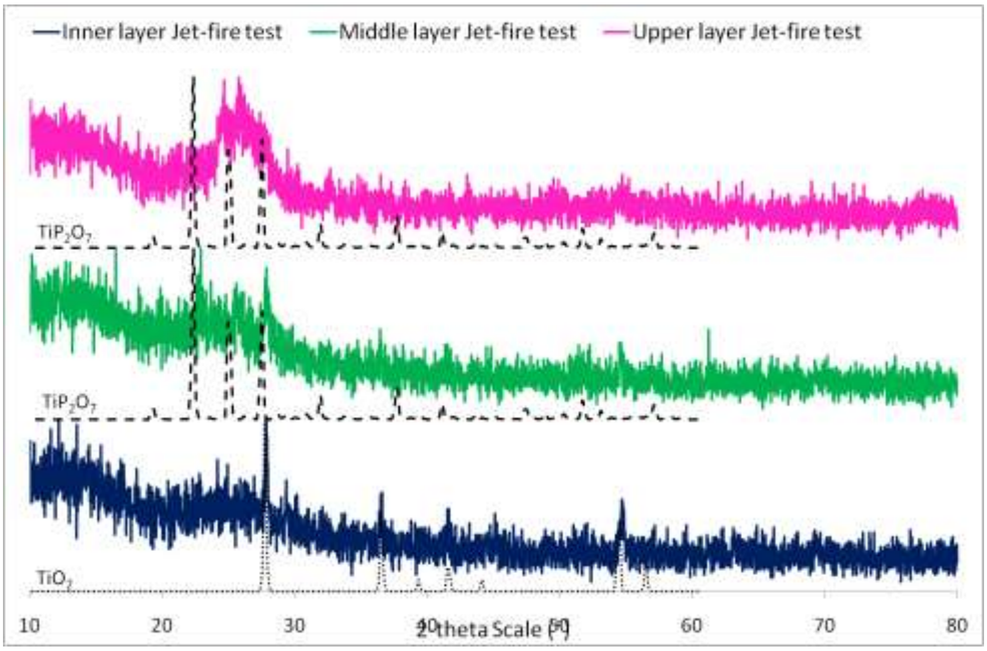

Figure 110 : X-Ray diffractograms of IF-4 residues from jet-fire resistance test

Therefore, we have highlighted the formation of TiP_2O_7 for IF-2 (all along the depth) and for IF-4 (less crystallized compound). Furthermore, we have determined a high concentration of amorphous carbons on the surface. These results should however be put into perspective with the wide temperature range reached for jet-fire test. Indeed, locations of specimen from jet-fire box are not well specified and knowing the temperature gradient existing all along the box, we can highly think that on some zones temperature reached is higher than 800°C and permits TiP_2O_7 formation as for IF-2 sample and inversely some zones are cooler and does not allow the reaction (as we suppose for IF-4 sample).

Nevertheless, with the detection of TiP_2O_7 in piece taken from jet-fire specimen, our chemical pathways proposed in this chapter for each coating are validated. We can assume that whatever the carbon sources used, titanium pyrophosphate is formed. Our analyses have demonstrated however, that the temperature range at which it is formed is different. Indeed, reactivity between APP and the different carbon sources are different, dipentaerythritol react with APP at lower temperature than pentaerythritol. Consequently, the substitution of PER by dipentaerythritol (IF-3 becomes IF-4) allows chemical steps of degradation occurring at lower temperature, notably the formation of TiP_2O_7.

We could finally correlate the formation of such structure and the results exposed for jet-fire resistance test. Indeed, literature shows that formation of TiP_2O_7 could enhance the mechanical resistance of the coating. So it would be rather to form such structure as soon as possible after the beginning of the incident in order to protect reliably the substrate. The next chapter with the development of a labscale tool mimicking large fire test should show the consequence of the chemical pathways on the fire performance of each coating.

Chapter V: Development of an efficient labscale test mimicking large scale jet-fire test

Thick intumescent coatings are usually evaluated in large furnace tests by the test UL 1709 [101] If they pass this test, they are then evaluated by the jet-fire OTI 95634 [103]. Both these tests are essential since they give a good simulation of a real fire and give means of determining whether or not fire protection products present minimum performance criteria required in an offshore platform. However, as these tests are very expensive and time consuming, they reduce the possibilities of testing a large number of formulations.

Nevertheless, significant differences have been highlighted about the behaviours of the four intumescent formulations after large-scale jet-fire resistance test, suspecting their physical properties, notably mechanical resistance or visco-elastic behaviours, being important parameters. These influences have been determined and confirmed by an investigation of the physical behaviours, we have suggested that high mechanical resistance of IF-1 is due to boric acid while other formulations (without H_3BO_3) exhibit low mechanical resistance facing to jet-fire impact. So use of mesh in those intumescent coatings is required to provide an additional reinforcement of the fragile barrier and to keep in place the protective shield. Furthermore the viscosity decrease observed for IF-3 has been stated as an explanation to the jet-fire failure and can be explained by the presence of PER. Indeed, PER is known to cause modification of the visco-elastic behaviours of the coating at lower temperature. The substitution of PER by dipentaerythritol (IF-3 → IF-4) allows to avoid this prejudicial change.

In a second approach, we have determined the chemical pathways of the three intumescent formulations IF-2, IF-3 and IF-4, where only carbon sources change (epoxy resin in IF-2, epoxy resin and PER in IF-3 and epoxy resin and dipentaerythritol in IF-4). Effect of TiO_2 has also been investigated, resulting to formation of TiP_2O_7 at high temperature thanks to a reaction with the phosphorus components of the char with TiO2. Regarding the results, it may be proposed that the substitution of PER by dipentaerythritol allows to increase the reactivity of APP with the carbon source and thus allows occurrences at lower temperature, notably the formation of TiP_2O_7. Similar pathways have been observed for jet-fire resistance test in IF-2 and IF-4 leading to formation of a carbonaceous structure and of a crystallized compound of TiP_2O_7. This product based on titanium and on phosphorus is described in literature to enhance greatly the fire performance of intumescent systems and the mechanical properties of the char, acting as a ceramic binder to reinforce the shield [113].

Knowing all these aspects, the aim of this last chapter is to try to develop experimental and reliable tools at the lab scale which could provide information about the development and the efficiencies of the intumescent structure. These tools could constitute a predictive approach to determine the fire behaviour of the evaluated formulations and give us a low cost and fast test allowing rapid and reliable results of a large number of different coating formulations in order to correlate observations made by our physical or chemical approaches with the results obtained in large scale fire tests.

Therefore, in the first section of this chapter, we introduce a labscale test developed to mimic industrial furnaces used for UL 1709 standards (Figure 111). Equipped with a powerful burner this test allows to evaluate samples according to standardized temperature profiles specified for hydrocarbon fires.

Figure 111 : Industrial furnaces used for UL 1709 standards

Then, previous jet-fire experiments done with the four intumescent formulations and introduced on the 2nd chapter have shown the crucial effect of pressure and temperature during the test. Careful analysis of the chars after the jet-fire test revealed zones of high pressure and zones of high temperature (Figure 112).

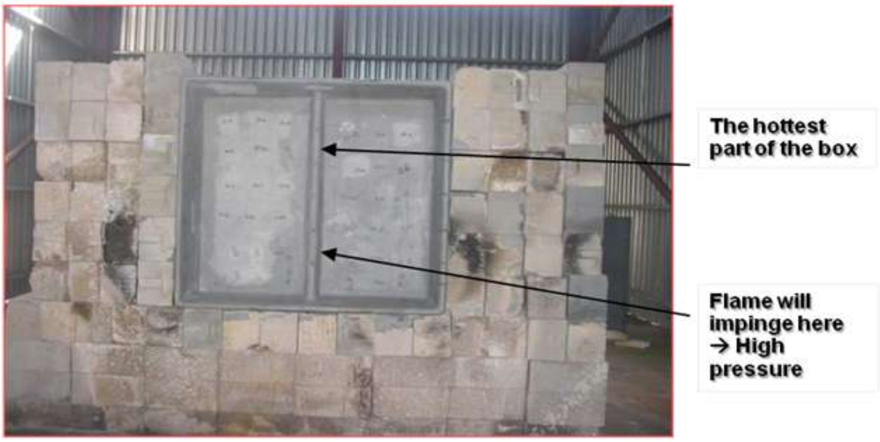

Figure 112 : Jet-fire box test and zones of high temperature and/or high pressure

The work on the second section of this chapter has so to detail the development of a small scale test mimicking jet-fire conditions. The setup of this test should take into account these two parameters (pressure and temperature), provide similar distributions of heat and pressure and thus permit observation of coating behaviours in agreement with large scale ones.

I. Preliminary fire test in furnace conditions

The aim of this test is to evaluate the efficiency of the intumescent coating in terms of heat transfer similarly to industrial standardized furnace tests but at laboratory scale.

I. 1. Experimental apparatus and materials

Contrary to large industrial fire test, our test occurs in $50cm^3$-sized furnace but its design remains close to that of bigger furnaces (Figure 113). In addition, advantages of our test are the small scale and the easy handling of the tool to screen several formulations and to test quickly the performance of different formulations. As in the case of large furnace test, time/temperature profiles are measured on the back of a coated steel plate.

In our test, the heat source is a powerful propane burner generating 35kW. Steel plates used are squares of $10*10\ cm^2$, 3.5mm thick, the steel is exactly the same as that used in the industrial test. About 1mm of the intumescent coating is applied on the surface of the steel plate. A black coating, provided by Medtherm Corporation (Huntsville, Alabama), resistant to 800°C and having a constant emissivity of 0.92 is applied on the non-heated side of the steel plates. The constant emissivity of the backside of the plate allows accurate measurement of the surface temperature of the plate using an infrared pyrometer or infrared camera. The infrared camera is positioned at a constant distance from the steel plate and focused on the back surface of the plate. It detects the temperature on the non heated face of the steel plate and records the time / temperature curve on a computer. The measurement of temperature without contact has several advantages: it is instantaneous and can be carried out in places which are difficult to access. It enables measurement over a larger range of temperatures without corrosion or degradation. However, it is still important to carefully control various parameters which could affect the measurements, such as for example the presence of fumes or dust.

Figure 113 : Pictures of the small scale furnace test

The aim of intumescent coatings is to decrease as much as possible the slope of the time/temperature curve, i.e. reaching 400°C as late as possible. Indeed, steel begins to lose most of its structural properties between 470 and 550°C. The temperature of 400°C has been thus unofficially adopted as critical temperature for heavily loaded structural components. So, time of failure, namely the time when the steel temperature reaches 400°C, is obviously one of the parameters to be improved: the best result is obtained when the longest time of failure is reached. It means that the coating has the best protective effect.

I. 2. Temperature profiles and results

Small furnace tests have then been carried out on the different intumescent formulations comparing virgin panel and a panel coated only with the epoxy resin (DGEBA + hardener). The time/temperature curves obtained in labscale furnace tests are shown on Figure 114.

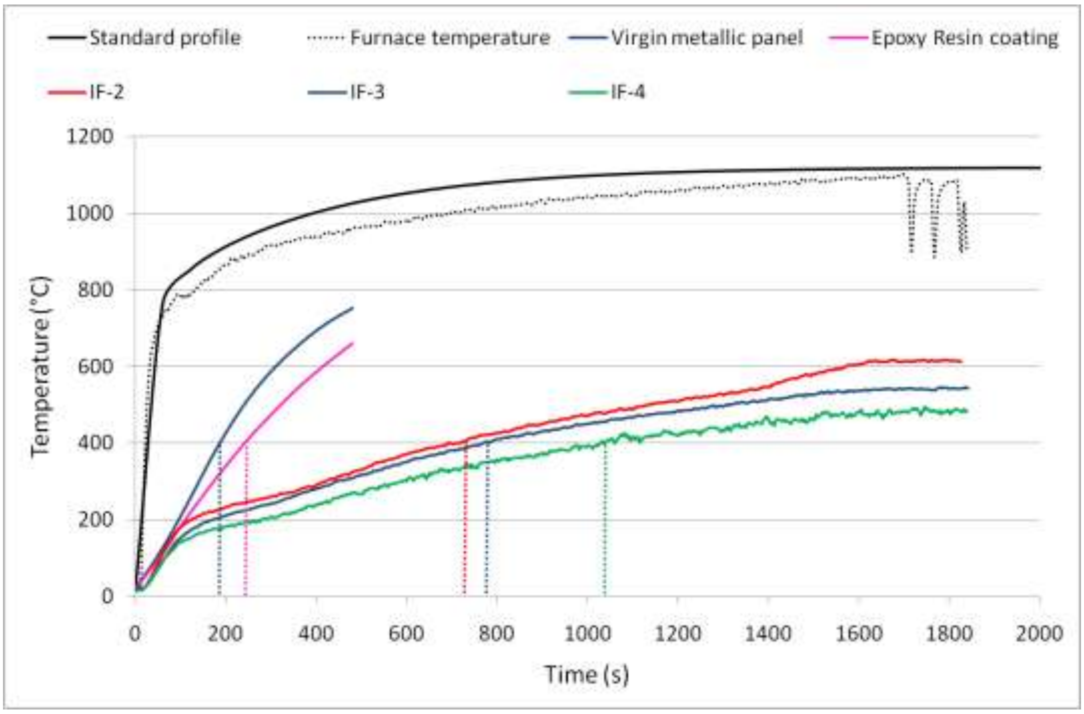

Figure 114 : Comparison of the time/temperature curves obtained for IF-2, IF-3, IF-4 and for epoxy resin using the small scale furnace test

Firstly, we can note the good agreement between the specified temperature profile of the standard and the temperature taken by thermocouple inside furnace during test, even if the first goal of this test is not a certification but a preliminary observation of the fire behaviour of the different coatings. The temperature rises rapidly to 900°C within 4 minutes and significantly higher overall temperatures are reached (between 1100°C and 1200°C).

Then the virgin plate reaches 400°C in 3 minutes and the epoxy resin coating whose quality is of course not the thermal insulation does not improve the thermal behaviour of the panel (time of failure is 3 minutes and 30 seconds). However, when the intumescent coatings are applied, time of failure increases significantly. It is multiplied by 4 whatever the formulation: IF-2 and IF-3 exhibit a similar behaviour with a time of failure between 750 and 800 seconds while substitution of PER by dipentaerythritol in IF-4 provides an increase of 25% more of time of failure up to 1050 seconds i.e. 17 minutes.

This improvement of time of failure can be correlated with the previous chemical properties introduced in the previous chapter. X-Ray diffractograms of residues are plotted on Figure 115.

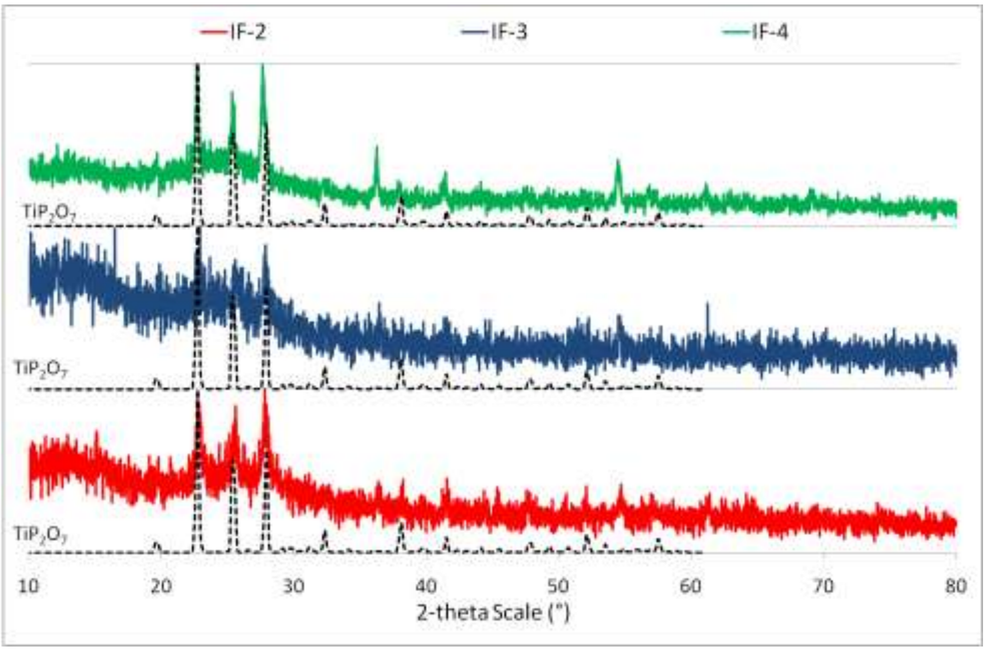

Figure 115 : X-Ray diffractograms of residues of IF-2, IF-3 and IF-4 after small furnace tests

Whatever the formulations, analyses have shown the formation of TiP_2O_7 for a testing time of 30 minutes. This formation is in agreement with the temperature measured on furnace and with the chemical investigation of the previous chapter. Indeed at 800°C, TiP_2O_7 is formed whatever the carbon source, nevertheless diffractograms in Figure 115 show clearly that its crystallinity are not the same in the case of IF-4 with dipentaerythritol than in the cases of IF-2 and IF-3 with respectively PER or epoxy resin. On diffractogram of IF-4, we observe three well-defined peaks attributed to TiP_2O_7 (similarly to what we observe after tubular furnace heat treatment at 800°C for IF-4) showing the great crystallinity of the residue. On the contrary, for IF-2 and IF-3, the ratio signal to noise is higher even if the three peaks of TiP_2O_7 are detected (similar to what we observe after tubular furnace heat treatment at 800°C for these two intumescent formulations). Therefore, based on conclusions demonstrated in the previous chapter about the formation of TiP_2O_7 at lower temperature with dipentaerythritol (IF-4), we assume that titanium pyrophosphate have been yielded earlier for fire test and we can suggest that the better efficiency observed with IF-4 than with IF-2 and IF-3 is correlated to the chemical changes of the formulation.

Therefore, thanks to this first test according to hydrocarbon fire and UL 1709 standard, we have highlighted a clear correlation between the chemical evolution and TiP_2O_7 formation in a first hand and the thermal efficiency and the time of failure in the other hand. It appears that the formation at lower temperature of the crystalline structure based on titanium can provide an additional efficiency of the coating. We suspect thus that TiP_2O_7 formation enhances fire protection because of formation of a ceramic-like protective material in char structure, as suggested elsewhere [113, 124]. Moreover, the thermal properties of such structure could allow a better reflection and a lower absorption of heat, these characteristics being responsible for the bulk and surface temperature of the shield.

Exhibiting good correlation with previous investigation about physical and chemical properties of the intumescent formulations, the first experimental setup appears as a reliable, fast and low cost tool to evaluate fire performance of intumescent coatings in furnace conditions. However, similar to standard conditions, a second tool must be developed to take into account the specificity of jet-fires that occur on offshore platforms and their characteristics due to high velocities, such as heat flux and erosion.

II. Development of a fire test mimicking jet-fire

The aim of the jet-fire test is to simulate an accidental load from a gas line rupture on an offshore oil rig. So, similarly to what we have developed for hydrocarbon furnace test, a small scale test mimicking jet-fire experimental settings will be beneficial to multiply the data and to minimize the cost. Moreover, a second objective of this test will be to separate the two phenomena that take place in a jet-fire and the two crucial parameters that we have highlighted on the second chapter:

- A **high momentum** of the jet due to the **velocity** of the jet and flame impact on the panel causing important **pressure** notably on the impact zone
- A **radiative** phenomenon due to the flames and providing the most part of the heat and causing the greater **temperature** change.

II. 1. Experimental settings and optimisation

II. 1. a) Experimental apparatus

Tests have been firstly carried out on 10*10cm²-sized squared metallic panels coated with 1.5mm of each coating. Eventually a mesh has been included into the coating to reinforce the structure similarly to specimen used for large-scale jet-fire test and described in the second chapter. In a last section, we have also evaluated the performance of intumescent formulations coated in panels with central flange, similarly to the ones used in large scale jet-fire test.

An experimental setup (Figure 116) has been home-built using two different heating devices in order to observe precisely the behaviours of the coating and to control independently and separately the two main phenomena characterizing a jet-fire.

Figure 116 : Experimental setup of the labscale jet-fire test

In a first hand, an electrical cone heater provides pure radiative heat and in a second hand an air jet of controlled temperature and pressure providing pure convective heat is used. The combination of the cone heater and the air jet should then provide a mix of convective and radiative heat at the same time with accurate controlled parameters (heat flux, pressure or velocity of air jet, temperature of air jet). Therefore, our work starts with the determination of the optimal setting parameters to discriminate the behaviours of the four intumescent formulations according to the previous observations during jet-fire test exposed in the second chapter.

II. 1. b) Determination of the optimal parameters

First experiments have been carried out to determine the appropriate experimental conditions: heat flux of the cone heater, velocity of the air jet, time to deliver the air jet (an early air jet can avoid the expansion of the intumescent coating). The studied parameters are summarized in Table 11. All these parameters have been chosen in agreement with the standard of the large scale jet-fire resistance test focusing on nozzle geometry and gas flow of propane but also based on the literature review about jet-fire highlighting important role of the jet length (varying with velocity) and heat radiation (taking into account with the heat flux from conical heater).

Table 11 : Screening of the different setting parameters used in the labscale jet-fire test

Air temperature	Air speed (Air pressure)	Heat flux of cone heater	Delayed time to switch on air jet	Total Time
450°C	15m/s (0.5bar)	35kW/m²	Immediately	15min
-	30m/s (1bar)	50kW/m²	After 150 seconds	-
-	-	-	After 300 seconds	-

Concerning the heat flux from the cone heater, several tests have been carried out at 35 and 50kW/m² on the four coatings. Results are presented in Figure 117. Increasing the external heat flux of the cone does not have a great effect on the time/temperature profiles (air jet is switched on at time zero and the air speed is fixed at 15m/s). Whatever the heat fluxes, temperatures on the plateau (steady state zone) are similar; however the time to reach it is as expected shorter at 50kW/m² than at 35kW/m². Similar intumescence factors (expansion) and observations of the hole caused by the air jet are found at the two irradiances (see the pictures on Figure 118).

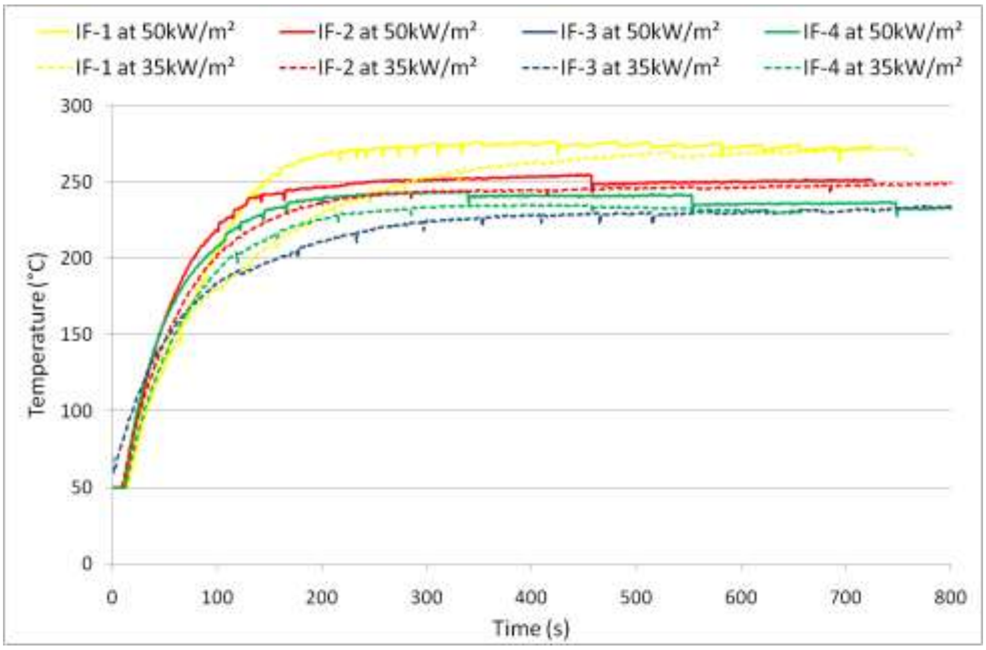

Figure 117 : Temperature profiles on the backside of panels coated by IF-1, IF-2, IF-3 and IF-4 in labscale jet-fire test at two heat fluxes, 50kW/m² (full curves) and 35kW/m² (dotted curves)

Figure 118 : Char aspect after labscale jet-fire test at 35kW/m² (on the left) and at 50kW/m² (on the right) – Example of IF-2

However, heat flux of 50kW/m² targets a forced-flaming combustion scenario that is typical of developed fires. Consequently, we have chosen **the higher irradiance (50kW/m²)** to continue the optimisation of the tests.

Typical experimental conditions are then: (i) cone heater supplying an external heat flux of 50kW/m² and (ii) air jet exhibiting a velocity of 15m/s heated at 500°C. In spite of this high temperature, it is noteworthy that the main heat contribution is provided by the radiative heat flux (surface temperature of the sample is equal to 730°C) while air jet provides mainly an impacting force at the surface of the sample (momentum effect) causing damage due to air speed. Indeed when we compare the profiles with and without air jet (Figure 119), the temperatures reached are very close, except for IF-3.

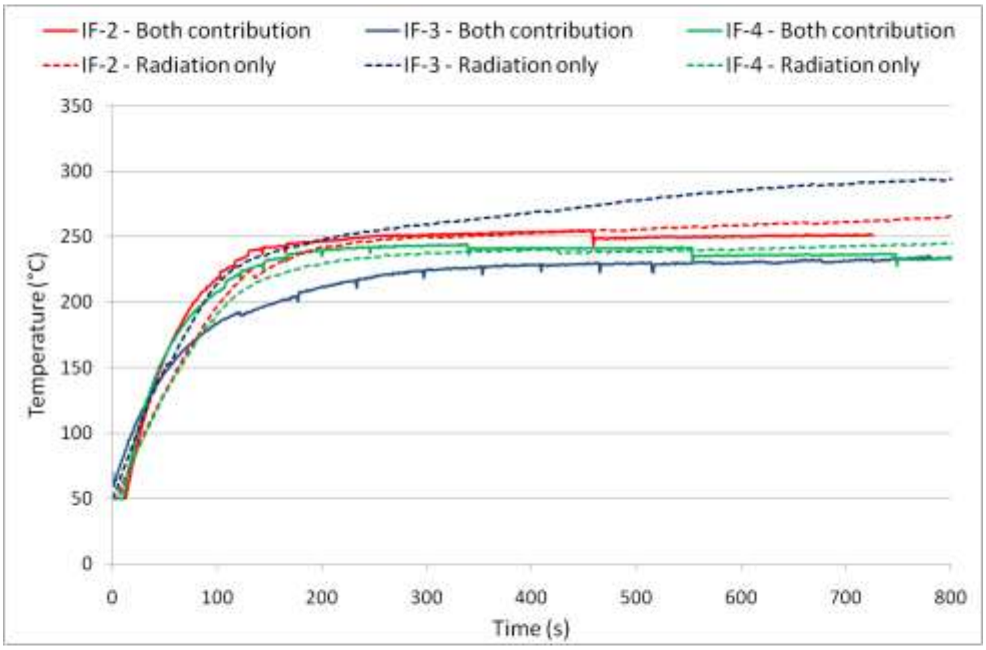

Figure 119 : Temperature profiles on the backside of panels coated by IF-1, IF-2, IF-3 and IF-4 in labscale jet-fire test according to air jet contribution, with air jet (plain curves) and without air jet (dotted curves)

Another observation is that differentiation between the coatings is not significant. Even with air jet, no change can be detected to differentiate the char resistance of the coatings. To improve our protocol, we have examined different setups by varying the time when air jet is turning on. Without air jet, the coating can expand freely, after full expansion of the intumescent coating, the air jet is turned on and observations can be made concerning the char resistance. Figure 120 shows the consequence of delaying the air jet. Indeed, after switching on the air jet at 150 seconds, we observe a quick increase of the temperature on the backside of the panel because of partial destruction of the protective coating. This destruction is evidenced by the pictures taken after the test that show only a print when air jet and cone heater are switching on together (Figure 121, left picture) while important damage is observed when air jet is delayed (Figure 121, right picture).

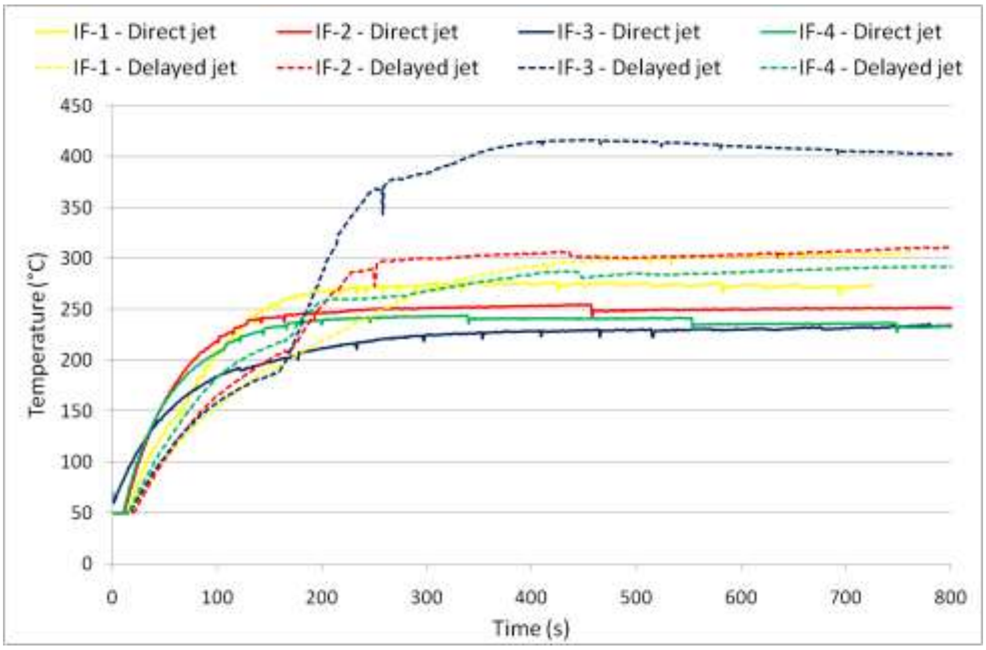

Figure 120 : Temperature profiles on the backside of panels coated by IF-1, IF-2, IF-3 and IF-4 according to time when air jet is switching on: air jet is switched on at the beginning of the test (plain curves) or air jet is switched on 150 seconds after the beginning of the test (dotted curves)

Figure 121 : Char aspect after labscale jet-fire test without time delaying (on the left) and with time delaying (on the right) – Example of IF-2

According to the above results, we have decided to apply a ‘delayed time’ for turning air jet in order to improve the differentiation of the coatings. Two values of delayed time have been selected at **150 seconds and 300 seconds**. Time delaying allows the char develops freely and then to be impacted by the air jet.

Finally, the velocity of the air jet or pressure must be determined. At 30m/s, all the coatings, except IF-1, exhibit severe damage but differences cannot be distinguished (results are not presented). We have thus fixed the velocity of the air jet at 15m/s. This velocity allows observing significant difference between the coatings and provides a sufficient impact to damage the more fragile coating without modifying the behaviour of the most robust one.

In Table 12, we have summarized the optimal parameters permitting to discriminate the behaviour of the four intumescent coatings.

Table 12 : Optimized configurations used to evaluate the four coatings with the labscale jet-fire test

	Air temperature	Air speed	Heat flux of cone heater	Delayed time to switch on air jet	Total Time
1st configuration	450°C	15m/s	50 kW/m²	After 300 seconds	15min
2nd configuration	450°C	15m/s	50 kW/m²	After 150 seconds	15min

In order to be as clear as possible, we propose to present only the results obtained with the 1st configuration both when coatings are applied alone on square panels and when mesh is included to reinforce the intumesced structure. Others results obtained with the 2nd configuration can be found in appendix.

II. 2. Tests on squared panels coated by intumescent formulations

The four coatings have been evaluated using squared panels according to the optimisation done above. Before presenting the results and thanks to previous analyses notably determination of the mechanical resistance using our rheological approach, the behaviour of our coatings can be summarized as follows:

- IF-1 is known to be a robust coating exhibiting a dense and compact char. This coating is our reference in terms of resistance facing to jet and the preliminary experiments confirms this information.
- The three other coatings, IF-2, IF-3 and IF-4, are coatings with relatively low resistance facing to strain, jet and impact.

Temperature profiles obtained with the four coatings on the backside of the panel are shown in Figure 122.

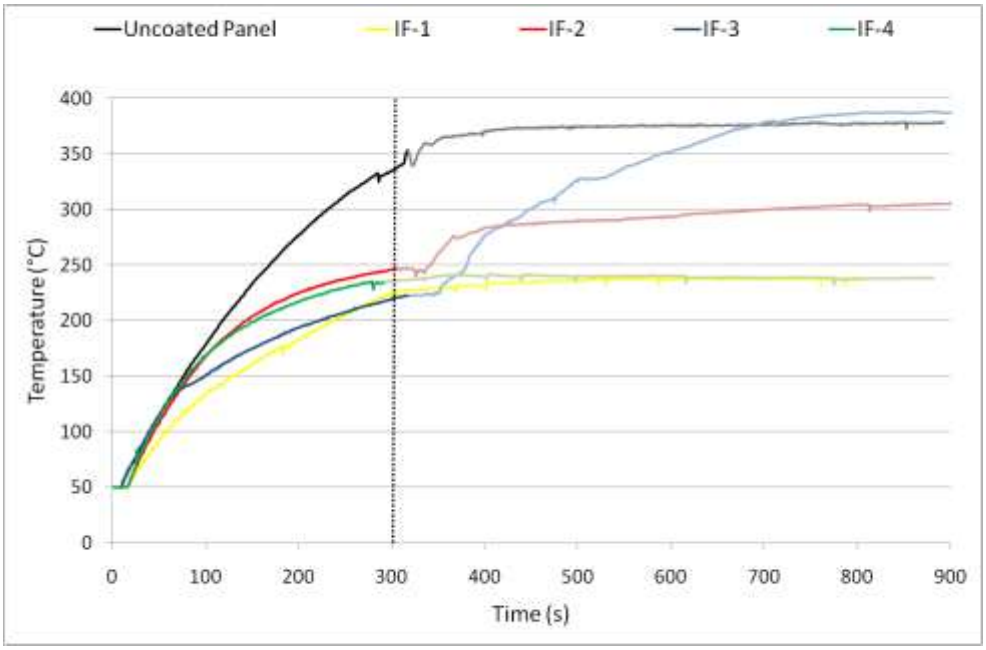

Figure 122 : Temperature profiles obtained in labscale jet-fire test for IF-1, IF-2, IF-3 and IF-4 (heat flux of 50kW/m², air speed of 15m/s, delayed time of 300 seconds)

Analysing the temperature profiles of the four coatings, we can suggest two behaviours. A type of coating is sensitive to air jet because IF-2 and IF-3 exhibit increasing slopes on the time/temperature profiles when turning on air jet. The other types of coating, IF-1 and IF-4, exhibit smooth time/temperature profiles. It can be explained by the remaining charred layer on the panel while chunks of intumescent char are blasted off by air jet leaving unprotected steel at the location of the impact zone in the case of IF-2 and IF-3.

Careful investigation of the char after performing the test provides additional information. IF-1 char (Figure 123) does not present any trace of the air jet impact. The swelling is relatively low (0.7cm – 450%) but the char is very dense and it provides a homogeneous protection characterized by no temperature gradient on the backside.

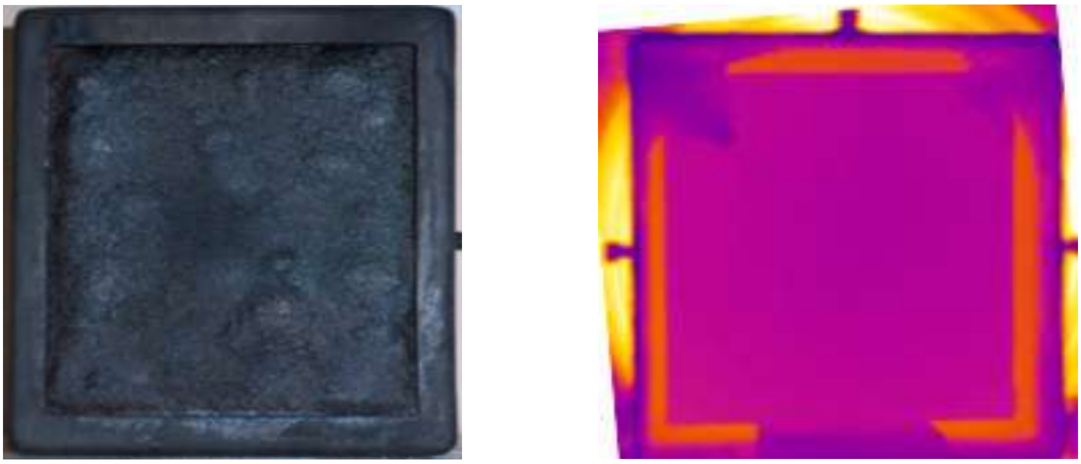

Figure 123 : Picture of IF-1 char after labscale jet-fire test and thermal image for labscale jet-fire test (heat flux of 50kW/m², air speed of 15m/s, delayed time of 300 seconds)

Concerning the ‘fragile’ coatings (IF-2 and IF-3), damage on IF-2 (Figure 124) caused by air jet is very significant. After test, different concentric circular zones from the centre to the edge are observed. At the centre, a 1.2cm-diameter zone is almost uncoated which explains the increase of the temperature and the ‘halo’ in the middle of the IR image (Figure 124). Swelling up to 1.3cm with eroded char is observed on the edge of the impact zone.

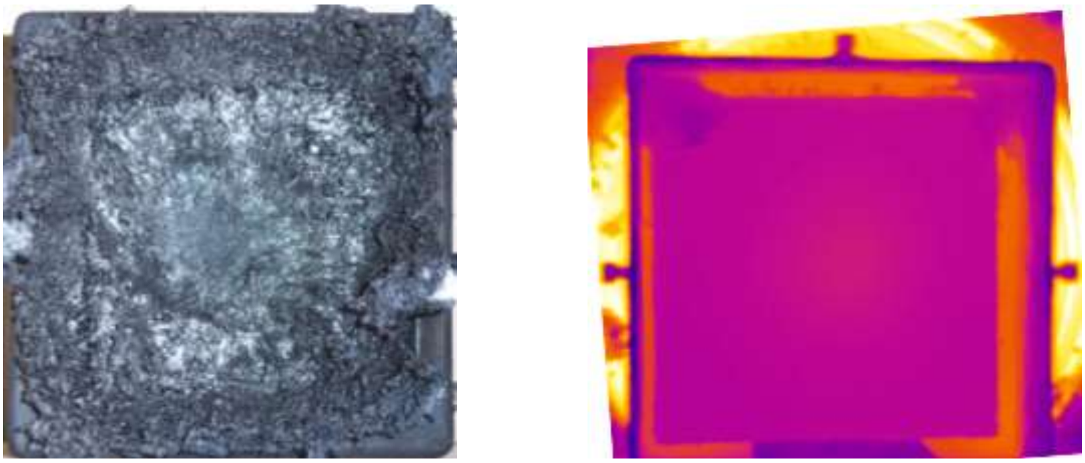

Figure 124 : Picture of IF-2 char after labscale jet-fire test and thermal image for labscale jet-fire test (heat flux of 50kW/m^2, air speed of 15m/s, delayed time of 300 seconds)

IF-3 is known to be the most fragile coating. After turning on the air jet, IF-3 exhibits temperature close to that obtained with virgin panel (Figure 122). By observing the char after test (Figure 125), the reason is self-explanatory. Indeed due to air jet impact, the structure is totally destructed and lets a large unprotected zone. In this zone, a quick increase of temperature is measured since this temperature reaches that of virgin panel. Obviously, no swelling measurement is available. This behaviour can be explained both by a bad adhesion and a bad mechanical resistance to air jet. The large zone of unprotected steel should be compared to the observations done after the jet-fire test where IF-3 failed for the same reasons. In fact, under strain caused by a jet, the intumescing structure does not adhere to the metallic substrate and is ejected by the jet.

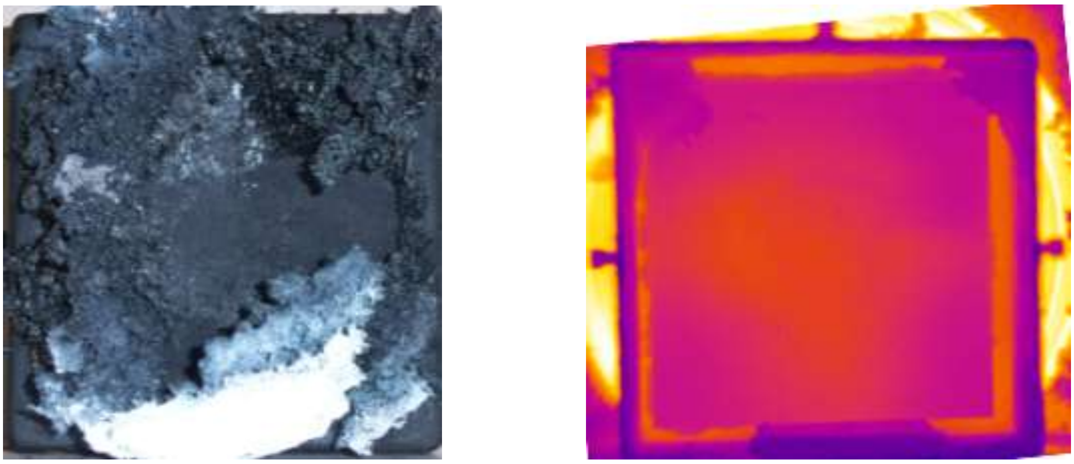

Figure 125 : Picture of IF-3 char after labscale jet-fire test and thermal image for labscale jet-fire test (heat flux of 50kW/m², air speed of 15m/s, delayed time of 300 seconds)

Concerning IF-4, the difference with IF-3 is very significant. Firstly, on the temperature profiles (Figure 122) we can observe that the temperature does not change when the air jet is switched on. This good insulation is confirmed by the char aspect (Figure 126). Indeed, we can see that a stronger protective layer (thickness = 1cm) remains stuck on the panel all along the test. Consequently, the protection is homogeneous and the temperature on the backside of the panel remains lower than 250°C. However, it is noteworthy that the upper part of the intumescent structure is partially damaged by the air jet although it provides protection.

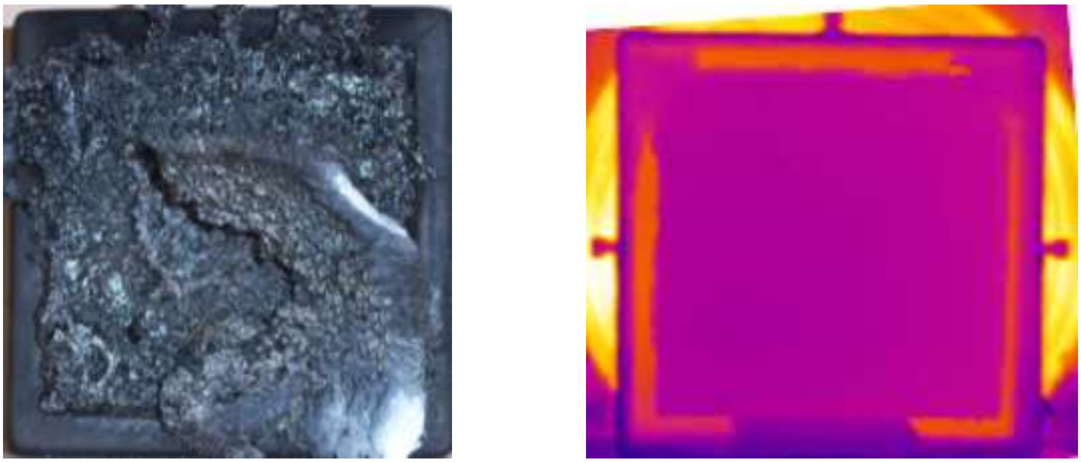

Figure 126 : Picture of IF-4 char after labscale jet-fire test and thermal image for labscale jet-fire test (heat flux of 50kW/m², air speed of 15m/s, delayed time of 300 seconds)

As a conclusion with this experimental configuration, the formation of a cohesive structure and the superior impact resistance of IF-1 are confirmed. Differences between the formulations can be commented as follows:

- **IF-1 does not exhibit any damage caused by air jet impact. Nevertheless, expansion is relatively low.**

- **The intumescent structure developed from IF-3 is completely destructed while that of IF-2 is partially destroyed at the location of impact and the rest of the structure is kept on the panel.**
- **Substitution of PER by dipentaerythritol provides a significant improvement of the resistance of the char. Containing dipentaerythritol in IF-4, a residual protective layer is maintained on the panel even if the upper part is partially damaged while with PER on IF-3, all the coating is pulled out.**

II. 3. Tests on squared panels coated by intumescent formulations reinforced with mesh

The use of mesh in intumescent coating provides an additional reinforcement of the barrier formed when burning. The efficiency of this reinforcement has been demonstrated for large scale jet-fire resistance test with IF-2 and IF-3, particularly because of their low mechanical resistance whereas its effect is not significant for a robust coating as IF-1. Therefore, to improve the mechanical resistance and to keep a sufficient insulation, mesh has been incorporated inside the three “fragile” coatings. Except this incorporation, experimental configuration remains similar and the temperature profiles are shown on Figure 127.

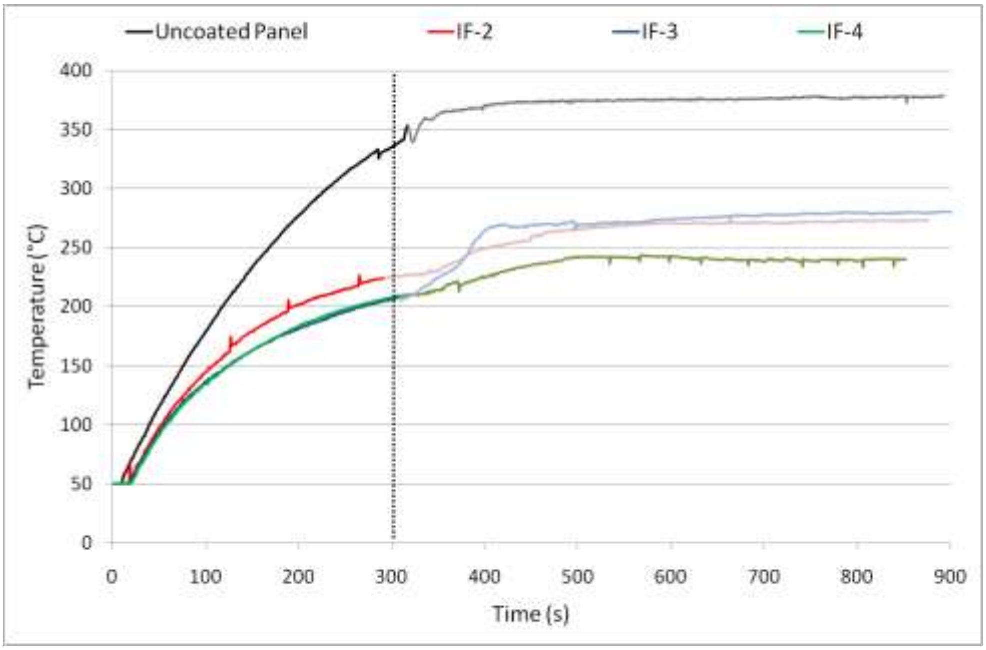

Figure 127 : Temperature profiles obtained in labscale jet-fire test for IF-2, IF-3 and IF-4 reinforced by mesh (heat flux of 50kW/m², air speed of 15m/s, delayed time of 300 seconds)

The inclusion of mesh improves the resistance of the coating facing to air jet. Although the temperature profiles of IF-2 and IF-3 still exhibit an increasing slope directly link with the switching on of the air jet, this phenomenon is attenuated and almost disappeared for IF-2 thanks to the reinforcement provided by mesh.

Concerning IF-4 coating, knowing that its behaviours without mesh are relatively good and damage does not appear as dramatic, effect of mesh are not significant and have just confirmed a better resistance of IF-4 facing to air jet than IF-2 and IF-3. No temperature variation has been detected on its temperature profile. This difference of behaviours between IF-3 and IF-4 is much more highlighted by the similar evolution of the temperature before onset of the air jet (curves are superimposed) while a gap appears after applying the air jet.

Therefore, mesh provides a great improvement for the resistance of the coating. To confirm information provided by temperature profile, an investigation of the char aspects after test is shown on Figure 128. First observations of the chars suggest that a higher amount of residues remain on the steel plate than with the previous settings. Incorporating mesh in the coating permits to keep the intumescent structure on the panels and to protect them.


IF-2 IF-3 IF-4

Figure 128 : Pictures of the char obtained with intumescent coatings reinforced by mesh after labscale jet-fire test (heat flux of 50kW/m², air speed of 15m/s, delayed time of 300 seconds)

IF-2 develops an intumescent structure with a swelling of 1.7cm with mesh. On this structure, a 1.3cm diameter central hole is formed by the impact of the air jet which does not reach the panel. A residual dense layer remains stuck on the panel, this layer is kept thanks to mesh and its presence is not observed for previous experiments carried out without mesh.

Char developed from IF-3 exhibits large differences with and without mesh after the test. Mesh keeps the structure on the panel except on the impact zone where a 1.9cm-diameter zone of non protected steel is formed which can explain the increase of temperature. However, by comparison with first experiments we can note that panels remains mainly protected. Of course thermal conductivity of steel and local weakness of the coating cause a temperature profile exhibiting quick increase when air jet impacts.

Finally, the behaviour of IF-4 is similar with and without mesh. Indeed, the temperature profiles are similar reaching 250°C in the steady state zone. Similar intumescence factor and damages are observed. No effect of mesh must however be put into perspective with the great behaviour exhibited without mesh similarly to IF-1.

Using the experimental parameters defined in the beginning of this section, **the benefit of mesh is shown. It permits to enhance the impact char resistance and the thermal insulation keeping char at the surface of the substrate.** Nevertheless, mesh is not sufficient to maintain the structure of IF-3 on the impact zone.

II. 4. Tests on flanged panels coated by intumescent formulations

To mimic the specific setup of the panel during jet-fire test, our panels have been modified accordingly. The panels have been designed with a flange located in the middle of the steel plate (Figure 129). This geometry could modify the swelling of the systems especially at the edge between the flange and the back faces. Holes have been drilled right through the flange and thermocouples have been embedded in the flange so that the thermocouple is located at the interface coating/panel during the test. The panel undergoes an external flux of 50kW/m^2 and the jet is turned on at 300 seconds after the beginning of the test. Jet impacts at level of the second hole i.e. in the middle of the flange. However, with this geometry, it is not possible to measure temperature profiles and to observe thermal cartography by IR camera, only measurements with thermocouples at three positions is possible for measuring time/Temperature profiles.

3 thermocouples, positioned at the interface between panel and coating, follow the panel temperature and highlight the efficiency of the coating

Figure 129 : Experimental setup to use flanged panels in labscale jet-fire test

Using this specific design IF-1 exhibits superior impact resistance against air jet. The temperature profiles taken in three points (Figure 130) show a constant increase of temperature except when the air jet is turned on. At this time (300 seconds), we observe a slight decrease of the temperature and then its stabilization. We have attributed this change to the variation of the temperature and the contribution of the air jet cooling down the surface of the coating (convective effect) as previously discussed.

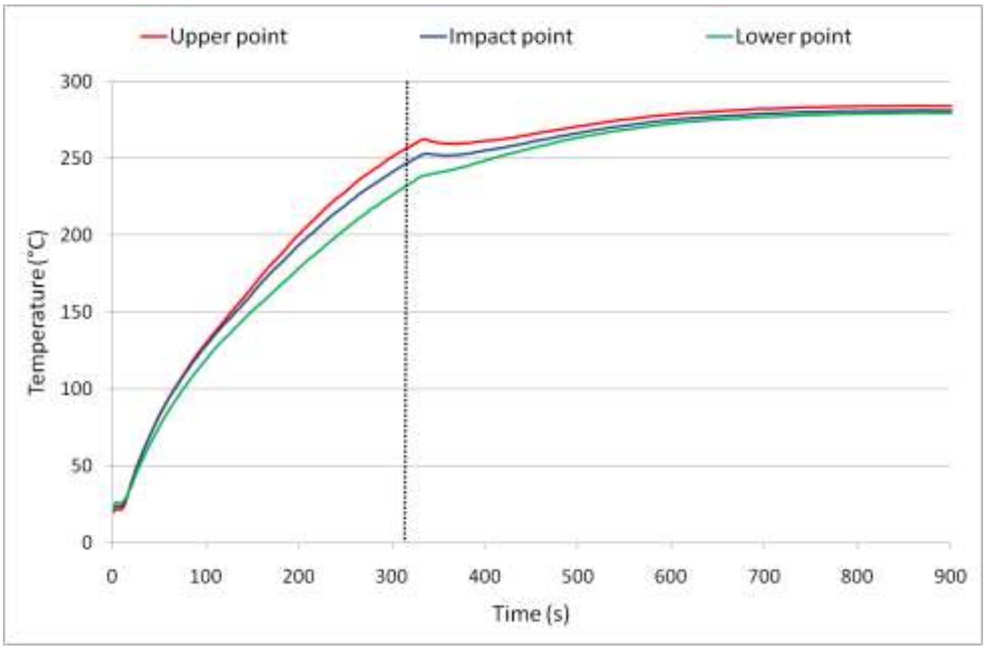

Figure 130 : Temperature profiles obtained in labscale jet-fire test for IF-1 coated on flanged panel (heat flux of 50kW/m², air speed of 15m/s, delayed time of 300 seconds)

Before onset of the air jet, temperature evolutions are very smooth. Radiative effect causes a temperature gradient from the bottom to the top of the flange. However, we can detect one inflexion point on the temperature profiles when the air jet is switched on. These variations cannot really be explained by observing the samples after test. Indeed, visual investigation of the char (Figure 131) after the test confirms the good resistance of the coating facing to heat and to impact. No damage is detected on the char surface, a compact and dense char with some bubbles coats the whole panel.

Figure 131 : Char obtained from IF-1 after labscale jet-fire test on flanged panel (heat flux of 50kW/m², air speed of 15m/s, delayed time of 300 seconds)

Concerning the three other formulations, the intumescent chars are affected facing to jet, notably on the impact zone, as shown on Figure 132.

IF-2 IF-3 IF-4

Figure 132 : Pictures of chars obtained from IF-2, IF-3 and IF-4 after labscale jet-fire test on flanged panel (heat flux of 50kW/m², air speed of 15m/s, delayed time of 300 seconds)

For IF-2 (Figure 132), the central part of the flange exposed to the jet is no longer coated by intumescent structure at the end of the test while the upper and lower places are still protected. The surface adjacent to the flange is also damaged by air jet because we can observe on the left part a partial blast of the coating caused by air flow. However, contrary to the experiments carried out with flat panels, temperature profiles obtained with thermocouples on the interface metal/coating does not show this destruction on the flange. Indeed, in agreement with the observation done on IF-2 char, we expected to observe significant increase of temperature, notably on the impact zone where coating is destructed. Instead of this, IF-2 profiles (Figure 133) exhibit curves that are initially superimposed representing the uniform evolution of the coating facing to heat flux from cone heater. But when air jet is switched on (after 300 seconds), temperature increases slightly on the boundaries and more strongly on the impact zone. However, the differences are not significant to make conclusions.

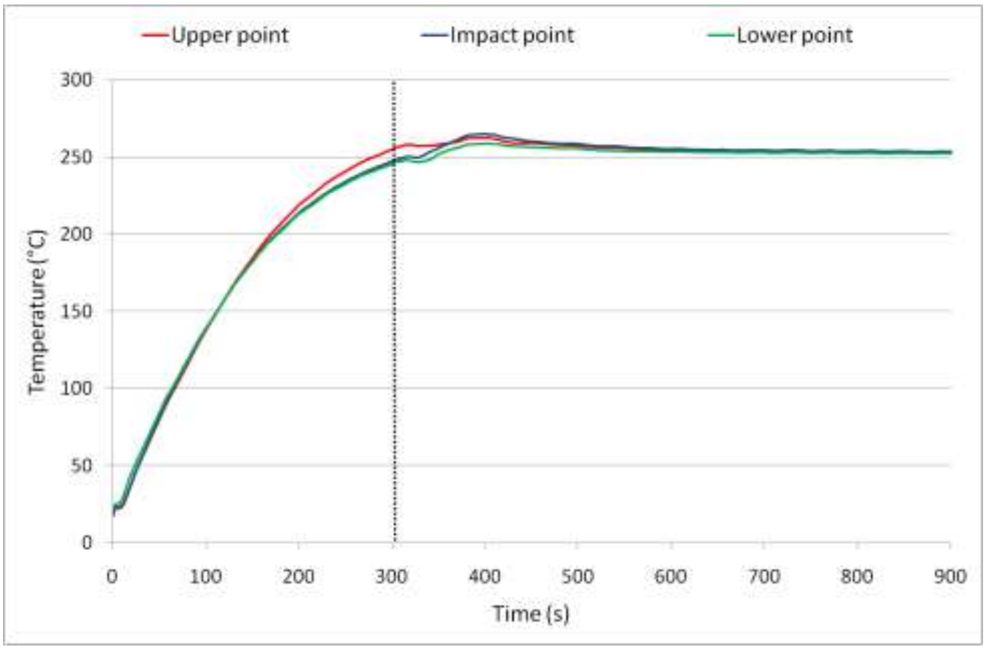

Figure 133 : Temperature profiles obtained in labscale jet-fire test for IF-2 coated on flanged panel (heat flux of 50kW/m², air speed of 15m/s, delayed time of 300 seconds)

For IF-3 (Figure 132), picture shows that the part of the flange where the jet impacts is totally unprotected. Furthermore, we can also detect damage at the surface adjacent to the flange. Jet impacts the flange and damages a central band perpendicular to the flange by erosive effect. On this band, the residual layer is very thin (not measurable) while on top and bottom of the side face a swelling of 0.7cm is observed and usually sufficient to provide protection. On temperature profiles, the effect of the air jet can be detected. Indeed, initially superimposed until turning on the air jet, the three curves exhibit different temperature changes. As soon as the air jet is switched on, the temperature on the impact zone increases rapidly while on the edges of the flange it continues to increase smoothly. To highlight the larger damage on IF-3 than on IF-2, we can also remark that higher temperatures are reached on temperature profiles of IF-3 (> 300°C) than those of IF-2. Thus these conclusions have been stated investigating the char aspect and have been confirmed by the thermal evolutions, even if temperature gaps are very slight and only trend can be proposed.

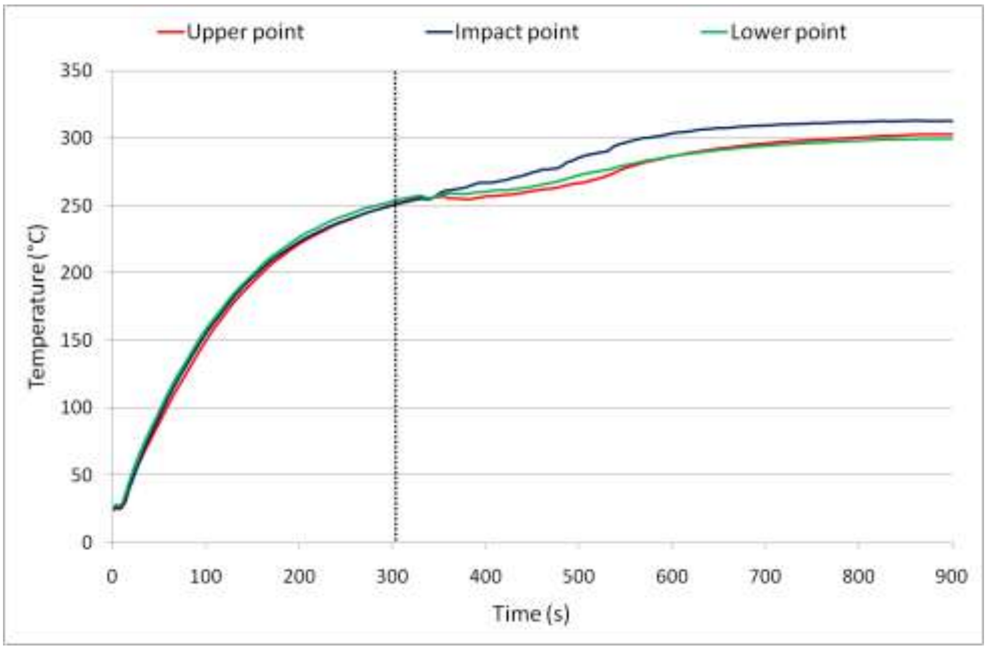

Figure 134 : Temperature profiles obtained in labscale jet-fire test for IF-3 coated on flanged panel (heat flux of 50kW/m², air speed of 15m/s, delayed time of 300 seconds)

For IF-4 (Figure 132), the coating is damaged on the flange where the air jet impacts the char. Nevertheless, the char developed on the back faces exhibits an enhanced resistance facing to air jet. In terms of swelling, we can measure a swelling on the side face of 1.5cm at the highest point. About the temperature evolution (Figure 135), the temperatures increase similarly until turning on the air jet. We then observe a higher increase of temperature at the impact zone than at the top and at the bottom in agreement with major location of the damage. However, the differences are small and prevent any further discussions.

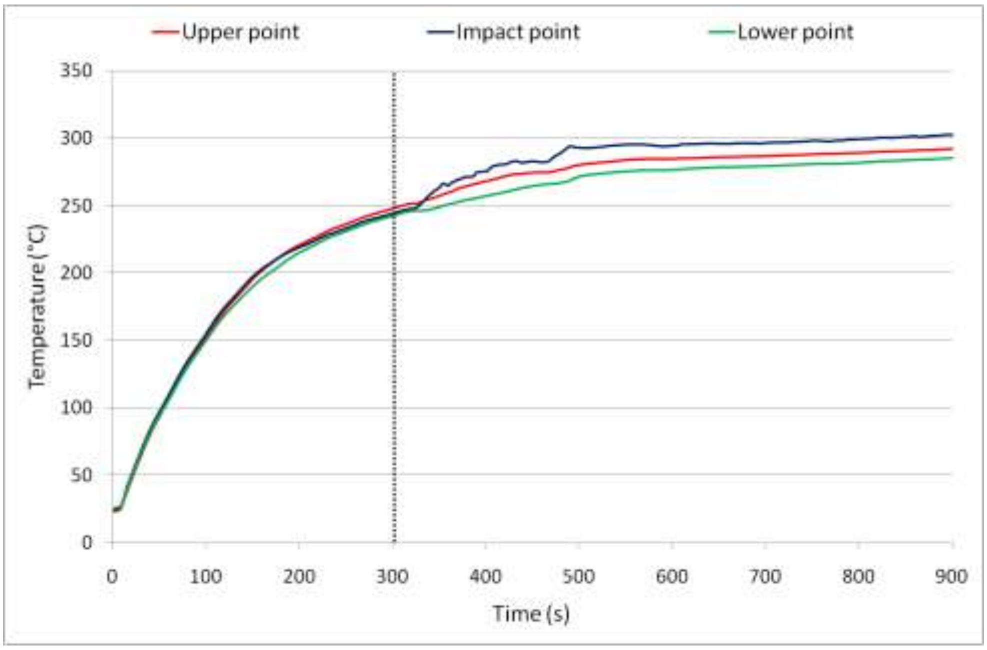

Figure 135 : Temperature profiles obtained in labscale jet-fire test for IF-4 coated on flanged panel (heat flux of 50kW/m², air speed of 15m/s, delayed time of 300 seconds)

To conclude this part and this experimental settings about the use of this specific design of panel, temperature measurements do not permit any significant discriminations between the formulations. Our first explanation is the inappropriate location of the thermocouples. Steel has a high heat conductivity which permits a rapid distribution of the temperature in all directions (isotropic heat conductivity). Accepting this, the rapid increase of the temperature on the impact zone (because of the partial destruction of the intumescent char) is propagated along the flange and a temperature gradient cannot be detected. The design and the techniques used to measure the temperatures have thus to be improved in order to obtain results mimicking jet-fire test in terms of geometrical aspect. Nevertheless, we can observe some consequences of the panel design on the expansion of the intumescent coatings, showing less homogeneous swelling along the panels due to presence of flange and complexity of the geometry. Others conclusions can be established about the thermal insulative provided by coatings and the temperature exhibited by coated panels where IF-2 seems to better insulate metallic panels than IF-3 and IF-4 in spite of superficial damage: final temperature measured by thermocouples are lower in the case of IF-2 than in the two others cases.

II. 5. Conclusions and discussion about the benefit of a new experimental tool

To underline the importance of the chemical difference and to understand the behaviours of the different coatings facing to jet-fire, we have undertaken to develop a labscale air-jet test. After optimizing the experimental parameters, a setup was proposed to evaluate the different coatings and their resulting resistance facing to impact.

The first conclusions and the correlations with large-scale results are very promising. Indeed if IF-1 appears as a robust coating without equivalent in terms of resistance, the three other coatings suggest significant and interesting differences. For IF-2, its mechanical resistance is poor. Localized on the impact zone, damage caused by the air jet provides a large insulation loss. This low resistance can be improved by incorporating mesh inside coating to avoid critical damage of the intumescent structure. However, mesh does not completely solve the insulation loss at the impact. For IF-3, its behaviour is the worst. Indeed facing to air jet, the intumescent shield is totally blasted off while this coating flows away of the panel due to its low viscosity during the jet-fire test. The intumescent structure does not resist to impact and is pushed from the centre to the edge because it does not adhere to panel. Once again, mesh provides significant improvement to this coating, allowing to keep the structure on the whole panel except at the impact zone. The best improvement is provided by the substitution of PER by dipentaerythritol. Indeed using dipentaerythritol in IF-4, a residual protective layer is maintained on the panel and allow a homogeneous protection of the substrate, as efficient as IF-1 in terms of insulation and apparent swelling.

So the conclusions of this section are drawn as follows:

- **Whatever the conditions, IF-1 exhibits the same behaviour developing a hard and compact char resistant to air jet.**
- **Concerning IF-2 and IF-3, correlations have been found between our labscale air jet test and the jet-fire test about the low mechanical resistance and the destruction of the structure.**
- **Substitution of PER by dipentaerythritol causes modification of the behaviour of the coating. IF-3 and IF-4 react differently facing to impact, with total destruction for the first formulation while a robust protective layer remains to protect panels with the second one.**
- **Mesh reinforces significantly the coatings, notably for IF-2 and IF-3 and appears as a solution to pass severe test with impact of flames.**

Correlations with the large scale jet-fire test can be sum up in the Table 13.

Table 13 : Evaluation and correlation of the behaviours of coatings

	IF-2	IF-3	IF-4
Labscale test	Weakness on the front of the jet, impact causes destruction on the centre of the panel	Reaction of the char facing to the air flow, structure is destroyed all along the surface due to blast	Dipentaerythritol provides appearance of a residual layer resistant to impact and protecting panel
Large-scale jet-fire test	Failure due to low resistance of the char after 35min	Failure due to low viscosity, flowing of the char on the back face after 13min	The char peels back as the adhesion is very poor, failure after 51min

Therefore, thanks to this labscale tool, we are able to observe and to explain the four different behaviours exhibited by the intumescent coatings. Some of these behaviours are self explanatory, similarly to large-scale jet-fire test and highlight the weaknesses of the formulations. Indeed to correlate these two scales, we can find some common points and similar observation about the intumescent formulations as the low swelling abilities of IF-1 even if its robustness allow a great fire performance for 60 minutes, or the low mechanical resistance of IF-2 and of IF-3, causing their test failures at both two scales. But the main link that we can establish between the two tests is mainly due to visual investigation of the char and thermal consequence that damage can cause on the insulative efficiencies of the coatings. Effectively, if main heat is provided by cone heater and radiation, the impingement of an air jet on a flat plate can reproduce the erosive effect on the fire protection material and can damage strongly the most fragile char as observed when IF-3 is completely blasted by air jet from the beginning of the test.

To conclude about the labscale test, even if no quantitative information have been obtained after this test in terms of fire-resistance rating, experiments and observations permit to obtain reliable information about the behaviour of the different coatings. Some aspects are still different between the two scales tests but we manage to establish some correlations. In addition with the first tool developed in laboratory to mimic industrial furnaces, this labscale test mimicking the characteristics of the jet-fire test constitutes a new tool to make 'high throughput' screening of new formulations.

General Conclusions

This Ph-D work was based on the study and explanations of the behaviours of four epoxy-based thick film intumescent coating, applied on offshore platforms and which has to resist in very strong conditions, such as jet-fires.

Our studying methods have investigated three different approaches about high fire risks on offshore locations. These approaches are all based on a starting assessment introduced on the chapter II about the behaviours of our four studied coatings for large scale jet-fire resistance test. Each coatings exhibit behaviour that highlights their weaknesses facing to impact of jet-fire or heat generated by such phenomenon. Clearly, intumescent formulation 1 produces a very hard and not flexible char that does not expand very much. As it does not expand enough, it fails at the hottest part of the box due to lack of insulation. On the contrary intumescent formulation 2 failure occurs on flange edge where the flame impacts. The char evolved from this product seems not to be sufficiently resistant and is destroyed by the high momentum delivered by the flame impact. Reinforcement provided by inclusion of carbon and glass fibre mesh system before testing can permit a great improvement of the mechanical resistance. Then intumescent formulation 3, a compromise between the two first coatings, appears as strong enough to resist on edge of flange and exhibit an expanded insulative char. However its failure occurs on the back face of the box: an area where neither intumescent formulation 1 nor intumescent formulation 2 fail. Finally, intumescent formulation 4, based on a slight modification of IF-3, introduces also a new type of failure caused by appearance of large voids at the steel/coating interface.

Regarding these four different failures highlighting mechanical resistance and visco-elastic properties, we have firstly investigated the physical properties of the intumescent coatings. Differences in terms of viscosity are shown by the use of different carbon sources. Indeed effect of the carbon sources (epoxy resin alone or with PER or with dipentaerythritol) are clearly determined by comparison between IF-2, IF-3 and IF-4. PER causes the shift of the viscosity decrease at lower temperature (270°C) and consequently swelling and intumescence process begin also at lower temperature for IF-3. Substitution of PER by dipentaerythritol (IF-4) allows to modify the behaviour of IF-3. These results must be linked with the results of jet-fire tests because the IF-3 failure and the flowing of char observed for jet-fire test can be partially explained by the visco-elastic properties. Indeed we can suggest that phenomena of flowing that occurs on the back faces can be the consequence of a too low viscosity of the melt phase, as observed at 270°C in our rheological experiments. Nevertheless, this flowing disappears for jet-fire test when PER is substituted by dipentaerythritol. Secondly, the mechanical resistance is also suspected for explaining the failure of IF-2 and IF-3 without mesh. Our experiments allow to conclude that IF-1 is the most robust and dense char, not sensitive to any strain while the three other coatings do not exhibit any resistance facing to the less force applied on the top of the char. This sensitivity to strain confirms thus results observed of IF-2 and IF-3 for jet-fire test resistance that fail in the impact zone where pressure is maximal and no coating resist to impact. Therefore physical approach provides us interesting information about the intumescent process and main conclusions target the role of the carbon sources in intumescent formulations.

Strongly linked with the efficiency of the char of these mixtures, these properties have been underlined by physical approach but could be also explained by the investigation of the mechanism of degradation that takes place inside these formulations. By analysing several residues from intumescent coatings at different characteristic temperatures mechanism of degradation as a function of the char former has been proposed. Indeed, investigations have been focused on the effect of the different carbon sources used on the intumescent formulations (epoxy resin in IF-2, epoxy resin and pentaerythritol on IF-3, epoxy resin and dipentaerythritol in IF-4). The chemical interactions that occur between the main components have then been investigated by thermo-gravimetric analyses, X-Ray diffraction and solid state NMR. Firstly, we have shown the effect of the carbon source on the chemical changes. We have demonstrated that epoxy resin could play the role of carbon source on IF-2 if no other component is present. However when PER or dipentaerythritol is added, no reaction between epoxy resin and acid source (APP) is detected. In a first step APP and the carbon source react together to yield to the development of a protective shield but also intermediate products containing phosphorus residues. Then, whatever the formulation, the formation of TiP_2O_7 is observed at high temperature: phosphorus residues react with TiO_2 to yield to a crystalline structure of TiP_2O_7. This crystallized compound is reported in literature to enhance mechanical properties and flame retardant performance. However, the temperature range at which it is formed is different. Indeed, TiP_2O_7 can be detected from 800°C for IF-3 whereas it is only clearly observable from 450°C for IF-4. For IF-2 without additional carbon source added to the formulation, epoxy resin alone plays a similar role leading to the formation of TiP_2O_7 at around 800°C. Consequently, it may be proposed that the substitution of PER by dipentaerythritol allows to increase the reactivity of APP with the carbon source and thus enables reaction to occur at lower temperature, notably the formation of TiP_2O_7. The formation of TiP_2O_7 have been shown for furnace jet-fire and linked between fire performance and chemical pathway are proposed focusing on the formation of TiP_2O_7 and its benefit to thermal efficiency of IF-4 compared to IF-3.

Finally, knowing all these properties and chemical changes exhibited by our four intumescent formulations and explaining their fire performance, the development of an experimental and reliable tool has been reported. This tool could provide information about the development and the efficiencies of the intumescent structure. These tools could constitute a predictive approach to determine the fire behaviour of the evaluated formulations. Moreover, thanks to these experimental tools, a low cost and fast test would permit rapid and reliable results of a large number of different coating formulations in good correlation with the results obtained in large scale standardized fire tests. First test mimicking hydrocarbon fire standard, we have highlighted a clear correlation between the chemical pathway and the TiP_2O_7 formation in a first hand and the thermal efficiency and the time of failure in the other hand. The second test tries to create a similar phenomenon that takes place for large scale jet-fire. Using a radiative heater and air jet with high momentum, the setup permits to focus on the two key parameters of hazardous jet-fire. Thanks to this experimental setup and to optimized settings, we have success to find again similar behaviours of the four coatings and to explain them. Some conclusions can thus be drawn to sum up these behaviours. Whatever the conditions, IF-1 exhibits the same behaviour developing a hard but low expanded char resisting to jet-fire. Concerning IF-2 and IF-3, correlations have been found between our labscale air jet test and the jet-fire test about the low mechanical resistance and the destruction of the structure letting unprotected the metallic substrate. Mesh can however reinforce significantly the intumesced structure and appears as a solution to pass severe test with impact of flames. Finally, the substitution of PER by dipentaerythritol allows to modify behaviour of the coatings. On the contrary, from IF-3, IF-4 forms a robust protective layer that remains to protect panels and avoids the increase of the temperature.

Therefore, although the labscale jet-fire test is not completely optimised to detect behaviour of the coating with the specific geometry of the large scale test (with a central flange), the combination of the fundamental conclusions about the physical properties and the degradation pathways of the different formulations and these experimental tools permit to highlight the weaknesses of the intumescent coatings and to propose solutions to improve this defaults. Indeed substitution of PER by dipentaerythritol and use of mesh appear as two solutions developed in this report, evaluated with similar experiments and exhibited satisfying results to enhance the fire performance of IF-2 and IF-3.

Finally, to end this Ph-D work, we can consider some outlooks. Indeed, thanks to investigation about role of carbon sources, we have highlighted its influence on the chemical degradation pathway and temperature at which it occurs, using epoxy resin either alone, or with PER, or with dipentaerythritol. Our conclusions are based on chemical analyses at different specific temperatures to determine the changes but it would be interesting to obtain quantitative information about the kinetic parameters. Indeed, the kinetic of degradation is a major concern and could be simulated using TGA device. A thermo-kinetic model could be determined in order to calculate kinetic parameters. This study should allow to refine the degradation mechanism of the material, notably the reaction between APP and the carbon source. Our study by chemical analyses has shown differences in terms of reactivity between APP and the different carbon sources, this approach by modelling could quantify this reactivity and compute the activation energy of each reaction. It would be so possible to confirm the better reactivity of APP with dipentaerythritol and the formation of the protective structure at lower temperature. To complete this study, new carbon sources (as tripentaerythritol) could be added to the main ingredients in order to screen the reactivity of APP with carbons sources.

Second, to go further to explain the effect of mesh and the improvement viewable for labscale jet-fire test, we could propose a specific study highlighting its role for severe test as jet-fire resistance one. Indeed, the use of mesh in the intumescent coating was an aspect quickly broached in this report but not really investigated except by observing its consequence on temperature profiles. However, in hot and severe conditions, hybrid carbon and glass fibre mesh show an interesting behaviour and the observation made after the jet fire tests as well as the composition of the mesh led us to suspect an influence of the oxygen on the thermal degradation of the mesh. Indeed, if the glass fibres do not degrade until 1000°C whatever the atmosphere, the carbon fibres are greatly sensitive to oxygen. Mesh can so remain in the zone where the oxygen level is low (pyrolysis conditions) whereas if oxygen is present the mesh completely degrades. In both cases, the glass fibres will be melted. Taking into account this information, this difference of behaviours according to the oxygen level can be a clue to determine the zone of pyrolysis and zone of combustion on the test panels during the jet-fire resistance test.

Appendix: Experimental results obtained with 2nd configuration

In order to better discriminate the coatings, we have used the same protocol as described in the last chapter of this report except that the delayed time of the air jet was reduced at 150 seconds. By decreasing the time delaying, we hope to observe a lower expanded structure and consequently a lower resistance of the char. So we hope to better differentiate coatings and to observe significant differences between the three fragile coatings (IF-2, IF-3 and IF-4), knowing that IF-1 exhibit the same behaviour whatever the settings used to test it.

2nd configuration without mesh

Firstly, without mesh, we have observed similar results and similar behaviours at 150 seconds and at 300 seconds (Figure 136 compare to Figure 122). The temperature profiles allow to highlight the potential local destruction of the coating. As observed previously, IF-1 and IF-4 exhibit smooth time/temperature profiles underlining good toughness of the char. On the contrary, temperature change can already be observed on temperature profiles of IF-2 and IF-3 when air jet is turning on. At the end of the experiment, IF-2 exhibits temperature close to virgin panels, confirming that destruction of the structure and stop of the protection. About IF-2, the consequences of air jet are smaller, but temperature variation points to potential local damages.

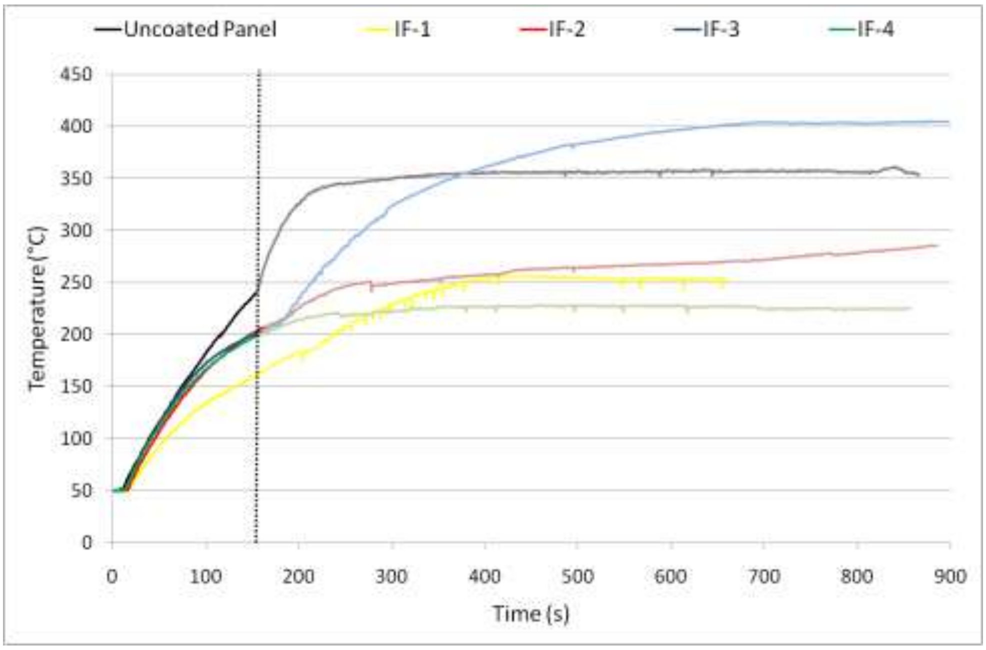

Figure 136 : Temperature profiles obtained in labscale jet-fire test for IF-1, IF-2, IF-3 and IF-4 (heat flux of 50kW/m², air speed of 15m/s, delayed time of 150 seconds)

Picture analyses confirm all the information obtained by temperature profiles. Once again, behaviour of IF-1 is not modified whatever the experimental configuration: the coating exhibited a low expanded char without sign of any strain.

Then concerning the three other coatings, a good agreement can also be stated between the temperature profiles and the pictures exposed on Figure 137.

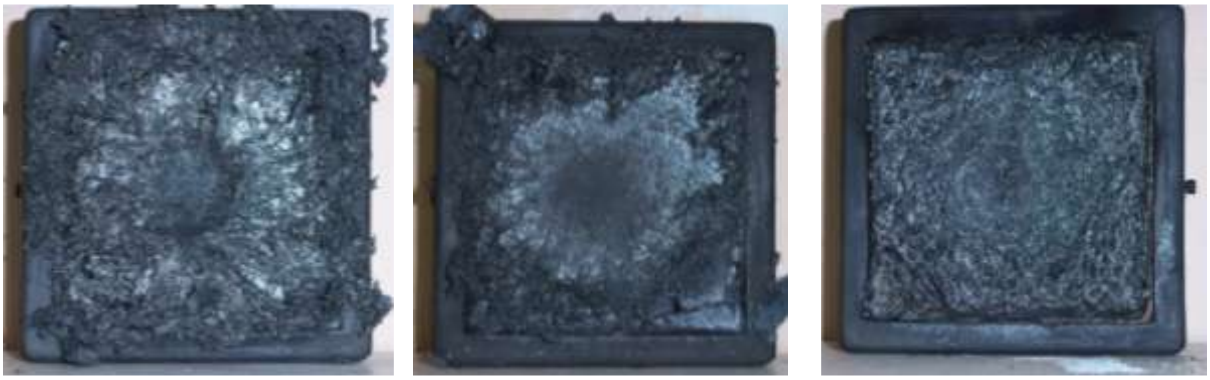
IF-2 IF-3 IF-4

Figure 137 : Picture of chars after labscale jet-fire test and thermal image for labscale jet-fire test (heat flux of 50kW/m², air speed of 15m/s, delayed time of 150 seconds)

Indeed, we can observe severe damage on structure issued of IF-2 and IF-3. Impact cause hole on the surface of IF-2 and destruction of the structure, nevertheless this destruction is not sufficient to observe a total destruction up to the substrate. This explains the gap already viewable between virgin panel and IF-2 coated panel. Damage are more important on IF-3 char, structure is totally destroyed from the centre to the edge in a radius of 3cm. The intumesced structure is pulled out, letting a large non-protected zone where temperature increases. Finally, for IF-4, an upper fragile intumescent layer that is destructed and pulled out by air jet, but a lower layer that resists to the jet continues to protect the panels all along the surface. With a low thickness (0.7cm), IF-4 exhibits behaviour and resistance close to IF-1, with a low expanded layer avoiding exposition of the panel to heat and fluxes.

Therefore, this 2nd configuration confirms the properties and the differences of each coating. The resistance of IF-2 and IF-3 and the appearance of a residual layer on IF-4 have been the main conclusions provided by this new series of experiments.

2nd configuration with mesh

A last series of experiments have been carried out. The delayed time is still reduced at 150 seconds and inclusion of mesh to improve the holding of the char facing to air jet. No new information have been obtained, however temperature profiles (Figure 138) and pictures describing the char aspect after test (Figure 139) confirm the previous conclusions and illustrate the behaviours of the coatings and the role of the mesh.

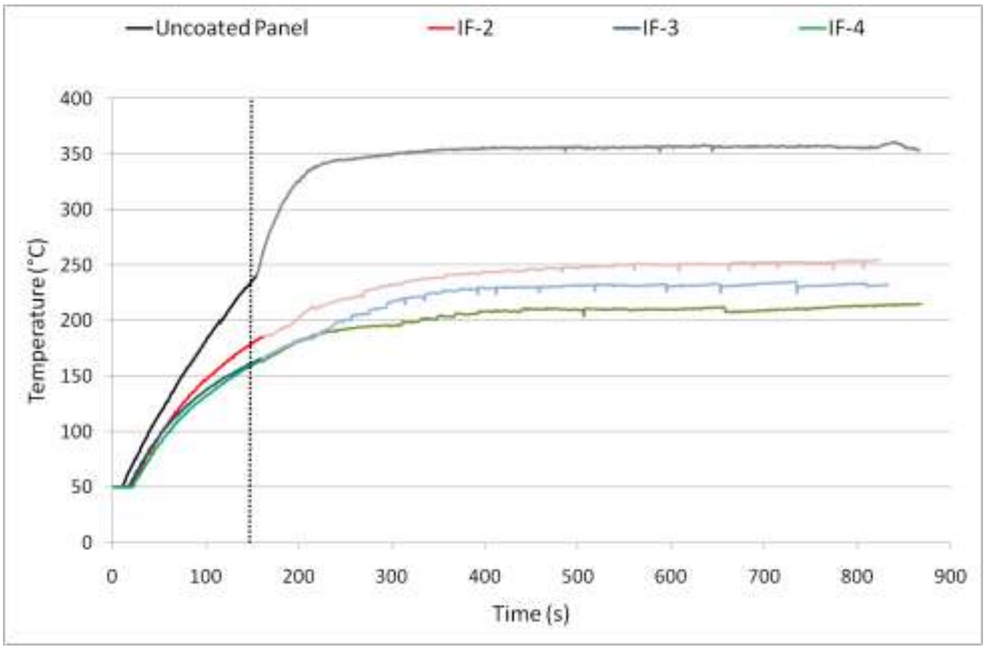

Figure 138 : Temperature profiles obtained in labscale jet-fire test for IF-2, IF-3 and IF-4 reinforced by mesh (heat flux of 50kW/m², air speed of 15m/s, delayed time of 150 seconds)

Indeed, by observing temperature profiles, an improvement of the coating resistance facing to air jet is exhibited thanks to inclusion of mesh. The quick variation of temperature (viewable usually when air jet is switching on) is less significant for IF-2 and IF-3. Their behaviours are still modified due to air jet but IF-3 is now clearly differentiated to virgin panels: residual material remains stuck to protect substrate.


IF-2 **IF-3** **IF-4**

Figure 139 : Pictures of the char obtained with intumescent coatings reinforced by mesh after labscale jet-fire test (heat flux of 50kW/m², air speed of 15m/s, delayed time of 150 seconds)

Char aspects are consistent with the temperature variations. All damages are superficial without reaching the panels and cancelling the thermal protection. Nevertheless, we continue to observe print where jet impacts: pressure caused by air jet and mesh limit the swelling on the central point. Swelling on the edge is 8mm while mesh on the central point limits the development but maintains the lower layer. On IF-3, a maximal swelling is measured at 1.6cm and mesh is positioned at 0.6cm from the panel. So it remains a residual layer on the whole panel to protect it. Finally on IF-4, a very low swelling (0.7cm) is viewable all along the surface without mark of any impact or mesh undiscovered. Large blocks of materials, initially the upper layer of the structure, are however pulled out.

Bibliography

[1] Recent Steel market developments, in *Seventh OECD High-Level Meeting on Steel Issues*, 28 June 2004, Paris.

[2] S. Melnick, Structural Steel Brings Environmental Advantages to Construction, *American Institute of Steel Construction*, http://www.prleap.com/pr/33400.

[3] F.S. Kelly and W. Sha, A comparison of the mechanical properties of fire-resistant and S275 structural steels, *Journal of Constructional Steel Research*, 1999, 50(3): p. 223-233.

[4] Fourth Revisions and Errata: National Building Code, 2002, *National Research Council Canada*.

[5] M. Haller and L.G. Cajot, Fire resistance of steel structures, *Arcelor LCS Research Report*, 2006.

[6] R. Pula, F.I. Khan, B. Veitch and P.R. Amyotte, Revised fire consequence models for offshore quantitative risk assessment, *Journal of Loss Prevention in the Process Industries*, 2005, 18(4-6): p. 443-454.

[7] V.P. Molchanov, A.N. Giletich, A.A. Makeev and Y.N. Shebeko, Fire safety of offshore stationary steelproof oil-producing platforms, *Neftyanoe Khozyaistvo - Oil Industry*, 2004(9): p. 82-87.

[8] J. Krueger and D. Smith, A practical approach to fire hazard analysis for offshore structures, *Journal of Hazardous Materials*, 2003, 104(1-3): p. 107-122.

[9] P.J. Rew, W.G. Hulbert and D.M. Deaves, Modelling of thermal radiation from external hydrocarbon pool fires, *Process Safety and Environmental Protection*, 1997, 75(2): p. 81-89.

[10] M.J. Pritchard and T.M. Binding, A new approach for predicting thermal radiation levels from hydrocarbon pool fires, in *Institution of Chemical Engineers Symposium Series*, 1992, Manchester.

[11] A.D. Johnson, Model for predicting thermal radiation hazards from large-scale LNG pool fires, in *Institution of Chemical Engineers Symposium Series*, 1992, Manchester.

[12] T. Roberts, A. Gosse and S. Hawksworth, Thermal radiation from fireballs on failure of liquefied petroleum gas storage vessels, *Process Safety and Environmental Protection: Transactions of the Institution of Chemical Engineers, Part B*, 2000, 78(3): p. 184-192.

[13] OTI 92596: Oil and gas fires: characteristics and impact, 1992, *HSE Offshore Technology Report*.

[14] OTI 92597: Behaviour of oil and gas fires in the presence of confinement and obstacles, 1992, *HSE Offshore Technology Report*.

[15] M. Gomez-Mares, L. Zarate and J. Casal, Jet fires and the domino effect, *Fire Safety Journal*, 2008, 43(8): p. 583-588.

[16] The Honourable Lord Cullen, The Public Inquiry into the Piper Alpha Disaster, *H.S. Office*, 1990.

[17] K. Sonju and J. Hustad, An experimental study of turbulent jet diffusion flames, *Norwegian maritime research*, 1984, 12(4): p. 2-11.

[18] Recommended Practice 521: Pressure-relieving and depressuring systems. - 5th edition, 2007, *American Petroleum Institute*.

[19] R. McMurray, Flare radiation estimated, *Hydrocarbon processing*, 1981: p. 175-181.

[20] A.L. Suris, E.V. Flankin and S.N. Shorin, Length of free diffusion flames, *Combustion, Explosion, and Shock Waves*, 1978, 13(4): p. 459-462.

[21] B.J. McCaffrey, Momentum diffusion flame characteristics and the effects of water spray, *Combustion science and technology*, 1989, 63(4-6): p. 315-335.

[22] W.R. Hawthorne, D.C. Weddell and H.C. Hottel, Mixing and combustion in turbulent gas jets, in *International symposium on Combustion*, 1998, Pittsburgh.

[23] H.A. Becker and S. Yamazaki, Entrainment, momentum flux and temperature in vertical free turbulent diffusion flames, *Combustion and Flame*, 1978, 33(C): p. 123-149.

[24] G.T. Kalghatgi, Blow-out stability of gaseous jet diffusion flames I. In still air, *Combustion science and technology*, 1981, 26(5-6): p. 233-239.

[25] GexCon UK Ltd, Jet Fire - Flame shape, Available from: http://www.gexcon.com/calculators/new/flame_shape.php (in 2009).

[26] H.G. Wertenbach, Spread of flames on cylindrical tanks for hydrocarbon fluids, *Gas and Erdgas*, 1971, 112(8).

[27] B.J. Lowesmith, G. Hankinson, M.R. Acton and G. Chamberlain, An overview of the nature of hydrocarbon jet fire hazards in the oil and gas industry and a simplified approach to assessing the hazards, *Process Safety and Environmental Protection*, 2007, 85(3 B): p. 207-220.

[28] G.A. Chamberlain, Developments in design methods for predicting thermal radiation from flares, *Chemical Engineering Research and Design*, 1987, 65(4): p. 299-309.

[29] L.T. Cowley and M.J. Pritchard, Large-scale natural gas and LPG jet fires and thermal impact on structures, in *14th International LNG/LPG Conference - Gastech 90*, 1990, Amsterdam.

[30] J. Hustad and K. Sonju, Heat transfer to pipes submerged in turbulent jet diffusion flames, in *Eurotherm N°17*, 1990, Cascais (Portugal).

[31] Saga Petroleum, Jet-fire explosion test for passive fire protection, *The design specification for the Snorre field*, 1987.

[32] L.C. Shirvill, Efficacy of water spray protection against propane and butane jet fires impinging on LPG storage tanks, *Journal of Loss Prevention in the Process Industries*, 2004, 17(2): p. 111-118.

[33] J.F. Bennett, L.T. Cowley, J.N. Davenport and J.J. Rowson, Large scale natural gas and LPG jet fires, final report to EC, *Shell Report*, 1991, TNER 91.022.

[34] J.N. Davenport, Large scale natural gas/kerosene mixed fuel jet fires, final report to the API, *Shell report*, 1994, TNER.94.061.

[35] J.N. Davenport, Large scale natural gas/butane mixed fuel jet fires, final report to EC, *Shell report*, 1994, TNER.94.030.

[36] Advantica, Horizontal jet fires of oil and gas, in *Unpublished Advantica report*, 1997.

[37] D.K. Cook, M. Fairweather, J. Hammonds and D.J. Hughes, Size and radiative characteristics of natural gas flares I. Field scale experiments, *Chemical Engineering Research and Design*, 1987, 65(4): p. 310-317.

[38] ISO 13702: Petroleum and natural gas industries - Control and mitigation of fires and explosions on offshore production installations - Requirements and guidelines, 1999, *International Organization for Standardization*.

[39] H. Shoub, Early history of fire endurance testing in the United States, *American Society for Testing and Materials, Special Technical Publication 301*, 1961, Fire Test Methods, Philadelphia, PA: p. 1-9.

[40] G.C. Gosselin, Structural fire protection, predictive methods, *Proceedings of building science insight*, 1987.

[41] M.G. Goode, Fire Protection of Structural Steel in High-Rise Buildings, *National Institute of Standards and Technology Report*, 2004, NIST GCR 04-872.

[42] G. Ellicott, The passive advantage, *Fire protection safety and security*, World hydrocarbon: p. 67-68.

[43] R. Smith, Sprayed mineral coatings and intumescent coatings for the fire protection of structural steel, *Journal of Protective Coatings and Linings*, 2003, 20(4): p. 12-21.

[44] P. Barber, Offshore cementitious passive fire protection - A proven and cost effective solution, in *Plastics & Rubber Institution*, 1987, London.

[45] D. Mistry, Laboratory testing of hydrocarbon fire protection coatings and effect of wet environments, in *NACE - International Corrosion Conference Series*, 2006, Orlando.

[46] J. Gordon, How to specify intumescent coatings, *Building Engineer*, 2008, 83(9): p. 12-13.

[47] E.L. Garrett, Ceramic fibre materials for fire protection, *Insulation*, 1978, 22(2).

[48] W.R. Parlor, Utilisation of mineral wool for offshore fire protection, in *Plastic & Rubber Institution*, 1987, London.

[49] P. Mather, Fire protection gets passive, International Coatings Limited.

[50] J.V. Dunk, Advantages of an epoxy medium as the basis of a durable passive fire protection, in *Plastics & Rubber Institution*, 1987, London.

[51] A. Fainleib, J. Galy, J.P. Pascault and H.J. Sue, Two ways of synthesis of polymer networks based on diglycidyl ether of bisphenol A, bisphenol A, and sulfanilamide: Kinetics study, *Journal of Applied Polymer Science*, 2001, 80(4): p. 580-591.

[52] J. Galy, A. Sabra and J.-P. Pascault, Characterization of epoxy thermosetting systems by differential scanning calorimetry, *Polymer Engineering and Science*, 1986, 26(21): p. 1514-1523.

[53] V. Rebizant, A.S. Venet, F. Tournilhac, E. Girard-Reydet, C. Navarro, J.P. Pascault and L. Leibler, Chemistry and mechanical properties of epoxy-based thermosets reinforced by reactive and nonreactive SBMX block copolymers, *Macromolecules*, 2004, 37(21): p. 8017-8027.

[54] S. Horold, Phosphorus flame retardants for composites, in *International SAMPE Technical Conference*, 1999, Chicago, IL, USA.

[55] J.T. Carter, G.T. Emmerson, C. Lo Faro, P.T. McGrail and D.R. Moore, The development of a low temperature cure modified epoxy resin system for aerospace composites, *Composites Part A: Applied Science and Manufacturing*, 2003, 34(1): p. 83-91.

[56] H. Lee and K. Neville, Hanbook of epoxy resins, Vol. 1, 1967, edited by McGraw-Hill.

[57] E. Girard-Reydet, J.P. Pascault, A. Bonnet, F. Court and L. Leibler, A new class of epoxy thermosets, *Macromolecular Symposia*, 2003, 198: p. 309-322.

[58] J.M. Laza, E. Bilbao, M.T. Garay, J.L. Vilas, M. Rodriguez and L.M. Leon, Thermal properties and fire behaviour of materials produced from curing mixed epoxy and phenolic resins, *Fire and Materials*, 2008, 32(5): p. 281-292.

[59] M.I.B. Tavares, J.R.M. D'Almeida and S.N. Monteiro, 13C solid-state NMR analysis of the DGEBA/TETA epoxy system, *Journal of Applied Polymer Science*, 2000, 78(13): p. 2358-2362.

[60] A. GroÃŸ, H. Kollek and H. Brockmann, The nucleophilicity as the determining parameter in the curing of epoxy resins, *International Journal of Adhesion and Adhesives*, 1988, 8(4): p. 225-233.

[61] Dow Liquid Epoxy Resins, *Dow Plastics*.

[62] National Institute of Industrial Research Board, Polymers And Plastics Technology Handbook, Vol. 1, edited by Asia Pacific Business Press Inc.

[63] C. Barrere and F. Dal Maso, Epoxy-resins crosslinked with Polyamines: Structure and Properties, *Revue de l'Institut Français du Pétrole*, 1997, 52(3): p. 317-335.

[64] Y.F. Shih and R.J. Jeng, Carbon black-containing interpenetrating polymer networks based on unsaturated polyester/epoxy II. Thermal degradation behavior and kinetic analysis, *Polymer Degradation and Stability*, 2002, 77(1): p. 67-76.

[65] R.N. Rothon and P.R. Hornsby, Flame retardant effects of magnesium hydroxide, *Polymer Degradation and Stability*, 1996, 54(2-3 SPEC. ISS.): p. 383-385.

[66] G. Matuschek, Thermal degradation of different fire retardant polyurethane foams, *Thermochimica Acta*, 1995, 263(C): p. 59-71.

[67] J. Jang, H. Chung, M. Kim and H. Sung, The effect of flame retardants on the flammability and mechanical properties of paper-sludge/phenolic composite, *Polymer Testing*, 2000, 19(3): p. 269-279.

[68] R. Seddon and J.F. Harper, Influence of flame retardant additives on the processing characteristics and physical properties of ABS, *Macromolecular Symposia*, 2001, 169: p. 109-119.

[69] S.R. Owen and J.F. Harper, Mechanical, microscopical and fire retardant studies of ABS polymers, *Polymer Degradation and Stability*, 1999, 64(3): p. 449-455.

[70] S. Bourbigot, M. Le Bras, L. Gengembre and R. Delobel, XPS study of an intumescent coating application to the ammonium polyphosphate/pentaerythritol fire-retardant system, *Applied Surface Science*, 1994, 81(3): p. 299-307.

[71] S. Duquesne, M. Le Bras, S. Bourbigot, R. Delobel, H. Vezin, G. Camino, B. Eling, C. Lindsay and T. Roels, Expandable graphite: A fire retardant additive for polyurethane coatings, *Fire and Materials*, 2003, 27(3): p. 103-117.

[72] S. Duquesne, S. Magnet, C. Jama and R. Delobel, Intumescent paints: Fire protective coatings for metallic substrates, *Surface and Coatings Technology*, 2004, 180-181: p. 302-307.

[73] C. Drevelle, S. Duquesne, M. Le Bras, J. Lefebvre, R. Delobel, A. Castrovinci, C. Magniez and M. Vouters, Influence of ammonium polyphosphate on the mechanism of thermal degradation of an acrylic binder resin, *Journal of Applied Polymer Science*, 2004, 94(2): p. 717-729.

[74] M. Jimenez, S. Duquesne and S. Bourbigot, Intumescent fire protective coating: Toward a better understanding of their mechanism of action, *Thermochimica Acta*, 2006, 449(1-2): p. 16-26.

[75] US-2106938, Fireproofing of wood, patented by H. Tramm, C. Clar, P. Kuhnel and W. Schuff for RUHRCHEMIE AG in 1938, http://www.freepatentsonline.com/2106938.html.

[76] H.L. Vandersall, Intumescent coating systems, their development and chemistry, *Journal of Fire and Flammability*, 1970, 1: p. 97-140.

[77] US-2452054, Fire-retardant composition and process, patented by J. Grinnell, J. Walter and S. Samuel for ALBI MFG Inc. in 1948, http://www.freepatentsonline.com/2452054.html.

[78] R. Delobel, M. Le Bras, N. Ouassou and F. Alistiqsa, Thermal behaviour of ammonium polyphosphate-pentaerythritol and ammonium pyrophosphate – pentaerythritol intumescent additives in polypropylene formulations, *Journal of Fire Sciences*, 1990, 8(2): p. 85-108.

[79] G. Camino, L. Costa and G. Martinasso, Intumescent fire-retardant systems, *Polymer Degradation and Stability*, 1989, 23(4): p. 359-376.

[80] M. Wladyka-Przybylak and R. Kozlowski, Thermal characteristics of different intumescent coatings, *Fire and Materials*, 1999, 23(1): p. 33-43.

[81] R. Delobel, N. Ouassou, M. Le Bras and J.M. Leroy, Fire retardance of polypropylene: Action of diammonium pyrophosphate-pentaerythritol intumescent mixture, *Polymer Degradation and Stability*, 1989, 23(4): p. 349-357.

[82] R. Delobel, M. Le Bras, N. Ouassou and R. Descressain, Fire retardance of polypropylene by diammonium pyrophosphate-pentaerythritol: Spectroscopic characterization of the protective coatings, *Polymer Degradation and Stability*, 1990, 30(1): p. 41-56.

[83] S. Bourbigot, M. Le Bras, S. Duquesne and M. Rochery, Recent advances for intumescent polymers, *Macromolecular Materials and Engineering*, 2004, 289(6): p. 499-511.

[84] M. Gao, W. Wu and Y. Yan, Thermal degradation and flame retardancy of epoxy resins containing intumescent flame retardant, *Journal of Thermal Analysis and Calorimetry*, 2009, 95(2): p. 605-608.

[85] J.W. Gu, G.C. Zhang, S.I. Dong, Q.Y. Zhang and J. Kong, Study on preparation and fire-retardant mechanism analysis of intumescent flame-retardant coatings, *Surface and Coatings Technology*, 2007, 201(18): p. 7835-7841.

[86] S. Bourbigot, M. Le Bras, R. Delobel, P. Breant and J.M. Tremillon, Carbonization mechanisms resulting from intumescence-part II. Association with an ethylene terpolymer and the ammonium polyphosphate-pentaerythritol fire retardant system, *Carbon*, 1995, 33(3): p. 283-294.

[87] G. Camino, L. Costa, L. Trossarelli, F. Costanzi and A. Pagliari, Study of the mechanism of intumescence in fire retardant polymers: Part VI-Mechanism of ester formation in ammonium polyphosphate-pentaerythritol mixtures, *Polymer Degradation and Stability*, 1985, 12(3): p. 213-228.

[88] S. Duquesne, S. Magnet, C. Jama and R. Delobel, Thermoplastic resins for thin film intumescent coatings - Towards a better understanding of their effect on intumescence efficiency, *Polymer Degradation and Stability*, 2005, 88(1): p. 63-69.

[89] A.R. Horrocks, Developments in flame retardants for heat and fire resistant textiles - The role of char formation and intumescence, *Polymer Degradation and Stability*, 1996, 54(2-3 SPEC. ISS.): p. 143-154.

[90] M. Bugajny, M. Le Bras and S. Bourbigot, New approach to the dynamic properties of an intumescent material, *Fire and Materials*, 1999, 23(1): p. 49-51.

[91] P. Anna, G. Marosi, I. Csontos, S. Bourbigot, M. Le Bras and R. Delobel, Influence of modified rheology on the efficiency of intumescent flame retardant systems, *Polymer Degradation and Stability*, 2001, 74(3): p. 423-426.

[92] F. Carpentier, S. Bourbigot, M. Le Bras and R. Delobel, Rheological investigations in fire retardancy: Application to ethylene-vinyl-acetate copolymer-magnesium hydroxide/zinc borate formulations, *Polymer International*, 2000, 49(10): p. 1216-1221.

[93] S. Duquesne, R. Delobel, M. Le Bras and G. Camino, A comparative study of the mechanism of action of ammonium polyphosphate and expandable graphite in polyurethane, *Polymer Degradation and Stability*, 2002, 77(2): p. 333-344.

[94] M.L. Bras, M. Bugajny, J.M. Lefebvre and S. Bourbigot, Use of polyurethanes as char-forming agents in polypropylene intumescent formulations, *Polymer International*, 2000, 49(10): p. 1115-1124.

[95] M. Jimenez, S. Duquesne and S. Bourbigot, Characterization of the performance of an intumescent fire protective coating, *Surface and Coatings Technology*, 2006, 201(3-4): p. 979-987.

[96] M. Jimenez, S. Duquesne and S. Bourbigot, Multiscale experimental approach for developing high-performance intumescent coatings, *Industrial and Engineering Chemistry Research*, 2006, 45(13): p. 4500-4508.

[97] I.S. Reshetnikov, A.N. Garashchenko and V.L. Strakhov, Experimental investigation into mechanical destruction of intumescent chars, *Polymers for Advanced Technologies*, 2000, 11(8-12): p. 392-397.

[98] I.S. Reshetnikov, M.Y. Yablokova, E.V. Potapova, N.A. Khalturinskij, V.Y. Chernyh and L.N. Mashlyakovskii, Mechanical stability of intumescent chars, *Journal of Applied Polymer Science*, 1998, 67(10): p. 1827-1830.

[99] E. Kandare, B.K. Kandola and J.E.J. Staggs, Global kinetics of thermal degradation of flame-retarded epoxy resin formulations, *Polymer Degradation and Stability*, 2007, 92(10): p. 1778-1787.

[100] I. Reshetnikov, A. Antonov, T. Rudakova, G. Aleksjuk and N. Khalturinskij, Some aspects of intumescent fire retardant systems, *Polymer Degradation and Stability*, 1996, 54(2-3 SPEC. ISS.): p. 137-141.

[101] UL 1709: Rapid rise fire tests of protection materials for structural steel, 1994, *Underwriter Laboratories*.

[102] RWS Curve, *SP Swedish national testing and research Institute*.

[103] OTI 95634: Jet fire resistance - Test of passive fire protection materials, 1996, *HSE Offshore Technology Report*.

[104] ISO 22899-1: Determination of the resistance to jet fires of passive fire protection materials - General requirements, 2007, *International Organization for Standardization*.

[105] M. Jimenez, Etude des mécanismes de protection et de réaction au feu dans les revêtements intumescents, Thesis defended at Université des Sciences et Technologies de Lille, Lille, on 5th October 2006.

[106] Beerenberg Corp. AS, Benarx F Epoxy Box Performance, Available from: http://www.benarx.com/products/benarx-f-epoxy-box-1/benarx-f-epoxy-box-performance (in 2009).

[107] C. Reti, M. Casetta, S. Duquesne, S. Bourbigot and R. Delobel, Flammability properties of intumescent PLA starch and lignin, *Polymers for Advanced Technologies*, 2008, 19(6): p. 628-635.

[108] G. Camino, G. Martinasso and L. Costa, Thermal degradation of pentaerythritol diphosphate, model compound for fire retardant intumescent systems: Part I-Overall thermal degradation, *Polymer Degradation and Stability*, 1990, 27(3): p. 285-296.

[109] A. Andersson, S. Landmark and F.H.J. Maurer, Evaluation and characterization of ammonium polyphosphate-pentaerythritol- based systems for intumescent coatings, *Journal of Applied Polymer Science*, 2007, 104(2): p. 748-753.

[110] V. Babrauskas, CONE CALORIMETER - A VERSATILE BENCH-SCALE TOOL FOR THE EVALUATION OF FIRE PROPERTIES, in 1986, Luxembourg, Luxemb.

[111] V. Babrauskas and W.J. Parker, IGNITABILITY MEASUREMENTS WITH THE CONE CALORIMETER, *Fire and Materials*, 1987, 11(1): p. 31-43.

[112] F. Samyn, S. Bourbigot, S. Duquesne and R. Delobel, Effect of zinc borate on the thermal degradation of ammonium polyphosphate, *Thermochimica Acta*, 2007, 456(2): p. 134-144.

[113] Z. Wang, E. Han, F. Liu and W. Ke, Thermal behavior of nano-TiO2 in fire-resistant coating, *Journal of Materials Science and Technology*, 2007, 23(4): p. 547-550.

[114] A. Laachachi, M. Cochez, E. Leroy, P. Gaudon, M. Ferriol and J.M. Lopez Cuesta, Effect of Al2O3 and TiO2 nanoparticles and APP on thermal stability and flame retardance of PMMA, *Polymers for Advanced Technologies*, 2006, 17(4): p. 327-334.

[115] G. Camino and L. Costa, Performance and mechanisms of fire retardants in polymers-A review, *Polymer Degradation and Stability*, 1988, 20(3-4): p. 271-294.

[116] N. Grassie, M.I. Guy and N.H. Tennent, Degradation of epoxy polymers: Part 4-Thermal degradation of bisphenol-A diglycidyl ether cured with ethylene diamine, *Polymer Degradation and Stability*, 1986, 14(2): p. 125-137.

[117] J.C. Paterson-Jones, V.A. Percy, R.G.F. Giles and A.M. Stephen, The thermal degradation of model compounds of amine-cured epoxide resins II. The thermal degradation of 1,3-diphenoxypropan-2-ol and 1,3-diphenoxypropene, *Journal of Applied Polymer Science*, 1973, 17(6): p. 1877-1887.

[118] M.A. Keenan and D.A. Smith, Further aspects of the thermal degradation of epoxide resins, *Journal of Applied Polymer Science*, 2003, 11(7): p. 1009-1026.

[119] G. Camino, L. Costa, L. Trossarelli, F. Costanzi and G. Landoni, Study of the mechanism of intumescence in fire retardant polymers: Part IV-Evidence of ester formation in ammonium polyphosphate-pentaerythritol mixtures, *Polymer Degradation and Stability*, 1984, 8(1): p. 13-22.

[120] M. Le Bras, S. Bourbigot, Y. Le Tallec and J. Laureyns, Synergy in intumescence - Application to Î²-cyclodextrin carbonisation agent in intumescent additives for fire retardant polyethylene formulations, *Polymer Degradation and Stability*, 1997, 56(1): p. 11-21.

[121] S. Bourbigot, M.L. Bras and R. Delobel, Carbonization mechanisms resulting from intumescence association with the ammonium polyphosphate-pentaerythritol fire retardant system, *Carbon*, 1993, 31(8): p. 1219-1230.

[122] A. Marchal, R. Delobel, M. Le Bras, J.M. Leroy and D. Price, Effect of intumescence on polymer degradation, *Polymer Degradation and Stability*, 1994, 44(3): p. 263-272.

[123] S.T. Norberg, G. Svensson and J. Albertsson, A TiP2O7 superstructure, *Acta Crystallographica Section C: Crystal Structure Communications*, 2001, 57(3): p. 225-227.

[124] Z. Wang, E. Han and W. Ke, Effect of nanoparticles on the improvement in fire-resistant and anti-ageing properties of flame-retardant coating, *Surface and Coatings Technology*, 2006, 200(20-21): p. 5706-5716.

[125] G.E. Maciel, V.J. Bartuska and F.P. Miknis, Characterization of organic material in coal by proton-decoupled 13C nuclear magnetic resonance with magic-angle spinning, *Fuel*, 1979, 58(5): p. 391-394.

[126] S. Bourbigot, M. Le Bras, P. Breant, J.M. Tremillon and R. Delobel, Zeolites: New synergistic agents for intumescent fire retardant thermoplastic formulations - Criteria for the choice of the zeolite, *Fire and Materials*, 1996, 20(3): p. 145-154.

[127] S. Bourbigot, M. Le Bras, R. Delobel, R. Decressain and J.P. Amoureux, Synergistic effect of zeolite in an intumescence process: Study of the carbonaceous structures using solid-state NMR, *Journal of the Chemical Society - Faraday Transactions*, 1996, 92(1): p. 149-158.

[128] S. Bourbigot, M. Le Bras, R. Delobel and J.M. Tremillon, Synergistic effect of zeolite in an intumescence process: Study of the interactions between the polymer and the additives, *Journal of the Chemical Society - Faraday Transactions*, 1996, 92(18): p. 3435-3444.

[129] J.R. Van Wazer, C.F. Callis, J.N. Shoolery and R.C. Jones, Principles of phosphorus chemistry II. Nuclear magnetic resonance measurements, *Journal of the American Chemical Society*, 1956, 78(22): p. 5715-5726.

[130] T.M. Duncan and D.C. Douglas, On the 31P chemical shift anisotropy in condensed phosphates, *Chemical Physics*, 1984, 87(3): p. 339-349.

[131] M. Bugajny, S. Bourbigot, M. Le Bras and R. Delobel, The origin and nature of flame retardance in ethylene-vinyl acetate copolymers containing hostaflam AP 750, *Polymer International*, 1999, 48(4): p. 264-270.

[132] S.A. Sojka and W.B. Moniz, Curing of an epoxy resin as followed by carbon 13NMR spectroscopy, *Journal of Applied Polymer Science*, 1976, 20(7): p. 1977-1982.

[133] S. Bourbigot, M. Le Bras, R. Delobel and L. Gengembre, XPS study of an intumescent coating II. Application to the ammonium polyphosphate/pentaerythritol/ethylenic terpolymer fire retardant system with and without synergistic agent, *Applied Surface Science*, 1997, 120(1-2): p. 15-29.

[134] G. Camino, L. Costa and L. Trossarelli, Study of the mechanism of intumescence in fire retardant polymers: Part II-Mechanism of action in polypropylene-ammonium polyphosphate-pentaerythritol mixtures, *Polymer Degradation and Stability*, 1984, 7(1): p. 25-31.

INVESTIGATION OF INTUMESCENT COATINGS FOR FIRE PROTECTION - APPLICATION TO JET-FIRE

Résumé : Cette étude s'intéresse aux comportements de 4 peintures intumescentes développées pour protéger des plateformes offshores et susceptibles de résister aux « jet-fires ». Un jet-fire peut intervenir sur un site pétrochimique suite à une fuite d'hydrocarbures sous pression et causer de sérieux dommages de part la chaleur dégagées et surtout la quantité de mouvement générées. Les aspects physiques et chimiques de ces formulations ont été développés permettant de mettre en avant les effets du pentaérythritol sur le comportement viscoélastiques et le processus d'intumescence. Par diffraction des rayons X et par RMN à l'état solide, nous avons montré les interactions entre ammonium et polyphosphate et différentes sources de carbones (pentaérythritol, dipentaérythritol, réseau époxyde) permettant la formation d'un char. Les résidus phosphorés réagissent ensuite avec TiO_2 pour former une structure cristalline TiP_2O_7 suspectées d'améliorer la résistance au feu et la résistance mécanique du char. Des tests feu ont confirmés ces améliorations. Dans un dernier chapitre nous avons développé un test permettant de reproduire à l'échelle laboratoire les phénomènes radiatifs et convectifs du jet-fire. Les premiers résultats ont montré de bonnes corrélations entre les observations faites à grande échelle et celles réalisées au laboratoire.

Mots clefs : *Résine époxyde, Dégradation thermique, Intumescence, Polyphosphate d'ammonium, Pentaerythritol, Dioxyde de titane, RMN du solide, Diffraction des rayons X, Développement de test feu.*

Abstract: The aim of this study is to understand and to explain behaviours exhibited by four epoxy-based intumescent formulations used on offshore platforms facing to jet-fire. A jet-fire is a turbulent diffusion flame resulting from the combustion of a fuel continuously released with some significant momentum. It represents a significant element of the risk on offshore installations. Regarding the formulation studied, we have developed three approaches. Firstly, the visco-elastic behaviour and mechanical resistance of the formulations have been investigated. The results show that pentaerythritol causes a viscosity decrease at lower temperature that appears as prejudicial to maintain efficient char on steel substrate. In a second part, chemical evolutions of the intumescent formulation have been determined thanks to solid-state NMR and X-Ray diffraction. Interactions between ammonium polyphosphate and respective carbon sources present in formulations have been assumed, yielding to the formation of char and production of phosphorus residues. Then these phosphorus residues react at high temperature with TiO_2 to form a crystalline structure TiP_2O_7 suspected to enhance mechanical properties and flame retardant performance. In a last part, furnace fire tests confirm this enhancement. Furthermore, a new small-scale experimental setup is developed mimicking large scale jet-fire resistance test in order to obtain rapidly and at low cost reliable behaviours of a large number of formulations facing to high load mixing radiative heat and flame impact. First results have been correlated with the large-scale ones and different geometries have been considered.

Keywords: *Epoxy resin, Thermal degradation, Intumescence, Ammonium polyphosphate, Pentaerythritol, Titanium dioxide, Solid state NMR, X-Ray diffraction, Fire testing development.*

Intitulé et adresse du laboratoire:

Laboratoire LSPES – Equipe PERF CNRS UMR 8008
E.N.S.C.L, Cité Scientifique, Bât. C7
F-59652 Villeneuve d'Ascq Cedex

INVESTIGATION OF INTUMESCENT COATINGS FOR FIRE PROTECTION - APPLICATION TO JET-FIRE

Résumé : Cette étude s'intéresse aux comportements de 4 peintures intumescentes développées pour protéger des plateformes offshores et susceptibles de résister aux « jet-fires ». Un jet-fire peut intervenir sur un site pétrochimique suite à une fuite d'hydrocarbures sous pression et causer de sérieux dommages de part la chaleur dégagées et surtout la quantité de mouvement générées. Les aspects physiques et chimiques de ces formulations ont été développés permettant de mettre en avant les effets du pentaérythritol sur le comportement viscoélastiques et le processus d'intumescence. Par diffraction des rayons X et par RMN à l'état solide, nous avons montré les interactions entre ammonium et polyphosphate et différentes sources de carbones (pentaérythritol, dipentaérythritol, réseau époxyde) permettant la formation d'un char. Les résidus phosphorés réagissent ensuite avec TiO_2 pour former une structure cristalline TiP_2O_7 suspectées d'améliorer la résistance au feu et la résistance mécanique du char. Des tests feu ont confirmés ces améliorations. Dans un dernier chapitre nous avons développé un test permettant de reproduire à l'échelle laboratoire les phénomènes radiatifs et convectifs du jet-fire. Les premiers résultats ont montré de bonnes corrélations entre les observations faites à grande échelle et celles réalisées au laboratoire.

Mots clefs : *Résine époxyde, Dégradation thermique, Intumescence, Polyphosphate d'ammonium, Pentaerythritol, Dioxyde de titane, RMN du solide, Diffraction des rayons X, Développement de test feu.*

Abstract: The aim of this study is to understand and to explain behaviours exhibited by four epoxy-based intumescent formulations used on offshore platforms facing to jet-fire. A jet-fire is a turbulent diffusion flame resulting from the combustion of a fuel continuously released with some significant momentum. It represents a significant element of the risk on offshore installations. Regarding the formulation studied, we have developed three approaches. Firstly, the visco-elastic behaviour and mechanical resistance of the formulations have been investigated. The results show that pentaerythritol causes a viscosity decrease at lower temperature that appears as prejudicial to maintain efficient char on steel substrate. In a second part, chemical evolutions of the intumescent formulation have been determined thanks to solid-state NMR and X-Ray diffraction. Interactions between ammonium polyphosphate and respective carbon sources present in formulations have been assumed, yielding to the formation of char and production of phosphorus residues. Then these phosphorus residues react at high temperature with TiO_2 to form a crystalline structure TiP_2O_7 suspected to enhance mechanical properties and flame retardant performance. In a last part, furnace fire tests confirm this enhancement. Furthermore, a new small-scale experimental setup is developed mimicking large scale jet-fire resistance test in order to obtain rapidly and at low cost reliable behaviours of a large number of formulations facing to high load mixing radiative heat and flame impact. First results have been correlated with the large-scale ones and different geometries have been considered.

Keywords: *Epoxy resin, Thermal degradation, Intumescence, Ammonium polyphosphate, Pentaerythritol, Titanium dioxide, Solid state NMR, X-Ray diffraction, Fire testing development.*

Intitulé et adresse du laboratoire:

Laboratoire LSPES – Equipe PERF CNRS UMR 8008
E.N.S.C.L, Cité Scientifique, Bât. C7
F-59652 Villeneuve d'Ascq Cedex